

# User Guide



Version 4.0

April 16, 2019

## License

This document is licensed under  
Creative Commons Attribution-NonCommercial-NoDerivs 3.0 Unported License  
<http://creativecommons.org/licenses/by-nc-nd/3.0/legalcode>



## Acknowledgments

The work leading to the preparation of this document has received funding from the European Research Council under the European Union's Seventh Framework Programme (FP7/2007-2013)/ERC Grant agreement n° 307499. The collaboration with Professor Fernando T. Pinho (University of Porto, Portugal), Professor Paulo J. Oliveira (University of Beira Interior, Portugal) and Dr Alexandre Afonso (University of Porto, Portugal) in the development of numerical methods for computational rheology is also acknowledged.

## Disclaimer

This offering is not approved or endorsed by OpenCFD Limited, producer and distributor of the OpenFOAM software via [www.openfoam.com](http://www.openfoam.com), and owner of the OPENFOAM® and OpenCFD® trade marks.

The recommendations expressed in this document are those of the authors and are not necessarily the views of, or endorsement by, third parties named in this document.

RheoTool, where this guide is included, is distributed in the hope that it will be useful, but WITHOUT ANY WARRANTY. See the GNU General Public License (<http://www.gnu.org/licenses/>) for more details.

## Trademarks

**Linux** is a registered trademark of Linus Torvalds.

**OpenFOAM** is a registered trademark of OpenCFD Limited.

**Paraview** is a registered trademark of Kitware.

Typeset in L<sup>A</sup>T<sub>E</sub>X.

© 2016-2019 Francisco Pimenta, Manuel A. Alves

# Contents

|          |   |           |
|----------|---|-----------|
| <b>1</b> | <b>Introduction</b>   | <b>1</b>  |
| 1.1      | Motivation . . . . .  | 1         |
| 1.2      | Guide organization . . . . .                                    | 2         |
| 1.3      | Changelog . . . . .   | 3         |
| 1.4      | Citing <i>rheoTool</i> . . . . .                                | 7         |
| 1.5      | Contacts . . . . .  | 7         |
| 1.6      | Contributing . . . . .  | 7         |
| <b>2</b> | <b>Installation</b>   | <b>8</b>  |
| 2.1      | Compatibility with OpenFOAM® and foam-extend versions . . . . . | 8         |
| 2.2      | Differences between versions . . . . .                          | 8         |
| 2.3      | System requirements . . . . .                                   | 9         |
| 2.4      | Step-by-step instructions . . . . .                             | 9         |
| 2.4.1    | Download/clone <i>rheoTool</i> . . . . .                        | 9         |
| 2.4.2    | Download Eigen library . . . . .                                | 10        |
| 2.4.3    | Install Petsc library . . . . .                                 | 11        |
| 2.4.4    | Compile <i>rheoTool</i> . . . . .                               | 13        |
| <b>3</b> | <b>Theoretical background</b>                                   | <b>15</b> |
| 3.1      | Governing equations of complex fluid flows . . . . .            | 15        |
| 3.2      | Stabilization of viscoelastic fluid flow simulations . . . . .  | 16        |
| 3.2.1    | The both-sides-diffusion (BSD) technique . . . . .              | 16        |
| 3.2.2    | The log-conformation tensor approach . . . . .                  | 17        |
| 3.3      | Coupling algorithms . . . . .                                   | 18        |
| 3.3.1    | Pressure-velocity coupling . . . . .                            | 18        |
| 3.3.2    | Stress-velocity coupling . . . . .                              | 19        |
| 3.4      | High-resolution schemes . . . . .                               | 20        |
| 3.5      | Moving grids . . . . .  | 21        |
| 3.6      | Segregated vs coupled solvers . . . . .                         | 22        |
| 3.7      | Electrically-driven flow models . . . . .                       | 22        |
| 3.7.1    | Poisson-Nernst-Planck model . . . . .                           | 23        |
| 3.7.2    | Splitting the electric potential . . . . .                      | 24        |
| 3.7.3    | Poisson-Boltzmann model . . . . .                               | 24        |
| 3.7.4    | Debye-Hückel model . . . . .                                    | 25        |
| 3.7.5    | Slip model . . . . .  | 25        |
| 3.7.6    | Ohmic (leaky dielectric) model . . . . .                        | 26        |

---

|          |   |           |
|----------|---|-----------|
| 3.8      | Brownian dynamics simulations . . . . .   | 27        |
| 3.8.1    | The bead-spring model . . . . .   | 27        |
| 3.8.2    | Governing equations of beads motion . . . . .   | 30        |
| 3.8.3    | Spring force models . . . . .   | 30        |
| 3.8.4    | Time integration algorithm . . . . .  | 31        |
| <b>4</b> | <b>Overview of <i>rheoTool</i></b>  | <b>33</b> |
| 4.1      | The <i>constitutiveEquations</i> library . . . . .  | 33        |
| 4.1.1    | Available GNF and viscoelastic models . . . . .   | 33        |
| 4.1.2    | A note on FENE-type models . . . . .  | 41        |
| 4.1.3    | Multi-mode modeling . . . . .   | 43        |
| 4.1.4    | Analysis of a code sample . . . . .   | 43        |
| 4.1.5    | Advanced settings . . . . .   | 49        |
| 4.1.6    | Adding new viscoelastic or GNF models . . . . .   | 49        |
| 4.2      | The <i>EDFModels</i> library . . . . .  | 50        |
| 4.2.1    | Available EDF models . . . . .  | 50        |
| 4.2.2    | The potentials splitting approach and multi-species modeling in the PNP, PB and DH models . . . . . | 52        |
| 4.2.3    | Electrokinetic coupling loop in the PNP model . . . . .   | 52        |
| 4.2.4    | Coupled PNP model . . . . .   | 52        |
| 4.2.5    | Analysis of a code sample . . . . .   | 53        |
| 4.2.6    | Adding new EDF models . . . . .   | 60        |
| 4.3      | The <i>BDmolecule</i> library . . . . .   | 61        |
| 4.3.1    | Organization of variables . . . . .   | 61        |
| 4.3.2    | Solution sequence . . . . .   | 62        |
| 4.3.3    | External forcing type . . . . .   | 65        |
| 4.3.4    | External forcing interpolation . . . . .  | 65        |
| 4.3.5    | Spring force and time-integration schemes . . . . .   | 68        |
| 4.3.6    | Tethering and fixing the molecules center of mass . . . . .   | 70        |
| 4.3.7    | Beads tracking . . . . .  | 71        |
| 4.3.8    | Data output for post-processing . . . . .   | 71        |
| 4.3.9    | Limitations . . . . .   | 72        |
| 4.4      | The <i>sparseMatrixSolvers</i> library . . . . .  | 73        |
| 4.4.1    | Conditions to reuse the preconditioner/factorization . . . . .                                      | 73        |
| 4.4.2    | Residuals and tolerances . . . . .  | 74        |
| 4.4.3    | Generic parameters . . . . .  | 74        |
| 4.4.4    | OpenFOAM interface . . . . .  | 76        |
| 4.4.5    | Eigen interface . . . . .   | 76        |
| 4.4.6    | Hypre interface . . . . .   | 77        |
| 4.4.7    | Petsc interface . . . . .   | 80        |
| 4.4.8    | Coupled solvers . . . . .   | 82        |
| 4.4.9    | How to use <i>sparseMatrixSolvers</i> library in my own application? . . . . .                      | 84        |
| 4.4.10   | Limitations . . . . .   | 85        |
| 4.5      | Solvers . . . . .   | 86        |
| 4.5.1    | <i>rheoFoam</i> . . . . .   | 87        |
| 4.5.2    | <i>rheoTestFoam</i> . . . . .   | 95        |

|          |   |            |
|----------|---|------------|
| 4.5.3    | <i>rheoInterFoam</i>  | 97         |
| 4.5.4    | <i>rheoEFoam</i>  | 98         |
| 4.5.5    | <i>rheoBDFoam</i>   | 99         |
| 4.6      | Boundary conditions   | 101        |
| 4.6.1    | <i>linearExtrapolation</i>                                      | 101        |
| 4.6.2    | <i>navierSlip</i>   | 101        |
| 4.6.3    | <i>zeroIonicFlux</i>  | 102        |
| 4.6.4    | <i>boltzmannEquilibrium</i>                                     | 102        |
| 4.6.5    | <i>inducedPotential</i>   | 103        |
| 4.6.6    | <i>slipSmoluchowski</i>   | 103        |
| 4.6.7    | <i>slipSigmaDependent</i>                                       | 103        |
| 4.6.8    | A note on wall boundary conditions for pressure                 | 103        |
| 4.7      | Utilities   | 105        |
| 4.7.1    | <i>GaussDefCmpw</i> schemes for convective terms                | 105        |
| 4.7.2    | Generic post-processing: <i>ppUtil</i>                          | 107        |
| 4.7.3    | <i>writeEfield</i>  | 109        |
| 4.7.4    | <i>initMolecules</i>  | 110        |
| 4.7.5    | <i>averageMolcN</i>   | 114        |
| 4.7.6    | <i>averageMolcX</i>   | 114        |
| <b>5</b> | <b>Tutorials</b>  | <b>116</b> |
| 5.1      | <i>rheoFoam</i>   | 116        |
| 5.1.1    | General guidelines  | 116        |
| 5.1.2    | A note on <i>coded FunctionObjects</i>                          | 122        |
| 5.1.3    | Case 1: flow between parallel plates                            | 123        |
| 5.1.4    | Case 2: lid-driven cavity flow                                  | 125        |
| 5.1.5    | Case 3: flow in a 4:1 planar contraction                        | 126        |
| 5.1.6    | Case 4: flow around a confined cylinder                         | 129        |
| 5.1.7    | Case 5: bifurcation in a 2D cross-slot flow                     | 132        |
| 5.1.8    | Case 6: blood flow simulation in a real-model aneurysm          | 134        |
| 5.1.9    | Case 7: viscous fluid damper (moving mesh)                      | 138        |
| 5.2      | <i>rheoTestFoam</i>   | 140        |
| 5.2.1    | General guidelines  | 140        |
| 5.2.2    | Case I: Herschel-Bulkley model                                  | 143        |
| 5.2.3    | Case II: FENE-CR model  | 143        |
| 5.3      | <i>rheoInterFoam</i>  | 147        |
| 5.3.1    | General guidelines  | 147        |
| 5.3.2    | Case 1: impacting drop  | 148        |
| 5.3.3    | Case 2: planar die swell  | 150        |
| 5.4      | <i>rheoEFoam</i>  | 152        |
| 5.4.1    | General guidelines  | 152        |
| 5.4.2    | Case I: EDF of power-law and PTT fluids in a microchannel       | 155        |
| 5.4.3    | Case II: induced-charge electroosmosis around a cylinder        | 159        |
| 5.4.4    | Case III: charge transport across an ion-selective membrane     | 161        |
| 5.4.5    | Case IV: electrokinetic instabilities in a flow-focusing device | 163        |
| 5.4.6    | Case V: electrokinetic mixer                                    | 167        |

---

|   |   |            |
|---|---|------------|
| 5.4.7   | Case VI: electro-elastic instabilities in cross-shaped geometries | 169        |
| 5.5   | <i>rheoBDFoam</i>   | 171        |
| 5.5.1   | General guidelines  | 171        |
| 5.5.2   | Molecules visualization with Paraview                             | 176        |
| 5.5.3   | Case 1: $\lambda$ -DNA extension in a planar extensional flow     | 177        |
| 5.5.4   | Case 2: $7\lambda$ -DNA extension in a flow-focusing device       | 180        |
| 5.5.5   | Case 3: $\lambda$ -DNA dynamics in LAOE                           | 183        |
| <b>6</b>  | <b>FAQS</b>   | <b>186</b> |
| <b>Appendix A Parameters and variables in <i>rheoTool</i></b> |   | <b>188</b> |
| <b>Bibliography</b>   |   | <b>193</b> |

# Chapter 1

## Introduction

### 1.1 Motivation

The open-source OpenFOAM® toolbox can be used as a versatile finite-volume solver for CFD simulations in general polyhedral grids. A number of constitutive equations for Generalized Newtonian Fluids (GNF) are already available in the toolbox for a long time. More recently, Favero et al. [1] created a library containing a wide range of constitutive equations to model viscoelastic fluids, along with a solver named *viscoelasticFluidFoam* which makes use of this library. However, *viscoelasticFluidFoam* presents stability issues in certain conditions, such as, for example, in the simulation of high Weissenberg number ( $Wi$ ) flows or when there is no solvent viscosity contribution (e.g. in the upper-convected Maxwell model).

In Ref. [2], we attempted to minimize those issues by modifying critical points in the *viscoelasticFluidFoam* solver and in the handling of viscoelastic models. The modified solver was tested in benchmark flows and second-order accuracy, both in space and time, was observed, in addition to an enhanced stability [2]. The package that we present in this document – *rheoTool* – implements the method described in [2].

Afterwards, the capability to simulate electrically-driven flows was added to *rheoTool* [3] and is available since version 2.0.

Recognizing the importance of modeling polymeric flows at different scales, a Brownian dynamics solver has been implemented in *rheoTool* [4], which is available since version 3.0.

In [5] we implemented coupled solvers for electrically-driven flows, which can be also used for pressure-driven flows. Moreover, *rheoTool* was interfaced to external libraries (Petsc, Hypre, Eigen) that widen the range of available (direct and iterative) sparse matrix solvers.

*rheoTool* is more than a collection of solvers and libraries. In addition to robust solvers for the simulation of pressure- and electrically-driven flows of both GNF and viscoelastic fluids, we provide also tutorials and utilities that can be useful for the users starting to apply the OpenFOAM® toolbox in the simulation of complex fluid flows. In particular, some of the distinguishing features of *rheoTool* are:

- both GNF and viscoelastic models can be selected on run time and applied to

single-phase laminar flows. A solver for two-phase flows is also being developed and an experimental (but fully functional) version is already available.

- the log-conformation tensor methodology [6] is available for a wide range of viscoelastic models. This minimizes the numerical instabilities frequently observed for high Weissenberg number flows.
- a stress-velocity coupling term can be selected on run time in order to avoid checkerboard fields under specific conditions, such as in the simulation of the Upper-Conveyed Maxwell (UCM) model in strong extensional flows.
- high-resolution schemes for convective terms are available in a component-wise and deferred correction approach, avoiding numerical instabilities (see Ref. [2] for details). Additional schemes were added to the newly created library, which are not available by default in the OpenFOAM® toolbox.
- a solver (*rheoTestFoam*) is provided to compute the relevant material functions of each GNF/viscoelastic model included in the library. The user can select any canonical flow to be tested (shear flow, extensional flow, etc.).
- a number of models for electrically-driven flows is available and can be coupled with any rheological model. Mixed pressure- and electrically-driven flows are also allowed.
- transient flow solvers use the SIMPLEC algorithm for pressure-velocity coupling, instead of the PISO implementation. Large time-steps can be used without decoupling problems, and the use of under-relaxation is not required (except for pressure in some problems using non-orthogonal grids).
- a solver is provided for Brownian dynamics simulations of polymer molecules in generic meshes. Molecules can be linear or circular and they can also have branches. The external forcing can be steady or transient.
- coupled and segregated solvers are available.
- *rheoTool* can use sparse matrix solvers from Petsc, Hypre and Eigen.
- the tool is provided with a user-guide (this document) and a selected set of tutorials reproducing relevant benchmark or real-life flow problems.
- *rheoTool* is available for both <sup>1</sup>OpenFOAM® and <sup>2</sup>foam-extend versions.

## 1.2 Guide organization

The remainder of this guide is organized as follows:

- Chapter 2 describes the basic steps to install *rheoTool*.

---

<sup>1</sup><http://openfoam.org/>

<sup>2</sup><http://www.extend-project.de/>

- Chapter 3 provides a succinct overview of the theory behind the governing equations being solved. More details can be found in Refs. [2–4, 7].
- Chapter 4 presents an overview of the functionalities available in *rheoTool*, and discusses technical details about the code implementation.
- Chapter 5 contains several tutorials, guiding the reader into the use of *rheoTool*.

The language and the content used in this guide assumes that the reader has a basic knowledge on the use of the OpenFOAM® toolbox and is familiar with the finite-volume method applied to CFD problems. Thus, it is out the scope of this document to serve as an introduction on those subjects.

Although *rheoTool* is available for different OpenFOAM® and foam-extend versions, for historical reasons Chapters 4 and 5 are still mainly based on OpenFOAM® version 2.2.2 to describe the contents (except the content related with Brownian dynamics simulations, described for OpenFOAM® version 5.x). However, the small differences among different versions should not be an obstacle to the readers using any other version.

The readers interested in the theory behind *rheoTool* are strongly encouraged to first read Refs. [2], [3] and [4] before this guide.

## 1.3 Changelog

### Version 4.0

Released on 04/04/2019.

#### Generic

- Add: added interfaces to Petsc, Hypre and Eigen libraries, allowing the use of their (direct and iterative) sparse matrix solvers. All the interfaces can be used in parallel, except the one for Eigen. Only for the OpenFOAM® version.
- Add: *rheoTool* needs Petsc as an extra dependency. Added a script to install this package. The instructions to install *rheoTool* have been updated (see Chapter 2). Only for the OpenFOAM® version.
- Add: added coupled solvers for both pressure- and electrically-driven flows. Most viscoelastic models can be solved within a coupled solution method. Only for the OpenFOAM® version.
- Change: *rheoTool* version compatible with OpenFOAM® v4.0/4.1 is discontinued.

#### Electrically-driven flows

- Add: added coupled Poisson-Nernst-Planck model to EDF models (Type-Name = *NernstPlanckCoupled*). Only for the OpenFOAM® version.

## Constitutive equations

- Change: the eXtended Pom-Pom model implementation has been changed in order to allow using its thermodynamically consistent version [8]. Parameter  $n$  has been added (see Table 4.1) and should be adjusted by the user ( $n = 1$  for thermodynamic consistency and  $n = 0$  otherwise).
- Change: the code for the constitutive equations of viscoelastic models has been modified to allow integration with coupled solvers. Only for the OpenFOAM® version.

## Solvers

- Fix: fixed bug in *rheoInterFoam* for OpenFOAM® version 6.0, which was preventing post-processing (missing call to *update()*).

## Tutorials

- Change: tutorial *rheoFoam/Cavity* now uses sparse matrix solvers from Eigen library and is 1.6 times faster. Only for the OpenFOAM® version.
- Change: tutorial *rheoFoam/Cylinder* is now solved coupled, being 30 times faster. Only for the OpenFOAM® version.
- Change: tutorial *rheoEFoam/ICE0/NernstPlanck* is now solved with the coupled implementation of the PNP model and is 30 times faster. The name of the tutorial was changed to *rheoEFoam/ICE0/NernstPlanckCoupled*. Only for the OpenFOAM® version.
- Change: tutorial *rheoEFoam/selecMembrane/NernstPlanck/solution1D* is now solved with the coupled implementation of the PNP model and is twice faster. Moreover, under-relaxation is not needed anymore to avoid numerical divergence. Only for the OpenFOAM® version.
- Fix: fixed bug related to the old flag for stabilization methods in several tutorials, which was aborting the runs.

## Version 3.0

Released on 18/09/2018.

### Brownian dynamics solver

- Add: solvers, libraries, utilities and tutorials for Brownian dynamics simulations of polymer molecules.

### Generic

- Add: all solvers are now compatible with dynamic meshes. Due to this change, and for convenience, momentum equation is the first to be solved, followed by pressure equation and then the equations for the remaining variables (extra-stresses, passive scalar, etc.).
- Add: tutorial *fluidDamper* showing the use of *rheoFoam* with dynamic meshes.
- Add: added an explicit Navier slip boundary condition for velocity.
- Change: Namespace encapsulation of several derived classes.
- Change: *rheoTool* version compatible with OpenFOAM® v2.2.2 is discontinued.
- Add: added *rheoTool* patch for OpenFOAM® v6.0.
- Add: added note in the user-guide (Section 2.4.4) about parallel compilation of *rheoTool*.

## Constitutive equations

- Add: Papanastasiou regularization is now available for yield-stress GNF models (Hershel-Bulkley/Bingham and Casson models).
- Add: Casson model has been added to the library of constitutive equations.
- Add: the Multi-Lambda Isotropic Kinematic Hardening (MLK-IKH) model has been added to the library of constitutive equations.
- Add: the Vasquez-Cook-Mckinley (VCM) model has been added to the library of constitutive equations.
- Add: the Reactive Rod Model (RRM) model has been added to the library of constitutive equations.
- Add: Saramito's elastoviscoplastic model has been added to the library of constitutive equations. Both stress and log-conformation versions are available.
- Add: the Bautista-Manero-Puig (BMP) model has been added to the library of constitutive equations. Both stress and log-conformation versions are available.
- Change: implemented functions *tauTotal()* and *tauTotalMF()* in base classes. Solver *rheoTestFoam* and the utility retrieving the wall shear-stresses were modified accordingly.

## Version 2.0

Released on 09/02/2018.

### Electrically-driven flows

- Add: solvers, libraries, utilities and tutorials for electrically-driven flows.

### Constitutive equations

- Add: the Rolie-Poly viscoelastic model has been added to the library of constitutive equations. Both the stress and log-conformation versions are available.
- Add: the (single-equation) eXtended Pom-Pom viscoelastic model has been added to the library of constitutive equations. Both the stress and log-conformation versions are available.
- Change: sPTT models have been generalized to their full form by replacing the upper-convected derivative by the Gordon-Schowalter derivative. It is now possible to simulate PTT models with non-affine deformation, in both the stress and log-conformation versions.
- Change: the stabilization method in viscoelastic simulations has been made general and run time selectable: *none*, *BSD* or *coupling*.
- Change: a verification step has been added to the *WhiteMetznerLog* model in order to prevent its incorrect use (see the note in the table displaying the constitutive equations).

### Post-Processing

- Add: class *ppUtil* for post-processing purposes has been added to the versions for OpenFOAM® and the one existing for foam-extend has been modified. Enable the use of multiple *ppUtil* in simultaneous.
- Fix: sampling error was fixed for the tutorials of versions *of40* and *fe40*.

### Multiphase flows

- Change: `(fvc::grad(U)&fvc::grad(etaS())*alpha))` has been replaced by `fvc::div(etaS())*alpha*dev2(T(fvc::grad(U)))` for the use in multiphase flows (*constitutiveEq.C*).
- Fix: call to *constrainPressure()* in *rheoInterFoam*, version *of40*, has been corrected for the SIMPLEC algorithm (*pEqn.H*). Added a section in the user-guide on how to use properly the *fixedFluxPressure* BC with *rheoInterFoam* in versions *of222* and *fe40*.
- Add: tutorials on the die swell problem.

### Generic

- Change/Fix: code cleanup and bug fix (BC evaluation of the explicit `fvc::div(phi, X)` operator) in class `GaussDefCmpw`.
- Change/Add: replace boundary condition `extST` by the *Type*-independent `linearExtrapolation` boundary condition (no backward compatibility). Added optional second-order regression.
- Change: major update of the user guide to include electrically-driven flows. Other changes were made in its content and organization, and some typos were corrected.
- Change: ensure compatibility with foam-extend 4.0 and OpenFOAM® v4.1.

## Version 1.0

Released on 6/12/2016.

Initial version.

## 1.4 Citing *rheoTool*

If you found *rheoTool* useful and want to cite it in your work, the following BibTeX entry can be used for that purpose:

```
@misc{rheoTool,
  author = "F. Pimenta and M.A. Alves",
  title = "rheoTool",
  howpublished = "\url{https://github.com/fppimenta/rheoTool}",
  year = "2016"}
```

Since the underlying theory of *rheoTool* has been mainly presented in technical papers [2–5], these can also be used for citation purposes.

## 1.5 Contacts

*rheoTool* is under continuous development and new features and improvements will be added in the future. If you have any suggestions, comments or doubts regarding the tool, or if you found a bug or error, feel free to contact us:

✉ Francisco Pimenta: [fpimenta@fe.up.pt](mailto:fpimenta@fe.up.pt)

✉ Manuel A. Alves: [mmalves@fe.up.pt](mailto:mmalves@fe.up.pt)

## 1.6 Contributing

In the open-source spirit, *rheoTool* is open to contributions from the community. If you believe that your piece of code is worth to be incorporated in *rheoTool*'s next version, feel free to contact us.

# Chapter 2

## Installation

### 2.1 Compatibility with OpenFOAM® and foam-extend versions

The development and testing of *rheoTool* is usually performed in the most recent stable release of OpenFOAM®. However, an effort has been made to keep *rheoTool* also compatible with foam-extend, although not all features available for the OpenFOAM® version can be found there (see Section 2.2). Currently, we provide versions of *rheoTool* for:

- OpenFOAM® v6.0 (`of60/`).
- foam-extend 4.0 (`fe40/`).

The list above includes the versions which were effectively tested. This means that a given version of *rheoTool* may be compatible with other OpenFOAM® or foam-extend versions not included in this list. The versions above were tested in Ubuntu 16.04, but other operating systems running OpenFOAM® can eventually support some version of *rheoTool*. However, the installation is only described here for a Linux OS.

### 2.2 Differences between versions

The complete version of *rheoTool* is the one available for OpenFOAM®, since this is the one used for development. There are two main components of this version that are not available for the foam-extend version: the Brownian dynamics module and the interfaces to external libraries (Petsc, Hypre and Eigen) providing access to a wider range of sparse matrix solvers (including coupled solvers).

Besides those major differences, in order to make *rheoTool* compatible with each OpenFOAM®/foam-extend version, several modifications were required at the programming level for each case. Still, the user-interface remained almost unchanged among the different versions. The main exception is on the *codedStreamFunctionObjects* and *coded* boundary conditions, which are used in the tutorials of Chapter 5. Indeed, while these functionalities are available in OpenFOAM®,

it is not the case for foam-extend. Thus, the *coded* boundary conditions and the utilities implemented as *codedStream FunctionObjects* in OpenFOAM® versions had to be assembled and compiled in a library for the foam-extend version.

A second point to be taken into account is that *rheoTool* may perform differently in each OpenFOAM®/foam-extend version, as it may happen with any other default solver of OpenFOAM®/foam-extend. This is naturally a consequence of the evolution of the core machinery of OpenFOAM®/foam-extend, transversal to many solvers and libraries. Fortunately, in most of the cases the differences will be small. The following issues were detected in the tests that we performed:

- in general, a tutorial of *rheoTool* for OpenFOAM® versions may be run either in serial or parallel while keeping the same numerical settings. However, in the tests using the foam-extend version, it was observed that parallel simulations are less stable than serial ones, usually requiring a smaller time-step or some under-relaxation of the velocity (sometimes as low as 0.97).

## 2.3 System requirements

Only standard requirements are needed to install *rheoTool*:

- a compatible and functional version of OpenFOAM® or foam-extend should be already installed.
- the machine should be connected to the Internet.

OpenFOAM® users might additionally need *sudo* privilege to install Petsc. This is discussed in more detail in Section 2.4.3.

## 2.4 Step-by-step instructions

After ensuring that the prerequisites are fulfilled, the user is ready to start the installation, which includes four (three) major steps:

1. Download/clone *rheoTool* (Section 2.4.1);
2. Download Eigen library (Section 2.4.2);
3. **(Only for OpenFOAM® users)** Install Petsc library (Section 2.4.3);
4. Compile *rheoTool* (Section 2.4.4).

### 2.4.1 Download/clone *rheoTool*

**ⓘ** This step is common to both OpenFOAM® and foam-extend users.

*rheoTool* is publicly available as a GitHub repository. There is a single branch (master) in the repository, which always contains the most recent, stable version of the code (there is no public dev branch or similar). Once a new version is pushed to the master branch, the previous, old version is tagged as a *release*. Therefore, *releases* are only checkpoints for older versions and **should not** be used to get the most recent version of the code.

As explained in the `Readme` file of the repository, *rheoTool* can be either downloaded or cloned from GitHub. The structure of *rheoTool* (<https://github.com/fppimenta/rheoTool>) is depicted in Fig. 2.1.

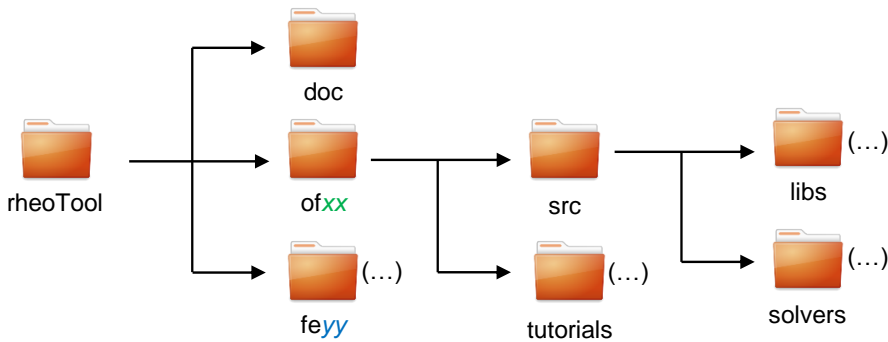


**Figure 2.1:** Directory organization of *rheoTool*.

The top-level directory of *rheoTool* contains the versions available for different OpenFOAM® (*of*) and foam-extend (*fe*) versions. The folder `doc/`, containing the user guide, is also in the top-level directory. Inside the folder for each version, there are two directories: `src/`, where the source code can be found, and `tutorials/`, containing several tutorial cases showing the use of *rheoTool*. The `src/` directory is further subdivided in a directory with the applications (`solvers/`) and another one containing libraries (`libs/`).

After cloning/downloading *rheoTool*, the user is free to remove from the top-level directory all the versions not needed and keep only the one(s) of interest.

#### 2.4.2 Download Eigen library

**!** This step is common to both OpenFOAM® and foam-extend users.

In the directory corresponding to a given *rheoTool* version (e.g. `of60`, where you will find file `downloadEigen`), open a terminal and check that file `etc/bashrc` of your installed OpenFOAM® or foam-extend version has been sourced. This is particularly relevant if you have defined *alias* for different versions of OpenFOAM® or foam-extend. If this is the case, be sure that the alias pointing to the desired version has been typed. Shortly, you should only advance to the next step if a command like `~$ icoFoam -help` is recognized in the terminal. Note that in this document we use the prepending `~$` for any instruction to be typed in the

command line (thus, `~$ icoFoam -help` means that you only type `icoFoam -help`). If this check is successful, run the script `downloadEigen` in that terminal:

```
~$ ./downloadEigen
```

This script downloads Eigen version 3.2.9 (other versions close to that would also work adequately) from the Internet (using `wget`), extracts it and moves it to directory:

```
$WM_PROJECT_USER_DIR/ThirdParty/Eigen3.2.9
```

Eigen is used in *rheoTool* for computation of eigenvalues and eigenvectors and there is no need to install the library, since the inclusion of the required headers is enough for our purposes.

However, its location in the system must be defined and exported. This is achieved by attributing to variable `EIGEN_RHEO` – the one used and recognized by *rheoTool* – the actual path of Eigen. The command to do so has been displayed to the terminal after running script `downloadEigen` (if everything was ok) and looks like:

```
~$ echo "export EIGEN_RHEO=/home/user/OpenFOAM/user-4.0/ThirdParty/Eigen3.2.9">>>/home/user/.bashrc
```

Do not copy this command, it is just an example of what is displayed to the screen. Instead, copy-paste and run the command appearing in your terminal.

If, for some reason, the user wants to move Eigen to another directory (or already has an Eigen version in another directory), then move Eigen to its final location (if already not) and define variable `EIGEN_RHEO` accordingly. **Note that Eigen only needs to be installed once per system.** Even if the user has installed multiple versions of *rheoTool* in the same system, the above procedure only needs to be run once (for the first version being installed), as long as the directory containing Eigen since the first installation is not deleted, or renamed.

### 2.4.3 Install Petsc library

**❶** This step is only for OpenFOAM® users.

Petsc [9–11] has been added to the dependencies used by *rheoTool* starting from version 4.0. This library provides a number of efficient and scalable sparse matrix solvers, that can be used in *rheoTool* with both segregated and coupled solvers.

The script `installPetsc` is responsible for downloading Petsc and the dependencies it needs, configuring Petsc, compiling the libraries and exporting the variables needed to call and use Petsc from any location. While the script is running, the user will be prompted to insert its password (and Yes or No) to allow the installation of some dependencies needed by Petsc:

```
libatlas-dev,libatlas-base-dev,libblas-dev,liblapack-dev,flex,bison,git,make,cmake,gfortran
```

Some of these dependencies might already exist in the system, and in those cases nothing is done. Only the nonexistent dependencies will be downloaded and

installed. This is the only part of the script requiring *sudo* mode (password confirmation). If the user is sure that all these packages are already installed in the system, then commenting section *## Install dependencies* inside the script is enough to avoid the need for *sudo*, which can be problematic for non-administrator users.

The script has been tested on fresh installs of Ubuntu 18.04 and 16.04, after installing OpenFOAM® binaries. The system OpenMPI is being used by both OpenFOAM® and Petsc in such conditions. This is a point worth to emphasize: both OpenFOAM® and Petsc should be compiled with the same MPI software, which, however, can be different from OpenMPI. At the beginning of script `installPetSc`, the user can change the paths to the MPI library and wrappers upon need.

Petsc library is configured with standard options, that the user can found and modify under section *## Configure Petsc*. To check the full range of options available, please consult Petsc references [9, 10]. The configuration that we set as default will download and install the following additional packages from within Petsc:

```
hypre,parmetis,metis,ptscotch,mumps,scalapack
```

Note that Petsc could be also installed via *apt-get* (there are binaries available), but this would not allow configuring and using the most recent versions of the software.

For most of the users, the script to install Petsc can be run without any modification. In such cases, go the directory corresponding to one of the *rheoTool* versions (where you will find file `installPetSc`), open a terminal and ensure that file `etc/bashrc` of your installed OpenFOAM® version was sourced (as for Eigen). Then run the script `installPetSc` in that terminal:

```
~$ ./installPetSc
```

Petsc library is saved and compiled to directory:

```
$ WM_PROJECT_USER_DIR/ThirdParty
```

which can be changed by the user inside the script (before running it).

Installing Petsc only needs to be performed once per system. For example, if you have multiple versions of *rheoTool* in the same machine, only a single install of Petsc is needed (recommended). Note that script `installPetSc` modifies your `~/.bashrc` file by appending Petsc variables to it (see the code at the end of the script). If you have multiple versions of Petsc installed, or if you change the location or version of Petsc, do not forget to manage these variables. Running (until completion) `installPetSc` multiple times will duplicate these variables and possibly cause conflicts of paths. After installing Petsc with success, it is good idea to check your `~/.bashrc` and verify if the three variables `PETSC_DIR`, `PETSC_ARCH` and `LD_LIBRARY_PATH` appended at the end are correctly defined and not duplicated.

### 2.4.4 Compile *rheoTool*

**i** This step is common to both OpenFOAM® and foam-extend users.

It is recommended to save *rheoTool* in a location with write permission, otherwise you will need to use *sudo* mode to run all the commands. A good location for *rheoTool* is, for example, directory `$WM_PROJECT_USER_DIR`, which is defined by default when OpenFOAM® or foam-extend is installed.

---

**Note (only for OpenFOAM® users):** in **some** combinations of OpenFOAM® patches/OS versions, it was observed that the linker is unable to locate PETSc, whose path is absent in variable `$LD_LIBRARY_PATH`. Indeed, `echo $LD_LIBRARY_PATH` will not include the path to PETSc libs in such situations. This is most frequently observed when there are **aliases to different OpenFOAM® versions**, since in these situations sourcing the `etc/bashrc` of OpenFOAM® cleans `$LD_LIBRARY_PATH`. When this happens, running the `Allwmake` script as described below results in linking errors similar to:

```
/usr/bin/ld:warning:libpetsc.so.3.10,neededby/home/user/OpenFOAM/us
er-6/platforms/linux64GccDPInt320pt/lib/libconstitutiveEquations.so
,notfound(tryusing-rpathor-rpath-link)

/home/user/OpenFOAM/user-6/platforms/linux64GccDPInt320pt/lib/libsp
arseMatrixSolvers.so:undefinedreferenceto‘VecSet’...
```

To avoid this situation, the user needs to ensure that the path to PETSc library is added to `$LD_LIBRARY_PATH` after sourcing the `etc/bashrc` of OpenFOAM®, such that it survives. Among the several possibilities, a simple one is to modify the alias. For that, open your system `~/.bashrc` in edit mode, for example running `gedit ~/.bashrc`, find your alias (typically at the bottom of the file) and modify it appending command

```
export LD_LIBRARY_PATH=$PETSC_DIR/$PETSC_ARCH/lib:$LD_LIBRARY_PATH
```

at its end. Thus, an alias of the form (this is just an example)

```
alias of60='source /opt/openfoam6/etc/bashrc'
```

before the modification should look like this (single line)

```
alias of60='source /opt/openfoam6/etc/bashrc; export
LD_LIBRARY_PATH=$PETSC_DIR/$PETSC_ARCH/lib:$LD_LIBRARY_PATH'
```

after the modification. Note that there are other ways that would lead to the same result, as for example modifying the `$LD_LIBRARY_PATH` variable at the end of the `etc/bashrc` file of OpenFOAM®, creating symbolic links of PETSc libraries inside one of the locations included by default by OpenFOAM® in `$LD_LIBRARY_PATH`, etc.

How do you know if the above procedure applies to your system? If you do not have aliases for OpenFOAM® versions, then you should not have this problem. If you do have aliases, then this problem might happen or not. It will happen if

command `echo $LD_LIBRARY_PATH` does not include the path to PETSc libs, which you can test before compiling *rheoTool*. Otherwise, the compilation error similar to the one displayed above should be suggestive of this issue.

---

After you move *rheoTool* to its final location, **open a new terminal** (to ensure that your system `~/.bashrc` is sourced and contains the path of Eigen and Petsc) in the top-level directory of *rheoTool* (ensuring that the OpenFOAM® or foam-extend environment has been sourced, as previously) and enter the directory with the version of *rheoTool* that is compatible with your OpenFOAM® or foam-extend version, and then go to directory `src/`. For example, for OpenFOAM® v6.0, it would be:

```
~$ cd of60/src
```

Now, run the script `Allwmake` to build the libraries and applications of *rheoTool*. In order to speed up the compilation, several processors can be used, if available. For OpenFOAM® users, run

```
~$ ./Allwmake -j N
```

for parallel compilation with  $N$  processors. For example, `./Allwmake -j 3` will compile in parallel using 3 processors. If the number of processors is not specified, all available processors are used. If option `-j` is not passed to the script, the compilation will use `WM_NCOMPPROCS` processors, where this variable is usually defined in the `etc/bashrc` file of your OpenFOAM® installation. For foam-extend users, option `-j` is not recognized by the script, therefore simply run

```
~$ ./Allwmake
```

The compilation in foam-extend will typically make use of all processors available in the system, since variable `WM_NCOMPPROCS` is set by default in such way.

Both the libraries and applications installed with *rheoTool* can be "cleaned" by running the script `Allwclean`.

Since the user will probably not need the remaining versions of *rheoTool* that remain in the top-level directory, they can simply be deleted, if already not.

To check if the installation succeeded, the user should try running one of the tutorials in Chapter 5.

# Chapter 3

## Theoretical background

The equations governing pressure- and electrically-driven flows of incompressible, complex fluids are discussed in this Chapter, along with some important aspects related with their discretization in the finite-volume framework. Since a thorough discussion on this subject can be found in Refs. [2, 3, 5], some intermediate steps are skipped and only the more relevant equations are presented.

The last Section of this Chapter is concerned with the theory of Brownian dynamics simulations using coarse-grained models. Again, we will only present the more relevant aspects for the scope of this user guide and more details can be found in Ref. [4].

### 3.1 Governing equations of complex fluid flows

The basic equations governing isothermal, single-phase, transient flows, under laminar conditions, for incompressible fluids, in static grids, establish mass conservation (Eq. 3.1) and momentum balance (Eq. 3.2),

$$\nabla \cdot \mathbf{u} = 0 \quad (3.1)$$

$$\rho \left( \frac{\partial \mathbf{u}}{\partial t} + \mathbf{u} \cdot \nabla \mathbf{u} \right) = -\nabla p + \nabla \cdot \boldsymbol{\tau}' + \mathbf{f} \quad (3.2)$$

where  $\mathbf{u}$  is the velocity vector,  $t$  is the time,  $p$  is the pressure,  $\boldsymbol{\tau}'$  is the extra-stress tensor and  $\mathbf{f}$  is any external body-force, such as the electric force discussed in Section 3.7. To simulate viscoelastic fluid flows, it is a common approach to split the total extra-stress tensor in a solvent contribution ( $\boldsymbol{\tau}_s$ ) and a polymeric contribution ( $\boldsymbol{\tau}$ ),  $\boldsymbol{\tau}' = \boldsymbol{\tau} + \boldsymbol{\tau}_s$ . In order to have a closed set of equations, a constitutive equation is required for each tensor contribution, which can be generally written as in Eqs. (3.3) and (3.4), for a wide range of models,

$$\boldsymbol{\tau}_s = \eta_s(\dot{\gamma})(\nabla \mathbf{u} + \nabla \mathbf{u}^T) \quad (3.3)$$

$$f(\boldsymbol{\tau})\boldsymbol{\tau} + \lambda(\dot{\gamma}) \nabla \boldsymbol{\tau} + \mathbf{h}(\boldsymbol{\tau}) = \eta_p(\dot{\gamma})(\nabla \mathbf{u} + \nabla \mathbf{u}^T) \quad (3.4)$$

In Eqs. (3.3) and (3.4),  $\eta_s$  is the solvent viscosity,  $\eta_p$  is the polymeric viscosity coefficient,  $\lambda$  is the relaxation time,  $\dot{\gamma}$  is the shear-rate,  $f(\boldsymbol{\tau})$  is a general scalar function depending on an invariant of  $\boldsymbol{\tau}$ ,  $\mathbf{h}(\boldsymbol{\tau})$  is a tensor-valued function depending on  $\boldsymbol{\tau}$  and  $\overset{\nabla}{\boldsymbol{\tau}} = \frac{\partial \boldsymbol{\tau}}{\partial t} + \mathbf{u} \cdot \nabla \boldsymbol{\tau} - \boldsymbol{\tau} \cdot \nabla \mathbf{u} - \nabla \mathbf{u}^T \cdot \boldsymbol{\tau}$  represents the upper-convected time derivative, which renders the models frame-invariant. Some models use the Gordon-Schowalter derivative ( $\overset{\square}{\boldsymbol{\tau}} = \overset{\nabla}{\boldsymbol{\tau}} + \zeta (\boldsymbol{\tau} \cdot \mathbf{D} + \mathbf{D} \cdot \boldsymbol{\tau})$ , with  $\mathbf{D} = \frac{1}{2}(\nabla \mathbf{u} + \nabla \mathbf{u}^T)$ ) instead of the upper-convected derivative, in order to take non-affine deformation into account (controlled by parameter  $\zeta$ ). In *rheoTool*, this is the case of PTT-type models. Other constitutive models exist, which can also make use of the lower-convected time derivative, but those are not explored here. The constitutive equation for a GNF is limited to Eq. (3.3), since elasticity is not considered ( $\boldsymbol{\tau}' = \boldsymbol{\tau}_s$ ). In Table 4.1 presented in the next Chapter, Eqs. (3.3) and (3.4) are specified for several GNF and viscoelastic models.

Eqs. (3.1)–(3.4) represent the standard system of equations to be solved. However, due to numerical stability issues in viscoelastic fluid flow simulations, the system is rarely solved in that form. Indeed, several techniques are available for stabilization purposes (see, for instance, Ref. [12] for a comparison between the most popular techniques) and the ones used in *rheoTool* are addressed next.

## 3.2 Stabilization of viscoelastic fluid flow simulations

### 3.2.1 The both-sides-diffusion (BSD) technique

The both-sides-diffusion (BSD) is a technique already incorporated in the *viscoelasticFluidFoam* solver [1]. It consists in adding a diffusive term on both sides of momentum equation (Eq. 3.2), with the difference that one of them (left-hand side) is added implicitly, while the other one (right-hand side) is added explicitly. Once steady-state is reached, both terms cancel each other exactly. Such method increases the ellipticity of the momentum equation and, as such, has a stabilizing effect, mostly when there is no solvent contribution in the extra-stress tensor. Incorporating the terms arising from the both-sides-diffusion in the momentum equation, and making use of Eq. (3.3), then

$$\rho \left( \frac{\partial \mathbf{u}}{\partial t} + \mathbf{u} \cdot \nabla \mathbf{u} \right) - \nabla \cdot (\eta_s + \eta_p) \nabla \mathbf{u} = -\nabla p - \nabla \cdot (\eta_p \nabla \mathbf{u}) + \nabla \cdot \boldsymbol{\tau} + \mathbf{f} \quad (3.5)$$

Note that the added diffusive terms are scaled by the polymeric viscosity ( $\eta_p$ ), which is a common choice in the literature (e.g. Ref. [12]), although not mandatory. In order to simplify the reading, the possible dependence of the viscosity and relaxation time on the shear-rate will be dropped in the respective symbols, as already done in Eq. (3.5), although this relation still holds to keep generality.

### 3.2.2 The log-conformation tensor approach

The log-conformation tensor approach consists in a change of variable when evolving in time the polymeric extra-stress and it was devised to tackle the numerical instability faced at high Weissenberg number flows [6, 13].

The polymeric extra-stress tensor is related with the conformation tensor ( $\mathbf{A}$ ). For the Oldroyd-B model, for example, this relation is expressed as (see Table 4.1 for several viscoelastic models)

$$\boldsymbol{\tau} = \frac{\eta_p}{\lambda}(\mathbf{A} - \mathbf{I}) \quad (3.6)$$

In the log-conformation tensor methodology, a new tensor ( $\boldsymbol{\Theta}$ ) is defined as the natural logarithm of the conformation tensor

$$\boldsymbol{\Theta} = \ln(\mathbf{A}) = \mathbf{R} \ln(\mathbf{\Lambda}) \mathbf{R}^T \quad (3.7)$$

In Eq. (3.7), the conformation tensor was diagonalized ( $\mathbf{A} = \mathbf{R} \mathbf{\Lambda} \mathbf{R}^T$ ) because it is positive definite, where  $\mathbf{R}$  is a matrix containing in its columns the eigenvectors of  $\mathbf{A}$  and  $\mathbf{\Lambda}$  is a matrix whose diagonal elements are the respective eigenvalues resulting from the decomposition of  $\mathbf{A}$ . Eq. (3.4) written in terms of ( $\boldsymbol{\Theta}$ ) becomes [6]

$$\frac{\partial \boldsymbol{\Theta}}{\partial t} + \mathbf{u} \cdot \nabla \boldsymbol{\Theta} = \boldsymbol{\Omega} \boldsymbol{\Theta} - \boldsymbol{\Theta} \boldsymbol{\Omega} + 2\mathbf{B} + \frac{1}{\lambda} \mathbf{g}(\boldsymbol{\Theta}) \quad (3.8)$$

where  $\mathbf{g}(\boldsymbol{\Theta})$  is a model-specific tensorial function depending on  $\boldsymbol{\Theta}$  (see Table 4.1 for other viscoelastic models) and

$$\mathbf{B} = \mathbf{R} \begin{bmatrix} m_{xx} & 0 & 0 \\ 0 & m_{yy} & 0 \\ 0 & 0 & m_{zz} \end{bmatrix} \mathbf{R}^T \quad (3.9)$$

$$\boldsymbol{\Omega} = \mathbf{R} \begin{bmatrix} 0 & \omega_{xy} & \omega_{xz} \\ -\omega_{xy} & 0 & \omega_{yz} \\ -\omega_{xz} & -\omega_{yz} & 0 \end{bmatrix} \mathbf{R}^T \quad (3.10)$$

$$\mathbf{M} = \mathbf{R} \nabla \mathbf{u}^T \mathbf{R}^T = \begin{bmatrix} m_{xx} & m_{xy} & m_{xz} \\ m_{yx} & m_{yy} & m_{yz} \\ m_{zx} & m_{zy} & m_{zz} \end{bmatrix} \quad (3.11)$$

$$\omega_{ij} = \frac{\Lambda_j m_{ij} + \Lambda_i m_{ji}}{\Lambda_j - \Lambda_i} \quad (3.12)$$

After solving Eq. (3.8),  $\boldsymbol{\Theta}$  is diagonalized in the form

$$\boldsymbol{\Theta} = \mathbf{R} \mathbf{\Lambda}^\Theta \mathbf{R}^T \quad (3.13)$$

and the conformation tensor is recovered by the inverse relation of Eq. (3.7)

$$\mathbf{A} = \exp(\boldsymbol{\Theta}) = \mathbf{R} \exp(\mathbf{\Lambda}^\Theta) \mathbf{R}^T \quad (3.14)$$

Finally, the polymeric extra-stress tensor can be computed from  $\mathbf{A}$  (Eq. 3.6) and used in the momentum equation.

Note that for PTT-type models, which may include non-affine deformation through the Gordon-Schowalter derivative, the tensor  $\mathbf{M}$  (Eq. 3.11) is computed differently:  $\mathbf{M} = \mathbf{R} (\nabla \mathbf{u}^T - \zeta \mathbf{D}) \mathbf{R}^T$ .

It is worth to mention that the log-conformation approach can be considered a particular case of the kernel-conformation method [14]. However, from our experience, the *log* kernel is frequently the optimal kernel (in terms of robustness and accuracy) for generic problems, so that only this one is widely used in *rheoTool*. Nevertheless, for the Oldroyd-B model, the root<sup>k</sup> kernel [14] and the square-root transformation [15] are also included in *rheoTool* for demonstration purposes.

### 3.3 Coupling algorithms

#### 3.3.1 Pressure-velocity coupling

Although the OpenFOAM® toolbox is already able to solve linear systems of equations in a coupled way, most of the solvers still rely on segregated solutions (this is a rule for transient solvers). In segregated solvers, the equations for each variable are solved sequentially. Even for a fully-implicit method, if the coupling between variables is weak, then numerical divergence is prone to occur.

In the OpenFOAM® toolbox, common algorithms for pressure-velocity coupling are SIMPLE and SIMPLEC for steady-state solvers and either PISO or PIMPLE (a combination of SIMPLE(C) and PISO) for transient solvers. From the benchmark cases performed in Ref. [2], it was observed that SIMPLEC was particularly suitable for transient viscoelastic fluid flows at low Reynolds numbers, regarding stability and accuracy.

The continuity equation, implicit in the pressure variable, derived for SIMPLEC (a more detailed derivation is presented in Ref. [2]) leads to

$$\nabla \cdot \left( \frac{1}{a_P - H_1} (\nabla p)_P \right) = \nabla \cdot \left[ \mathbf{H} + \left( \frac{1}{a_P - H_1} - \frac{1}{a_P} \right) (\nabla p^*)_P \right] \quad (3.15)$$

where  $a_P$  are the diagonal coefficients from the momentum equation,  $H_1 = - \sum_{nb} a_{nb}$  is an operator representing the negative sum of the off-diagonal coefficients from momentum equation,  $\mathbf{H} = - \sum_{nb} a_{nb} \mathbf{u}_{nb}^* + \mathbf{b}$  is an operator containing the off-diagonal contributions, plus source terms (except the pressure gradient) of the momentum equation and  $p^*$  is the pressure field known from the previous time-step or iteration. Accordingly, the equation to correct the velocity after obtaining the continuity-compliant pressure field from Eq. (3.15) is

$$\mathbf{u} = \frac{\mathbf{H}}{a_P} + \left( \frac{1}{a_P - H_1} - \frac{1}{a_P} \right) (\nabla p^*)_P - \frac{1}{a_P - H_1} (\nabla p)_P \quad (3.16)$$

Importantly, in order to avoid the onset of checkerboard fields, the pressure gradient terms involved in the computation of face velocities, i.e., in Eqs. (3.15)

and (3.16), are directly evaluated using the pressure on the cells straddling the face, in a Rhee-Chow-like procedure (more details in Ref. [2]). Nonetheless, when Eq. (3.16) is used to correct the cell-centered velocity field, the pressure gradient terms are computed "in the usual way", for example using Green-Gauss integration.

Rhee-Chow methods used to avoid checkerboard fields, as the one described in the previous paragraph, are known to be affected by the use of small time-steps and they also present time-step dependency on steady-state results [16]. In OpenFOAM® solvers, a common strategy to avoid such effects is to add a corrective term to face-interpolated velocities, through functions `ddtPhiCorr()` or `ddtCorr()`. Recently, in foam-extend the time-step dependency was solved in a different way, by removing the transient term contribution from the  $a_p$  coefficients of the momentum equation [17]. However, this approach may be problematic when used with the SIMPLEC algorithm, since a division by zero is prone to happen. In *rheoTool*, we keep using the added corrective term, although, as mentioned in Ref. [2], this term can be improved in order to more efficiently avoid the small time-step dependency of steady-state solutions.

### 3.3.2 Stress-velocity coupling

Stress-velocity decoupling problems can arise for similar reasons as those described for pressure-velocity: the cell-centered velocity loses the influence of the forces (either polymeric extra-stress or pressure gradient) of its direct neighborhood (cells sharing a face in common). This usually happens in the interpolation from cell-centered to face-centered fields. In the case of polymeric extra-stresses, it is the divergence term ( $\nabla \cdot \boldsymbol{\tau}$ ) in the momentum equation, when  $\boldsymbol{\tau}$  is linearly interpolated from cell centers to face centers, which can be responsible for the decoupling.

In Ref. [2], we described a new stress-velocity coupling method, where the polymeric extra-stresses at face centers are computed as

$$\boldsymbol{\tau}_f = \bar{\boldsymbol{\tau}}_f + \eta_p \left[ (\nabla \mathbf{u} |_f + (\nabla \mathbf{u})^T |_f) - \left( \overline{\nabla \mathbf{u}} |_f + \overline{(\nabla \mathbf{u})^T} |_f \right) \right] \quad (3.17)$$

where terms with an overbar are linearly interpolated from cell-centered values, while the remaining velocity gradients are directly evaluated from the cell-centered velocities straddling the face. When the definition of  $\boldsymbol{\tau}_f$  in Eq. (3.17) is inserted in the momentum equation with the both-sides-diffusion terms already present (Eq. 3.5), then we obtain

$$\rho \left( \frac{\partial \mathbf{u}}{\partial t} + \mathbf{u} \cdot \nabla \mathbf{u} \right) - \nabla \cdot (\eta_s + \eta_p) \nabla \mathbf{u} = -\nabla p - \overline{\nabla \cdot \eta_p \nabla \mathbf{u}} + \nabla \cdot \bar{\boldsymbol{\tau}} + \mathbf{f} \quad (3.18)$$

where the term  $\overline{\nabla \cdot \eta_p \nabla \mathbf{u}}$  is a "special second-order derivative" (different from the *laplacian* operator of OpenFOAM®), defined as the divergence of the velocity gradient, where the velocity gradient at the faces is obtained by linear interpolation of the velocity gradient evaluated on the cell centers. More details are presented in Ref. [2], where it is shown that with mesh refinement Eq. (3.17) approaches  $\boldsymbol{\tau}_f = \bar{\boldsymbol{\tau}}_f$  and the additional terms cancel out. Note that when inserting Eq. (3.17)

in the momentum equation (resulting in Eq. 3.18), we drop the transpose velocity gradients for simplicity, since continuity imposes  $\nabla \cdot \nabla \mathbf{u}^T = \mathbf{0}$ .

### 3.4 High-resolution schemes

The discretization of convective terms within the finite-volume framework leads to

$$\int_V (\mathbf{u} \cdot \nabla \phi) dV = \sum_f \phi_f (\mathbf{u}_f \cdot \mathbf{S}_f) = \sum_f \phi_f F_f \quad (3.19)$$

where  $\phi$  is a generic variable being advected,  $\mathbf{S}_f$  is the face-area vector and  $F_f$  is the volumetric flux crossing face  $f$ . While fluxes are known at the faces from the Rhie-Chow-like interpolation (Eq. 3.16),  $\phi$  at face centers need to be interpolated from known values at cell centers. OpenFOAM® offers a wide range of schemes to perform such interpolation, from upwind – an unconditionally stable scheme, but only first-order accurate –, to central differences – a conditionally stable, second-order accurate scheme. A good compromise between both extremes is provided by High-Resolution Schemes (HRSs). When represented in a Normalized Variable Diagram (NVD), several HRSs are piecewise-linear functions and can be defined using the Normalized Weighting Factor (NWF) approach [18]:

$$\tilde{\phi}_f = \alpha \tilde{\phi}_C + \beta \quad (3.20)$$

where the following definitions hold

$$\tilde{\phi}_f = \frac{\phi_f - \phi_U}{\phi_D - \phi_U} \quad (3.21a)$$

$$\tilde{\phi}_C = \frac{\phi_C - \phi_U}{\phi_D - \phi_U} \quad (3.21b)$$

In Eq. (3.20),  $\alpha$  and  $\beta$  are scalars specific to each HRS and they can be functions of  $\tilde{\phi}_C$ . Subscripts in Eqs. (3.21a,b) have the following meaning: for a given face, cell C is the cell from which the flux comes (upstream), cell D (downstream) is the cell to which the flux goes and cell U (far-upstream) is the cell upstream to cell C. In a general unstructured mesh, cell U cannot be identified unequivocally, and  $\phi_U$  in Eqs. (3.21a,b) can be evaluated as [19]

$$\phi_U = \phi_D - 2(\nabla \phi)_C \cdot \mathbf{d}_{CD} \quad (3.22)$$

where  $\mathbf{d}_{CD}$  is the vector connecting the center of cells C and D. For a deferred correction implementation of HRSs, the upwind part of the HRS is discretized implicitly, while the remaining (difference between the HRS and the upwind differencing scheme) is discretized explicitly (cf. Ref. [2]), which, using Eqs. (3.20-3.22), results in

$$\phi_f = [\phi_C]_{\text{implicit}} + [(\alpha - 1)\phi_C + \beta\phi_D + (1 - \alpha - \beta)(\phi_D - 2(\nabla \phi)_C \cdot \mathbf{d}_{CD})]_{\text{explicit}} \quad (3.23)$$

Handling the HRSs in a deferred correction approach avoids, in some cases, numerical instabilities introduced by the central-differencing component of the

HRS. Additionally, in Ref. [2] it was observed that the usual methodology of OpenFOAM® to apply HRSs to non-scalar variables (tensors and vectors) can locally introduce numerical instabilities in some viscoelastic flow problems. This methodology consists in using a frame-invariant quantity for non-scalar variables, such as the squared magnitude for vectors, or the trace (or double-dot product) for tensors, to compute the  $\alpha$  and  $\beta$  parameters in Eq. (3.23). It was observed that such artificial instabilities can be significantly damped with a component-wise handling of non-scalar variables [2], at the cost of losing frame-invariance, which however is very weak and vanishes with grid refinement. Accordingly, non-scalar variables are split into its components and Eq. (3.23) is applied independently to each one of them. Note that this approach still generates one single matrix of coefficients for such variables, since the upwind differencing scheme coefficients are common to all the components (they only depend on the flux). The differentiation between components is only introduced in the explicit part of Eq. (3.23), generating a different source term for each individual tensor/vector component. This is possible due to the use of a deferred correction approach.

### 3.5 Moving grids

Some CFD problems require the simulation of a moving entity interacting with a fluid. There are several approaches than can be used to tackle such problems, and the choice is usually made based on a case-by-case analysis. Consider for example the flow induced inside a sphere due to its time-dependent rotation. Such case can be easily handled by defining adequate boundary conditions for the flow variables on the sphere surface, without further modifications of the usual solver setup. On the other hand, if we consider the time-dependent simulation of the flow inside an axisymmetric stirred tank reactor, such approach is no longer adequate. Instead, we can use, for example, a (rotating) non-inertial reference frame, which allows to keep the mesh steady and introduces some acceleration terms in the momentum equation (OpenFOAM® allows the use of such non-inertial reference frames). However, if the tank is not axisymmetric, the non-inertial reference frame becomes useless and a different approach is needed. An immersed boundary method can be used for that purpose, avoiding the use of moving grids. However, we will turn our attention to moving meshes, i.e. a computational mesh whose control volumes move in space over time.

For moving control volumes, the equations governing the flow need to be changed regarding convective terms, which should account for the grid motion [20],

$$\int_S \phi(\mathbf{u} - \mathbf{u}_b) \cdot \mathbf{n} dS = \sum_f \phi_f (\mathbf{u}_f - \mathbf{u}_{b,f}) \cdot \mathbf{S}_f \quad (3.24)$$

where  $\phi$  is any generic variable being advected and  $\mathbf{u}_b$  is the velocity at which surface  $S$  is moving. Moreover, the space conservation law (SCL) needs to be satisfied to ensure mass conservation [20],

$$\frac{d}{dt} \int_V dV - \int_S \mathbf{u}_b \cdot \mathbf{n} dS = 0 \quad (3.25)$$

If the SCL is ensured, the continuity equation remains unchanged and so does the pressure equation. In practice, the SCL is imposed while computing  $\int_S \mathbf{u}_b \cdot \mathbf{n} dS$  in Eq. (3.24), which is the flux due to mesh motion. According to Eq. (3.25), the form taken by this term involving the volume swept by the moving faces at different times depends on the discretization scheme of time-derivatives. More details can be found in [20].

In addition to changing the position of its control volumes, the mesh can also change its topology if cells are removed or added. This is at the basis of automatic mesh refinement (AMR), frequently used to locally (un)refine the mesh at particular regions of interest (e.g. zones where the gradient of a given variable is high). The introduction/removal of cells in the mesh requires defining the fields and their fluxes in the newly generated cells/faces, which is based on a interpolation procedure that uses the values in the neighboring cells.

## 3.6 Segregated vs coupled solvers

The governing equations in an implicit CFD code can be solved either segregated or coupled. In a segregated solution method, the equations are solved sequentially, one at a time (equations for multidimensional variables are further split into components). This is the standard method used in OpenFOAM® and in most CFD codes based on finite-volumes. In a coupled solution method, all the governing equations are solved simultaneously. There are also semi-coupled solvers, which lie somewhere between segregated and coupled solvers. In a semi-coupled solver, part of the equations are solved coupled and part are solved segregated.

The segregated solution method has been and continues being a popular strategy for its low computational cost *per* time-step and low memory usage, compared to the coupled solution method. Nonetheless, they are less stable than coupled solvers, usually requiring lower time-steps and/or more under-relaxation in order to avoid numerical divergence. Thus, the higher usage of resources by coupled solvers is sometimes compensated by its enhanced stability, which translates in a lower total time of computation. Moreover, due to its higher implicitness, coupled solvers can be also more accurate in transient flow simulations [5].

In [5] we discussed the implementation of coupled and semi-coupled solvers in *rheoTool*, in the context of electrically-driven flows. Semi-coupled solvers proved to be faster and more accurate (time accuracy) than segregated solvers in a number of situations. Similar advantages could be also observed in pressure-driven flows.

## 3.7 Electrically-driven flow models

Consider now that the fluid under analysis is a weak electrolyte subjected to an electric field. In such conditions, the momentum equation (Eq. 3.2) should include the contribution from an electric body-force,

$$\mathbf{f} = \mathbf{f}_E = \nabla \cdot \left[ \varepsilon \left( \mathbf{E} \mathbf{E} - \frac{\|\mathbf{E}\|^2}{2} \mathbf{I} \right) \right] = \rho_E \mathbf{E} - \frac{\|\mathbf{E}\|^2}{2} \nabla \varepsilon \quad (3.26)$$

where  $\mathbf{E}$  is the electric field,  $\varepsilon = \varepsilon_0 \varepsilon_R$  is the electric permittivity and  $\rho_E$  is the charge density (per unit volume). In order to close the system of equations for electrically-driven flows (EDFs), additional relations must be provided to compute the terms in Eq. (3.26). Some options, the ones available in *rheoTool*, are presented next. Note that when referring generically to EDFs, we do not exclude the possibility of having any other external forcing (for example due to an imposed pressure difference), in addition to the electric forcing. When only an electric forcing exists, we call this flow as pure EDF.

The second term of Eq. (3.26) is only non-zero for a system of two fluids, each having a different electric permittivity.

### 3.7.1 Poisson-Nernst-Planck model

In the absence of magnetic effects, the electric potential ( $\Psi$ ) can be computed by Gauss' law

$$\nabla \cdot (\varepsilon \nabla \Psi) = -\rho_E \quad (3.27)$$

where the electric field is  $\mathbf{E} = -\nabla \Psi$  in electrostatics. By definition, the charge density is

$$\rho_E = F \sum_{i=1}^N z_i c_i \quad (3.28)$$

where  $F$  is Faraday's constant,  $z_i$  is the charge valence of specie  $i$  and  $c_i$  is the concentration of specie  $i$  (mol/m<sup>3</sup>). The sum is over the  $N$  charged species in the electrolyte. The standard law governing the transport of charged species in a weak electrolyte, under the action of an electric field and neglecting any reaction, is embodied by the Nernst-Planck equation,

$$\frac{dc_i}{dt} + \mathbf{u} \cdot \nabla c_i = \nabla \cdot (D_i \nabla c_i) + \nabla \cdot \left[ \underbrace{\left( D_i \frac{e z_i}{k T} \nabla \Psi \right)}_{\mathbf{u}_{M,i}} c_i \right] \quad (3.29)$$

which closes the system of equations for an EDF. In Eq. (3.29),  $D$  is the diffusion coefficient,  $e$  is the elementary charge,  $k$  is Boltzmann's constant and  $T$  is the absolute temperature. The last term of Eq. (3.29), representing the transport of charged species due to an electric field, can be though as a standard convective term driven by an electromigration velocity ( $\mathbf{u}_{M,i}$ ). However, it may also be considered as the Laplacian operator applied to field  $\Psi$ , with a space and time varying diffusion coefficient,  $D_i \frac{e z_i}{k T} c_i$  (this last approach is used in *rheoTool* for discretization purposes).

The so-called Poisson-Nernst-Planck model (henceforth PNP model) is constituted by Eqs. (3.27)-(3.29) and, coupled with the continuity and momentum equations, is applicable to a wide range of EDFs. However, the coexistence of different scales of time and length in EDFs may originate a stiff system of equations when the PNP model is used. As such, several simplified models can be derived to

mitigate these numerical issues, as described next. Note that the PNP model does not take into account molecular crowding effects (e.g., the number of ions near a surface may grow unbounded), so care must be taken when using it to simulate electrolytes of mild to high ionic strength.

In the PNP model, the electric-related unknowns are  $c_i$  and  $\Psi$ . Due to the convective term in Eq. (3.29), there is a two-way coupling between the PNP and the momentum equations.

### 3.7.2 Splitting the electric potential

Before proceeding to the derivation of other EDF models, we introduce here a useful approach to simulate EDF problems. In the PNP model, a single electric potential variable has been used,  $\Psi$ . However, in certain situations this can pose some difficulties when defining the boundary conditions to solve the Poisson equation. A common approach to avoid such issues is the decomposition of the electric potential in two variables: the externally imposed electric potential,  $\phi_{\text{Ext}}$ , and the intrinsic electric potential,  $\psi$ , such that  $\Psi = \phi_{\text{Ext}} + \psi$  [3]. Following this approach, Gauss' law is also decomposed in two equations,

$$\nabla \cdot (\varepsilon \nabla \phi_{\text{Ext}}) = 0 \quad (3.30a)$$

$$\nabla \cdot (\varepsilon \nabla \psi) = -\rho_E \quad (3.30b)$$

An additional simplification which can be used simultaneously with the splitting approach is to consider  $\mathbf{f}_E = -\rho_E \nabla \phi_{\text{Ext}}$  in the momentum equation, i.e., the intrinsic electric potential contribution is ignored in the electric field definition. This can be justified by stating that this extra force not accounted for directly is balanced by a pressure gradient, which mutually cancel each other in the momentum equation [3], under the assumption that it would not affect the flow.

The splitting approach will be used in the derivation of the next two models.

### 3.7.3 Poisson-Boltzmann model

If we assume that the ions follow a Boltzmann equilibrium, then the PNP model can be simplified to the so-called Poisson-Boltzmann model (henceforth PB model), for which Gauss' law reads

$$\nabla \cdot (\varepsilon \nabla \psi) = -F \sum_{i=1}^N z_i c_{i,0} \exp\left(-\frac{e z_i}{kT} (\psi - \psi_0)\right) \quad (3.31)$$

with  $c_{i,0}$  being a reference concentration of specie  $i$ , where the intrinsic potential is  $\psi_0$ . Without loss of generality, we will assume that  $c_{i,0}$  is the bulk ionic concentration, where the intrinsic potential is  $\psi_0 = 0$ .

Note that the right hand side of Eq. (3.31) represents (minus) the charge density for the PB model. Thus, Eq. (3.31) provides the definition of Eq. (3.30b) for the PB model, under the splitting approach.

For this model, the only electric-related unknowns are the two electric potentials,  $\psi$  and  $\phi_{\text{Ext}}$ , computed from Eqs. (3.30a) and (3.31). Furthermore, as can be seen from Eq. (3.31), there is no influence of flow variables in the PB model (one-way coupling).

In order to increase the implicitness of Eq. (3.31), its source term can be linearized by expansion in Taylor series up to the first-derivative, transforming the equation into

$$\nabla \cdot (\varepsilon \nabla \psi) + \psi F \sum_{i=1}^N (a_i b_i)^* = -F \sum_{i=1}^N (a_i)^* + \psi^* F \sum_{i=1}^N (a_i b_i)^* \quad (3.32)$$

with  $b_i = -\frac{ez_i}{kT}$  and  $a_i = z_i c_{i,0} \exp(b_i \psi)$ . All the terms of Eq. (3.32) with a star are evaluated explicitly.

### 3.7.4 Debye-Hückel model

Considering the PB model, if we further simplify Eq. (3.31) assuming low electric potentials,  $\frac{ez_i}{kT} \psi \ll 1$ , then

$$\nabla \cdot (\varepsilon \nabla \psi) = -F \sum_{i=1}^N z_i c_{i,0} \left( 1 - \frac{ez_i}{kT} \psi \right) \quad (3.33)$$

which is the equation governing the electric potential distribution in the so-called Debye-Hückel model (henceforth DH model).

As for the PB model, the only electric-related unknowns are the two electric potentials,  $\psi$  and  $\phi_{\text{Ext}}$ , computed from Eqs. (3.30a) and (3.33). Also, there is no influence of flow variables in the DH model (one-way coupling).

### 3.7.5 Slip model

A common characteristic of electrokinetic problems is the spontaneous formation of an electric double layer (EDL) near a charged surface, upon contact with an electrolyte. The thickness of the EDL can be approximated by the Debye length ( $\lambda_D$ ), a physical parameter appearing when solving the Poisson equation for the electric potential,

$$\lambda_D = \sqrt{\frac{\varepsilon kT}{Fe \sum_{i=1}^N z_i^2 c_{i,0}}} \quad (3.34)$$

In several practical applications, the charge density is mainly located in the EDL region, while the bulk electrolyte is neutral. If the Debye length is much smaller than the characteristic dimension of the system ( $\frac{\lambda_D}{W} \ll 1$ ) and assuming a smooth, laminar flow inside the EDL, then it is possible to approximate the EDL effect by a slip velocity at the surface, avoiding the need to solve the flow inside the EDL. Such a case would be, for example, the pumping of a Newtonian electrolyte ( $\lambda_D \sim \mathcal{O}(10^{-9} \text{ m})$ ) in a microchannel of arbitrary shape ( $W \sim \mathcal{O}(10^{-6} \text{ m})$ ), by

electroosmosis, at low voltage ( $\frac{ez}{kT}\psi \ll 1$ ) – the last conditions is usually relaxed. The Helmholtz-Smoluchowski theory is frequently used to approximate the slip velocity in such conditions,

$$\mathbf{u}_{\text{Sch}} = \mu \mathbf{E} \quad (3.35)$$

where  $\mu = -\frac{\varepsilon\zeta}{\eta_0}$  is the electroosmotic mobility ( $\zeta$  is usually the surface zeta-potential). Thus, when Eq. (3.35) is used as a boundary condition for velocity in the momentum equation, both the electroosmotic mobility and the electric field at the surface must be known. The electroosmotic mobility is assumed to be known a priori – it can be a fixed value over all the surface or have a known distribution. On the other hand, the electric field on the surface must be computed, making use of the initial assumption that no free charge exists in the bulk electrolyte, thus  $\Psi = \phi_{\text{Ext}} + \psi = \phi_{\text{Ext}}$ , and

$$\nabla \cdot (\varepsilon \nabla \Psi) = 0 \quad (3.36)$$

When the slip model is used, the electric body-force is not included in the momentum equation – electric effects contribute uniquely via the slip boundary condition on the wall.

Note that slip models do not resolve any phenomena occurring in the EDL. Thus, this approach is highly inaccurate for some flows, even though the condition  $\frac{\lambda_D}{W} \ll 1$  is satisfied. For example, this kind of model is unable to predict the high values of shear-rate typically found in EDLs, which can trigger elastic instabilities for complex fluid flows [21] – using a slip model would simply retrieve a smooth flow in such cases.

### 3.7.6 Ohmic (leaky dielectric) model

The so-called Ohmic model [22] is particularly useful to simulate fluids of different conductivities, although a generalized Ohmic model has been recently proposed for different types of problems [23]. The model can be derived from the PNP equations, rewritten in terms of the conductivity and free-charge density, and assuming additionally instantaneous charge relaxation and electroneutrality [22]. The interested reader is directed to Ref. [22] for the full derivation of the Ohmic model. Here, only the final equations are presented. Furthermore, and contrarily to what was done for the previous models, we will restrict our analysis to a binary electrolyte, i.e., an electrolyte composed of only one positive and one negative species, with  $z_+ = -z_- = z$ , but no restrictions in the relation between  $D_+$  and  $D_-$ .

First, let's start defining the conductivity ( $\sigma$ ) and free-charge density ( $\rho_E$ ) for a binary electrolyte,

$$\sigma = \frac{F^2 z^2}{RT} (D_+ c_+ + D_- c_-) \quad (3.37)$$

$$\rho_E = Fz(c_+ - c_-) \quad (3.38)$$

where  $R$  is the universal gas constant. Imposing the conservation of each variable leads to (after the assumptions mentioned above; more details in Ref. [22])

$$\frac{\partial \sigma}{\partial t} + \mathbf{u} \cdot \nabla \sigma = D_{\text{eff}} \nabla^2 \sigma \quad (3.39)$$

$$\nabla \cdot (\sigma \nabla \Psi) = 0 \quad (3.40)$$

where the effective diffusivity is  $D_{\text{eff}} = \frac{2D_- D_+}{D_- + D_+}$ . The conductivity is transported through Eq. (3.39), while Eq. (3.40), derived from the conservation of charge-density (then simplified on the basis of electroneutrality), is actually used to compute the distribution of electric potential. The electric force entering the momentum equation assumes its standard form, taking into account that the charge density can be expressed as  $\rho_E = -\nabla \cdot (\varepsilon \nabla \Psi)$  from Gauss' law, then

$$\mathbf{f}_E = \rho_E \mathbf{E} = \nabla \cdot (\varepsilon \nabla \Psi) \nabla \Psi \quad (3.41)$$

In order to close the Ohmic model, the EDL effect is commonly represented by a slip velocity, which avoids detailing the flow inside the EDL using a very fine mesh. Since the zeta-potential of a surface depends generally on the ionic conductivity, a  $\sigma$ -dependent slip velocity is typically used [22], such as

$$\mathbf{u}_{\text{Sch}}(\sigma) = \mu_0 \left( \frac{\sigma}{\sigma_0} \right)^m \mathbf{E} \quad (3.42)$$

where  $\mu_0 = -\frac{\varepsilon \zeta_0}{\eta_0}$  is a reference electroosmotic mobility, at a reference conductivity ( $\sigma_0$ ), and  $m$  is an exponent governing the power-law dependence of the zeta-potential on the conductivity ( $m \in [-0.5, -0.3]$  is in agreement with several works, e.g. [22]). Note that  $\mathbf{E}$  in Eq. (3.42) is the electric potential at the surface where the slip velocity is computed.

## 3.8 Brownian dynamics simulations

In the previous Sections, polymeric fluid flows were addressed from a continuum mechanics perspective. In this Section, we zoom-in the scale of analysis, such that each polymer molecule is now modeled individually. We enter the kinetic theory domain, which lays somewhere between continuum mechanics and atomistic modeling. This means that even though each polymer molecule is simulated individually, we ignore atomic-size events. Moreover, the models discussed here and implemented in *rheoTool* neglect inter-molecular interactions, which is representative of dilute solutions. The interested reader is referred to [7] for a thorough discussion on the kinetic theory of polymers.

### 3.8.1 The bead-spring model

The most commonly used coarse-grained models to simulate polymer molecules are bead-spring and bead-rod models. Currently, only the bead-spring model is available in *rheoTool* (Fig. 3.1). According to this model, the molecules are

represented by a set of  $N$  beads connected by  $N_S = (N - 1)$  springs, for open chains, or  $N_S = N$  springs for closed chains. Each  $i$  bead owns a group denoted as  $\mathbf{g}_i$  that contains the index of all the beads to which it is directly connected to by springs. For chains without branches,  $\mathbf{g}_i$  has one (beads at the edges) or two elements, but more elements can be present for branched polymers, such as the ones depicted in Fig. 3.1. Note that each bead and spring in the chain aims to represent a group of atoms, and not an individual atom. In this guide, we use either  $|\mathbf{x}_{ij}| = |\mathbf{r}_j - \mathbf{r}_i|, j \in \mathbf{g}_i$ , or simply  $R_i$  to denote the length of all the springs associated with bead  $i$ .

Polymer molecules usually display a maximum contour length upon full-extension ( $L_{\max}$ ), which should be ideally reproduced by the numerical model. Therefore, each spring also has a maximum length,  $l = L_{\max}/N_S$ .

The minimum characteristic length featured in a spring is the so-called persistence length ( $\lambda_P$ ), below which the spring segments behave as rigid elements, with fixed orientation. The Kuhn step size, defined as  $b_k = 2\lambda_P$  is a measure commonly used in coarse-grained models, especially in bead-rod models, where it represents the fixed size of a single rod. For the physical representation of the springs to remain valid, a minimum number of Kuhn steps should be used to represent a (flexible) spring. The number of Kuhn steps per spring is denoted by  $N_{k,s} = l/b_k$  and is usually controlled by the choice of  $N$ .

In *rheoTool*, an individual molecule is represented by a set of beads and springs, and a group of molecules is composed by an ensemble of molecules sharing the same physical properties. Each simulation in *rheoTool* can handle simultaneously several groups of molecules (Fig. 3.1).

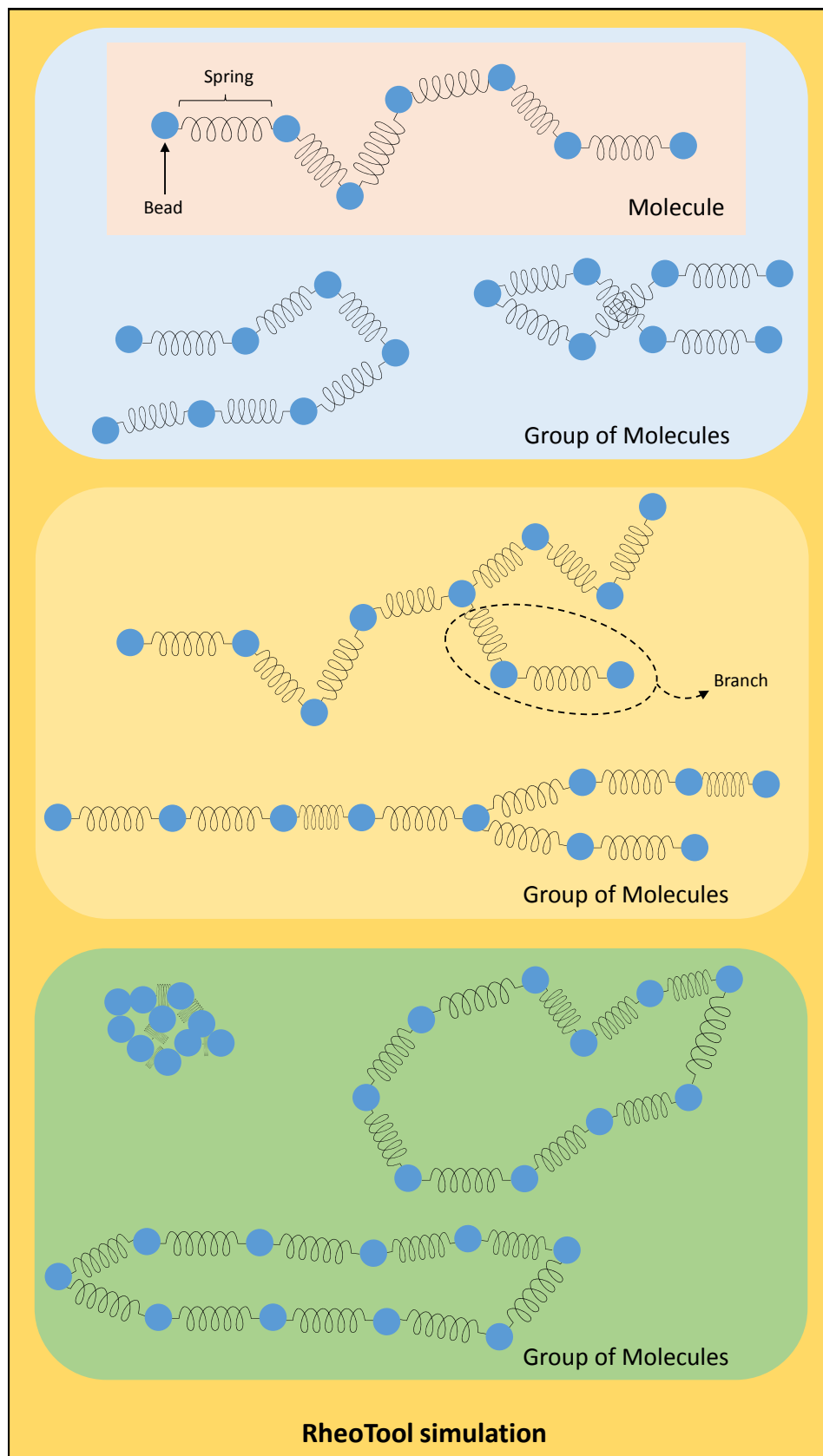


**Figure 3.1:** Polymer molecules representation by a bead-spring model. The organization levels used in *rheoTool* are also represented: beads and springs, molecules and groups of molecules.

### 3.8.2 Governing equations of beads motion

Consider a chain with an arbitrary topology, composed by  $N$  beads. The time evolution of the position vector corresponding to each bead ( $\mathbf{r}_i$ ) is governed by [24, 25]

$$\frac{\partial \mathbf{r}_i}{\partial t} = \mathbf{u}_f + \sum_{j=1}^N \frac{\partial \mathbf{D}_{ij}}{\partial \mathbf{r}_j} + \sum_{j=1}^N \frac{\mathbf{D}_{ij} \mathbf{F}_j}{kT} + \left( \frac{6}{\Delta t} \right)^{0.5} \sum_{j=1}^i \boldsymbol{\sigma}_{ij} \mathbf{n}_j \quad (3.43)$$

where  $\mathbf{u}_f$  is a velocity imposed by an external forcing,  $\mathbf{D}_{ij}$  is the diffusion tensor,  $k$  is Boltzmann's constant,  $T$  is the absolute temperature,  $\mathbf{F}_j$  is the sum of spring and exclusion volume (EV) forces ( $\mathbf{F}_j = \mathbf{F}_j^S + \mathbf{F}_j^{EV}$ ),  $\Delta t$  is the discrete time-step,  $\boldsymbol{\sigma}$  is a tensor satisfying  $\mathbf{D} = \boldsymbol{\sigma} \boldsymbol{\sigma}^T$  and  $\mathbf{n}_j$  is a vector whose 3 components are random numbers uniformly distributed in the range  $[-1; 1]$ .

$\mathbf{D}$  and  $\boldsymbol{\sigma}$  are  $(N \times N)$  symmetric tensors, whose  $ij$  elements are themselves  $(3 \times 3)$  tensors. The single model available in *rheoTool* to represent the diffusion tensor is the Rotne–Prager–Yamakawa (RPY) model [4],

$$\mathbf{D}_{ij} = \begin{cases} \frac{kT}{6\pi\eta a} \mathbf{I} = D\mathbf{I}, & i = j \\ \frac{3D}{4} \frac{a}{|\mathbf{x}_{ij}|} \left[ \left( 1 + \frac{2a^2}{3|\mathbf{x}_{ij}|^2} \right) \mathbf{I} + \left( 1 - \frac{2a^2}{|\mathbf{x}_{ij}|^2} \right) \frac{\mathbf{x}_{ij}\mathbf{x}_{ij}}{|\mathbf{x}_{ij}|^2} \right], & i \neq j \wedge |\mathbf{x}_{ij}| \geq 2a \\ D \left[ \left( 1 - \frac{9|\mathbf{x}_{ij}|}{32a} \right) \mathbf{I} + \frac{3}{32a} \frac{\mathbf{x}_{ij}\mathbf{x}_{ij}}{|\mathbf{x}_{ij}|} \right], & i \neq j \wedge |\mathbf{x}_{ij}| < 2a \end{cases} \quad (3.44)$$

where  $|\mathbf{x}_{ij}| = |\mathbf{r}_j - \mathbf{r}_i|$ ,  $\eta$  is the fluid viscosity,  $a$  is the bead radius and  $\mathbf{I}$  is the unit tensor  $(3 \times 3)$ . Note that in *rheoTool*,  $a$  and  $D$  are defined independently by the user and need not to be related. For the RPY tensor,  $\frac{\partial \mathbf{D}_{ij}}{\partial \mathbf{r}_j} = \mathbf{0}$  in Eq. (3.43). The decomposition of  $\mathbf{D}$ , a symmetric tensor, to obtain  $\boldsymbol{\sigma}$  is currently performed by a Cholesky decomposition, whereby  $\boldsymbol{\sigma}$  results in a lower triangular tensor (matrix).

The free-draining approach is sometimes assumed in bead-spring models, which results from ignoring the beads disturbance in the continuum velocity field. In such situations, hydrodynamic interactions are neglected and all the off-diagonal tensor elements of tensor  $\mathbf{D}$  become zero. The diffusion becomes isotropic and can simply be defined by coefficient  $D$ . The summations in Eq. (3.43) reduce to a single element contribution ( $j = i$ ), and  $\boldsymbol{\sigma}_{ii} = \sqrt{D}\mathbf{I}$ .

The exclusion volume forces impose a repulsive potential between beads, which, however, does not avoid any possible crossover between beads or springs (there is also no collision between beads). The following exclusion volume force is used [25],

$$\mathbf{F}_i^{EV} = -\frac{9}{2} \frac{kT}{l} \frac{\nu^{EV}}{l^3} \left( \frac{3}{4\sqrt{\pi}} \right)^3 (2N_{k,s})^{9/2} \sum_{j=1}^N \exp \left( -\frac{9}{2} N_{k,s} \frac{|\mathbf{x}_{ij}|^2}{l^2} \right) \frac{\mathbf{x}_{ij}}{l} \quad (3.45)$$

where  $\nu^{EV}$  is the exclusion volume parameter.

### 3.8.3 Spring force models

Several models can be used to express the spring force acting on each bead. Firstly, one should distinguish between the models that limit the maximum spring length

and the models that do not impose any restriction on the spring length. Among the mostly used models, the Marko-Siggia, Cohen Padé and FENE models fall into the first category, while the Hookean model falls in the second one.

The Hookean model is arguably the simplest model representing a spring [24],

$$\mathbf{F}_i^S = \sum_{j \in \mathbf{g}_i}^N H \mathbf{x}_{ij} \quad (3.46)$$

where  $H = \frac{3kTN_{k,s}}{l^2}$ . As can be seen, the force is linearly proportional to the spring extension and both are unlimited (here  $l$  is simply a parameter, and not the effective limit of maximum spring extension). Although unphysical for high deformations, the Hookean model is at the basis of the closed-form UCM and Oldroyd-B constitutive equations used in continuum mechanics simulations, available in *rheoTool*. Some of the difficulties felt in the continuum simulations with these two models arise precisely due to the unlimited stretch of Hookean springs, which usually translate in unbounded stresses.

For the extension-limited models, we have [24]:

- Marko-Siggia model

$$\mathbf{F}_i^S = \sum_{j \in \mathbf{g}_i}^N \frac{2}{3} H l \left[ \frac{|\mathbf{x}_{ij}|}{l} - \frac{1}{4} + \frac{1}{4(1 - |\mathbf{x}_{ij}|/l)^2} \right] \frac{\mathbf{x}_{ij}}{|\mathbf{x}_{ij}|} \quad (3.47)$$

- Cohen Padé model

$$\mathbf{F}_i^S = \sum_{j \in \mathbf{g}_i}^N \frac{H}{3} \left[ \frac{3 - (|\mathbf{x}_{ij}|/l)^2}{1 - (|\mathbf{x}_{ij}|/l)^2} \right] \mathbf{x}_{ij} \quad (3.48)$$

- FENE model (Warner spring law)

$$\mathbf{F}_i^S = \sum_{j \in \mathbf{g}_i}^N H \frac{1}{1 - (|\mathbf{x}_{ij}|/l)^2} \mathbf{x}_{ij} \quad (3.49)$$

The relation between the spring force and the spring extension is non-linear in these three models, and all are singular for  $|\mathbf{x}_{ij}| = l$ , which represents an asymptote for the springs extension. For low spring extension, the three models closely approach the Hookean model. For high spring extension (close to the asymptote), both FENE and Cohen Padé models present sharper gradients of force than the Marko-Siggia model, which directly impacts the numerical stability of the time integration algorithm.

### 3.8.4 Time integration algorithm

The integration over time of Eq. (3.43) can be performed with explicit, semi-implicit or implicit methods, which differ essentially in numerical stability and

computational cost. Most of the methods suggested in the literature are first-order accurate in time, using Euler schemes to discretize the time derivative (higher-order methods are not effective due to the random nature of the Brownian term [26]).

The explicit first-order Euler method evolves the beads positions from the previous time-step ( $t$ ) to the new time-step ( $t + \Delta t$ ) as,

$$\mathbf{r}_i^{t+\Delta t} = \mathbf{r}_i^t + \Delta t \mathbf{B}_i^t \quad (3.50)$$

where  $\mathbf{B}_i^t$  represents the whole right hand side of Eq. (3.43) evaluated at the previous time-step. This integration scheme only requires the explicit evaluation of mathematical expressions, presenting a low computational cost per time-step. However, the numerical stability of the scheme is highly dependent on  $\Delta t$ , which should be kept sufficiently small. The numerical stability is evaluated by the capability of the method in respecting the constraint  $R_i \leq l$ , when bounded spring force models are used. In practice, the time-step that satisfies such constraint is relatively small, leading to the need of a very high number of iterations (time-steps) to simulate a given period of physical time. Therefore, the explicit time integration is seldom used.

In the semi-implicit scheme described in [4], the explicit Euler scheme (Eq. 3.50) is used while  $R_i < \alpha l$ , where  $0 < \alpha \leq 1$  is defined by the user, and is usually close to 1. Once this condition is violated, a two-steps computation is used:

$$\mathbf{r}_i^* = \mathbf{r}_i^t + \Delta t \left[ \mathbf{u}_f + \sum_{j=1, j \neq i}^N \frac{\mathbf{D}_{ij} \mathbf{F}_j^S}{kT} + \frac{\mathbf{D}_{ii} \mathbf{F}_i^{EV}}{kT} + \left( \frac{6}{\Delta t} \right)^{0.5} \sum_{j=1}^i \boldsymbol{\sigma}_{ij} \mathbf{n}_j \right]_t \quad (3.51)$$

$$\mathbf{r}_i^{t+\Delta t} = \mathbf{r}_i^* + \Delta t \left( \frac{\mathbf{D}_{ii} \mathbf{F}_i^s}{kT} \right)_{t+\Delta t} \quad (3.52)$$

In Eq. (3.51), the intermediate beads positions ( $\mathbf{r}^*$ ) are obtained explicitly from the contribution of drag, Brownian and exclusion volume forces, and also from the off-diagonal spring force terms. This results in a non-linear system of equations that can be solved, for example, with the iterative Newton-Raphson method. As discussed in [4], the Newton-Raphson method requires solving a linear system of equations in each iteration ( $k$ ),

$$\mathbf{J}^k \Delta \mathbf{r}^k = -\mathbf{f}^k \quad (3.53)$$

where  $\mathbf{f}^k$  is a vector function whose expression depends on the spring model,  $\mathbf{J}^k$  is the Jacobian of  $\mathbf{f}^k$  and  $\Delta \mathbf{r}^k$  is a vector representing the difference in the beads positions between the previous and the current iteration. Further details are given in Ref. [4]. The linear system of equations (3.53) can be solved using different methods.

# Chapter 4

## Overview of *rheoTool*

In the previous Chapter, the main theoretical points behind *rheoTool* were briefly discussed. This Chapter focus on the numerical implementation of the governing equations in the OpenFOAM® environment, providing an overview of the functionalities available in *rheoTool*.

### 4.1 The *constitutiveEquations* library

#### 4.1.1 Available GNF and viscoelastic models

The *constitutiveEquations* library is a main component of *rheoTool*, since it contains all the viscoelastic and GNF constitutive equations, which can be called from the solvers. It was derived from the *viscoelasticTransportModels* library [1]. However, instead of restricting the library to viscoelastic models, we also extend it to include GNF models, most of them already present in OpenFOAM®. This was done in order to allow accessing both classes of models from a single library, hence from a single solver.

Most of the models available in the *constitutiveEquations* library are displayed in Table 4.1, along with the respective expressions to be used in Eqs. (3.3), (3.4), (3.6) and (3.8). However, some models falling in special categories as elastoviscoelasticity and multispecies modeling, are presented in the text following the table, in order to provide a more detailed discussion about them.

**Table 4.1:** Available constitutive models in the *constitutiveEquations* library.

### GNF models

| Model                            | <sup>1</sup> TypeName  | $\eta_s(\dot{\gamma})$  |
|----------------------------------|------------------------|---|
| Newtonian                        | <i>Newtonian</i>       | $\eta$  |
| <sup>2</sup> (Bounded) Power-Law | <i>PowerLaw</i>        | $\max [\eta_{\min}, \min (\eta_{\max}, k \dot{\gamma}^{n-1})]$  |
| Carreau-Yasuda                   | <i>CarreauYasuda</i>   | $\eta_{\infty} + (\eta_0 - \eta_{\infty})[1 + (k\dot{\gamma})^a]^{\frac{n-1}{a}}$   |
| <sup>2</sup> Herschel-Bulkley    | <i>HerschelBulkley</i> | Bounded: $\min (\eta_0, \tau_0 \dot{\gamma}^{-1} + k \dot{\gamma}^{n-1})$<br><sup>3</sup> Papanastasiou reg.: $\min \left\{ \eta_0, \tau_0 \dot{\gamma}^{-1} [1 - \exp(-m\dot{\gamma})] + k \dot{\gamma}^{n-1} \right\}$  |
| <sup>2</sup> Casson              | <i>Casson</i>          | Bounded: $\max \left\{ \eta_{\min}, \min \left[ \eta_{\max}, \left( \sqrt{\eta_{\infty}} + \sqrt{\frac{\tau_0}{\dot{\gamma}}} \right)^2 \right] \right\}$<br>Papanastasiou reg.: $\left\{ \sqrt{\eta_{\infty}} + \sqrt{\frac{\tau_0}{\dot{\gamma}}} [1 - \exp(-\sqrt{m\dot{\gamma}})] \right\}^2$ |

<sup>1</sup> Corresponds to the name entry identifying the model in the source code.

<sup>2</sup> Special care is taken in these models to avoid division by zero when  $\dot{\gamma}$  is zero or very small and  $n - 1 < 0$ . For  $\dot{\gamma} < VSMALL$ , the value  $\dot{\gamma} = VSMALL$  is used in the computation of the shear viscosity ( $VSMALL = 10^{-300}$  for versions using double precision).

<sup>3</sup> The original Papanastasiou regularization does not include the artificial upper-bounding by  $\eta_0$ . However, this bounding is needed to avoid an infinite viscosity for  $\dot{\gamma} \rightarrow 0$  (e.g. startup of flow) and  $n < 1$ . The original Papanastasiou regularization is recovered for  $\eta_0 \rightarrow \infty$ . In practice,  $\eta_0$  should be low enough to avoid an infinite viscosity in quiescent conditions and high enough to allow Papanastasiou regularization to take control in the remaining situations.

Notes:

- $\dot{\gamma} = \sqrt{\frac{\dot{\gamma} : \dot{\gamma}}{2}}$ , with  $\dot{\gamma} = \nabla \mathbf{u} + \nabla \mathbf{u}^T$ .
- $\mathbf{I}$  is the identity tensor and  $\frac{D}{Dt}(\phi) = \frac{\partial \phi}{\partial t} + \mathbf{u} \cdot \nabla \phi$  represents the material derivative of the generic variable  $\phi$ .
- $\overset{\nabla}{\tau} = \frac{\partial \tau}{\partial t} + \mathbf{u} \cdot \nabla \tau - \tau \cdot \nabla \mathbf{u} - \nabla \mathbf{u}^T \cdot \tau$  is the upper-convected derivative of  $\tau$ .
- $\overset{\square}{\tau} = \overset{\nabla}{\tau} + \zeta (\tau \cdot \mathbf{D} + \mathbf{D} \cdot \tau)$  is the Gordon-Schowalter derivative of  $\tau$ , with  $\mathbf{D} = \frac{1}{2}(\nabla \mathbf{u} + \nabla \mathbf{u}^T)$ .

Continuation of Table 4.1

Viscoelastic models solved in the standard extra-stress or conformation tensor variables

| Model                            | TypeName              | $\eta_s(\dot{\gamma})$ | $\eta_p(\dot{\gamma})$                           | $\lambda(\dot{\gamma})$                           | Constitutive Equation  |
|----------------------------------|-----------------------|------------------------|--|---|--|
| Oldroyd-B                        | <i>Oldroyd-B</i>      | $\eta_s$               | $\eta_p$   | $\lambda$   | $\boldsymbol{\tau} + \lambda \nabla \boldsymbol{\tau} = \eta_p (\nabla \mathbf{u} + \nabla \mathbf{u}^T)$  |
| WhiteMetzner<br>(Carreau-Yasuda) | <i>WhiteMetznerCY</i> | $\eta_s$               | $\eta_p [1 + (K\dot{\gamma})^a]^{\frac{n-1}{a}}$ | $\lambda [1 + (L\dot{\gamma})^b]^{\frac{m-1}{b}}$ | $\boldsymbol{\tau} + \lambda(\dot{\gamma}) \nabla \boldsymbol{\tau} = \eta_p(\dot{\gamma}) (\nabla \mathbf{u} + \nabla \mathbf{u}^T)$  |
| Giesekus                         | <i>Giesekus</i>       | $\eta_s$               | $\eta_p$   | $\lambda$   | $\boldsymbol{\tau} + \lambda \nabla \boldsymbol{\tau} + \alpha \frac{\lambda}{\eta_p} (\boldsymbol{\tau} \cdot \boldsymbol{\tau}) = \eta_p (\nabla \mathbf{u} + \nabla \mathbf{u}^T)$  |
| PTT linear                       | <i>PTTlinear</i>      | $\eta_s$               | $\eta_p$   | $\lambda$   | $\left[ 1 + \frac{\varepsilon \lambda}{\eta_p} \text{tr}(\boldsymbol{\tau}) \right] \boldsymbol{\tau} + \lambda \square \boldsymbol{\tau} = \eta_p (\nabla \mathbf{u} + \nabla \mathbf{u}^T)$  |
| PTT exponential                  | <i>PTTexp</i>         | $\eta_s$               | $\eta_p$   | $\lambda$   | $\left[ e^{\frac{\varepsilon \lambda}{\eta_p} \text{tr}(\boldsymbol{\tau})} \right] \boldsymbol{\tau} + \lambda \square \boldsymbol{\tau} = \eta_p (\nabla \mathbf{u} + \nabla \mathbf{u}^T)$  |
| FENE-CR                          | <i>FENE-CR</i>        | $\eta_s$               | $\eta_p$   | $\lambda$   | $\left[ 1 + \lambda \frac{D}{Dt} \left( \frac{1}{f} \right) \right] \boldsymbol{\tau} + \frac{\lambda}{f} \nabla \boldsymbol{\tau} = \eta_p (\nabla \mathbf{u} + \nabla \mathbf{u}^T)$<br>where $f = \frac{L^2 + \frac{\lambda}{\eta_p} \text{tr}(\boldsymbol{\tau})}{L^2 - 3}$  |
| FENE-P                           | <i>FENE-P</i>         | $\eta_s$               | $\eta_p$   | $\lambda$   | $\boldsymbol{\tau} + \frac{\lambda}{f} \nabla \boldsymbol{\tau} = \frac{a \eta_p}{f} (\nabla \mathbf{u} + \nabla \mathbf{u}^T) - \frac{D}{Dt} \left( \frac{1}{f} \right) [\lambda \boldsymbol{\tau} + a \eta_p \mathbf{I}]$<br>where $f = \frac{L^2 + \frac{\lambda}{a \eta_p} \text{tr}(\boldsymbol{\tau})}{L^2 - 3}$ and $a = \frac{L^2}{L^2 - 3}$   |
| <sup>3</sup> Rolie-Poly          | <i>Rolie-Poly</i>     | $\eta_s$               | $\eta_p$   | $\lambda_D$                                       | $\lambda_D \nabla \mathbf{A} = -(\mathbf{A} - \mathbf{I}) - 2k \frac{\lambda_D}{\lambda_R} \left( 1 - \sqrt{3/\text{tr}(\mathbf{A})} \right) \left[ \mathbf{A} + \beta \left( \frac{\text{tr}(\mathbf{A})}{3} \right)^{\delta} (\mathbf{A} - \mathbf{I}) \right]$<br>where $k = \frac{\left( 3 - \frac{\chi^2}{\chi_{\max}^2} \right) \left( 1 - \frac{1}{\chi_{\max}^2} \right)}{\left( 1 - \frac{\chi^2}{\chi_{\max}^2} \right) \left( 3 - \frac{1}{\chi_{\max}^2} \right)}$ and $\chi = \sqrt{\frac{\text{tr}(\mathbf{A})}{3}}$   |
| eXtended Pom-Pom                 | <i>XPomPom</i>        | $\eta_s$               | $\eta_p$   | $\lambda_B$                                       | $f \boldsymbol{\tau} + \lambda_B \nabla \boldsymbol{\tau} + \alpha \frac{\lambda_B}{\eta_p} (\boldsymbol{\tau} \cdot \boldsymbol{\tau}) + \frac{\eta_p}{\lambda_B} (f - 1) \mathbf{I} = \eta_p (\nabla \mathbf{u} + \nabla \mathbf{u}^T)$<br>where $f = 2 \frac{\lambda_B}{\lambda_S} e^{\frac{2}{q}(\Lambda-1)} \left( 1 - \frac{1}{\Lambda^{n+1}} \right) + \frac{1}{\Lambda^2} \left[ 1 - \frac{\alpha}{3} \frac{\text{tr}(\boldsymbol{\tau} \cdot \boldsymbol{\tau})}{(\eta_p / \lambda_B)^2} \right]$ and $\Lambda = \sqrt{1 + \frac{\text{tr}(\boldsymbol{\tau})}{3\eta_p / \lambda_B}}$ |

<sup>3</sup> See Ref. [27]. This model is exclusively solved in the conformation tensor variable, which is then converted to  $\boldsymbol{\tau}$  using,  $\boldsymbol{\tau} = \frac{\eta_p}{\lambda_D} k(\mathbf{A} - \mathbf{I})$ .

Continuation of Table 4.1

‡Viscoelastic models solved with the log-conformation approach

| Model   | TypeName                 | $\Theta \rightarrow \tau$  | <sup>4,5</sup> Constitutive Equation   |
|---|--------------------------|--|--|
| <sup>6</sup> Oldroyd-B                        | <i>Oldroyd-BLog</i>      | $\tau = \frac{\eta_p}{\lambda} (e^\Theta - \mathbf{I})$          | $\Upsilon = \frac{1}{\lambda} (e^{-\Theta} - \mathbf{I})$  |
| <sup>7</sup> WhiteMetzner<br>(Carreau-Yasuda) | <i>WhiteMetznerCYLog</i> | $\tau = \frac{\eta_p}{\lambda} (e^\Theta - \mathbf{I})$          | $\Upsilon = \frac{1}{\lambda(\dot{\gamma})} (e^{-\Theta} - \mathbf{I})$  |
| Giesekus                                      | <i>GiesekusLog</i>       | $\tau = \frac{\eta_p}{\lambda} (e^\Theta - \mathbf{I})$          | $\Upsilon = \frac{1}{\lambda} \left[ (e^{-\Theta} - \mathbf{I}) - \alpha e^\Theta (e^{-\Theta} - \mathbf{I})^2 \right]$  |
| PTT linear                                    | <i>PTTlinearLog</i>      | $\tau = \frac{\eta_p}{\lambda(1-\zeta)} (e^\Theta - \mathbf{I})$ | $\Upsilon = \frac{1}{\lambda} \left\{ 1 + \frac{\varepsilon}{1-\zeta} [\text{tr}(e^\Theta) - 3] \right\} (e^{-\Theta} - \mathbf{I})$   |
| PTT exponential                               | <i>PTTexpLog</i>         | $\tau = \frac{\eta_p}{\lambda(1-\zeta)} (e^\Theta - \mathbf{I})$ | $\Upsilon = \frac{1}{\lambda} e^{\frac{\varepsilon}{1-\zeta} (\text{tr}(e^\Theta) - 3)} (e^{-\Theta} - \mathbf{I})$  |
| FENE-CR                                       | <i>FENE-CRLog</i>        | $\tau = \frac{\eta_p f}{\lambda} (e^\Theta - \mathbf{I})$        | $\Upsilon = \frac{f}{\lambda} (e^{-\Theta} - \mathbf{I})$ , where $f = \frac{L^2}{L^2 - \text{tr}(e^\Theta)}$  |
| FENE-P  | <i>FENE-PLog</i>         | $\tau = \frac{\eta_p}{\lambda} (f e^\Theta - a \mathbf{I})$      | $\Upsilon = \frac{1}{\lambda} (a e^{-\Theta} - f \mathbf{I})$ , where $a = \frac{L^2}{L^2 - 3}$ and $f = \frac{L^2}{L^2 - \text{tr}(e^\Theta)}$  |
| <sup>8</sup> Rolie-Poly                       | <i>Rolie-PolyLog</i>     | $\tau = \frac{\eta_p}{\lambda_D} k (e^\Theta - \mathbf{I})$      | $\Upsilon = -\frac{1}{\lambda_D} e^{-\Theta} \left\{ (e^\Theta - \mathbf{I}) + 2k \frac{\lambda_D}{\lambda_R} \left( 1 - \sqrt{3/\text{tr}(e^\Theta)} \right) \left[ e^\Theta + \beta \left( \frac{\text{tr}(e^\Theta)}{3} \right)^\delta (e^\Theta - \mathbf{I}) \right] \right\}$  |
| eXtended Pom-Pom                              | <i>XPomPomLog</i>        | $\tau = \frac{\eta_p}{\lambda_B} (e^\Theta - \mathbf{I})$        | $\Upsilon = -\frac{1}{\lambda_B} e^{-\Theta} [(f - 2\alpha) e^\Theta + \alpha e^\Theta e^\Theta + (\alpha - 1) \mathbf{I}]$<br>where $f = 2 \frac{\lambda_B}{\lambda_S} e^{\frac{2}{q}(\Lambda-1)} \left( 1 - \frac{1}{\Lambda^{n+1}} \right) + \frac{1}{\Lambda^2} [1 - \alpha - \frac{\alpha}{3} \text{tr}(e^\Theta (e^\Theta - 2\mathbf{I}))]$ and $\Lambda = \sqrt{\frac{\text{tr}(e^\Theta)}{3}}$ |

‡ The solvent viscosity, the polymeric viscosity coefficient and the relaxation time for the models solved in variable  $\Theta$  are the same as those for the models solved in variable  $\tau$  or  $\mathbf{A}$ , in the previous page.

<sup>4</sup> For the shortness of notation, we have introduced the operator:  $\Upsilon = \frac{\partial \Theta}{\partial t} + \mathbf{u} \cdot \nabla \Theta - (\boldsymbol{\Omega} \Theta - \Theta \boldsymbol{\Omega}) - 2\mathbf{B}$ .

<sup>5</sup> The following equivalences hold true:  $e^\Theta = \mathbf{A} = \mathbf{R} \mathbf{A} \mathbf{R}^T$  and  $e^{-\Theta} = \mathbf{A}^{-1} = \mathbf{R} \mathbf{A}^{-1} \mathbf{R}^T$ .

<sup>6</sup> For this model, we also included the square-root conformation approach [15] (TypeName: *Oldroyd-BSqrt*) and the root<sup>k</sup> kernel approach [14] (TypeName: *Oldroyd-BRootk*), for demonstration purposes.

<sup>7</sup> This log-conformation tensor approach of the White-Metzner model is **only applicable when**  $\frac{\eta_p(\dot{\gamma})}{\lambda(\dot{\gamma})} = \frac{\eta_p}{\lambda}$  **is constant**, i.e., for  $K = L$ ,  $a = b$  and  $n = m$ . The version based on the extra-stress tensor variable is more general and does not have this restriction.

<sup>8</sup> The expression for  $k$  is the same as for the model solved in variable  $\mathbf{A}$ , in the previous page, considering that  $\mathbf{A} = e^\Theta$ .

In a footnote of Table 4.1, the (invariant) shear-rate used to compute shear-rate dependent variables was defined as

$$\dot{\gamma} = \sqrt{\frac{\dot{\gamma} : \dot{\gamma}}{2}} = \sqrt{2\mathbf{D} : \mathbf{D}}, \text{ with } \dot{\gamma} = \nabla \mathbf{u} + \nabla \mathbf{u}^T \text{ and } \mathbf{D} = \frac{1}{2}\dot{\gamma} \quad (4.1)$$

In the code, the shear-rate is returned by function *strainRate()* as

*strainRate() = sqrt(2.0)\*mag(symm(fvc::grad(U())))*

and it is equivalent to Eq. (4.1). Indeed,

$$\text{symm}(fvc::grad(U())) = \frac{1}{2}(\nabla \mathbf{u} + \nabla \mathbf{u}^T) = \frac{1}{2}\dot{\gamma} = \mathbf{D}$$

thus,

$$\text{sqrt}(2.0)*\text{mag}(\text{symm}(fvc::grad(U()))) = \sqrt{2}\sqrt{\frac{1}{2}\dot{\gamma} : \frac{1}{2}\dot{\gamma}} = \sqrt{\frac{\dot{\gamma} : \dot{\gamma}}{2}} = \sqrt{2\mathbf{D} : \mathbf{D}}$$

which is equal to Eq. (4.1) – the definitions of operators *symm()*, *mag()* and  $:$  (double contraction) can be found in the OpenFOAM® programmers' guide. Note that the invariant computed in Eq. (4.1) is actually the magnitude of the rate-of-strain tensor, which is usually called shear rate or strain rate for shear-dominated or extensional-dominated flows, respectively.

All the viscoelastic models presented in Table 4.1 can be solved in the standard extra-stress tensor  $\boldsymbol{\tau}$  (Eq. 3.4) or using the log-conformation approach (Eq. 3.8). The selection is made in dictionary **constitutiveProperties**, which should be located inside the folder **constant/** of the case (see more details in section 5.1.1). For the Oldroyd-B model, we provide two additional methods for demonstration purposes. One of them (TypeName: *Oldroyd-BSqrt*) consists in solving the constitutive equation using the square-root of the conformation tensor, according to Ref. [15]. The second approach (TypeName: *Oldroyd-BRootk*) allows to apply a general root<sup>k</sup> kernel, as described in Ref. [14]. Both can be used in 2D or 3D simulations, as any other model in the library. Since both models are only illustrative, their implementation and theory are not described in this guide, although both can be easily understood after a close inspection of the source code and taking as reference the literature cited for each one. Furthermore, tutorials for both methodologies are included in *rheoTool* (see the tutorial of Section 5.1.7).

## ❖ Other models:

### ⊕ VCM model (TypeName: *VCM*)

The Vasquez-Cook-McKinley (VCM) model [28] can be used to simulate worm-like micellar solutions, being able to predict the shear-banding behavior typically observed in these fluids. The model represents such fluids as a combination of large (subscript A) and small chain (subscript B) species that can convert into each other. A transport equation is solved for each species [28],

$$\frac{\partial n_A}{\partial t} + \mathbf{u} \cdot \nabla n_A = 2D_A \nabla^2 n_A + \frac{1}{2\lambda_A} c_B n_B^2 - \frac{c_A n_A}{\lambda_A} \quad (4.2)$$

$$\frac{\partial n_B}{\partial t} + \mathbf{u} \cdot \nabla n_B = 2D_B \nabla^2 n_B - \frac{c_B n_B^2}{\lambda_A} + 2\frac{c_A n_A}{\lambda_A} \quad (4.3)$$

where  $n$  is the dimensionless number density of the species,  $\lambda$  is the relaxation time,  $D$  is the diffusivity coefficient and  $c_A$  and  $c_B$  are, respectively, the dimensionless breakage and reformation rates, expressed as

$$c_A = c_{A_{\text{Eq}}} + \frac{\chi}{3} \left( \dot{\gamma} : \frac{\mathbf{A}}{n_A} \right) \quad (4.4)$$

$$c_B = c_{B_{\text{Eq}}} \quad (4.5)$$

In Eqs. (4.2) and (4.3), the double contraction term originally presented in [28] is not included, in order to simplify the definition of no-flux boundary conditions for  $n_A$  and  $n_B$  at impermeable walls (which reduce to a zero-gradient condition). The contribution of these omitted terms is typically negligible.

A constitutive equation is also solved for each species [28],

$$\lambda_A \frac{\nabla}{\nabla} \mathbf{A} + \mathbf{A} - n_A \mathbf{I} - \lambda_A D_A \nabla^2 \mathbf{A} = c_B n_B \mathbf{B} - c_A \mathbf{A} \quad (4.6)$$

$$\epsilon \lambda_A \frac{\nabla}{\nabla} \mathbf{B} + \mathbf{B} - \frac{n_B \mathbf{I}}{2} - \epsilon \lambda_A D_B \nabla^2 \mathbf{B} = -2\epsilon c_B n_B \mathbf{B} + 2\epsilon c_A \mathbf{A} \quad (4.7)$$

where  $\mathbf{A}$  and  $\mathbf{B}$  represent the conformation tensor of each species, and  $\epsilon = \frac{\lambda_B}{\lambda_A}$ . The contribution of each species to the polymeric extra-stress tensor is given by [28],

$$\boldsymbol{\tau} = G_0 [(\mathbf{A} + 2\mathbf{B}) - (n_A + n_B) \mathbf{I}] \quad (4.8)$$

where  $G_0$  is the elastic modulus. In the absence of flow,  $n_A = 1$ ,  $n_B = \sqrt{2 \frac{c_{A_{\text{Eq}}}}{c_{B_{\text{Eq}}}}}$ ,  $\mathbf{A} = \mathbf{I}$ ,  $\mathbf{B} = \frac{n_B}{2} \mathbf{I}$  and  $\boldsymbol{\tau} = \mathbf{0}$ .

### ⊕ RRM (TypeName: *RRM*)

Also in the context of modeling the flow of wormlike micellar solutions, Dutta and Graham proposed recently the Reactive Rod Model (RRM), accounting for the formation/destruction of flow-induced structures [29]. In this model, micelles are approached by rods, whose orientation tensor,  $\mathbf{S}$ , evolves according to [29],

$$\frac{d\mathbf{S}}{dt} = -6D_r \left( \mathbf{S} - \frac{\mathbf{I}}{3} \right) + \nabla \mathbf{u}^T \cdot \mathbf{S} + \mathbf{S} \cdot \nabla \mathbf{u} - 2\nabla \mathbf{u}^T : < \mathbf{u} \mathbf{u} \mathbf{u} \mathbf{u} > \quad (4.9)$$

where

$$D_r = \frac{D_{r,0}}{L^{*3}} \left( \frac{\ln L^* + m}{m} \right) \quad (4.10)$$

is a time-varying diffusion coefficient (units are  $\text{s}^{-1}$ ),  $L^* = L/L_0$  is the time-varying rod length normalized by its initial value and  $m$  is the initial aspect ratio of the rods (see [29] for more details). In Eq. (4.9), the last term is approximated by [29]

$$\nabla \mathbf{u}^T : < \mathbf{u} \mathbf{u} \mathbf{u} \mathbf{u} > \approx \frac{1}{5} [\mathbf{S} \cdot \mathbf{D} + \mathbf{D} \cdot \mathbf{S} - \mathbf{S} \cdot \mathbf{S} \cdot \mathbf{D} - \mathbf{D} \cdot \mathbf{S} \cdot \mathbf{S} + 2\mathbf{S} \cdot \mathbf{D} \cdot \mathbf{S} + 3(\mathbf{S} : \mathbf{D})\mathbf{S}] \quad (4.11)$$

and  $\mathbf{D} = \frac{1}{2}(\nabla \mathbf{u} + \nabla \mathbf{u}^T)$  is the rate of deformation tensor. The variation of the normalized rod length is computed from [29]

$$\frac{dL^*}{dt} = \frac{\lambda_S D_{r,0}}{1 - \left(\frac{L^*}{\alpha + \beta/Pe}\right)^2} (1 - L^*) + k D_{r,0} \sqrt{\frac{3}{2} \hat{\mathbf{S}} : \hat{\mathbf{S}}} \quad (4.12)$$

where  $\lambda_S$ ,  $\alpha$ ,  $\beta$  and  $k$  are parameters of the model,  $\hat{\mathbf{S}} = \mathbf{S} - \frac{\mathbf{I}}{3}$  and  $Pe$  is a Péclet number computed locally,  $Pe = \frac{\dot{\gamma}}{D_{r,0}}$  ( $\dot{\gamma}$  is the strain-rate defined in Eq. 4.1). The extra-stress due to the rods is accounted for as [29]

$$\boldsymbol{\tau} = \frac{G_0}{L^*} \left[ 3 \left( \mathbf{S} - \frac{\mathbf{I}}{3} \right) + \frac{1}{2D_r} \nabla \mathbf{u}^T : < \mathbf{u} \mathbf{u} \mathbf{u} \mathbf{u} > \right] \quad (4.13)$$

where  $G_0$  is the elastic modulus. Note that due to the generic strain-rate definition used in the Péclet number, the strain-rate retrieved for a pure shear-flow corresponds effectively to the local shear-rate, but for a pure extensional flow, the strain-rate computed does not correspond to the extension rate (it differs by a constant, that can be incorporated in parameter  $\beta$  of Eq. 4.12). Those considerations are important when using *rheoTestFoam*. Other measures of the hydrodynamic stresses can be used in the Péclet number definition in order to generalize it for any flow.

#### ⊕ Bautista-Manero-Puig model (TypeName: *BMP* and *BMPLog*)

The Bautista-Manero-Puig (BMP) model is still another option to simulate worm-like micellar solutions [30]. This model can also predict thixotropy and it results from the combination between the UCM model and Fredrickson's kinetic equation [30].

The polymeric extra-stress tensor is evolved according to

$$\varphi G_0 \boldsymbol{\tau} + \overset{\nabla}{\boldsymbol{\tau}} = G_0 (\nabla \mathbf{u} + \nabla \mathbf{u}^T) \quad (4.14)$$

and Fredrickson's kinetic equation governing the structure parameter ( $\varphi$ ) is represented by

$$\frac{\partial \varphi}{\partial t} + \mathbf{u} \cdot \nabla \varphi = \frac{\varphi_0 - \varphi}{\lambda} + k (\varphi_\infty - \varphi) \boldsymbol{\tau} : \mathbf{D} \quad (4.15)$$

In Eqs. (4.14) and (4.15),  $\mathbf{D} = \frac{1}{2}(\nabla \mathbf{u} + \nabla \mathbf{u}^T)$ ,  $G_0$  is the instantaneous relaxation modulus,  $\varphi$  is the fluidity ( $\equiv \eta_P^{-1}$ ),  $\varphi_0$  is the zero shear-rate fluidity,  $\varphi_\infty$  is the infinite shear-rate fluidity,  $\lambda$  is the structural relaxation time and  $k$  is a kinetic constant for structure breaking down [30].

The model is also implemented within the log-conformation approach, taking a form similar to the log-transformed Oldroyd-B equation presented in Table 4.1, with  $\lambda^{-1}$  replaced by  $\varphi G_0$  and  $\eta_P$  replaced by  $\varphi^{-1}$ .

#### ⊕ Saramito's model (TypeName: *Saramito* and *SaramitoLog*)

Elastoviscoplastic fluids exhibit a solid-like behavior below the yield stress and they flow as viscoelastic fluids when the yield stress is exceeded. The stress-strain relation in each regime can assume several forms.

The model proposed by Saramito [31] attempts to merge the Herschel–Bulkley model for yield-stress fluids with the Oldroyd-B/PTT model for viscoelastic fluids. Accordingly, the resulting constitutive relation is given by

$$f(\boldsymbol{\tau})\eta_p \max\left(0, \frac{\bar{\sigma} - \tau_0}{k\bar{\sigma}^n}\right)^{\frac{1}{n}} \boldsymbol{\tau} + \lambda \overset{\square}{\boldsymbol{\tau}} = \eta_p (\nabla \mathbf{u} + \nabla \mathbf{u}^T) \quad (4.16)$$

where  $\tau_0$  is the yield stress,  $f(\boldsymbol{\tau}) = 1$  and  $\bar{\sigma} = II_{\boldsymbol{\tau}_D} = \sqrt{\frac{\boldsymbol{\tau}_D \cdot \boldsymbol{\tau}_D}{2}}$  is the second invariant of the deviatoric stress tensor,  $\boldsymbol{\tau}_D = \boldsymbol{\tau} - \frac{\text{tr}(\boldsymbol{\tau})}{N} \mathbf{I}$ . An elastic modulus can be defined,  $G = \frac{\eta_p}{\lambda}$ , which is often found in the literature in the description of this model. We remember that  $\overset{\square}{\boldsymbol{\tau}}$  represents the Gordon-Schowalter derivative defined as,  $\overset{\square}{\boldsymbol{\tau}} = \overset{\nabla}{\boldsymbol{\tau}} + \zeta (\boldsymbol{\tau} \cdot \mathbf{D} + \mathbf{D} \cdot \boldsymbol{\tau})$ , with  $\mathbf{D} = \frac{1}{2}(\nabla \mathbf{u} + \nabla \mathbf{u}^T)$ , which reduces to the upper-convected derivative for  $\zeta = 0$ .

For  $n = 1$  and  $k = \eta_p$ , Saramito's model degenerates into a previous model proposed by the same author [32], that merges the Bingham model with the Oldroyd-B or PTT models, depending on the form taken by  $f(\boldsymbol{\tau})$ :

$$f(\boldsymbol{\tau}) = \begin{cases} 1 & , \text{Oldroyd-B} \\ 1 + \frac{\varepsilon \lambda}{\eta_p} \text{tr}(\boldsymbol{\tau}) & , \text{linear PTT} \\ e^{\frac{\varepsilon \lambda}{\eta_p} \text{tr}(\boldsymbol{\tau})} & , \text{exponential PTT} \end{cases} \quad (4.17)$$

The four variants of the model are available in *rheoTool*, where both the Herschel–Bulkley and PTT variants can avoid the possible infinite Oldroyd-B elongational viscosity for  $Wi \geq 0.5$  in extensional flows of Oldroyd-B fluids. In addition, the four variants can also be solved with the log-conformation approach and the governing equation becomes

$$\frac{\partial \boldsymbol{\Theta}}{\partial t} + \mathbf{u} \cdot \nabla \boldsymbol{\Theta} - (\boldsymbol{\Omega} \boldsymbol{\Theta} - \boldsymbol{\Theta} \boldsymbol{\Omega}) - 2\mathbf{B} = \frac{g(\boldsymbol{\tau})}{\lambda} (e^{-\boldsymbol{\Theta}} - \mathbf{I}) \quad (4.18)$$

with

$$g(\boldsymbol{\tau}) = \begin{cases} \eta_p \max\left(0, \frac{\bar{\sigma} - \tau_0}{k\bar{\sigma}^n}\right)^{\frac{1}{n}} & , \text{Oldroyd-B–Herschel-Bulkley} \\ \max\left(0, \frac{\bar{\sigma} - \tau_0}{\bar{\sigma}}\right) & , \text{Oldroyd-B–Bingham} \\ \max\left(0, \frac{\bar{\sigma} - \tau_0}{\bar{\sigma}}\right) \left\{1 + \frac{\varepsilon}{1-\zeta} [\text{tr}(e^{\boldsymbol{\Theta}}) - 3]\right\} & , \text{lin. PTT–Bingham} \\ \max\left(0, \frac{\bar{\sigma} - \tau_0}{\bar{\sigma}}\right) e^{\frac{\varepsilon}{1-\zeta} (\text{tr}(e^{\boldsymbol{\Theta}}) - 3)} & , \text{exp. PTT–Bingham} \end{cases} \quad (4.19)$$

and the polymeric extra-stress tensor is recovered using  $\boldsymbol{\tau} = \frac{\eta_p}{\lambda(1-\zeta)} (e^{\boldsymbol{\Theta}} - \mathbf{I})$ .

### ⊕ ML-IKH model (TypeName: *ML-IKH*)

Elastoviscoplastic models can be rendered more complex (and realistic) once thixotropy is added to them. This is the case of the Multi-Lambda Isotropic Kinematic Hardening (MLK-IKH) model [33]. According to this model, the equation governing the polymeric extra-stress tensor is given by [33]

$$\max\left(0, 1 - \frac{\lambda k_y}{\bar{\sigma}}\right) \boldsymbol{\tau}_{\text{eff}} + \lambda \lambda_E \overset{\nabla}{\boldsymbol{\tau}} = \lambda \eta_p (\nabla \mathbf{u} + \nabla \mathbf{u}^T) \quad (4.20)$$

where  $\lambda_E$  is the viscoelastic relaxation time,  $\boldsymbol{\tau}_{\text{eff}} = \boldsymbol{\tau} - \boldsymbol{\kappa}_{\text{back}}$ , with  $\boldsymbol{\kappa}_{\text{back}} = k_h (\mathbf{A} + 2\mathbf{A}^2)$ , and  $\bar{\sigma} = II_{\boldsymbol{\tau}_{\text{eff}}^D} = \sqrt{\frac{\boldsymbol{\tau}_{\text{eff}}^D : \boldsymbol{\tau}_{\text{eff}}^D}{2}}$ , where  $\boldsymbol{\tau}_{\text{eff}}^D = \boldsymbol{\tau}_{\text{eff}} - \frac{\text{tr}(\boldsymbol{\tau}_{\text{eff}})}{N} \mathbf{I}$  ( $N$  is the number of dimensions of the problem). Eq. (4.20) closely resembles the governing equation for  $\boldsymbol{\tau}$  in Saramito's model (Eq. 4.16). Tensor  $\mathbf{A}$  is related with material hardening and its evolution follows [33]

$$\frac{\partial \mathbf{A}}{\partial t} + \mathbf{u} \cdot \nabla \mathbf{A} + \boldsymbol{\Omega} \cdot \mathbf{A} - \mathbf{A} \cdot \boldsymbol{\Omega} = \mathbf{D}_p \cdot \mathbf{A} + \mathbf{A} \cdot \mathbf{D}_p + \mathbf{D}_p - q d_p \mathbf{A} \quad (4.21)$$

where  $\boldsymbol{\Omega} = (\nabla \mathbf{u} - \nabla \mathbf{u}^T)/2$  is the vorticity tensor,  $d_p = \sqrt{\frac{\mathbf{D}_p : \mathbf{D}_p}{2}}$  and

$$\mathbf{D}_p = \begin{cases} \mathbf{0} & , \text{ if } \bar{\sigma} < \lambda k_y \\ \frac{(\bar{\sigma} - \lambda k_y)}{2\lambda\eta_p} \cdot \frac{\boldsymbol{\tau}_{\text{eff}}}{\bar{\sigma}} & , \text{ if } \bar{\sigma} \geq \lambda k_y \end{cases} \quad (4.22)$$

is the plastic component of the rate of deformation tensor. In the previous equations,  $\lambda$  is a structure parameter regulating the thixotropic behavior and is obtained from the multi-lambda model [33],

$$\lambda = \sum_{i=1}^M C_i \lambda_i \quad (4.23)$$

where each of the  $M$  modes of  $\lambda$  obeys

$$\frac{d\lambda_i}{dt} = D_i [-k_1 \phi^a \lambda_i^n + k_2 \phi^b (1 - \lambda_i) + k_3 (1 - \lambda_i)] \quad (4.24)$$

and  $\phi$  can be computed in two ways [33],

$$\phi = \begin{cases} \max(0, \bar{\sigma} - \lambda k_y) & , \text{ Stress-controlled form} \\ 2d_p & , \text{ Rate-controlled form} \end{cases} \quad (4.25)$$

The model implementation in *rheoTool* allows for arbitrary  $M$  modes, where lists  $C$  and  $D$  (size  $M$ ) should be provided as input by the user. Thus, the complete list of input parameters for this model is:  $\eta_p, C, D, a, n, b, k_1, k_2, k_3, k_y, k_h, q$  and  $\lambda_E$ , to which we should add the solvent viscosity ( $\eta_s$ ) and the fluid density ( $\rho$ ). If no initial conditions are provided for each  $\lambda_i$ , the solvers assume  $\lambda_{i,0} = 1$  by default.

As discussed in [33], the transformation of the ML-IKH model from its scalar version to the above tensorial version assumes some simplifications, which impose restrictions on the model applicability (see [33] for more details).

#### 4.1.2 A note on FENE-type models

The Finitely Extensible Non-linear Elastic (FENE) models were originally developed based on the representation of polymer molecules by elastic dumbbells [7]. In such analysis, the end-to-end vector for each molecule is naturally related with the conformation tensor, such that the constitutive equations for this family of models is frequently written and handled as a function of the conformation tensor. The polymeric contribution to the momentum equation is then accounted for by

transforming the conformation tensor ( $\mathbf{A}$ ) in the extra-stress tensor ( $\boldsymbol{\tau}$ ), using the relations in Table 4.1 (for the models expressed in the log-conformation approach, considering that  $e^\Theta = \mathbf{A}$ ). The same applies for the Roly-Polie model.

In order to write the constitutive equation for FENE-type models as a function of  $\boldsymbol{\tau}$ , some terms arise, which may compromise the numerical stability. Furthermore, the computational cost to evaluate the resulting expression is higher than for the original model. As such, some authors simplify the constitutive equation by neglecting certain terms [34]. For the FENE-CR and FENE-P models, the complete constitutive equation written as a function of  $\mathbf{A}$  and  $\boldsymbol{\tau}$  and the modified formulation in  $\boldsymbol{\tau}$  are:

- FENE-CR

- Complete in  $\mathbf{A}$ :

$$\lambda \overset{\nabla}{\mathbf{A}} = -f(\text{tr}(\mathbf{A}))(\mathbf{A} - \mathbf{I}), \text{ where } f(\text{tr}(\mathbf{A})) = \frac{L^2}{L^2 - \text{tr}(\mathbf{A})}$$

- Complete in  $\boldsymbol{\tau}$  (see Table 4.1):

$$\left[1 + \lambda \frac{D}{Dt} \left(\frac{1}{f}\right)\right] \boldsymbol{\tau} + \frac{\lambda}{f} \overset{\nabla}{\boldsymbol{\tau}} = \eta_p (\nabla \mathbf{u} + \nabla \mathbf{u}^T), \text{ where } f = \frac{L^2 + \frac{\lambda}{\eta_p} \text{tr}(\boldsymbol{\tau})}{L^2 - 3}$$

- Modified in  $\boldsymbol{\tau}$  (usually known as FENE-MCR):

$$\boldsymbol{\tau} + \frac{\lambda}{f} \overset{\nabla}{\boldsymbol{\tau}} = \eta_p (\nabla \mathbf{u} + \nabla \mathbf{u}^T), \text{ where } f = \frac{L^2 + \frac{\lambda}{\eta_p} \text{tr}(\boldsymbol{\tau})}{L^2 - 3}$$

- FENE-P

- Complete in  $\mathbf{A}$ :

$$\lambda \overset{\nabla}{\mathbf{A}} = -[f(\text{tr}(\mathbf{A}))\mathbf{A} - a\mathbf{I}], \text{ where } f(\text{tr}(\mathbf{A})) = \frac{L^2}{L^2 - \text{tr}(\mathbf{A})} \text{ and } a = \frac{L^2}{L^2 - 3}$$

- Complete in  $\boldsymbol{\tau}$  (see Table 4.1):

$$\boldsymbol{\tau} + \frac{\lambda}{f} \overset{\nabla}{\boldsymbol{\tau}} = \frac{a\eta_p}{f} (\nabla \mathbf{u} + \nabla \mathbf{u}^T) - \frac{D}{Dt} \left(\frac{1}{f}\right) [\lambda \boldsymbol{\tau} + a\eta_p \mathbf{I}], \text{ where } f = \frac{L^2 + \frac{\lambda}{a\eta_p} \text{tr}(\boldsymbol{\tau})}{L^2 - 3}$$

and  $a = \frac{L^2}{L^2 - 3}$

- Modified in  $\boldsymbol{\tau}$ :

$$\boldsymbol{\tau} + \frac{\lambda}{f} \overset{\nabla}{\boldsymbol{\tau}} = \frac{a\eta_p}{f} (\nabla \mathbf{u} + \nabla \mathbf{u}^T), \text{ where } f = \frac{L^2 + \frac{\lambda}{a\eta_p} \text{tr}(\boldsymbol{\tau})}{L^2 - 3} \text{ and } a = \frac{L^2}{L^2 - 3}$$

In *rheoTool*, all the formulations are available and can be used (see Section 5.1.1 to know how to select each one). The steady material functions evaluated for canonical flows are the same for all the formulations. However, this is not true when evaluating the transient material functions: the modified formulations have a different behavior comparing with the complete ones, which are themselves similar. For a generic flow, the complete formulations, either in  $\mathbf{A}$  or  $\boldsymbol{\tau}$ , should provide similar results, since they are mathematically equivalent. Due to discretization

errors and stability issues, this may not be true. Regarding the modified formulations, they are not expected to behave exactly as the complete ones, even in the limit of highly refined grids.

From our experience, we strongly recommend using the formulations written and solved as a function of  $\mathbf{A}$  for FENE-type models. Those are the most stable, the most accurate regarding the original theory presented in [7] and the ones for which there is direct correspondence with the models solved with the log-conformation approach, since those were derived from the constitutive equations written as a function of the conformation tensor. Note that the FENE-CR and FENE-P models available in the *viscoelasticTransportModels* library of *viscoelasticFluidFoam* [1] are expressed in the modified form presented above.

### 4.1.3 Multi-mode modeling

Similarly to the *viscoelasticTransportModels* library [1], the *constitutiveEquations* library also supports multi-mode modeling for viscoelastic models. In such cases, the total extra-stress tensor is the sum of the extra-stress tensor resulting from each  $k^{th}$  mode

$$\boldsymbol{\tau}' = \sum_{k=1}^N (\boldsymbol{\tau}^k + \boldsymbol{\tau}_s^k) \quad (4.26)$$

In practice, this is achieved by assembling and solving one constitutive equation for each  $k^{th}$  mode, that is, Eq. (3.3) – solvent contribution – and Eq. (3.4) or (3.8) – polymer contribution – are built and solved  $N$  times each time-step. A warning should be made at this point, since this approach is probably not the most conventional. Indeed,  $\boldsymbol{\tau}_s$  in Eq. (4.26) is commonly placed outside the summation symbol, since multiple modes are only assigned to the polymeric contribution. To achieve this in *rheoTool*, and considering the expression for  $\boldsymbol{\tau}_s$  in Eq. (3.3), **the user must split the "single-solvent viscosity" by the  $N$  modes considered**, in any way, such that this "single-solvent viscosity" is recovered summing all these  $N$  values in Eq. (4.26).

### 4.1.4 Analysis of a code sample

For the readers still initiating their journey in OpenFOAM®, we will explore in this section the implementation of the Oldroyd-B constitutive model, solved with the log-conformation tensor approach. This example will establish the link between part of the theory described in Chapter 3 and its implementation in the source code.

The source code displayed in Listing 4.1 is taken from file `src/libs/constitutiveEquations/constitutiveEqs/Oldroyd-B/Oldroyd-BLog/Oldroyd_BLog.C`. Let's analyze the most important lines:

- lines 1-91: this section initializes the variables used in the constitutive model. In terms of field variables, we have (lines 23-84): `tau_`( $\boldsymbol{\tau}$ ), `theta_`( $\Theta$ ), `eigVals_`( $\Lambda$ ) and `eigVecs_`( $\mathbf{R}$ ). All those fields must be defined by the user when

starting a simulation, except *eigVals\_* and *eigVecs\_*, which can be defined or not. If defined (typical of a restart from a previous simulation), they are used in the first time-step; otherwise, they are both initialized as the identity tensor/matrix, corresponding to a null extra-stress tensor ( $\boldsymbol{\tau}$ ). Afterwards, the fluid properties are read from a dictionary (lines 85-88), along with the stabilization method selected by the user (line 90): none, BSD or the stress-velocity coupling described in Section 3.3.2.

- lines **94-151**: this section implements the member function *correct()*, whose purpose is to update the polymeric extra-stress field, by evolving  $\Theta$  according to the constitutive equation. From line 96 to 105, variables  $\mathbf{M}$ ,  $\boldsymbol{\Omega}$  and  $\mathbf{B}$ , defined in Eqs. (3.9)–(3.11), are computed. The function *decomposeGradU()* is a member function of the base class *constitutiveEq* (find it in the file *constitutiveEq.C*), since it is used by all the models based on the log-conformation tensor approach. Then, in lines 107-140, the constitutive equation (Eq. 3.8) is built and solved, after which  $\Theta$  is diagonalized to compute its eigenvectors/eigenvalues (line 144). The function doing this task (*calcEig()*) is also a member function of the class *constitutiveEq* and the algorithm being used by default for that purpose is the QR method provided by the Eigen library [35]. Another method is also available, as discussed in Section 4.1.5. Note that the eigenvalues retrieved by function (*calcEig()*) are already **exponentiated**, so that they correspond to  $\Lambda = \exp(\Lambda^\Theta)$ . Finally, with the currently computed eigenvectors/eigenvalues, the polymeric extra-stress tensor ( $\boldsymbol{\tau}$ ) is recovered from the conformation tensor (line 148), according to the relation established in Eqs. (3.6) and (3.14) (check Table 4.1 for other models), and will be used in the *divTau()* function described below.
- in the *viscoelasticTransportModels* library [1] each model was in charge to define its own contribution to the momentum equation, i.e., the term  $(\nabla \cdot \boldsymbol{\tau}')$ . In the *constitutiveEquations* library there is a default definition of this term in the base class. In fact, the function *divTau()* is now defined in class *constitutiveEq* and can be found in file *constitutiveEq.C*, Listing 4.2. This function starts by distinguishing between GNF and viscoelastic models in line 7. For a GNF model (lines 8-14), the extra-stress contribution is  $\nabla \cdot \boldsymbol{\tau}' = \nabla \cdot \eta(\dot{\gamma}) \nabla \mathbf{u} + \nabla \mathbf{u} \cdot \nabla \eta(\dot{\gamma})$ , divided by the density to be compliant with the usual strategy of OpenFOAM® for single-phase, incompressible fluid flows. Note that the second term is included to account for a shear-rate dependent viscosity coefficient. By definition, a GNF fluid has no elasticity, thus  $\boldsymbol{\tau} = \mathbf{0}$ . For a viscoelastic fluid (lines 17-49), the output depends on the stabilization method selected (see function *checkForStab()* in *constitutiveEq.C* for the correspondence between indexes and the method): if *none*, there is no added stabilization and  $\nabla \cdot \boldsymbol{\tau} = \nabla \cdot \bar{\boldsymbol{\tau}} - \nabla \cdot \eta_s \nabla \mathbf{u}$ ; if *BSD*, then the both-sides-diffusion technique is used and  $\nabla \cdot \boldsymbol{\tau} = \nabla \cdot \bar{\boldsymbol{\tau}} - \nabla \cdot \eta_p \nabla \mathbf{u} + \nabla \cdot (\eta_s + \eta_p) \nabla \mathbf{u}$  (Eq. 3.5); otherwise (if *coupling*), the stress-velocity coupling technique of Eq. (3.17) is used and  $\nabla \cdot \boldsymbol{\tau} = \nabla \cdot \bar{\boldsymbol{\tau}} - \overline{\nabla \cdot \eta_p \nabla \mathbf{u}} + \nabla \cdot (\eta_s + \eta_p) \nabla \mathbf{u}$ . Note that using the *coupling* stabilization is the method recommended for most of the cases,

being the one used by default if no information is provided by the user. However, some cases may require the use of no stabilization, as for example the simulation of multimode models with  $\eta_P \gg \eta_S$  – the amount of artificial diffusion may mask the real phenomena in transient simulations. For the cases using stabilization, the explicit behavior effects on transient results can be minimized by performing inner iterations at each time-step, a subject discussed later in this guide (see Section 4.5.1). In file `constitutiveEq.C`, a function `divTauS()` is also included, which retrieves part of the extra-stress contribution to the momentum equation, when solving two-phase flows (this topic will be discussed later).

```

41         U.mesh(),
43             IOobject::MUST_READ,
44             IOobject::AUTO_WRITE
45         ),
46         U.mesh()
47     ),
48     eigVals_
49     (
50         IOobject
51         (
52             "eigVals" + name,
53             U.time().timeName(),
54             U.mesh(),
55             IOobject::READ_IF_PRESENT,
56             IOobject::AUTO_WRITE
57         ),
58         U.mesh(),
59         dimensionedTensor
60         (
61             "I",
62             dimless,
63             pTraits<tensor>::I
64         ),
65         zeroGradientFvPatchField<tensor>::typeName
66     ),
67     eigVecs_
68     (
69         IOobject
70         (
71             "eigVecs" + name,
72             U.time().timeName(),
73             U.mesh(),
74             IOobject::READ_IF_PRESENT,
75             IOobject::AUTO_WRITE
76         ),
77         U.mesh(),
78         dimensionedTensor
79         (
80             "I",
81             dimless,
82             pTraits<tensor>::I
83         ),
84         zeroGradientFvPatchField<tensor>::typeName
85     ),
86     rho_(dict.lookup("rho")),
87     etaS_(dict.lookup("etaS")),
88     etaP_(dict.lookup("etaP")),
89     lambda_(dict.lookup("lambda")),
90 {
91     checkForStab(dict);
92 }
93 // * * * * * * * * * * * * * * * * * * Member Functions * * * * *
94 // * * * * * //
95 void Foam::constitutiveEqs::Oldroyd_BLog::correct()

```

```

// Decompose grad(U).T()
97
98 volTensorField L = fvc::grad(U());
99
100 dimensionedScalar c1( "zero", dimensionSet(0, 0, -1, 0, 0, 0, 0),
101     0. );
102 volTensorField B = c1 * eigVecs_;
103 volTensorField omega = B;
104 volTensorField M = (eigVecs_.T() & L.T() & eigVecs_);
105
106 decomposeGradU(M, eigVals_, eigVecs_, omega, B);
107
108 // Solve the constitutive Eq in theta = log(c)
109
110 dimensionedTensor Itensor
111 (
112     "Identity",
113     dimensionSet(0, 0, 0, 0, 0, 0, 0),
114     tensor::I
115 );
116
117 fvSymmTensorMatrix thetaEqn
118 (
119     fvm::ddt(theta_)
120     + fvm::div(phi(), theta_)
121     ==
122     symm
123     (
124         (omega&theta_)
125         - (theta_&omega)
126         + 2.0 * B
127         + (1.0/lambda_)
128         *
129             (
130                 eigVecs_ &
131                 (
132                     inv(eigVals_)
133                     - Itensor
134                     )
135                 & eigVecs_.T()
136             )
137     )
138 );
139
140 thetaEqn.relax();
141 thetaEqn.solve();
142
143 // Diagonalization of theta
144
145 calcEig(theta_, eigVals_, eigVecs_);
146
147 // Convert from theta to tau
148
149 tau_ = (etaP_/lambda_) * symm( (eigVecs_ & eigVals_ & eigVecs_
150 .T()) - Itensor);

```

```
151 }  
    tau_.correctBoundaryConditions();
```

**Listing 4.1:** Source code for the *Oldroyd-BLog* constitutive model (Oldroyd\_BLog.C)

```
1 tmp<fvVectorMatrix> constitutiveEq::divTau  
(  
3     const volVectorField& U  
) const  
5 {  
  
7     if (isGNF())  
8     {  
9         return  
10        (  
11            fvm::laplacian( eta() / rho(), U, "laplacian(eta,U)"  
12            + (fvc::grad(U) & fvc::grad(eta() / rho()))  
13        );  
14    }  
15    else  
16    {  
17        if (stabMeth_ == 0) // none  
18        {  
19            return  
20            (  
21                fvc::div(tau() / rho(), "div(tau)")  
22                + fvm::laplacian(etaS() / rho(), U, "laplacian(eta,U")  
23            );  
24        }  
25        }  
26    else if (stabMeth_ == 1) // BSD  
27    {  
28        return  
29        (  
30            fvc::div(tau() / rho(), "div(tau)")  
31            - fvc::laplacian(etaP() / rho(), U, "laplacian(eta,U")  
32            + fvm::laplacian((etaP() + etaS()) / rho(), U, "laplacian(eta,U")  
33        );  
34    }  
35    }  
36    }  
37    else // coupling  
38    {  
  
40        return  
41        (  
42            fvc::div(tau() / rho(), "div(tau)")  
43            - (etaP() / rho()) * fvc::div(fvc::grad(U))  
44            + fvm::laplacian((etaP() + etaS()) / rho(), U, "laplacian(eta,U")  
45        );  
46    }
```

```

47         }
49     }
}

```

**Listing 4.2:** Source code of the virtual function *divTau()* defined in file *constitutiveEq.C*

### 4.1.5 Advanced settings

As aforementioned, the eigenvectors/eigenvalues used in the models based on the log-conformation approach are computed, by default, using the QR algorithm provided by the Eigen library [35]. However, there is also the possibility to use an iterative Jacobi method [36]. While both options offer good accuracy and stability, the QR algorithm was seen to be slightly faster and this is the reason of being the default option. Switching between either methods is not run time selectable, but hard-coded, instead. This can be controlled in member function *calcEig()* of class *constitutiveEq*, located in file *constitutiveEq.C*. The Jacobi method can be selected by uncommenting the currently commented block (*// Eigen decomposition using the iterative jacobi algorithm*) and commenting the block (*// Eigen decomposition using a QR algorithm of Eigen library*), i.e., all the remaining lines inside the function. The source code of *jacobi()* function is located in *utils/jacobi.H*. Note that, independently of which method is used in function *calcEig()*, this function will return the eigenvectors of the input tensor, and the **exponential** of the eigenvalues of the same tensor. After re-compiling the library with those modifications, all the log-conformation-based models will be affected by those changes.

### 4.1.6 Adding new viscoelastic or GNF models

For the users with minimal programming skills in OpenFOAM®, adding new viscoelastic or GNF models should be a straightforward task. The main steps are:

- copy-paste the folder of an existing model (that we will call template model) in directory *src/libs/constitutiveEquations/constitutiveEqs/* for viscoelastic models, or *src/libs/constitutiveEquations/constitutiveEqs/GNF/* for GNF models. Rename the folder and the files inside it (.C and .H files) with the new model's name. Remove the *.dep* file inside the folder, as well as the folder for the log-implementation (if not needed), in case of viscoelastic models.
- inside the source .C and header .H files, find-replace the old model's name by the new one (e.g. *Ctrl + H* in *gedit*). This is to change the name of the class, which is usually equal to the name given to the respective source file. However, it is a good idea to always check first the name given to the class of the template model.

- add the source code of the new model to the compilation list of the library. For that, edit file `src/libs/constitutiveEquations/Make/files` by adding the path for the source code (see the entries for the other models already there).
- make a first compilation of the new model, by running the script `Allwmake` in directory `src/`. Note that, until this point, the source code of the new model is the one from the original template model, where only the name of the class has been changed. Thus, the model should compile without errors. If not, something wrong occurred in the previous steps.
- the last step is to change the source code of the model in order to implement the desired constitutive equation. Typically, the changes will be in three main places: (i) the header file, where the new variables and parameters of the model have to be declared (delete the ones from the template model that are not needed); (ii) the constructor in the source file, where those new entries should be added and initialized (delete the ones not needed); (iii) function `correct()`, which is aimed to either update the viscosity (GNF) or the polymeric extra-stresses (viscoelastic model). Note that you may also need to define functions `divTau()` and `divTauS()` for your new model, if the ones defined and used by default in the base class (see `constitutiveEq.C`) are not adequate. After all the changes on the code had been completed, compile again by running script `Allwmake`.

If all the steps listed above were successfully executed, then the new model is now available to all the solvers of *rheoTool*. In order to use library *constitutiveEquations* in any solver other than the ones provided with *rheoTool*, the user should:

- add the header `#include "constitutiveModel.H"` to the main solver.
- create a *constitutiveModel* object by calling the constructor, with the correct arguments, for example: `constitutiveModel constEq(U, phi)`.
- add the library *constitutiveEquations* to the `Make/options`, and specify its path (check the `Make/options` of the solvers in *rheoTool* for an example).

## 4.2 The *EDFModels* library

### 4.2.1 Available EDF models

The list of runtime selectable EDF models is presented in Table 4.2.

**Table 4.2:** Available models for electrically-driven flows in the *EDFModels* library. The last column indicates the section in the user guide where the model has been described.

| Model                          | <sup>1</sup> TypeName   | <sup>2,3,4</sup> $\mathbf{f}_E$  | <sup>5</sup> Governing Equations  | Section       |
|--------------------------------|---|--|---|---------------|
| Poisson-Nernst-Planck<br>(PNP) | <sup>6</sup> <i>NernstPlanck</i><br><sup>6</sup> <i>NernstPlanckCoupled</i> | $- \left( F \sum_{i=1}^N z_i c_i \right) (\nabla \Psi - \mathbf{E}_a)$   | $\begin{cases} \nabla \cdot (\varepsilon \nabla \phi_{\text{Ext}}) = 0 \\ \nabla \cdot (\varepsilon \nabla \psi) = -F \sum_{i=1}^N z_i c_i \\ \frac{\partial c_i}{\partial t} + \mathbf{u} \cdot \nabla c_i = \nabla \cdot (D_i \nabla c_i) + \nabla \cdot \left[ (D_i \frac{e z_i}{kT} \nabla \Psi) c_i \right] \end{cases}$ | Section 3.7.1 |
| Poisson-Boltzmann<br>(PB)      | <i>PoissonBoltzmann</i>   | $\left[ -F \sum_{i=1}^N z_i c_{i,0} \exp(-\frac{e z_i}{kT} \psi) \right] (\nabla \Psi - \mathbf{E}_a)$             | $\begin{cases} \nabla \cdot (\varepsilon \nabla \phi_{\text{Ext}}) = 0 \\ \nabla \cdot (\varepsilon \nabla \psi) + \psi F \sum_{i=1}^N (a_i b_i)^* = -F \sum_{i=1}^N (a_i)^* + \psi^* F \sum_{i=1}^N (a_i b_i)^* \\ \text{with } b_i = -\frac{e z_i}{kT} \text{ and } a_i = z_i c_{i,0} \exp(b_i \psi) \end{cases}$           | Section 3.7.3 |
| Debye-Hückel<br>(DH)           | <i>DebyeHuckel</i>  | $\left[ -F \sum_{i=1}^N z_i c_{i,0} \left( 1 - \frac{e z_i}{kT} \psi \right) \right] (\nabla \Psi - \mathbf{E}_a)$ | $\begin{cases} \nabla \cdot (\varepsilon \nabla \phi_{\text{Ext}}) = 0 \\ \nabla \cdot (\varepsilon \nabla \psi) = -F \sum_{i=1}^N z_i c_{i,0} \left( 1 - \frac{e z_i}{kT} \psi \right) \end{cases}$  | Section 3.7.4 |
| Slip velocity                  | <i>slipSmoluchowski</i>   | $\mathbf{0}$   | $\nabla \cdot (\varepsilon \nabla \phi_{\text{Ext}}) = 0$   | Section 3.7.5 |
| Ohmic                          | <i>Ohmic</i>  | $[\nabla \cdot (\varepsilon \nabla \phi_{\text{Ext}})] (\nabla \phi_{\text{Ext}} - \mathbf{E}_a)$                  | $\begin{cases} \frac{\partial \sigma}{\partial t} + \mathbf{u} \cdot \nabla \sigma = D_{\text{eff}} \nabla^2 \sigma \\ \nabla \cdot (\sigma \nabla \phi_{\text{Ext}}) = 0 \end{cases}$  | Section 3.7.6 |

<sup>1</sup> Corresponds to the name entry identifying the model in the source code.

<sup>2</sup>  $\mathbf{f}_E$  is the electric body-force entering the momentum equation.

<sup>3</sup>  $\mathbf{E}_a$  is an optional argument - a single vector - representing a uniform electric field.

<sup>4</sup> When the splitting of potentials approach is selected for the PNP, PB and DH models, the user may choose to use  $(\nabla \phi_{\text{Ext}} - \mathbf{E}_a)$ , instead of  $(\nabla \Psi - \mathbf{E}_a)$ . Recall that the splitting of potentials is given by  $\Psi = \phi_{\text{Ext}} + \psi$  (cf. Section 3.7.2).

<sup>5</sup> For the PNP, PB and DH models, the equations are presented according to the splitting of potentials approach, which is optional. When a single electric potential is intended to be used, then replace  $\psi$  by  $\Psi$  and ignore the equations in terms of  $\phi_{\text{Ext}}$ .

<sup>6</sup> Both models solve the PNP equations, but *NernstPlanck* uses a segregated solver, whereas *NernstPlanckCoupled* solves the PNP equations in a fully-coupled way, which can be optionally coupled to the Navier-Stokes equations.

## 4.2.2 The potentials splitting approach and multi-species modeling in the PNP, PB and DH models

The possibility of splitting the electric potential into two variables, as described in Section 3.7.2, is available for the PNP, PB and DH models. When used, one Poisson equation for  $\psi$  and one Laplace equation for  $\phi_{\text{Ext}}$  are solved, as shown in Table 4.2. In practice, the choice between using one or two potentials is achieved in the following way: if only one potential ( $\text{psi} \Leftrightarrow \Psi$ ) is present in the starting-time folder, then it is assumed than a unique potential is to be used, while if two potentials ( $\text{phiE} \Leftrightarrow \phi_{\text{Ext}}$  and  $\text{psi} \Leftrightarrow \psi$ ) are defined, then the splitting approach is assumed. Under the splitting approach, the user still has the option to include or not the contribution of the intrinsic potential in the electric field definition of the body-force entering the momentum equation. The choice is through the variable *psiContrib*, which should be defined in a dictionary, as explained later in Section 5.4.1.

All the PNP, PB and DH models support multi-species modeling, with an arbitrary number of species, each having different properties (charge valence, and diffusivity, when it applies). On the other hand, the Ohmic model is only implemented for a binary, symmetric electrolyte, although the two species may have different diffusion coefficients.

## 4.2.3 Electrokinetic coupling loop in the PNP model

The PNP model has a loop for the coupling between the Nernst-Planck equations (ionic concentration) and the Poisson equation (electric potential). This loop was seen to be required to keep the second-order accuracy in time of the PNP model [3]. Furthermore, it also allows the use of higher time-steps, while ensuring the conservation of ions. Although it is allowed to select one single iteration for this loop, we recommend the use of at least two iterations in any generic case. Moreover, two coupling iterations is the default behavior for this model if no information is provided by the user.

## 4.2.4 Coupled PNP model

**i** This feature is only available for OpenFOAM® versions.

The PNP system of equations can be solved coupled instead of segregated. The segregated solution method is implemented in the *NernstPlanck* model, whereas the coupled solution method is implemented in the *NernstPlanckCoupled* model. The coupled solver, which has been presented in [5], displays a higher numerical stability, but consumes more computational resources (memory and CPU time) per time-step. The PNP system of equations can not only be solved coupled alone, as it can also be coupled with momentum and continuity equations.

The technical aspects related with the use of the *NernstPlanckCoupled* model are discussed in Section 4.4.8.

### 4.2.5 Analysis of a code sample

As previously done in Section 4.1.4 for the *constitutiveEquations* library, in this Section we analyze a piece of code from the *EDFModels* library in order to illustrate the connection between the code and the theory previously discussed. However, we should note that the differences, at the code level, between the different models of the *EDFModels* library are bigger than in the *constitutiveEquations* library, as can be deduced from Table 4.2.

The piece of code selected for that purpose, Listing 4.3, represents the implementation of the PNP model and can be found in `src/libs/EDFModels/models/NernstPlanck/NernstPlanck.C`. Let's start the analysis to the most important parts:

- lines **11-33**: this is the constructor of a subclass (*NPSpecie*), nested in the main class (*NernstPlanck*). Remember that the PNP, PB and DH models were all presented in a multi-species formulation, which is the form available in the code. The *NPSpecie* subclass is exactly each specie of the PNP model. For **each new** specie, we can see the initialization of the following attributes (members): the concentration field (*ci*), the charge valence (*zi*) and the diffusivity (*Di*). The *NernstPlanck* class may have *N* instances of the *NPSpecie* subclass, as much as defined by the user.
- lines **35-107**: this is the constructor of the main class, where the several fields and variables are initialized. The call to function *checkForPhiE()* in line 44, which is implemented in the base class (see *EDFEquation.C*), is checking for the existence of field *phiE* in the folder corresponding to the starting time. If it is found, the code will interpret that the electric potential should be split into 2 variables (*phiE*  $\Leftrightarrow \phi_{\text{Ext}}$  and *psi*  $\Leftrightarrow \psi$ ), otherwise, the code will consider that only a single potential should be used (*psi*  $\Leftrightarrow \Psi$ ). This is how we identify if the splitting of potentials approach should be used. We also highlight lines 89-107, where each specie of the PNP model is being constructed and saved in a *PtrList <>*, named *species\_*.
- lines **110-156**: as suggested by the function's name (*Fe*), these lines implement the function returning the electric body-force for the momentum equation. The charge density (*rhoE*) is computed in lines 114-120 (compare with Eq. 3.28), and multiplied by the electric field in lines 122-155 (compare with Eq. 3.26 and Table 4.2). The computation of the electric field may include, or not, the contribution from the intrinsic potential, as discussed in Section 3.7.2 – this is a user selection. Furthermore, the vector *extraE\_* is an extra, uniform electric field, which can be optionally defined by the user (see Table 4.2 and its footnotes).
- lines **158-252**: it is inside this function, named *correct()*, that the electric-related equations are solved for. The function is generally prepared to use the splitting approach, in which case three equations are solved: the Laplace equation for the external potential (lines 172-186), the Poisson equation for the intrinsic (or full, unique) potential (lines 188-218) and the Nernst-Planck

transport equation for each ionic specie (220-250) – all these equations can be seen in Table 4.2. Each equation is inserted in a *while* loop controlled by the number of cycles and by the initial residual of the equation solved for. This is to optionally converge the explicit terms inside each equation, for each inner-iteration. In addition, and as discussed in Section 4.2.3, all the equations are solved inside an electrokinetic coupling loop (lines 161-251), whose number of iterations is controlled by variable *nIterPNP\_*, that is read from dictionary *fvSolution* (line 86). If the variable is not specified by the user, 2 iterations are carried out by default.

All the other EDF models also have the functions *Fe()* and *correct()* in their structure, which are defined according to the given model. We believe that the readers/users will easily understand those functions by reading the comments included in the code, and by comparing the code with Table 4.2.

```
1 #include "NernstPlanck.H"
2 #include "addToRunTimeSelectionTable.H"
3
4 // * * * * * * * * * * Static Data Members * * * * * * * * //
5 namespace Foam{
6 namespace EDFEquations{
7     defineTypeNameAndDebug(NernstPlanck, 0);
8     addToRunTimeSelectionTable(EDFEquation, NernstPlanck, dictionary);
9 }
10 }
11
12 // * * * * * * * * * * Constructors * * * * * * * * //
13 Foam::EDFEquations::NernstPlanck::NPSpecie::NPSpecie
14 (
15     const word& name,
16     const surfaceScalarField& phi,
17     const dictionary& dict
18 )
19 :
20     ci_
21     (
22         IOobject
23         (
24             name,
25             phi.time().timeName(),
26             phi.mesh(),
27             IOobject::MUST_READ,
28             IOobject::AUTO_WRITE
29             ),
30             phi.mesh()
31         ),
32         zi_(dict.lookup("z")),
33         Di_(dict.lookup("D"))
34     {}
35
36 // * * * * * * * * * * Constructors * * * * * * * * //
37 Foam::EDFEquations::NernstPlanck::NernstPlanck
38 (
39     const word& name,
40     const surfaceScalarField& phi,
41     const dictionary& dict
42 )
43 :
44     EDFEquation(name, phi),
45     solvePhiE_(checkForPhiE(name, phi)),
46     psi_
47     (
48         IOobject
49         (
50             "psi" + name,
51             phi.time().timeName(),
52             phi.mesh(),
53             IOobject::MUST_READ,
54             IOobject::AUTO_WRITE
55             ),
56             phi.mesh()
57         ),
58     phiE_
```

```

58     (
59         IOobject
60         (
61             "phiE" + name,
62             phi.time().timeName(),
63             phi.mesh(),
64             IOobject::READ_IF_PRESENT,
65             solvePhiE_ == false ? (IOobject::NO_WRITE) : (IOobject::
66             AUTO_WRITE)
67         ),
68         phi.mesh(),
69         dimensionedScalar
70         (
71             "zero",
72             psi_.dimensions(),
73             pTraits<scalar>::zero
74         ),
75         zeroGradientFvPatchField<scalar>::typeName
76     ),
77     relPerm_(dict.lookup("relPerm")),
78     T_(dict.lookup("T")),
79     extraE_(dict.lookupOrDefault<dimensionedVector>"extraEFfield",
80             dimensionedVector("0", dimensionSet(1, 1, -3, 0, 0, -1, 0),
81             vector::zero)),
82     psiContrib_(dict.lookupOrDefault<bool>"psiContrib", true),
83     phiEEqRes_(phi.mesh().solutionDict().subDict("electricControls").
84                 subDict("phiEEqn").lookupOrDefault<scalar>"residuals", 1e-7),
85     psiEqRes_(phi.mesh().solutionDict().subDict("electricControls").
86                 subDict("psiEqn").lookupOrDefault<scalar>"residuals", 1e-7),
87     ciEqRes_(phi.mesh().solutionDict().subDict("electricControls").
88                 subDict("ciEqn").lookupOrDefault<scalar>"residuals", 1e-7),
89     maxIterPhiE_(phi.mesh().solutionDict().subDict("electricControls").
90                 subDict("phiEEqn").lookupOrDefault<scalar>"maxIter", 50),
91     maxIterPsi_(phi.mesh().solutionDict().subDict("electricControls").
92                 subDict("psiEqn").lookupOrDefault<scalar>"maxIter", 50),
93     maxIterCi_(phi.mesh().solutionDict().subDict("electricControls").
94                 subDict("ciEqn").lookupOrDefault<scalar>"maxIter", 50),
95     nIterPNP_(phi.mesh().solutionDict().subDict("electricControls").
96                 lookupOrDefault<int>"nIterPNP", 2)),
97     species_(),
98     nSpecies_(0)
99 {
100     PtrList<entry> specEntries(dict.lookup("species"));
101     nSpecies_ = specEntries.size();
102     species_.setSize(nSpecies_);
103
104     forAll (species_, specI)
105     {
106         species_.set
107         (
108             specI,
109             new NPSpecie
110             (
111                 specEntries[specI].keyword(),
112                 phi,
113                 specEntries[specI].dict()
114             )

```

```
    );
106 }
108 // * * * * * Member Functions * * * * *
110 Foam::tmp<Foam::volVectorField> Foam::EDFEquations::NernstPlanck::Fe()
111 {
112     const
113     {
114         volScalarField rhoE( psi_ * dimensionedScalar("norm", epsilonK_.
115             dimensions()/dimArea, 0.) );
116
117         forAll (species_, i)
118         {
119             rhoE
120             += (
121                 species_[i].zi()*species_[i].ci()*FK_
122             );
123
124             if (solvePhiE_)
125             {
126                 if (psiContrib_)
127                 {
128                     return
129                     (
130                         -rhoE * ( fvc::grad(phiE_+psi_) - extraE_ )
131                     );
132                 }
133                 else
134                 {
135                     return
136                     (
137                         -rhoE * ( fvc::grad(phiE_) - extraE_ )
138                     );
139                 }
140             }
141             else
142             {
143                 if (psiContrib_)
144                 {
145                     return
146                     (
147                         -rhoE * ( fvc::grad(psi_) - extraE_ )
148                     );
149                 }
150             }
151         }
152     }
153
154     void Foam::EDFEquations::NernstPlanck::correct()
155     {
156 }
```

```
160 // Electrokinetic coupling loop
162 for (int j=0; j<nIterPNP_; j++)
{
164     Info << "PNP Coupling iteration: " << j << endl;
166     scalar res=GREAT;
168     scalar iter=0;

170 //-- Equation for the external potential (loop for the case
//    of non-orthogonal grids)
172 if (solvePhiE_)
{
174     while (res > phiEEqRes_ && iter < maxIterPhiE_)
    {
176         fvScalarMatrix phiEEqn
        (
178             fvm::laplacian(phiE_)
        );
180
        phiEEqn.relax();
182     res=phiEEqn.solve().initialResidual();

184     iter++;
    }
186 }

188 //-- Equation for the intrinsic potential

190 res=GREAT;
191 iter=0;
192
    volScalarField souE(psi_ * dimensionedScalar("norm1", dimless/dimArea
        , 0.));
194
    forAll (species_, i)
195 {
    souE +=
196     (
197         -species_[i].zi()*species_[i].ci()*FK_
200         /(relPerm_*epsilonK_)
    );
202 }

204 while (res > psiEqRes_ && iter < maxIterPsi_)
{
206
    fvScalarMatrix psiEqn
208 (
        fvm::laplacian(psi_)
210     ==
        souE
    );
212

214 psiEqn.relax();
    res=psiEqn.solve().initialResidual();
```

```

216     iter++;
218 }

220 //-- Nernst-Planck equation for each ionic species
222 forAll (species_, i)
223 {
224     res=GREAT;
225     iter=0;
226
227     volScalarField& ci = species_[i].ci();
228
229     dimensionedScalar cf(species_[i].Di() * eK_ * species_[i].zi() / (kbK_
230                           *T_) );
231
232     while (res > ciEqRes_ && iter < maxIterCi_)
233     {
234
235         fvScalarMatrix ciEqn
236         (
237             fvm::ddt(ci)
238             +fvm::div(phi(), ci, "div(phi,ci)")
239             ==
240             fvm::laplacian(species_[i].Di(), ci, "laplacian(D,ci)")
241             +fvc::laplacian(ci*cf, phiE_+psi_, "laplacian(elecM)")
242         );
243
244         ciEqn.relax(phi().mesh().equationRelaxationFactor("ci"));
245         res=ciEqn.solve(phi().mesh().solver("ci")).initialResidual();
246
247         ci = Foam::max( dimensionedScalar("lowerLimit",ci.dimensions(), 0.),
248                         ci );
249         iter++;
250     }
251 }
252 }
```

**Listing 4.3:** Source code of the Poisson-Nernst-Planck model in file `NernstPlanck.C`.

#### 4.2.6 Adding new EDF models

The steps required to add new EDF models are similar to the ones described previously, in Section 4.1.6, for GNF and viscoelastic models. The main steps are:

- copy-paste the folder of an existing model (that we will call template model) in directory `src/libs/EDFModels/models/`. Rename the folder and the files inside it (`.C` and `.H` files) with the new model's name. Remove the `.dep` file inside the folder. We recommend to use model *slipSmoluchowski* as template, since it is the simplest one and does not contain other sub-classes, which would also need to be renamed in the next step.
- inside the source `.C` and header `.H` files, find-replace the old model's name by the new one (e.g. *Ctrl + H* in *gedit*). This is to change the name of the class, which is usually equal to the name given to the respective source file. However, it is a good idea to always check first the name given to the class of the template model.
- add the source code of the new model to the compilation list of the library. For that, edit file `src/libs/EDFModels/Make/files` by adding the path for the source code (see the entries for the other models already there).
- make a first compilation of the new model, by running the script *Allwmake* in directory `src/`. Note that, until this point, the source code of the new model is the one from the original template model, where only the name of the class has been changed. Thus, the model should compile without errors. If not, something wrong occurred in the previous steps.
- the last step is to change the source code of the model in order to implement the desired EDF model. Depending on the characteristics of the new model, several parts of the source and header files might need to be changed. Our recommendation is to look to the closest model among the ones available. After all the changes on the code had been completed, compile again by running script *Allwmake*.

If all the steps listed above were successfully executed, then the new model is now available to solver *rheoEFoam* (only). In order to use library *EDFModels* in any solver other than *rheoEFoam*, the user should:

- add the header `#include "EDFModel.H"` to the main solver.
- create an *EDFModel* object by calling the constructor with the correct arguments, for example: *EDFModel elecM(phi)*.
- add the library *EDFModels* to the *Make/options*, and specify its path (check the *Make/options* of *rheoEFoam* for an example).

## 4.3 The *BDmolecule* library

 This library is only available for OpenFOAM® versions.

Library *BDmolecule* contains the classes and routines implementing the Brownian dynamics algorithm. The library is based on the *solidParticle* library provided by OpenFOAM® to perform the tracking of rigid particles. This library has been copied and modified in order to allow the creation of molecules, which are simply organized ensembles of beads. The interface of library *BDmolecule* is embodied by class *sPCloudInterface*. The source code of the library can be found in `src/libs/brownianDynamics`.

### 4.3.1 Organization of variables

The base class *particle* is commonly used in OpenFOAM® to create a single Lagrangian entity that can be tracked. Several other classes are derived from this one, adding new features to it. A *Cloud* is a template class representing a set of *particles*, inheriting the properties of C++ doubly-linked lists. This type of lists is not the most versatile one when we need to perform operations between non-consecutive elements, as it happens when computing intra-molecular forces. Thus, directly creating a molecule from a *Cloud* class seemed not to be the best option, even more because this option would create  $4M$  files ( $M$  being the number of molecules) for each time-step saved, which would overburden any file transfer operation, notwithstanding the small disk space used by each file. Therefore, we decided to separate the particle tracking from the molecule-related tasks. As such, we created a single (blind) *Cloud* object to contain all the particles (beads) from all the molecules of the simulation and perform the tracking, and an additional structure establishing the link between each particle and the corresponding molecule, that takes care of all the molecule-related tasks. We classified object *Cloud* as blind, because it does not differentiate among the particles, ignoring the molecules and groups to which they belong. This solves the two previous issues related with indexing and the number of files generated, but requires the exchange of information between structures and, consequently, some internal duplication of data, which is not problematic in terms of performance, but hinders the efficient parallelization of the code.

In the interface class (*sPCloudInterface*), object *spc\_* (a *Cloud*) is the one dedicated to the particle tracking. In addition, we can find a number of *PtrList <>* whose name starts with *m* and ends with an underscore (e.g. *mx\_*, *mSigma\_*, *mU\_*, ...) which are used in the remaining operations. For example, *mx\_* is a *PtrList < Field < vector >>* holding the beads positions (Cartesian coordinates) for each molecule. The beads positions are also a member of *spc\_*, but the difference comparing to *mx\_* is in the data organization. While we can use *mx\_* to easily find the position of bead *i*, in molecule *m* of group *g*, this cannot be done from inside *spc\_*.

### 4.3.2 Solution sequence

For a proper understanding of the source code behind the Brownian dynamics module of *rheoTool*, the user first needs to understand the interplay between the local fields of *sPCloudInterface* and the particles fields inside *spc\_*, from *solidParticle* class. We believe that the comments left in the code will help in this task. It would be unfeasible (and probably useless) to explain all the code details in this guide, thus we decided to only explore the function controlling the main Brownian dynamics loop. This function, named *update()*, a public member of *sPCloudInterface*, is charged of evolving the position and configuration of the molecules each time-step. In what follows, we briefly discuss the structure of this function (Listing 4.4):

- line **3**: the beads positions at the beginning of a time-step (*mx\_*) are copied to *mx0\_*. The algorithm structure ensures that the beads positions in *mx0\_* are such that all the springs of the active molecules are shorter than *l*, for bounded models (Section 3.8.3).
- lines **5-6**: if the user selects to account for hydrodynamic interactions, tensor **D** is computed from the RPY model (Eq. 3.44), and its Cholesky decomposition results in tensor **σ** (Section 3.8.3). If hydrodynamic interactions are suppressed, the diffusion is isotropic and can be represented by a scalar (*D*; Eq. 3.44), which is used to compute each force acting on the beads (tensors **D** and **σ** are not even computed in this case).
- line **8**: this function computes the Brownian force contribution to the beads velocity (last term of Eq. 3.43). The function is also defined inside *sPCloudInterface.C*.
- lines **10-11**: if exclusion volume forces are activated by the user, then their contribution to the beads velocity is added through a call to function *fEV()*, defined inside *sPCloudInterface.C*.
- line **13**: function *sendU()* copies the beads velocity from the local *mU\_PtrList <>* to the particles field *U*. This function is defined inside *sPCloudInterface.C*.
- line **16**: function *moveAndReceive()* comprises two main steps. In the first step, there is a call to the *move()* function of the *solidParticleCloud* object *spc\_*. This executes the movement and tracking of all the beads, after adding the drag force contribution to the particles velocity, which is done outside class *sPCloudInterface* (see file *solidParticle.C*). In the second step, the function updates *mx\_* with the final positions resulting from the particle tracking. If for some reason a given particle (bead) is lost during the tracking (e.g. if it exits the mesh through a patch), then the corresponding molecule is labeled as non-active, and it is no more tracked. Up to this point, the beads experienced all the forces, except the spring force.

- line **19**: the current beads positions are saved in  $mxStar_-$ . Since the spring force still did not contributed to these positions, the computation of the spring vectors from  $mxStar_-$  would result eventually in overstretched springs ( $R_i > l$ ).
- line **20**: this call to a non-member function computes explicitly (Euler explicit) the spring force contribution to the beads velocity ( $mU_-$ ), using the current beads positions ( $mxStar_-$ ). The **local** beads positions ( $mx_-$ ) are also updated.
- line **23**: based on the current beads positions ( $mx_-$ ), the spring vectors are computed and a check is carried out for  $R_i < al$  (see Section 3.8.4). For each molecule, if any spring violates this condition  $mxStar_-$  is taken again and the spring force contribution is now added implicitly, using the Newton-Raphson method (Section 3.8.4). Of course, this is only done if the semi-implicit method is selected (Euler-explicit is also available), and for any of the bounded spring models. After the implicit call, the function checks if any spring is overstretched. This can happen if the time-step is too large. Any molecule having at least one spring overstretched is automatically deleted by the algorithm and a warning message is printed to the terminal.
- lines **26-27**: if the molecules are not tethered and if any of the components of the push-back vector defined by the user is non-zero, the molecules center of mass is pushed to its original position. This is equivalent to the translation of all the molecule's beads by a fixed vector. In this case, we add the corresponding velocity to  $mU_-$ , such that the translation can be effective in the next particle tracking stage.
- line **29**: see comment above for line **13**.
- line **32**: this is the second call to function *moveAndReceive()*, thus a second call to the particle tracking engine. The operations carried out are the same as described above for line 16, with the exception that, in this call, the beads velocity does not receive the drag force contribution, since this was already done in the first call (the distinction between calls is in the boolean argument passed to the function). At this point of the algorithm, the particles positions and  $mx_-$  are synchronized and it can be ensured that none of the active molecules has an overstretched spring. We do not care about the synchronization of the beads' velocity, because this field is not used in the next time-step, contrarily to the beads' positions.
- line **35**: function *writeM()* ensures that the molecules' data is written in the case directory at each *outputTime*. It will create directories *outputTime* /*lagrangian/molecules/* and *constant/runTimeInfo/outputTime/*, and write the molecules' data therein. Both directories are needed on restart of *rheoBDFoam*.
- lines **38-39**: function *writeStatistics()* can be optionally activated by the user, and will retrieve the molecules index/position/stretch over time.

- lines **41-48**: these lines enclose the conditional return value of function *update()*. A value of *true* is returned as long as at least one molecule is still active and under tracking. Otherwise, the function returns *false* and, as explained in Section 4.5.5, this will force *rheoBDFoam* to abort the run, even if the *endTime* was still not reached (there is no interest in keeping the solver running without any valid molecule).

While inspecting the source code, note that several intermediate operations are carried out in a dimensionless form to reduce round-off errors, but final results are always dimensional. Round-off errors can be an important source of numerical error in Brownian dynamics simulations (the situation is worse in atomistic simulations) if care is not taken with the different scales involved.

```

bool sPCloudInterface::update()
2 {
    mx0_ = mx_;
4
    if (isHI_)
6        computeDSigma();
8
    fBrownian();
10
    if (isExclusionVolumeF_)
      fEV();
12
    sendU();
14
    // Move particles: Drag + Brownian + Exclusion Volume
16 moveAndReceive(true);
18
    // Compute Spring force term explicitly and update local mU and
      mx.
    mxStar_ = mx_;
20 spModel_->fSpring();
22
    // Check for violations in spring lengths and add spring force
      implicitly if needed
    spModel_->checkSpringsLength(mxStar_, mx0_);
24
    // Push back the molecules if not tethered and if pushback
      vector is not negligible
26    if (!isTethered_ && mag(pBackV_)>SMALL)
      pushToX0();
28
    sendU();
30
    // Move particles: spring force only
32 moveAndReceive(false);
34
    // Write data (controlled by output time)
    writeM();
36
    // Write statistics (has its own control for output)
38    if (writeStats_)
```

```

        writeStatistics();

40   if (nMolc_>0)
41   {
42     return true;
43   }
44   else
45   {
46     return false;
47   }
48 }
```

**Listing 4.4:** Member function *update()* of class *sPCloudInterface*. The source code can be found in file *sPCloudInterface.C*.

### 4.3.3 External forcing type

The external forcing (drag) acting on the beads is embodied by term  $\mathbf{u}_f$  in Eq. (3.43). The forcing can be defined analytically or computed numerically.

In case it is defined analytically, tensor  $\nabla \mathbf{u}$ , provided by the user, defines the gradient of the forcing (spatially homogeneous and constant over time, by default). The computational mesh in those cases can (should) be simply a single cell. The computational domain can be made large in all the directions if an unconfined flow is intended, but a confined flow can also be imposed by shortening one or multiple directions. Importantly, the boundaries used to impose confined flow conditions must be of *wall* type (*patch* types will be crossed by the molecules, and remaining types give undefined behavior).

In case it is computed numerically, then two types are still available in *rheoTool*: hydrodynamic forcing, in which case  $\mathbf{u}_f$  is the fluid velocity; electric forcing for polyelectrolytes immersed in an electric field, in which case  $\mathbf{u}_f = \mu \mathbf{E}$  is the electrophoretic velocity ( $\mu$  is the electrophoretic mobility and  $\mathbf{E}$  is the electric field). Both types of forcing can coexist, and each one requires that the respective continuum field is available in the case directory.

Note that 2D meshes, and the corresponding continuum fields, are allowed in Brownian dynamics simulations, but the motion equation of the beads (Eq. 3.43) is **always** solved for the 3 Cartesian coordinates. This means, for example, that the molecules will not feel the *z*-component effect of a planar velocity field solved in the *Oxy* plane, but they still feel the Brownian force (and the remaining, except drag) in that direction.

### 4.3.4 External forcing interpolation

Independently of the forcing nature,  $\mathbf{u}_f$  must be interpolated to the current position of the bead. Therefore, the question addressed in this section is how to compute  $\mathbf{u}_f$  given a numerical field defined at cell centers (numerical forcing), or a forcing gradient valid over all the domain (analytical forcing)? The following methods are available in *rheoTool*:

- *Analytical*: this scheme is the only available for analytical forcing and cannot be used with a numerical forcing. The velocity is interpolated using  $\mathbf{u}_f = \nabla \mathbf{u}^T \cdot \mathbf{r}_i$ , where  $\nabla \mathbf{u}$  is user-defined.
- *BarycentricWeights*: this is the method that OpenFOAM® uses by default to compute the velocity of Lagrangian particles. Consider a generic cell and its decomposition in tetrahedrons, where one vertex of the tetrahedron is always the center of the cell, and the remaining vertices correspond to vertices of one of the cell's faces. For a rectangular cell, for example, one would end-up with 12 non-unique tetrahedrons, two per face of the cell. It is then possible to define a barycentric coordinate system for each tetrahedron, such that any point inside it can be uniquely identified by a quadruplet  $(b_1 \ b_2 \ b_3 \ b_4)$ , with  $\sum_{i=1}^4 b_i = 1$ . In addition to allow the spatial location of particles, these coordinates can also be used to weight the data at the vertexes of the tetrahedron, acting as interpolants of the data at the tetrahedron's vertices, which is the method adopted when selecting *BarycentricWeights*. Remember that the vertices of the tetrahedrons are either cell centers or vertices of cells. Therefore, the numerical field computed at the cell-centers (OpenFOAM® uses co-located grids) also needs to be interpolated to vertices, which is accomplished by simple inverse distance weighting.
- *Gradient*: in this approach, both the cell-centered field and its gradient are used for the interpolation. Assuming that  $\mathbf{u}_C$  is the forcing known (computed) at the cell center (located at  $\mathbf{x}_C$ ) and that  $\nabla \mathbf{u}_C$  is its gradient (computed numerically), then the velocity at any point  $\mathbf{x}_P$  inside the cell can be approximated by:  $\mathbf{u}_f = \mathbf{u}_C + (\mathbf{x}_P - \mathbf{x}_C) \cdot \nabla \mathbf{u}_C$ . The numerical scheme used to compute the cell-centered gradient ( $\nabla \mathbf{u}_C$ ) can be defined by the user under keyword *gradExternalForcing* in dictionary *fvSchemes*. In general, we recommend *Gauss linear* for hex-dominated grids and *leastSquares* in the remaining cases.

Although the *BarycentricWeights* and *Gradient* methods display sub-cell resolution, they both have some pitfalls, as illustrated in Fig. 4.1. The data/grid in this figure corresponds to a fully-developed field in the  $x$ -direction, which displays a maximum in the  $y$ -direction, for  $y = 0$ , and is symmetric about  $y = 0$ . The profile in the  $y$ -direction can be a parabola, a piecewise linear function or any other function satisfying the aforementioned conditions of maximum and symmetry. This could be the case, for example, of the velocity in a fully-developed Poiseuille flow sampled at the centerline. The behavior of the two interpolation methods for this case are plotted in the right of Fig. 4.1. For the case depicted, the interpolated  $u_f$  by the *BarycentricWeights* method is simply a field of quadrangular pyramids (apex at cell centers), with the height of each vertex corresponding to the local forcing value.

For a profile taken over  $y = 0$ , method *Gradient* approaches correctly the theoretical function (constant over the  $x$ -direction), whereas method *BarycentricWeights* retrieves a sawtooth profile. Consider now that the molecules' center

of mass is artificially fixed (see Section 4.3.6) somewhere between  $x = -1$  and  $x = 1$  (keeping  $y = 0$ ). For the *Gradient* method, the results will be independent of the specific abscissa selected, as one would expect for a fully-developed field in the  $x$ -direction. On the other hand, if the strain-rate in the sawtooth profile retrieved by method *BarycentricWeights* is such that  $Wi = \lambda\dot{\gamma} \gg 1$ , then the results will strongly depend on the specific abscissa selected.

For a profile taken over  $x = 0$ , method *Gradient* is unable to capture any variation of the field in that direction for the central cell, since it predicts  $\nabla \mathbf{u}_C = (0 \ 0 \ 0)$  for all the cells at the centerline, which is only true exactly at the cell's center. The issue arises from the gradient computation method, and is akin to the checkerboard problem that can happen for the  $U$ - $p$  coupling in the momentum equation. On the other hand, method *BarycentricWeights* performs better this time, retrieving a linear variation of  $u_f$  over the  $y$ -direction (the interpolation is exact if the original field displays a linear variation). If we consider a group of molecules traveling over the  $x$ -axis, and only spanning the central layer of cells, then we can easily conclude that they would not feel any forcing under the *Gradient* method, whereas method *BarycentricWeights* would be able to approach the forcing gradient in the  $y$ -direction (in addition to the artificial one in the  $x$ -direction).

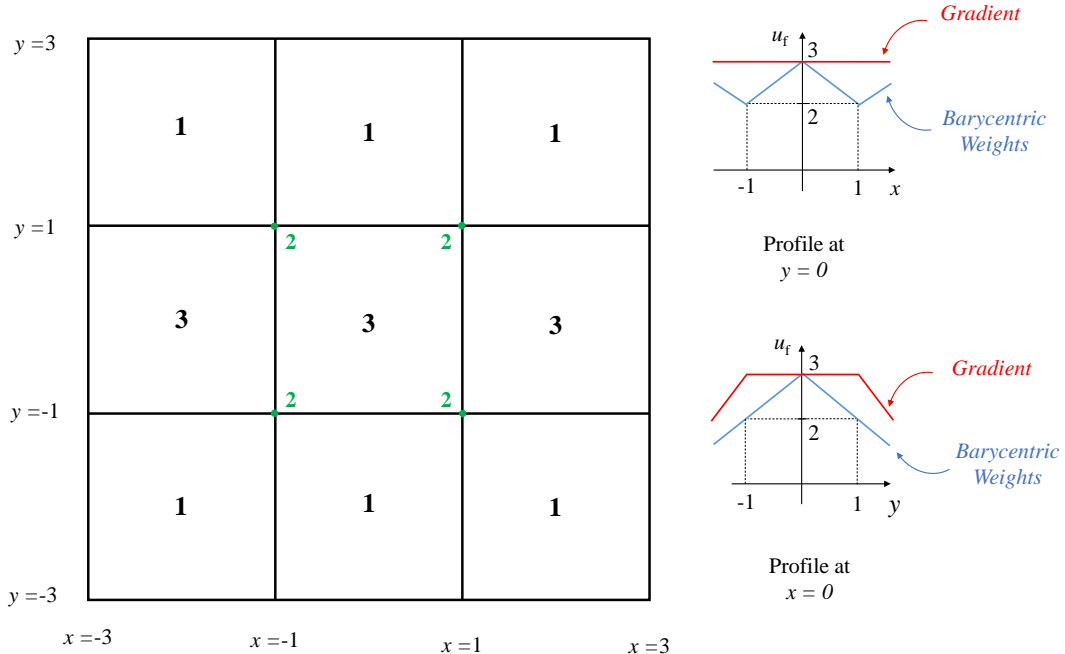


**Figure 4.1:** Hypothetical 2D external forcing field (a scalar field to simplify) in a co-located grid (values at cell centers), aiming to represent a fully-developed field in the  $x$ -direction. The green values defined at vertices are obtained by inverse distance weighting of the cell-centered data. On the right, the profiles of  $u_f$  taken at  $x = 0$  and  $y = 0$  are represented for two different interpolation methods.

The previous case has shown that the numerical interpolation methods available are prone to errors in certain conditions and care should be taken in their use. In the specific case presented above, the issues with the two methods could have been reduced by refining the grid in the  $y$ -direction, such that the molecules spanned more than one cell in that direction, and by allowing the molecules to travel at least one entire cell in the  $x$ -direction. Alternatively, the use of an unstructured grid could possibly solve the issues in that particular case. The message that we want to convey to the reader/user is to use refined meshes in BDS cases, even though the interpolation methods have sub-cell resolution. Moreover, grid-dependency studies are also advisable. In any generic situation, if *Analytical* interpolation can be used, then this should always be the preferred method, since it is not prone to such errors. If not possible, then method *BarycentricWeights* should be preferred over *Gradient*.

#### 4.3.5 Spring force and time-integration schemes

The spring force models available in library *BDmolecule* are presented in Table 4.3 and were briefly discussed in Section 3.8.3.

**Table 4.3:** Available spring force models for Brownian dynamics simulations.

| Model        | (1) TypeName       | (2) $\mathbf{F}_i^S$  | (3) $\mathbf{f}_i^k$   | (4,5) $J_{ij, a (j \neq i, j \in \mathbf{g}_i)}^k$   |
|--------------|--------------------|---|--|--|
| Hookean      | <i>Hookean</i>     | $H \sum_{j \in \mathbf{g}_i}^N \mathbf{x}_{ij}$   | —  | —  |
| Marko-Siggia | <i>MarkoSiggia</i> | $\frac{2}{3} H l \sum_{j \in \mathbf{g}_i}^N \left[ \frac{ \mathbf{x}_{ij} }{l} - \frac{1}{4} + \frac{1}{4(1- \mathbf{x}_{ij} /l)^2} \right] \frac{\mathbf{x}_{ij}}{ \mathbf{x}_{ij} }$ | $\mathbf{r}_i^k - \mathbf{r}_i^* - \Delta t \frac{D}{kT} \mathbf{F}_i^{S,k}$ | $\frac{2}{3} \frac{H'}{d} \left[ \left( \frac{1}{4(d-1)^2} + d - \frac{1}{4} \right) \left( \frac{\delta^2}{d^2} - 1 \right) - \frac{\delta^2}{d} \left( 1 - \frac{1}{2(d-1)^3} \right) \right]$ |
| Cohen Padé   | <i>CohenPade</i>   | $\frac{H}{3} \sum_{j \in \mathbf{g}_i}^N \left[ \frac{3 - ( \mathbf{x}_{ij} /l)^2}{1 - ( \mathbf{x}_{ij} /l)^2} \right] \mathbf{x}_{ij}$  | $\mathbf{r}_i^k - \mathbf{r}_i^* - \Delta t \frac{D}{kT} \mathbf{F}_i^{S,k}$ | $\frac{H'}{3} \frac{2\delta^2}{(d^2-1)} \left[ \frac{d^2-3}{d^2-1} - 1 - \frac{d^2-3}{2\delta^2} \right]$  |
| FENE         | <i>FENE</i>        | $H \sum_{j \in \mathbf{g}_i}^N \frac{1}{1 - ( \mathbf{x}_{ij} /l)^2} \mathbf{x}_{ij}$   | $\mathbf{r}_i^k - \mathbf{r}_i^* - \Delta t \frac{D}{kT} \mathbf{F}_i^{S,k}$ | $H' \left[ \frac{1}{d^2-1} - \frac{2\delta^2}{(d^2-1)^2} \right]$  |

(1) Corresponds to the name entry identifying the model in the source code.

(2)  $H = \frac{3kTN_{k,s}}{l^2}$ .

(3) Vectorial function used in the Newton-Raphson method (see Section 3.8.4). Superscript  $k$  denotes the iteration index.

(4) The expressions in this column are for the off-diagonal  $ij$  ( $j \neq i, j \in \mathbf{g}_i$ ) elements of the Jacobian matrix of the Cartesian component  $a = x, y, z$  of  $\mathbf{f}^k$ . All the off-diagonal elements for which  $j \notin \mathbf{g}_i$  are zero. The diagonal elements are obtained from the sum of the off-diagonal elements,  $J_{ii,a}^k = 1 - \sum_{m=1, m \neq i}^N J_{im,a}^k$ . This symmetric matrix is used in the Newton-Raphson method (see Section 3.8.4).

(5)  $H' = H \Delta t \frac{D}{kT}$ ,  $d = |\mathbf{x}_{ij}^k|/l = |\mathbf{r}_j^k - \mathbf{r}_i^k|/l$ ,  $\delta = (r_{j,a}^k - r_{i,a}^k)/l$

In general, the FENE and Cohen Padé models are stiffer to solve than the Marko-Siggia model, thus requiring smaller time-steps.

An explicit time integration scheme (*TypeName* = *explicit*) is available for all spring models. For the bounded spring models, the semi-implicit scheme (*TypeName* = *semiImplicit*) described in Section 3.8.4 is also available. The auxiliary functions used in the semi-implicit scheme are specified in Table 4.3 for all bounded models.

As mentioned in Section 3.8.4, several methods can be used to solve the linear system of equations (3.53). Four (direct) methods are available in library *BDmolecule*:

*TypeName* – *Description*

*QR* – uses the Householder rank-revealing QR decomposition (function *colPivHouseholderQr()*) of Eigen [35] to decompose matrix  $\mathbf{J}_a^k$ . It can be used in any situation, and it should be the default choice in case of doubt.

*LLT* – performs a standard Cholesky decomposition of matrix  $\mathbf{J}_a^k$ , using the *llt()* function of Eigen [35]. It should not be used for tethered molecules.

*TDMA* – implements Thomas algorithm for a tridiagonal matrix. It can be used for open, linear (no branches), not tethered molecules. Better performance than *QR* is achieved for a large number of beads per molecule (it only visits elements  $i-1, i, i+1$ ).

*Gaussian* – uses the Gaussian elimination method provided by OpenFOAM®. Restrictions are the same as for TDMA method.

The reader may be questioning the need and utility of so many methods. Theoretically, some methods should be faster than others, but possibly more stringent in their application (only tridiagonal matrices, diagonal-dominant matrices, etc.). In practice, we observe that the *QR* method is usually the best compromise. The *TDMA* method presents a CPU time typically equal or smaller than *QR*, but has restrictions in its application (see above). All the methods are implemented using full-matrices, notwithstanding the fact that most of the off-diagonal matrix elements are zero. Sparse matrices and sparse matrix (iterative/direct) solvers might be considered in a future version if memory overhead starts to be an issue of concern (say  $> 500$  beads per molecule).

#### 4.3.6 Tethering and fixing the molecules center of mass

*rheoTool* allows the simulation of tethered molecules, i.e., molecules with some specific part of the chain fixed in space. The only restriction is that solely the first bead of a given molecule (the one having *index* = 0 inside the chain) can be fixed. The numerical procedure to simulate tethered molecules is similar to that for generic molecules, with the exception that we impose a null resulting force acting on the tethered bead.

Fixing the center of mass of a molecule is different from tethering a molecule, and the use of both in simultaneous is not allowed (would it make sense?). When the option of fixing the molecules center of mass is selected, the molecules are simulated in the usual way, but at the end of  $n$  time-steps all the beads are translated by a same vector, which restores the original center of mass ( $n$  time-steps before). This option is useful, for instance, when simulating molecules under an analytical external forcing (homogeneous in space), or to equilibrate the molecules in a local flow. The value of  $n$ , the number of consecutive time-steps in which the molecules movement is unconstrained, is defined by the user. The existence of this tunable parameter is mainly to avoid some of the inconsistencies previously described in Section 4.3.4 for the *BarycentricWeights* interpolation method.

The reader should keep in mind that the molecules will always move in space (over the mesh) according to the external forcing if none of these options is selected, independently of the external forcing nature.

### 4.3.7 Beads tracking

The default particle tracking engine of OpenFOAM® is used to move the beads over the mesh. The algorithm has been greatly improved since OpenFOAM® v5.0, where barycentric coordinates for the beads' position have been generalized. It is out the scope of this user guide to explain the particle-tracking algorithm. However, it is worth mentioning that the drag force (and only that one) is re-interpolated inside the same time-step each time a particle (bead) crosses an internal face of the mesh.

Once a bead hits a *wall*, it is repositioned at the location where the wall is crossed or, optionally, at a given distance from that point, in the wall-normal direction. This artificial repulsion aims to reproduce the finite size of the beads, that would never let them to approach infinitely close to a surface in a real situation.

If a bead hits a *patch*, it will simply leave the mesh through such *patch* and the corresponding molecule is deleted. If a 2D flow is simulated, we recommend to make the *empty* direction long enough in order to avoid the unnecessary contact of the *empty* boundaries with the beads. The contact of a bead with any other boundary type will result in undefined behavior, although we expect the molecule to be deleted in most of the cases. The corollary is to create meshes having only *patch*, *wall* and *empty* boundary types for use in Brownian dynamics simulations. Other types can be used as long as the beads do not enter the cells owning those boundary faces.

It is well-known that the hydrodynamic interactions near a wall are different than in the bulk. However, the current version of *BDmolecule* does not make any correction at the walls. Therefore, care should be taken when simulating confined problems, or when the molecule-wall contact is recurrent.

### 4.3.8 Data output for post-processing

The *sPCloudInterface* class can optionally save some information about the molecules in runtime. When this option is active, a directory named `rheoTo`

`olPP/startTime/moleculesStates/groupName` is created for each group of molecules, and three files are written to this directory:

`IDs.txt`: contains three columns, where the first one is for the molecule name/ID, the second is for the number of beads in the molecule and the third is for the molecule's group ID. This file includes such information for all molecules starting the simulation, regardless of whether the molecule is deleted at some time during the simulation (e.g. if one of the springs becomes overstretched). Each row represents a molecule.

`stretch.txt`: the first column of this file is for the physical time and each of the remaining columns represents the *stretch* of a molecule. There is a direct and sequential one to one relation between the rows of `IDs.txt` and the columns of `stretch.txt` (excluding the first column for time). We define *stretch* as the maximum inter-bead distance in a molecule:  $\text{stretch} = \max(|\mathbf{r}_j - \mathbf{r}_i|)$ ,  $i, j = \{1..N\}$ . If a given molecule is deleted at some point of the simulation, then the column corresponding to that molecule will be filled with zeros starting from the row corresponding to that time. Since the length of a molecule can never be zero, these entries can be used as flags to detect the molecules that have been deleted during the simulation.

`X.txt`: the first column of this file is for the physical time and each of the following triplets of columns represents the *x*-, *y*- and *z*-coordinates of the molecule center of mass,  $\mathbf{x}_{\text{cm}} = \frac{1}{N} \sum_{i=1}^N \mathbf{r}_i$ . Again, there is a direct and sequential one to one correspondence between the rows of `IDs.txt` and each triplet of columns of `X.txt` (excluding the first column, for time).

### 4.3.9 Limitations

Some of the main limitations of the Brownian dynamics library have been previously described. However, to make them clear and to avoid any misuse of the library, they are summarized below:

- only single-core runs are allowed.
- only *patch*, *wall* and *empty* boundary types can be present in a mesh.
- hydrodynamic interactions near surfaces are not corrected and the algorithm for beads reflection at the walls is simplistic (accuracy in confined-flow conditions can be compromised).

Of course, all these limitations can be seen as points to improve in future work. Although the non-parallelization of the code is pointed out as an issue, we believe it is not the most important one. Indeed, we expect the solver to be used essentially with a steady external forcing. In such cases, if the code was parallelized we would distribute the ensemble of  $M$  molecules by  $P$  available processors ( $M/P$  molecules per processor), in a single run (single mesh, single fields, etc.). Since this is not

possible, we can prepare  $P$  cases, with  $M/P$  molecules per case and run each one in a processor. This is valid because all the molecules are similar objects and need not to communicate between them. The two methods should perform closely in terms of CPU time, although the non-parallel one consumes more memory (allocation of the mesh  $P$  times *vs* 1 time). For the cases with transient external forcing, parallelization would be indisputably advantageous regarding CPU time.

## 4.4 The *sparseMatrixSolvers* library

 This feature is only available for OpenFOAM® versions.

*rheoTool* has interfaces to three external libraries: Eigen [35], Hypre [37] and Petsc [9–11]. These interfaces allow solving "externally" the linear systems of equations built in OpenFOAM®, thus increasing the availability of sparse matrix solvers. Moreover, they also enable certain operations that would not be allowed by OpenFOAM® matrix solvers, as for example reusing the preconditioner. All interfaces are parallelized with MPI, except Eigen's interface, which can only be used for serial runs. These features are incorporated in library *sparseMatrixSolvers*, which also includes coupled solvers (Section 4.4.8).

The library is generic regarding the type of equations that can be handled by the interfaces (scalar, vector, tensor, symmTensor and sphericalTensor). In practice, we only use the library to solve the **pressure** and **momentum** equations in segregated solvers, since those are usually the ones consuming more CPU time. Note that the use of different sparse matrix solvers does not change the accuracy of the algorithm. Indeed, as long as the system of equations is solved to a tight tolerance, the solution retrieved by any solver should be the same. Speed is the only factor involved when selecting the sparse matrix solver.

### 4.4.1 Conditions to reuse the preconditioner/factorization

In some situations, the discretized equations result in matrices with a large condition number. For example, this happens often with the pressure equation. The default sparse matrix solvers available in OpenFOAM® might present convergence issues in such cases, which is visible in the high number of iterations taken to converge to the prescribed tolerance. The use of strong preconditioners can lower the number of iterations, but this does not necessarily translates in a lower time of computation, since computing and applying strong preconditioners is a costly procedure. However, in some particular situations the matrix of coefficients does not change over time, which allows computing the preconditioner only once. There are also situations where the matrix of coefficients only changes slightly between time-steps, such that a given preconditioner can be used more than once. Considering this range of situations, *sparseMatrixSolvers* library offers the possibility to reuse the preconditioner.

Considering pressure and momentum equations, the respective matrix of coefficients does not change over time when:

- the time-step/under-relaxation factor is fixed;
- momentum convection is negligible (this term is removed from the equation, see Section 4.7.1);
- the viscosity coefficient is constant over time;
- the density is constant over time.

These conditions are typically verified in inertialess microfluidic single-phase flows. They allow computing the preconditioner (iterative solver) or factorization (direct solver) once, at the first time-step, and reusing it in the remaining time-steps. If some of these conditions are not verified, it might still be possible to reuse the preconditioner/factorization in more than one time-step.

Note that using direct solvers or iterative solvers combined with strong preconditioners typically increases the memory usage. Therefore, users should always take this factor into consideration in order to prevent memory overflow.

#### 4.4.2 Residuals and tolerances

The residuals are an indicator typically used in CFD to monitor convergence. The definition of residuals is not consensual and each software package uses its own definition. In OpenFOAM®, the residuals of an equation are defined as

$$\text{Residual} = \frac{|\mathbf{Ax} - \mathbf{b}|_1}{|\mathbf{Ax} - \mathbf{A}\bar{x}\mathbf{I}|_1 + |\mathbf{b} - \mathbf{A}\bar{x}\mathbf{I}|_1} \quad (4.27)$$

where  $\mathbf{A}$  is the matrix of coefficients,  $\mathbf{b}$  is the right hand-side vector,  $\mathbf{x}$  is the solution vector,  $\mathbf{I}$  is a vector of ones,  $\bar{x}$  is the average value of  $\mathbf{x}$  and  $||_1$  represents the L<sub>1</sub> norm of a vector. For all the three interfaces, the residuals displayed to the screen follow the definition of Eq. (4.27), independently of the sparse matrix solver being used.

While solving a system of equations with an iterative solver, the iterative process stops once a convergence criteria is satisfied. The most used criteria are typically the absolute tolerance, the relative tolerance and an established maximum number of iterations. The formula used to define each tolerance is usually software-dependent. For example, OpenFOAM® solvers use the residuals to define the tolerance. In the *sparseMatrixSolvers* library, the solvers belonging to each interface use the tolerance definition imposed by the respective library. Therefore, whereas OpenFOAM® solvers present a direct relation between the absolute tolerance and the residuals, there is no such direct relation for the solvers from the external libraries. This question does not arise with direct solvers, since they always solve the equations to machine precision.

#### 4.4.3 Generic parameters

The access to the sparse matrix solvers from the external libraries takes place in dictionary *fvSolution*, under sub-dictionary *solvers*. There are four parameters common to all interfaces:

*solverType* – corresponds to the TypeName of the class of solvers to be used, one of *eigenSolver*, *hypreSolver*, *openFoamSolver* or *petscSolver*. Each option corresponds to one of the external libraries, except *openFoamSolver*, which is simply a wrapper to the default OpenFOAM® solvers. If *solverType* is not specified, then *openFoamSolver* is assumed by default, in order to keep backward compatibility, and the remaining three parameters have no effect.

*saveSystem* – this bool indicates whether to reuse or not the elements needed to solve the system of equations (matrix of coefficients, solver and preconditioner).

*updatePrecondFrequency* – the frequency at which the preconditioner is updated. The counter is updated each time the equation for the given field is assembled and solved. If the matrix of coefficients is not changing and *saveSystem* = true, this variable should be set to a high value (e.g.  $10^5$ ), such that, in practice, the preconditioner is only computed at the beginning of the simulation. If the matrix of coefficients is changing and *saveSystem* = true, this variable should be carefully adjusted. If the matrix of coefficients changes quickly, the value should be close to 1, whereas higher values can be selected otherwise. If this parameter is set equal to -1, then an empiric algorithm [5] is employed to automatically decide when to update the preconditioner. If a direct solver is used, this parameter must be set equal to 1 (the factorization needs to be computed each time-step) and an error message is retrieved if this condition is not satisfied. If *saveSystem* = false, then this parameter has no meaning and is not read.

*updateMatrixCoeffs* – this bool indicates whether to update or not the matrix of coefficients every time the equation is solved. It should be set equal to true if the matrix of coefficients changes over time and false otherwise. There is a (weak) verification procedure at the beginning of a simulation to check if the matrix of coefficients is changing. An error is retrieved if *updateMatrixCoeffs* is inconsistent with the result from this verification. If *saveSystem* = false, then this parameter has no meaning and is not read.

The set of options *saveSystem* = true, *updatePrecondFrequency* = 1 and *updateMatrixCoeffs* = true results in a close, but not equal setup as *saveSystem* = false. For the first set of options, some structures are reused, as for example the sparsity pattern in the matrix of coefficients, whereas in the latter case all structures are deleted after the equation is solved.

If the user is unsure about the possibility of reusing elements, then setting *saveSystem* = false should be the first approach. The resulting setup might be inefficient, but has unconstrained applicability (with the exceptions mentioned in Section 4.4.10).

For programming reasons, when *saveSystem* = true, *updatePrecondFrequency* = bigNumber and *updateMatrixCoeffs* = false, the factorization/preconditioner is computed in **the first two times the equation is solved**, and not only in the first time (that would be enough since the matrix is not changing from the first

time it is assembled). These two solution times are expected to be **significantly slower than the following ones**. Therefore, the user should not judge the speed of the simulation based on these two initial time-steps.

The parameters specific to each interface are presented in the following sections.

#### 4.4.4 OpenFOAM interface

This interface is selected by setting *solverType = openFoamSolver* and is simply a wrapper to the default OpenFOAM® sparse matrix solvers. Therefore, specifying the solver, preconditioner and their corresponding parameters is as usual.

#### 4.4.5 Eigen interface

**Note:** sparse matrix solvers from Eigen library can not be used in parallel runs.

The interface to Eigen library was built essentially due to the ease of use of this library. This class of solvers is selected by setting *solverType = eigenSolver*. The list of solvers available for this interface is presented in Table 4.4, and the list of preconditioners in Table 4.5. Note that only part of the solvers/preconditioners offered by Eigen is available through this interface. Moreover, the PCG solver is restricted to symmetric matrices and SparseLU is the only direct solver made available. The *tolerance* parameter owns Eigen’s definition. See Eigen’s documentation [35] for more details about each solver/preconditioner and its parameters.

The preconditioner must be defined under a sub-dictionary named *preconditioner*. It is not allowed using an iterative solver without preconditioner. In Listing 4.5 we present an example showing the use of a solver from Eigen library (an ILUT preconditioned BiCGSTAB Krylov solver).

**Table 4.4:** Available sparse matrix solvers from Eigen interface. The values inside brackets represent the default parameters used if they are not specified by the user. Note that additional parameters might be available for each solver, but only those listed in this Table can be changed through the interface (the ones not listed here get default values defined by Eigen).

| Solver   | Parameters                               | Available preconditioners |
|----------|--|---------------------------|
| BiCGSTAB | maxIter (1000), tolerance ( $10^{-12}$ ) | ILUT, Diagonal            |
| GMRES    | maxIter (1000), tolerance ( $10^{-12}$ ) | ILUT, Diagonal            |
| PCG      | maxIter (1000), tolerance ( $10^{-12}$ ) | ICC, Diagonal             |
| SparseLU | pivotThreshold ( $10^{-12}$ )            | (Direct Solver)           |

**Table 4.5:** Available preconditioners from Eigen interface. The values inside brackets represent the default parameters used if they are not specified by the user. Note that additional parameters might be available for each preconditioner, but only those listed in this Table can be changed through the interface (the ones not listed here get default values defined by Eigen).

| Preconditioner | Parameters                              |
|----------------|---|
| ILUT           | fillFactor (10), dropTol ( $10^{-12}$ ) |
| ICC            | —                                       |
| Diagonal       | —                                       |

```

1 solvers
{
3   " (p | U) "
{
5     solverType      eigenSolver;
7     saveSystem      true;
8     updatePrecondFrequency 10000;
9     updateMatrixCoeffs    false;

11    solver          BiCGSTAB;
12    tolerance       1e-12;
13    maxIter        1000;

15    preconditioner
{
17      preconditioner  ILUT;
18      dropTol         0;
19      fillFactor      5;
}
21  }
}

```

**Listing 4.5:** Example of a *solvers* dictionary in *fvSolution* showing the use of a sparse matrix solver from Eigen library to solve momentum and pressure equations.

#### 4.4.6 Hypre interface

The class of solvers in the Hypre interface is selected by setting *solverType = hypreSolver*. The list of solvers available for this interface is presented in Table 4.6, and the list of preconditioners in Table 4.7. Note that only part of the solvers/preconditioners offered by Hypre is available through this interface. The PCG solver is restricted to symmetric matrices and not all preconditioners can keep

symmetry when used with this solver. The *tolerance* and *relTol* parameters own Hypre's definition. Some preconditioners can only be used in parallel runs and preconditioner *none* is tantamount to not using any preconditioning method. See Hypre's documentation [37] for more details about each solver/preconditioner and its parameters.

The preconditioner must be defined under a sub-dictionary named *preconditioner*, even in the case it is *none*. In Listing 4.6 we present an example showing the use of a solver from Hypre library (a BoomerAMG preconditioned GMRES Krylov solver). Note that options *updatePrecond* and *updateMatrixCoeffs* are not specified in this example because *saveSystem* = false (see Section 4.4.3).

**Table 4.6:** Available sparse matrix solvers from Hypre interface. The values inside brackets represent the default parameters used if they are not specified by the user. Note that additional parameters might be available for each solver, but only those listed in this Table can be changed through the interface (the ones not listed here get default values defined by Hypre).

| Solver    | Parameters  | Available preconditioners          |
|-----------|---|------------------------------------|
| BiCGSTAB  | maxIter (1000), relTol (0), tolerance ( $10^{-8}$ ), printLevel (0), logging (0)  | BoomerAMG, Euclid, ParaSails, none |
| GMRES     | maxIter (1000), relTol (0), tolerance ( $10^{-8}$ ), KrylovSpaceDim (100), printLevel (0), logging (0)  | BoomerAMG, Euclid, ParaSails, none |
| PCG       | maxIter (1000), relTol (0), tolerance ( $10^{-8}$ ), useTwoNorm (true), recomputeEndResidual (false), printLevel (0), logging (0)   | BoomerAMG, Euclid, ParaSails, none |
| BoomerAMG | relTol (0), maxIter (1000), minIter (0), convergenceType (0), relaxationType (6), nSweeps (1), coarsenType (10), restrictionType (0), cycleType (1), AMGVariant (0), printLevel (0), relaxOrder (0), recoversOldDefault (true), logging (0) | none                               |

**Table 4.7:** Available preconditioners from Hypre interface. The values inside brackets represent the default parameters used if they are not specified by the user. Note that additional parameters might be available for each preconditioner, but only those listed in this Table can be changed through the interface (the ones not listed here get default values defined by Hypre).

| Preconditioner | Parameters  |
|----------------|---|
| Euclid         | ILUklevel (2), enableJacobiILU (false), enableRowScaling (false), dropTol (0)   |
| ParaSails      | printLevel (0), loadBalance (0)   |
| BoomerAMG      | relTol (0), maxIter (1000), minIter (0), convergenceType (0), relaxationType (6), nSweeps (1), coarsenType (10), restrictionType (0), cycleType (1), AMGVariant (0), printLevel (0), relaxOrder (0), recoversOldDefault (true), logging (0) |
| none           | —   |

```

solvers
2 {
    " (p | U) "
4   {
            solverType      hypreSolver;
6
            saveSystem      false;
8
            solver          GMRES;
10
            tolerance       0;
            relTol          1e-8;
12
            maxIter         1000;

14
            preconditioner
16           {
18             preconditioner      BoomerAMG;
20           }
}
}

```

**Listing 4.6:** Example of a *solvers* dictionary in *fvSolution* showing the use of a sparse matrix solver from Hypre library to solve momentum and pressure equations.

#### 4.4.7 Petsc interface

Petsc interface is the most complete among the three interfaces. This interface is selected by setting *solverType* = *petscSolver*. In opposition to the other two interfaces, no more parameters need to be specified under dictionary *solvers* of *fvSolution*, other than the four general parameters discussed in Section 4.4.3, as shown in the example of Listing 4.7. This is because all the parameters related with the solvers and preconditioners are read from a different file, named *petscDict*, that should be present in directory *system* of the case being solved. According to Petsc terminology, this file is the options database and allows for a great flexibility.

```

1 solvers
2 {
3     p
4     {
5         solverType      petscSolver;
6         saveSystem
7         updatePrecondFrequency 100000;
8         updateMatrixCoeffs   false;
9     }
10
11    U
12    {
13        solverType      petscSolver;
14        saveSystem
15        updatePrecondFrequency -1;
16        updateMatrixCoeffs   true;
17    }
18 }
```

**Listing 4.7:** Example of a *solvers* dictionary in *fvSolution* showing the use of a sparse matrix solver from Petsc library to solve momentum and pressure equations.

Listing 4.8 shows an example of a *petscDict* database, which, in the case illustrated, is used to control the solver options for momentum and pressure equations. The formating rules of this file are the same as for any Petsc database: the lines starting with a '#' are ignored and every option should be prepended with a '-'. One additional rule must hold, which is specific from the interface: any option related with the matrix/vector (*Mat* and *Vec* modules of Petsc) and solver (*ksp* module of Petsc) contexts should be prepended with the name of the field which is intended for, followed by an underscore. For example, option *-ksp\_type* aims at specifying the sparse matrix solver of a *ksp* context, but if we want to apply it to the pressure equation in particular, then this option should be written as *-p\_ksp\_type* (Listing 4.8). The prefix is the way Petsc distinguishes between options for different contexts (equations). Only the options which are generic, and not bounded to a particular context, should not be prepended. This is the case, for example, of option *-help*, which displays all the available options related with Petsc in a given simulation (see Petsc's documentation [9, 10] for the meaning of all options displayed). Note that the name of the prefixes should correspond to the names used to identify the solvers in dictionary *fvSolution* (lines 3 and 11 of Listing 4.7).

All the options that Petsc recognizes for the *Mat*, *Vec* and *ksp* modules can be used in Petsc interface and selected in run-time through the options database. Therefore, in opposition to the other two interfaces, there are no individual wrappers to each solver/preconditioner offered by Petsc, such that, in theory, all can be used. For the list of solvers/preconditioners available in Petsc, please consult Petsc's documentation [9, 10], or start a simulation with option *-help*. Note that some solvers/preconditioners are only available if additional packages are downloaded. This is the case, for example, of direct solvers from MUMPS. Moreover, some solvers/preconditioners are only available for sequential runs, as specified in Petsc's documentation.

In the example of Listing 4.8, it can be shown that a Cholesky decomposition (direct solver) is used to solve the pressure equation. Since *saveSystem* = true for *p* in Listing 4.7 and the matrix is not changing (*updateMatrixCoeffs* = false), the factorization is only computed once and reused in the remaining time-steps. For the velocity, a BiCGStab iterative solver (*bcgs*) preconditioned with an incomplete LU factorization (*ilu*) is employed. A number of options is further specified for this preconditioner (lines 28-32). The solver-preconditioner are created/destroyed each time the momentum equation is solved, as *saveSystem* = false in Listing 4.7. As a matter of curiosity, this setup could not be used in a parallel run, since the two preconditioners specified are not parallelized (see Petsc's documentation [9, 10]).

If the user followed the installation procedure of Chapter 2, in addition to the default solvers/preconditioners from Petsc, there are also available solvers/preconditioners from Hypre and MUMPS packages, which are downloaded via Petsc. It should be noted that some of the solvers/preconditioners wrapped in the Hypre interface (Section 4.4.6) can be also accessed from Petsc interface. However, they are based on different implementations, since the solvers/preconditioners from Hypre interface rely exclusively on Hypre's environment, whereas those accessible from Petsc's interface are intermediated by and depend on Petsc environment.

```

#####
2 ##### Global settings #####
#####
4 # -help
6 #####
8 ##### Settings for p #####
#####
10 #--> KSP
    -p_ksp_type preonly
12 #
14 #--> PC
    -p_pc_type cholesky
    -p_pc_factor_mat_solver_type petsc
16 #####
18 ##### Settings for U #####
#####
20 #--> KSP
    -U_ksp_type bcgs
22 -U_ksp_max_it 1000

```

```

24 -U_ksp_rtol 0
25 -U_ksp_atol 1e-12
26 -U_ksp_divtol 10
27
28 #--> PC
29 -U_pc_type ilu
30 -U_pc_factor_levels 10
31 -U_pc_factor_reuse_fill 1
32 -U_pc_factor_reuse_ordering 1
33 -U_pc_factor_mat_ordering_type rcm

```

**Listing 4.8:** Example of a *petscDict* options database showing the settings to solve momentum and pressure equations.

#### 4.4.8 Coupled solvers

Besides the three interfaces specified above for segregated solvers, library *sparse-MatrixSolvers* also has a class for coupled solvers. Coupled solvers are implemented based on Petsc, such that only the solvers/preconditioners available in Petsc can be used with coupled solvers.

In *rheoTool*, the coupled solvers can be used in the following scenarios:

- solve *p-u* coupled;
- solve *p-u-τ* coupled;
- solve the PNP system of equations coupled (restricted to the *NernstPlanck-Coupled* model);
- solve the PNP system of equations coupled with *p-u-τ* (restricted to the *NernstPlanckCoupled* model).

Coupled solvers are accessible from *rheoFoam*, *rheoEFoam* and *rheoBDFoam* applications. In order to use a coupled solver, dictionary *coupledSolvers* should be added to *fvSolution*. The options related with *p-u-τ* should be inserted under sub-dictionary *Uptau*, whereas the options related with the PNP system of equations (*NernstPlanckCoupled* model) should be inserted under sub-dictionary *ciPsi*. This is exemplified in Listing 4.9 and the options available are:

##### *Uptau* sub-dictionary

*solveCoupledUp* – true to solve *p-u* coupled and false to solve segregated.

*solveCoupledTau* – true to add *τ* to the *p-u* coupled system of equations and false to solve *τ* segregated. The variables *p-u-τ* are only solved coupled if both *solveCoupledUp* and *solveCoupledTau* are set to true.

*saveSystem* – see Section 4.4.3.

*updatePrecondFrequency* – see Section 4.4.3.

*updateMatrixCoeffs* – see Section 4.4.3.

*robustSumCheck*– this option is only enabled if *saveSystem* = true and controls the method used to check if the matrix of coefficients is changing over time. If this option is set to true, a robust method is employed, which, however, duplicates the matrix of coefficients, thus increasing the memory usage. If the option is set to true, the method used is the same as for segregated solvers and might fail for coupled systems of equations. We recommend using the robust method. If memory overflow is an issue of concern, simply run a few iterations in a coarse mesh to detect any variation in the matrix of coefficients and once the verification is done turn the option off and return to the fine mesh. Note that the verification algorithm is only run at the beginning of a simulation.

### ***ciPsi* sub-dictionary**

*solveWithUptau*– if true, the PNP system of equations is solved coupled with *p-u* and optionally  $\tau$ . In that case, no other options are read from dictionary *ciPsi* (the matrix controls are those of *Uptau*).

*Remaining options are the same as for Uptau*

```

coupledSolvers
2 {
3   Uptau
4   {
5     solveCoupledUp true;
6     solveCoupledTau true;
7
8     saveSystem true;
9     robustSumCheck true;
10    updatePrecondFrequency 1;
11    updateMatrixCoeffs true;
12  }
13
14  ciPsi
15  {
16    solveWithUptau      false;
17
18    saveSystem true;
19    robustSumCheck true;
20    updatePrecondFrequency 1;
21    updateMatrixCoeffs true;
22  }
}
```

**Listing 4.9:** Example of a *coupledSolvers* dictionary in *fvSolution*.

Note that the conditions enumerated in Section 4.4.1 that allow reusing the preconditioner/factorization still hold for the coupled *p-u* system of equations. However, if also  $\tau$  is solved coupled, the matrix of coefficients always changes over time due to the convective term of the constitutive equation (Eq. 3.4). In that case, *saveSystem* can still be set to true, with a user-defined *updatePrecondFrequency* (-1

for an automatic decision method), but *updateMatrixCoeffs* must be set equal to true or an error will be retrieved otherwise (if the verification algorithm is working correctly). For the coupled PNP system of equations, the matrix of coefficients changes every time-step due to the implicit discretization of the electromigration term.

Since coupled solvers are based on Petsc, the options database file (`petscDict`) controls the solution settings, as described in Section 4.4.7. The prefixes are now '`Uptau_`' and '`ciPsi_`'.

While solving a coupled system of equations, *rheoTool* will still output the information for each sub-equation (solver name, residuals and number of iterations to convergence). However, only the residual is different between sub-equations, which are computed individually according to Eq. 4.27.

As shown in [5], semi-coupled solvers show a better performance than coupled solvers in some cases, among other advantages. Therefore it is recommended to first try semi-coupled solvers, before coupled solvers. A semi-coupled solver solves part of the equations coupled and part segregated. For example, the set of options `solveCoupledUp = true`, `solveWithUptau = true` and `solveCoupledTau = true` corresponds to a coupled solver, but if `solveWithUptau = false` or `solveCoupledUp = solveWithUptau = false`, then a semi-coupled solver is obtained.

Coupled solvers in  $\tau$  can be only used with viscoelastic fluid models solved in  $\tau$  variable, which excludes all the implementations based on transformation of variables (conformation and log-conformation tensor). For GNF models,  $p\text{-}\mathbf{u}$  can be solved coupled, but the viscosity is a fully-explicit function of the strain-rate.

#### 4.4.9 How to use *sparseMatrixSolvers* library in my own application?

##### ☒ Segregated solvers

In order to use the interfaces from *sparseMatrixSolvers* library in a segregated solver, follow these steps:

- include header *sparseMatrixSolvers.H* in your application. Note that this header file should be ideally the first to be included, in order to avoid namespace conflict with Petsc;
- create an object `autoPtr < sparseSolver < Type >>`, where *Type* can be any of the valid OpenFOAM® types. The constructor requires the field for which the equation will be built and solved. See an example in `createSolvers.H` of solver *rheoEFoam*;
- call function `solve(fvMatrix < Type >)` of the object created to solve the equation. The *Type* of the matrix should be consistent with the *Type* used in the constructor. See an example in `pEqn.H` of solver *rheoEFoam*;
- add the path of *sparseMatrixSolvers* library and its dependencies to the Make/option file of your application. See, for example, the Make/option file of solver *rheoEFoam*.

### ❖ Coupled solvers

In order to use the interfaces from *sparseMatrixSolvers* library in a coupled solver, follow these steps:

- include headers *sparseMatrixSolvers.H* and *blockOperators.H* in your application. Note that header *sparseMatrixSolvers.H* should be ideally the first to be included, in order to avoid namespace conflict with Petsc;
- create an object *autoPtr < coupledSolver >*;
- insert **all** the fields being solved in the object created, using function *insertField(volField < Type >)*. *Type* is any valid OpenFOAM® type. Note that **all** fields must be already inserted before the first equation is inserted in the next step. You can *lookup* the *autoPtr < coupledSolver >* object to add fields from other compilation units, since the class is object-registered;
- insert all the equations in the *autoPtr < coupledSolver >* object with a call to function *insertEquation(word, word, eqType)*, where *eqType* is either an *fvMatrix < Type >* or a *LMatrix < Type >*, with *Type* being any valid OpenFOAM® type. Note that class *LMatrix < Type >* has been created in *rheoTool* to handle special coupling terms that are discretized with *fvmf* operators. The first and second arguments of function *insertEquation()* correspond to the names of the field for which the equation is being written and the field which is contributing to that equation, respectively. These are technical details related with new classes added to OpenFOAM® through *rheoTool*. It is not expected that the reader (programmer) understand them without having examined the code before;
- after **all** the equations and coupling terms have been inserted, solve the coupled system of equations through a call to function *solve()*. Note that in a coupled solution method all the governing equations are solved simultaneously;
- add the path of *sparseMatrixSolvers* and *fvmf* libraries and their dependencies to the Make/option file of your application. See, for example, the Make/option file of solver *rheoEFoam*.

The above explanation for coupled solvers might seem abstract if the code behind was not analyzed before. Therefore, we strongly recommend programmers to first take a look into directories *fvmf* and *sparseMatrixSolvers* and any application using coupled solvers, as for example *rheoEFoam* and model *Nernst-PlanckCoupled*.

#### 4.4.10 Limitations

These are some known limitations of the *sparseMatrixSolvers* library:

- the interfaces were not tested with *cyclic*-derived patches other than *cyclic* itself. For example, *cyclicAMI* is untested.
- some preconditioners in Hypre (mostly) and Petsc interfaces do not work correctly in serial runs.
- the residuals retrieved by coupled solvers in the **first time** the system of equation is solved do not correspond to the reality for any non-zero initial solution (field).
- Eigen interface can not be used in parallel.
- coupled solvers are not using the block matrix structures of Petsc, which is probably deteriorating performance.
- the coupled PNP system of equations (*NernstPlanckCoupled* model) shows some instability in non-orthogonal grids due to the electromigration term. To mitigate this issue, use *cellLimited* gradient schemes for electric-related variables.
- boundary condition *fixedFluxExtrapolatedPressure* for pressure can not be used if  $p\text{-}\mathbf{u}$  are solved coupled.

It is worth noting that the default OpenFOAM® sparse matrix solvers display the best performance in most of the times. The sparse matrix solvers from the external libraries are only advantageous when OpenFOAM® sparse matrix solvers require a high number of iterations to converge. In those cases, it is typically possible to setup a solver from an external library that outperforms the *openFoamSolver* interface. We simply want to alert that the default sparse matrix solvers of OpenFOAM® will continue being a good (the best) option in most of the situations where a segregated solver is applied.

## 4.5 Solvers

**!** The discussion presented in this Section assumes a segregated solution method. However, a coupled solution method is also available for some solvers in the OpenFOAM® version.

The solvers available in *rheoTool* are summarized in Table 4.8. Each one is discussed in detail in the following sections.

**Table 4.8:** Brief description of the solvers available in *rheoTool*.

| Name | Description |
|------|-------------|
|------|-------------|

---

|                      |  |
|----------------------|--|
| <i>rheoFoam</i>      | Transient solver for pressure-driven, single-phase, laminar, isothermal flows. Selection of rheology is general among all the available GNF and viscoelastic models.   |
| <i>rheoInterFoam</i> | Transient solver for pressure-driven, two-phase, laminar, isothermal flows, using the volume-of-fluid (VOF) approach. Selection of rheology for each phase is general among all the available GNF and viscoelastic models.                   |
| <i>rheoTestFoam</i>  | Application to compute steady and transient material properties for any of the available GNF and viscoelastic models.  |
| <i>rheoEFoam</i>     | Transient solver for electrically-driven, single-phase, laminar, isothermal flows. Mixed electric-/pressure-driven flows are also allowed. Selection of rheology is general among all the available GNF and viscoelastic models.             |
| <i>rheoBDFoam</i>    | Solver for Brownian dynamics simulations. The external forcing can be analytical or numerical (transient or steady). The external numerical forcing can be electrophoresis, electroosmosis, a pressure-driven flow or a combination of them. |

---

### 4.5.1 *rheoFoam*

Solver *rheoFoam* implements the transient, incompressible Navier-Stokes equations for single-phase flows of GNF or viscoelastic fluids. Figure 4.2 displays the solving sequence when the equations are solved segregated.

The solver has three main loops: *L1*, which is advancing the time; *L2*, which is an inner-loop used to converge the solution at each time-step; and *L3*, a loop which can be enabled for non-orthogonal grids, in order to update (inside each time-step and each inner-iteration) the explicit correction of the pressure Laplacian, avoiding stability problems and reducing the error in transient computations. More than understanding each step identified in Fig. 4.2, we want to help the reader to identify them in the source code and relate them with the theory presented in the previous Chapter. With this purpose in mind, we will do a tour to the source code of the solver and the most important points will be discussed, skipping the lines not essential to understand the algorithm.

The solver *rheoFoam* is composed of one main file (*rheoFoam.C*) and other associated header files, among which (*createFields.H*, *createPPutil.H*, *UEqn.H*, *pEqn.H*, *CEqn.H*), that can be found in directory *src/solvers/rheoFoam/*. All the header files are included from the main *.C* file. We will start

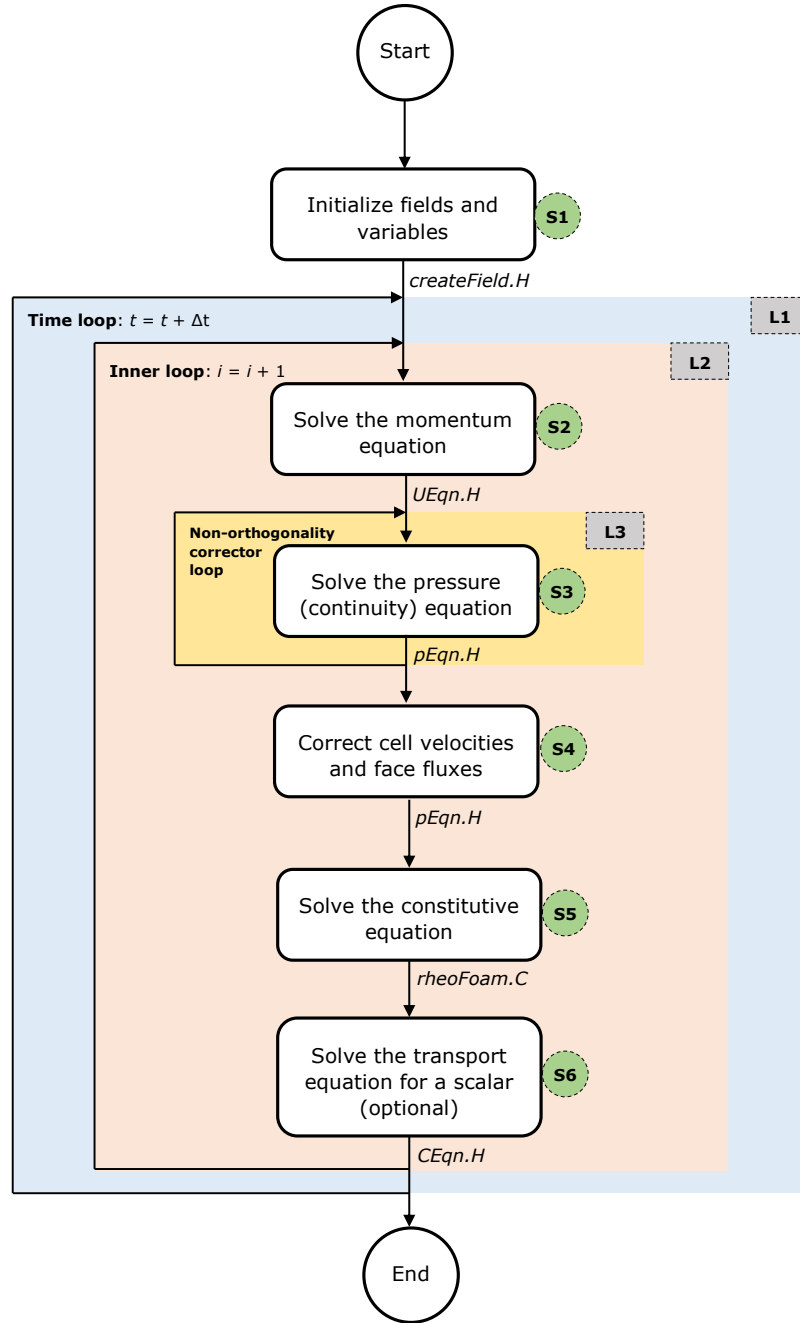


**Figure 4.2:** Solving sequence of *rheoFoam* under a segregated solution method (steps related with mesh motion are omitted for simplicity).

by digging into *rheoFoam.C*, whose source code is displayed in Listing 4.10.

- lines **1-9**: those *# include* lines load classes used by OpenFOAM® for standard tasks, transversal to most of the OpenFOAM® solvers.
- line **11**: this *# include* is providing access to a library of post-processing

utilities, that we discuss later in Section 4.7.2.

- line **12**: this `# include` allows the solver to access the models defined in the *constitutiveEquations* library.
- lines **17-29**: fields, variables, controls and the mesh are created (step *S1* of Fig. 4.2). Lines 23 and 27 point to the header files `createFields.H` and `createPPutil.H`, respectively, located in the same directory as `rheoFoam.C`. The later is responsible for the creation of post-processing utilities.
- lines **36-93**: represents the time loop, i.e., *L1* of Fig. 4.2. The solver will keep running until the final specified time is reached or once the residuals of the solved variables drop below some tolerance (this dual criterion is specific of class *simpleControl*).
- lines **38-40**: those `# include` allow automatic time-step adjustment, based on the maximum Courant number specified by the user. This control can be switched off by the user (more details in Section 5.1.1).
- lines **66-85**: this is the inner loop, *L2*, of Fig. 4.2. Inside this loop, all the conservation equations are solved *nIter* times inside the same time-step. This reduces the explicitness of the method, which exists, for example, in the non-linear convective term of the momentum equation, in the both-sides-diffusion technique and in several terms of the constitutive equation (for a given equation, only the terms introduced through a *fvm::* operator are implicit). Furthermore, these iterations also strengthen the coupling between velocity and pressure.
- lines **44**: this function executes the mesh motion if the mesh is dynamic. For a static mesh, this function has no practical effects.
- lines **46-63**: these lines are only executed for dynamic meshes and include an optional correction of fluxes (line 53). Note that the term  $\mathbf{u}_b$  of Eq. (3.24) is subtracted from  $\mathbf{u}$  in line 57.
- line **73**: the momentum equation is solved. The header file `UEqn.H` (Listing 4.11) will be explored later.
- line **74**: the pressure equation is solved. The header file `pEqn.H` (Listing 4.12) will be explored later.
- line **78**: function *correct()* of the constitutive model is called. As seen before, this function updates variable  $\boldsymbol{\tau}$  by solving the constitutive equation(s).
- line **81-84**: the equation for a passive scalar is optionally solved, depending on a user-defined selection (more details in Section 5.1.1). The header file `CEqn.H` (Listing 4.13) will be explored later.
- lines **87**: this is where the post-processing utilities are evaluated, if any has been selected by the user.

```
1 #include "fvCFD.H"
2 #include "IFstream.H"
3 #include "OFstream.H"
4 #include "simpleControl.H"
5 #include "fvOptions.H"
6 #include "extrapolatedCalculatedFvPatchField.H"
7 #include "dynamicFvMesh.H"
8 #include "CorrectPhi.H"
9 #include "adjustCorrPhi.H"

11 #include "ppUtilInterface.H"
12 #include "constitutiveModel.H"
13 // * * * * * * * * * * * * * * * * * * * * * * * * * * * * * * * * * * *
14 * * * * * //

15 int main(int argc, char *argv[])
{
16
17     #include "postProcess.H"
18     #include "setRootCase.H"
19     #include "createTime.H"
20     #include "createDynamicFvMeshDict.H"
21     #include "createDynamicFvMesh.H"
22     #include "initContinuityErrs.H"
23     #include "createFields.H"
24     #include "createControls.H"
25     #include "createUfIfNeeded.H"
26     #include "createFvOptions.H"
27     #include "createPPutil.H"
28     #include "CourantNo.H"
29     #include "setInitialDeltaT.H"
30     // * * * * * * * * * * * * * * * * * * * * * * * * * * * * * * * * *
31     * * * * * //
32
33     Info<< "\nStarting time loop\n" << endl;
34
35     // --- Time loop ---
36
37     while (simple.loop())
38     {
39         #include "readControls.H"
40         #include "CourantNo.H"
41         #include "setDeltaT.H"
42
43         Info<< "Time = " << runTime.timeName() << nl << endl;
44
45         mesh.update();
46
47         if (mesh.changing())
48         {
49             // Calculate absolute flux from the mapped surface
50             // velocity
51             phi = mesh.Sf() & Uf();
52
53             if (correctPhi)
54             {
55                 #include "correctPhi.H"
```

```

55
56     }
57
58     // Make the flux relative to the mesh motion
59     fvc::makeRelative(phi, U);
60
61     if (checkMeshCourantNo)
62     {
63         #include "meshCourantNo.H"
64     }
65
66     // --- Inner loop iterations ---
67     for (int i=0; i<nInIter; i++)
68     {
69         Info << "Inner iteration: " << i << nl << endl;
70
71         // --- Pressure-velocity SIMPLEC corrector
72         {
73             // ---- Solve U and p ----
74             #include "UEqn.H"
75             #include "pEqn.H"
76         }
77
78         // ---- Solve constitutive equation ----
79         constEq.correct();
80
81         // --- Passive Scalar transport
82         if (sPS)
83         {
84             #include "CEqn.H"
85         }
86
87         postProc.update();
88         runTime.write();
89
90         Info << "ExecutionTime = " << runTime.elapsedCpuTime() << " "
91             << " s"
92             << " ClockTime = " << runTime.elapsedClockTime() << " "
93                 << " s"
94                 << nl << endl;
95     }
96
97     Info << "End\n" << endl;
98
99     return 0;
}

```

**Listing 4.10:** Source code of *rheoFoam.C*.

The source code in file *createFields.H* will not be discussed, since it mainly contains standard declaration/initialization of fields and variables. However, it is worth mentioning the creation of a *constitutiveModel* object, named *constEq*, which stores the data of the constitutive equation selected.

According to the SIMPLEC algorithm, the momentum equation is first solved

to obtain an estimated velocity field, using the pressure field of the previous inner-iteration or time-step. Then, we solve for the pressure field enforcing continuity. Finally, using the correct pressure field, the previously estimated velocity is corrected, both on faces and cell centers. This is what is being executed in `UEqn.H` and `pEqn.H`. We follow the discussion by analyzing the content of `UEqn.H`, whose code is displayed in Listing 4.11.

- lines **5-13**: this is where the momentum equation is built. We can identify the transient term in line 7, an eventual acceleration term arising from a non-inertial reference frame in line 8, the convective term in line 9, an extra momentum source term in line 11 (term  $\mathbf{f}$  in Eqs. 3.5 and 3.18) and the extra-stress divergence in line 12 ( $\nabla \cdot \boldsymbol{\tau}'$ ), containing both the solvent and the polymeric contributions (remember the output of `divTau()` function, analyzed in Section 4.1.4).
- line **21**: the momentum equation is solved considering the pressure gradient contribution, where the pressure field from the last time-step or inner-iteration is used. This term was not added before in order for operator  $\mathbf{H}$  obtained from the momentum equation to be free of such contribution, as discussed in Section 3.3.1. This is required to avoid the onset of checkerboard fields, since a traditional Rhie-Chow interpolation is not used (cf. Ref. [2]).

```

1 // Momentum predictor
2
3     MRF.correctBoundaryVelocity(U);
4
5     tmp<fvVectorMatrix> tUEqn
6     (
7         fvm::ddt(U)
8         + MRF.DDt(U)
9         + fvm::div(phi, U)
10        ==
11        fvOptions(U)
12        + constEq.divTau(U)
13    );
14
15     fvVectorMatrix& UEqn = tUEqn.ref();
16
17     UEqn.relax();
18
19     fvOptions.constrain(UEqn);
20
21     solve(UEqn == -fvc::grad(p));
22
23     fvOptions.correct(U);

```

**Listing 4.11:** Source code of `UEqn.H`.

After having a guessed (non-conservative) velocity field, we will see how it is used inside `pEqn.H` (Listing 4.12):

- lines **1-32**: variables required to solve the pressure equation (Eq. 3.15) are assembled. The sequence of steps can be easily understood, keeping in mind

that  $UEqn().A()$  retrieves diagonal coefficients ( $a_P$ ) and that  $UEqn().H()$  and  $UEqn().H1()$  stand for operators  $\mathbf{H}$  and  $H_1$ , respectively. As previously discussed in Section 3.3.1, pressure gradient terms entering the definition of face fluxes (line 26) are directly evaluated on cell faces to avoid checkerboard fields. Also, in line 8/11 there is the addition of the corrective term for time-step dependency, described in Section 3.3.1.

- lines **35-50**: this is the non-orthogonality corrector loop ( $L3$ ) displayed in Fig. 4.2. The goal is similar to the one of the inner loop: minimizing the explicitness of the algorithm. At this point, the reader may be asking why do this loop exists if the inner loop is already there doing a similar task? To clarify this point, it should be noted that the non-orthogonality corrector loop only makes sense to exist for non-orthogonal meshes. For those meshes, the *laplacian* operator in line 39 is not completely handled in an implicit way, but an explicit corrective term is added. For highly non-orthogonal meshes, this term has an important contribution and, due to being explicit, the pressure solution will not be continuity-compliant, which can afterwards introduce continuity problems and lead the simulation to diverge. For this reason, in such cases the implicitness of the Laplacian term is increased by continuously solving that equation with the updated pressure-field, and the fluxes are only corrected at the last iteration of this loop (lines 46-49). Is the non-orthogonal corrector loop absolutely necessary when dealing with non-orthogonal meshes? No, as long as the simulation does not diverge and if only steady-state results are required. Otherwise, this loop should be active. For a number of cases, doing 2-3 non-orthogonal iterations keeps the solver stable, without the need of under-relaxing the pressure. Even if only one non-orthogonal correction is performed, the Laplacian term should still be discretized with the corrective term to keep the accuracy in non-orthogonal meshes.
- lines **39,44**: the pressure equation (Eq. 3.15) is assembled (line 39) and solved (line 44).
- line **48**: this is the equation which corrects the face fluxes (Eq. 3.16 interpolated to the faces). Again, pressure gradient terms are directly evaluated on cell faces: the *snGrad()* operator in line 26, when building *phiHbyA*, and the one coming from the *laplacian()* operator in line 39, from which the *flux()* operator is derived.
- line **57**: this is the equation which corrects the cell-centered velocity field (Eq. 3.16).
- line **69**: the term  $\mathbf{u}_b$  of Eq. (3.24) is subtracted from  $\mathbf{u}$  (the operation is on face fluxes, variable *phi*).

```

1 volScalarField rAU(1.0/UEqn.A());
volVectorField HbyA(constrainHbyA(rAU*UEqn.H(), U, p));
3 surfaceScalarField phiHbyA

```

```

(
5   "phiHbyA",
6   mesh.changing() == true ?
7   fvc::flux(HbyA)
8   + fvc::interpolate(rAU)*fvc::ddtCorr(U, Uf())
9   :
10  fvc::flux(HbyA)
11  + fvc::interpolate(rAU)*fvc::ddtCorr(U, phi)
);
13
MRF.makeRelative(phiHbyA);
15
if (p.needReference())
17 {
18   fvc::makeRelative(phiHbyA, U);
19   adjustCorrPhi(phiHbyA, U, p);
20   fvc::makeAbsolute(phiHbyA, U);
21 }

23 tmp<volScalarField> rAtU(rAU);

25 rAtU = 1.0/(1.0/rAU - UEqn.H1());
26 phiHbyA += fvc::interpolate(rAtU() - rAU)*fvc::snGrad(p)*mesh.
27   magSf();
28 HbyA -= (rAU - rAtU())*fvc::grad(p);

29 tUEqn.clear();

31 // Update the pressure BCs to ensure flux consistency
32 constrainPressure(p, U, phiHbyA, rAtU(), MRF);
33
34   // Non-orthogonal pressure corrector loop
35   while (simple.correctNonOrthogonal())
36   {
37     fvScalarMatrix pEqn
38     (
39       fvm::laplacian(rAtU(), p, "laplacian(p|(ap-H1))" ) ==
40         fvc::div(phiHbyA)
41     );
42
43     pEqn.setReference(pRefCell, pRefValue);
44
45     pEqn.solve();
46
47     if (simple.finalNonOrthogonalIter())
48     {
49       phi = phiHbyA - pEqn.flux();
50     }
51
52   #include "continuityErrs.H"
53
54   // Explicitly relax pressure for momentum corrector
55   p.relax();
56
57   U = HbyA - rAtU*fvc::grad(p);

```

```

U.correctBoundaryConditions();
59 fvOptions.correct(U);

61 if (mesh.changing())
{
63     Uf() = fvc::interpolate(U);
     surfaceVectorField n(mesh.Sf()/mesh.magSf());
65     Uf() += n*(phi/mesh.magSf() - (n & Uf()));
}
67
// Make the fluxes relative to the mesh motion
69 fvc::makeRelative(phi, U);

```

**Listing 4.12:** Source code of pEqn.H.

After pEqn.H is executed, both the pressure and the face fluxes are continuity-compliant, but not the cell-centered velocity field. The conservative fluxes can now be used to solve any transport equation. In *rheoFoam*, we offer the possibility to solve a transport equation for a passive scalar. The governing equation, included in file CEqn.H, is simply a convection-diffusion transport equation, as can be seen in lines 5-11 of Listing 4.13.

```

1 // Transport of passive scalar

3 dimensionedScalar D_ = cttProperties.subDict("passiveScalarProperties").lookup("D");

5 fvScalarMatrix CEqn
(
7     fvm::ddt(C)
+ fvm::div(phi, C)
9     ==
11     fvc::laplacian(D_, C)
);

13 CEqn.relax();
CEqn.solve();
15
17 if (U.time().outputTime())
{
18     C.write();
19 }

```

**Listing 4.13:** Source code of CEqn.H.

### 4.5.2 *rheoTestFoam*

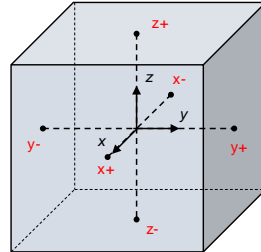
The main purpose of solver *rheoTestFoam* is to evaluate the behavior of the constitutive models for a user-defined  $\nabla\mathbf{u}$  tensor. At the same time, it can also be envisaged as a basic debugging tool to check for the correct implementation of the constitutive models, since an analytical or semi-analytical solution usually exists, which can be used for comparison.

Shortly, *rheoTestFoam* solves for the solvent and polymeric constitutive equations, Eqs. (3.3) and (3.4), respectively, for a prescribed  $\nabla\mathbf{u}$  tensor, assuming

homogeneous flow conditions ( $\nabla \cdot \boldsymbol{\tau} = 0$ ;  $\mathbf{u} \cdot \nabla \boldsymbol{\tau} = 0$ ). Since there are no approximations related with spatial discretization, the resulting steady-state solution  $\boldsymbol{\tau}' = \boldsymbol{\tau} + \boldsymbol{\tau}_s$  is exact, and OpenFOAM® is simply acting as a nonlinear matrix solver. To obtain unsteady solutions, the temporal discretization introduces numerical errors during the transient period, which can be reduced using a small time-step.

The computational domain used with this solver is composed of a single cell: a cube with unitary edge length (1 m). The boundary conditions for  $\mathbf{u}$  are internally manipulated inside the code, in order to get the tensor  $\nabla \mathbf{u}$  defined by the user, Fig. 4.3. Thus, **the default mesh and boundary conditions should not be changed** by the user when working with *rheoTestFoam*. We note that the following definition holds in this guide (and in OpenFOAM®, in general):

$$(\nabla \mathbf{u})_{ij} = \frac{\partial u_j}{\partial x_i} = \begin{bmatrix} \frac{\partial u}{\partial x} & \frac{\partial v}{\partial x} & \frac{\partial w}{\partial x} \\ \frac{\partial u}{\partial y} & \frac{\partial v}{\partial y} & \frac{\partial w}{\partial y} \\ \frac{\partial u}{\partial z} & \frac{\partial v}{\partial z} & \frac{\partial w}{\partial z} \end{bmatrix} \quad (4.28)$$



$$\mathbf{u}_{x-} = \left( \kappa_1 - \left( \frac{\partial u_x}{\partial x} \right) \frac{\delta x}{2}, \kappa_2 - \left( \frac{\partial u_y}{\partial x} \right) \frac{\delta x}{2}, \kappa_3 - \left( \frac{\partial u_z}{\partial x} \right) \frac{\delta x}{2} \right) \quad \mathbf{u}_{x+} = \left( \kappa_1 + \left( \frac{\partial u_x}{\partial x} \right) \frac{\delta x}{2}, \kappa_2 + \left( \frac{\partial u_y}{\partial x} \right) \frac{\delta x}{2}, \kappa_3 + \left( \frac{\partial u_z}{\partial x} \right) \frac{\delta x}{2} \right)$$

$$\mathbf{u}_{y-} = \left( \kappa_1 - \left( \frac{\partial u_x}{\partial y} \right) \frac{\delta y}{2}, \kappa_2 - \left( \frac{\partial u_y}{\partial y} \right) \frac{\delta y}{2}, \kappa_3 - \left( \frac{\partial u_z}{\partial y} \right) \frac{\delta y}{2} \right) \quad \mathbf{u}_{y+} = \left( \kappa_1 + \left( \frac{\partial u_x}{\partial y} \right) \frac{\delta y}{2}, \kappa_2 + \left( \frac{\partial u_y}{\partial y} \right) \frac{\delta y}{2}, \kappa_3 + \left( \frac{\partial u_z}{\partial y} \right) \frac{\delta y}{2} \right)$$

$$\mathbf{u}_{z-} = \left( \kappa_1 - \left( \frac{\partial u_x}{\partial z} \right) \frac{\delta z}{2}, \kappa_2 - \left( \frac{\partial u_y}{\partial z} \right) \frac{\delta z}{2}, \kappa_3 - \left( \frac{\partial u_z}{\partial z} \right) \frac{\delta z}{2} \right) \quad \mathbf{u}_{z+} = \left( \kappa_1 + \left( \frac{\partial u_x}{\partial z} \right) \frac{\delta z}{2}, \kappa_2 + \left( \frac{\partial u_y}{\partial z} \right) \frac{\delta z}{2}, \kappa_3 + \left( \frac{\partial u_z}{\partial z} \right) \frac{\delta z}{2} \right)$$

**Figure 4.3:** Boundary conditions manipulation in the single-cell mesh used with *rheoTestFoam*. The constants currently used to represent the cell-centered velocity are  $\kappa_1 = \kappa_2 = \kappa_3 = 0$ , although any other values could be used. The edge length of the cubic cell is set to  $\delta x = \delta y = \delta z = 1\text{m}$ .

Two operation modes are available with this solver:

- **ramp mode:** the user defines a list of  $\nabla \mathbf{u}$  tensors and the solver will retrieve the steady solution for each entry. In this mode, the solver automatically selects the ideal time-step value to be used and the steady-state is also automatically detected (either the relative variation of the extra-stress magnitude

drops below  $10^{-8}$ , or after a predefined number of time-steps has been exceeded – this last condition is used to avoid infinite loops).

- **transient mode:** the user defines one single  $\nabla\mathbf{u}$  tensor and the solver will return the evolution over time of the monitored variables. In this case, both the time-step and the end time are controlled by the user. This mode allows to determine the transient material functions of the constitutive model selected.

As default behavior, *rheoTestFoam* writes a file named `Report` containing all the components of the total extra-stress tensor,  $\boldsymbol{\tau}'$  (remember that  $\boldsymbol{\tau}' = \boldsymbol{\tau} + \boldsymbol{\tau}_s$  is the total extra-stress tensor, including both solvent and polymeric contributions). In ramp mode, also the status (*Converged* or *Exceed\_Niter*) is returned, along with the relative error. The user can compute any relevant material function from the tensor components retrieved. If for some reason the status *Exceed\_Niter* is retrieved for any  $\nabla\mathbf{u}$  entry in *ramp* mode, we recommend to run *rheoTestFoam* in *transient* mode for that same  $\nabla\mathbf{u}$ , using a small time-step – at convergence, the steady material properties will be obtained. This may happens, for example, when using a multimode model with very different modes, for which the automatic time-stepping procedure fails to choose a stable time-step for the given  $\nabla\mathbf{u}$ . On the other hand, some viscoelastic models are naturally unbounded under certain flow conditions, such as the UCM and Oldroyd-B models for  $Wi \geq 0.5$  in extensional flow. Care should be taken for such situations, since the solver will most likely retrieve a non-physical solution close to those limits and eventually diverge.

Note that *rheoTestFoam* is only adapted to work optimally in ramp mode with the models implemented in the extra-stress tensor variable, which excludes the models solved with the log-conformation approach or with the conformation tensor (FENE-type). However, the material functions for a given model are the same independently of the variable in which it is solved for, as long as all the terms are accounted for. Thus, it is possible to extract the material functions of all the models provided in *rheoTool*.

In a future release of *rheoTool*, we anticipate that the solver *rheoTestFoam* will be able to fit the available constitutive models to experimental data input by the user and return the best-fit model, along with the best-fit parameters ( $\lambda, \eta, \dots$ ). This will allow to run simulations with a numerical model reproducing properly the material functions of real fluids.

### 4.5.3 *rheoInterFoam*



*Section 4.5.3 is under development.*

The solver *rheoInterFoam* is a generalization of *rheoFoam* for two-phase flows, using the Volume of Fluid (VOF) method of OpenFOAM® to represent the interface between the two phases.

Currently, *rheoInterFoam* solves a constitutive equation for each phase and the extra-stress tensor contributing to the momentum equation is the weighted average of the extra-stress tensor for each phase, where the weighing is ensured by the indicator function used in VOF. This approach allows to have phases represented by different constitutive equations, although this is possibly not the most accurate and stable way to do the computations. Additionally, the SIMPLEC algorithm used for single-phase flows may need to be improved when used in *rheoInterFoam*. Other aspects are still under test, which makes the current version of *rheoInterFoam* still experimental. Nonetheless, this version is fully functional.

#### 4.5.4 *rheoEFoam*

The solver *rheoEFoam* is the extension of *rheoFoam* to electrically-driven flows – note the additional *E* in the solver name, which points to its *Electric* component. Thus, with no surprise, both solvers share the same basic structure and only minor differences exist between both at the code level. For this reason, we will not discuss again the common parts. Instead, we refer the reader to Section 4.5.1 to eventually recall the structure of *rheoFoam* and in this Section we only highlight the main differences introduced in *rheoEFoam*. Note that *rheoEFoam* allows the combination of both electrically- and pressure-driven flows with no restrictions. Pure pressure-driven flows can be also simulated with *rheoEFoam*, for which the solver becomes functionally equivalent to *rheoFoam*, although directly using *rheoFoam* is the more efficient option in these situations.

Starting by the file `createFields.H`, there is an extra line for the creation of the electric model, as shown in Listing 4.14.

```
1 // Create the electric model
  EHDEKModel elecM(phi);
```

**Listing 4.14:** Line in the file `createFields.H` of *rheoEFoam*, where the electric model is created.

In file `rheoEFoam.C`, the header `# include "EDFModel.H"` has been added in order to enable the use of the *EDFModels* library, whose path had also to be added to file `Make/options`. The other change is in the inner-iteration loop, which now includes solving the electric-related equations (line 21, Listing 4.15), calling the function `correct()` of the electric model (recall an example of that function in lines 188-281 of Listing 4.3). The user may also choose not to solve the equations governing the fluid flow (see the `if` condition in line 7 of Listing 4.15). This is useful when only the electric component of the problem is of interest.

```
// --- Inner loop iterations ---
2   for (int i=0; i<nInIter; i++)
{
4
    Info << "Inner iteration: " << i << nl << endl;
6
    if (solveFluid)
8
    {
        // --- Pressure-velocity SIMPLEC corrector
10 }
```

```

12          // ---- Solve U and p ----
13          #include "UEqn.H"
14          #include "pEqn.H"
15      }
16
17          // ---- Solve constitutive equation ----
18          constEq.correct();
19      }
20
21          // ---- Update electric terms ----
22          elecM.correct();
23
24          // --- Passive Scalar transport
25          if (sPS)
26          {
27              #include "CEqn.H"
28          }
29      }

```

**Listing 4.15:** Inner-iteration loop of *rheoEFoam* (source code: *rheoEFoam.C*).

Finally, the last change at the code level is in file *UEqn.H*, containing the momentum equation, which has been modified to include the electric body-force (line 9, Listing 4.16) – it can be a null vector, depending on the EDF model selected.

```

1 tmp<fvVectorMatrix> tUEqn
2 (
3     fvm::ddt(U)
4     + MRF.DDt(U)
5     + fvm::div(phi, U)
6     ==
7     fvOptions(U)
8     + constEq.divTau(U)
9     + elecM.Fe() / constEq.rho()
) ;

```

**Listing 4.16:** Momentum-balance equation in *rheoEFoam* (source code: *UEqn.H*).

### 4.5.5 *rheoBDFoam*

Solver *rheoBDFoam* is intended for Brownian dynamics simulations in generic meshes. In a glance, the source code of *rheoBDFoam* is simply the one of *rheoEFoam*, to which we added an object of class *sPCloudInterface*, that is updated over time. Therefore, we recommend the reader to first take a look at Sections 4.3 and 4.5.4. The pieces of code specifically devoted to Brownian dynamics are mainly contained in header files *createLagrangianFields.H* and *moleculesEqns.H*. In *createLagrangianFields.H*, a *sPCloudInterface* object is created and named *molecules*. This header file is called once in *rheoBDSFoam.C*, at the beginning of the simulation. On the other hand, header

file `moleculesEqns.H` is included in `rheoBDSFoam.C` each iteration of the main time loop. Let's take a look on its source code (Listing 4.17):

- lines **8-14**: these lines enclose a special loop, which first divides the Eulerian time-step by  $nSubCycles$ , and then performs the operations inside it. The old time is incremented by this new time-step in each iteration of the loop, such that an entire original (Eulerian) time-step is elapsed upon completion of the loop. This procedure allows to use the original Eulerian time-step everywhere outside the loop (e.g. in solving continuum equations), while a lower time-step can be used for the operations enclosed in the loop, as long as  $nSubCycles > 1$  (this variable should be a positive integer different from 0; line 1). The operation executed inside the loop is defined at line 10, which basically consists in a call to function `update()` of object `molecules`. The tasks carried out by this function have been discussed in Section 4.3.2 and result essentially in the update of the molecules' state. The return value of the function is *true* if at least one valid molecule remains in the computational mesh, otherwise it is *false* and forces an early exit from the loop (lines 12-13).
- lines **20-24**: the main time loop of the solver is exited if no valid molecules remain inside the mesh.

```

1   int nSubCycles = mesh.solutionDict().subDict("SIMPLE") .
2     lookupOrDefault<int>("nSubCycles", 1);
3
4   Info<< "Moving molecules." << endl;
5
6   scalar t0(runTime.elapsedCpuTime());
7
8   bool cont;
9   for (subCycleTime molcSubCycle(runTime, nSubCycles); !(++molcSubCycle).end())
10  {
11    cont = molecules.update();
12    // Exit subcycle
13    if (!cont)
14      break;
15  }
16
17  execTimeLagrang += (runTime.elapsedCpuTime() - t0);
18  Info<< "ExecutionTime Lagrangian = " << execTimeLagrang << " s"
19  << endl;
20
21  // Exit simple loop
22  if (!cont)
23  {
24    Info << nl << "No more valid molecules inside the computational
25    domain." << nl << "Exiting time loop." << nl << endl;
26    break;
27  }

```

**Listing 4.17:** Source code of header file `moleculesEqns.H` used by solver `rheoBDFoam` to update the molecules' state.

If an analytical external forcing is used, or if a numerical one is used but not solved for (frozen flow), then *rheoBDFoam* is basically just updating the molecules state. Otherwise, it also solves the continuum equations. Note that the algorithm used for Brownian dynamics follows a one-way coupling approach: the continuum fields affect the molecules motion, but not the opposite. Therefore, the momentum equation, as well as any other equation related with the continuum, keeps unchanged upon inclusion of molecules. Moreover, this also allows to decouple continuum computations from Brownian dynamics computations, and, in practice, a steady-state continuum field previously computed can be simply used and kept frozen over time to move the molecules. The sole exception is when we need to study the molecules dynamics in a transient continuum field. Details on the simulation settings to run *rheoBDFoam* and to select between analytical/numerical, steady/transient forcing, etc., are provided in Section 5.5.1.

## 4.6 Boundary conditions

### 4.6.1 *linearExtrapolation*

**TypeName:** *linearExtrapolation*

**Type:** fixed-value (any type field).

**Formula:**  $T_{ij,f} = T_{ij,P} + (\nabla T_{ij})_P \cdot \mathbf{d}_{Pf}$ , where  $T_{ij}$  is the  $ij$  component of the generic field  $T$  (scalar, vector or tensor), indices  $f$  and  $P$  represent the boundary face and the cell owning that face, respectively, and  $\mathbf{d}_{Pf}$  is the vector connecting their geometrical centers.

**Description:** linear extrapolation of each field component from boundary cells to boundary faces. Shortly, this boundary condition starts by computing the gradient of each component at the center of the cell owning the boundary face (using the previous iteration/time-step known values on the boundary face). Then, with both the value and the gradient of each component at those locations, the components at the boundary faces are estimated by linear extrapolation. The discretization scheme to compute the gradients enrolled in the process is run time selectable and can be adjusted in dictionary *fvSchemes*, through the entry *linExtrapGrad* followed by the selected scheme, in the *gradSchemes* subDict. In general, using linear extrapolation for the polymeric extra-stress tensor on walls should be preferred in relation to a zero-gradient boundary condition, which has a lower order of accuracy [2].

Since version 2.0, an optional second-order accurate linear regression (see [38]) can be selected by adding the entry *useRegression true* to the dictionary defining the BC, i.e., below keyword *type*, for example. If not present, the solver will execute by default the linear extrapolation defined above.

### 4.6.2 *navierSlip*

**TypeName:** *navierSlip*

**Type:** fixed-value (vector).

**Formula:**

$$\mathbf{u}_f^{t+\Delta t} = (1 - URF) \mathbf{u}_f^t + URF \begin{cases} -k_{nl} |\boldsymbol{\tau}'_{w,f}|^m \frac{\boldsymbol{\tau}'_{w,f}}{|\boldsymbol{\tau}'_{w,f}|} & , \text{model} = \text{nonLinearNavierSlip} \\ -\alpha (1 - \beta |\boldsymbol{\tau}'_{w,f}|) \boldsymbol{\tau}'_{w,f} & , \text{model} = \text{slipTT} \end{cases}$$

where  $URF$  is the under-relaxation factor ( $0 < URF \leq 1$ ),  $\mathbf{u}_f^t$  is the boundary velocity at the previous time-step, and  $k_{nl}$ ,  $m$ ,  $\alpha$  and  $\beta$  are input model-dependent parameters (the model name should be also defined). The wall stress vector is tangent to the wall and is given by  $\boldsymbol{\tau}'_{w,f} = \boldsymbol{\tau}'_f \cdot \mathbf{n}_f - [(\boldsymbol{\tau}'_f \cdot \mathbf{n}_f) \cdot \mathbf{n}_f] \mathbf{n}_f$  with  $\boldsymbol{\tau}'_f$  corresponding to the total (solvent and polymeric) extra-stress tensor at the wall.

**Description:** fully-explicit implementation of slip models according to [39]. Supports both two-phase flows and moving meshes. In the latter case, the moving wall velocity is added to the slip component computed as above. Lower values of  $URF$  increase the numerical stability, but are not adequate for time-dependent flows.

#### 4.6.3 *zeroIonicFlux*

**TypeName:** *zeroIonicFlux*

**Type:** fixed-gradient (scalar).

**Formula:**  $\nabla c_i|_f \cdot \mathbf{n}_f = -c_{i,f} \frac{e z_i}{kT} \nabla \Psi|_f \cdot \mathbf{n}_f$ , with  $c_{i,f} = c_{i,P} \exp \left[ -\frac{e z_i}{kT} (\psi_f - \psi_P) \right]$ . Indices  $f$  and  $P$  represent the boundary face and the cell owning that face (see the definition of the other variables in Section 3.7.1).

**Description:** imposing a no-flux condition for an ionic specie, in the Poisson-Nernst-Planck model. This boundary condition results from the balance of diffusion and electromigration at the patch, assuming that a no-penetration condition holds there. The expression being used has been derived from a Robin-type boundary condition [3].

#### 4.6.4 *boltzmannEquilibrium*

**TypeName:** *boltzmannEquilibrium*

**Type:** fixed-value (scalar).

**Formula:**  $c_{i,f} = c_{i,0} \exp \left[ \frac{e z_i}{kT} (\psi_f - \psi_0) \right]$ , where  $c_{i,0}$  is the reference concentration (user-defined) at which the intrinsic electric potential is  $\psi_0$  (user-defined; see the definition of the other variables in Section 3.7.1). A common choice is to set  $c_{i,0}$  as the bulk concentration of ions and  $\psi_0 = 0$ .

**Description:** ionic concentration derived from the assumption of Boltzmann equilibrium near the patch. This boundary condition is intended to be used when the electric potential is split, in which case only the intrinsic potential is used in the formula. This boundary condition does not guarantee the zero-flux of a given specie in all the situations, and, in general, it is not accurate for transient simulations.

#### 4.6.5 *inducedPotential*

**TypeName:** *inducedPotential*

**Type:** fixed-value (scalar).

**Formula:**  $\psi_f = -\phi_{Ext,f} + \psi_{Fix} + \left( \frac{1}{\sum_{f=1}^{N_f} |\mathbf{S}_f|} \right) \sum_{f=1}^{N_f} \phi_{Ext,f} |\mathbf{S}_f|$ , where  $\psi_{Fix}$  is the bias

voltage (user-defined) of the patch, i.e., the electric potential of the surface in the absence of an external electric field.

**Description:** intrinsic potential induced in a conducting surface placed over an electric field and having a bias voltage [40]. The last term in the formula represents the area-averaged external electric potential over the surface. This boundary condition can be used with the Poisson-Boltzmann and Debye-Hückel models, under the potentials splitting approach.

#### 4.6.6 *slipSmoluchowski*

**TypeName:** *slipSmoluchowski*

**Type:** fixed-value (vector).

**Formula:**  $\mathbf{u}_{Sch,f} = \mu(-\nabla\phi_{Ext,f})$ , where  $\mu$  is the electroosmotic mobility (user-defined), as defined in Section 3.7.5.

**Description:** slip velocity derived from the Helmholtz-Smoluchowski theory (Section 3.7.5). Although this boundary condition can be used with any EDF model for which  $\phi_{Ext}$  is defined, it is primarily intended to be used with the slip model.

#### 4.6.7 *slipSigmaDependent*

**TypeName:** *slipSigmaDependent*

**Type:** fixed-value (vector).

**Formula:**  $\mathbf{u}_{Sch,f} = \mu_0 \left( \frac{\sigma_f}{\sigma_0} \right)^m (-\nabla\phi_{Ext,f})$ , as defined in Section 3.7.6. Parameters  $\mu_0$ ,  $\sigma_0$  and  $m$  are user-defined.

**Description:** slip velocity derived from the Helmholtz-Smoluchowski theory for a space-variable conductivity field (Section 3.7.6). This boundary condition can be used with the Ohmic model.

#### 4.6.8 A note on wall boundary conditions for pressure

In the simulation of incompressible flows, it is a common approach to assign a zero-gradient boundary condition for the pressure at walls. This approach is efficient to ensure no-penetration in the wall (continuity equation), but it results in a lower-order approximation for the pressure gradient in the momentum equation and, in some cases, it may significantly unbalance the remaining sources of momentum.

A more general approach is to derive the pressure gradient at the boundary from the continuity equation, by enforcing the no-penetration condition. Indeed, if Eq. (3.16) is interpolated to the faces of a bounding wall, then setting the velocity, or more correctly the flux, to zero (no-penetration condition) results in

$$\mathbf{u}_f \cdot \mathbf{n} = 0 \Rightarrow (\nabla p)_f \cdot \mathbf{n} = (a_P - H_1) \left[ \frac{H_f}{a_P} + \left( \frac{1}{a_P - H_1} - \frac{1}{a_P} \right) (\nabla p^*)_f \right] \cdot \mathbf{n} \quad (4.29)$$

Eq. (4.29) is generic since it does not depend on a specific form of the momentum equation. It can also be seen that if both sides of Eq. (4.29) are forced to be zero – the zero-gradient approach –, the equality is still satisfied and the no-penetration condition is still valid. The advantage in using Eq. (4.29) is that the resulting normal pressure gradient is going to effectively balance the remaining local forces in the momentum equation. In practice, the difference between using Eq. (4.29) or the zero-gradient approximation is only noticeable when the stresses at the wall are significant (high  $\frac{H_f}{a_P}$ ), as for example in EDFs, where a strong electric force normal to the wall may exist. In the tutorials provided with *rheoTool*, the zero-gradient approximation is frequently used.

Since OpenFOAM® version 4.0, the boundary equation embodied by Eq. (4.29) is available by default under the name *fixedFluxExtrapolatedPressure*. However, this boundary condition may not be usable in some cases, as for example in cases with a zero velocity assigned to all boundaries. In such cases, there is a conflict created by function *adjustPhi()* when it attempts to artificially adjust the fluxes. This issue can be avoided by commenting the line where function *adjustPhi()* is called in the code (typically inside file *pEqn.H*), provided the user is sure that the set of boundary conditions under use verifies continuity. This limitation in the boundary condition might be eventually solved in future releases of OpenFOAM®.

Importantly, in multiphase flows with non-zero surface tension and/or gravity effects, the zero-gradient condition for pressure is generally incorrect. Indeed, for such flows it is usual to compute the fluxes in two steps in OpenFOAM®, i.e., the term  $\frac{H_f}{a_P}$  in Eq. (4.29) is built in two steps. The last step adds the flux contribution from surface-tension and gravity without enforcing a null contribution at the wall. Thus, in general the right hand side of Eq. (4.29) is non-null in these cases and simply setting  $(\nabla p)_f \cdot \mathbf{n} = 0$  creates a local mass imbalance. The boundary conditions *fixedFluxPressure* (available in OpenFOAM® and foam-extend) and *fixedFluxExtrapolatedPressure* (only available in OpenFOAM® starting from version 4.0) solve this issue by equating the normal pressure gradient to this extra flux, and they should be employed in such situations. In addition, for *rheoTool* versions running foam-extend, when the SIMPLEC algorithm is selected for pressure-velocity coupling, the *fixedFluxPressure* BC requires that the entry *Dp* is defined and set to "rAtU" (check the tutorials provided). This is not needed for the PIMPLE coupling algorithm, or when using OpenFOAM® v4.x.

## 4.7 Utilities

### 4.7.1 *GaussDefCmpw* schemes for convective terms

The component-wise and deferred correction handling of HRSs, described in Section 3.4, is included as a library in *rheoTool*. If the installation procedure presented in Chapter 2 has been followed, this new class of schemes will only be available when using the family of solvers provided with *rheoTool*. However, there are several ways to make the schemes available to any solver of OpenFOAM®. One option (not requiring compilation) is to include this library (`libgaussDefCmpwConvectionSchemes.so`) as a *lib* entry of `controlDict` in the case directory. Another option is to compile the class inside library `finiteVolume`, which is included by most OpenFOAM® solvers. To access this class from a specific solver, `lgaussDefCmpwConvectionSchemes` should be added to the `Make/options` file of that solver, along with its path. We note that the component-wise and deferred correction handling of HRSs improved significantly the stability of viscoelastic fluid flow simulations [2], but its performance and advantage when used in other type of flows need to be tested (by no way we argue that this is a magic bullet for all purposes).

The new group of HRSs is accessible from class *GaussDefCmpw* and its use is similar to the standard HRSs of OpenFOAM®. For example, the CUBISTA scheme can be used by simply defining in dictionary `fvSchemes`: *GaussDefCmpw cubista*; in front of the divergence term being discretized (remember that keywords in OpenFOAM® are case-sensitive). To obtain a list of all the schemes available, simply type *GaussDefCmpw*; without any additional argument and you will obtain all the possibilities, listed in Table 4.9. There is a scheme named *none*, which corresponds to removing the convective term from the equation being discretized. Note that all the limiters implemented in class *GaussDefCmpw* are totally independent from the already existing limiters of OpenFOAM® and all are defined in file `limiters.H`. For example, you will have now *GaussDefCmpw minmod* and *Gauss Minmod*, which are two different schemes, or, actually, two different implementations of the same high-resolution scheme.

Details on the implementation of this class of schemes will not be presented in this guide, although the interested reader will easily find the analogy between the equations presented in Section 3.4 and the source code in files `gaussDefCmpwConvectionScheme.C` and `limiters.H`. Nevertheless, for documentation purposes, we summarize next the operations being executed by each member function of class *GaussDefCmpw*:

- *phifDefC()*: depending on the boolean value of *onlyDCphi*, this function returns either the interpolated variable on the faces – Eq. (3.23), with all the terms explicitly evaluated –, or the deferred correction to the upwind scheme – only the explicit term of Eq. (3.23).
- *lims()*: this function retrieves three variables: *alpha*, is a list containing  $\alpha$  for each interval of the function defined in Eq. (3.20); *beta* is a list containing  $\beta$  for each interval of the function defined in Eq. (3.20); *bounds* is a list of  $\phi_C$

**Table 4.9:** Available High-Resolution schemes for convective terms in class *gaussDefCmpw*. The schemes are defined using the NWF approach (Eq. 3.20).

| Scheme                     | <sup>1</sup> TypeName | <sup>2</sup> Equation  |
|----------------------------|-----------------------|--|
| Upwind                     | <i>upwind</i>         | $[\alpha, \beta] = [1, 0]$   |
| CUBISTA                    | <i>cubista</i>        | $[\alpha, \beta] = \begin{cases} [1, 0] & \tilde{\phi}_C \leq 0 \vee \tilde{\phi}_C \geq 1 \\ [7/4, 0] & 0 < \tilde{\phi}_C < 3/8 \\ [3/4, 3/8] & 3/8 \leq \tilde{\phi}_C \leq 3/4 \\ [1/4, 3/4] & 3/4 < \tilde{\phi}_C < 1 \end{cases}$ |
| MINMOD                     | <i>minmod</i>         | $[\alpha, \beta] = \begin{cases} [1, 0] & \tilde{\phi}_C \leq 0 \vee \tilde{\phi}_C \geq 1 \\ [3/2, 0] & 0 < \tilde{\phi}_C < 1/2 \\ [1/2, 1/2] & 1/2 \leq \tilde{\phi}_C < 1 \end{cases}$   |
| SMART                      | <i>smart</i>          | $[\alpha, \beta] = \begin{cases} [1, 0] & \tilde{\phi}_C \leq 0 \vee \tilde{\phi}_C \geq 1 \\ [3, 0] & 0 < \tilde{\phi}_C < 1/6 \\ [3/4, 3/8] & 1/6 \leq \tilde{\phi}_C \leq 5/6 \\ [0, 1] & 5/6 < \tilde{\phi}_C < 1 \end{cases}$       |
| WACEB                      | <i>waceb</i>          | $[\alpha, \beta] = \begin{cases} [1, 0] & \tilde{\phi}_C \leq 0 \vee \tilde{\phi}_C \geq 1 \\ [2, 0] & 0 < \tilde{\phi}_C < 3/10 \\ [3/4, 3/8] & 3/10 \leq \tilde{\phi}_C \leq 5/6 \\ [0, 1] & 5/6 < \tilde{\phi}_C < 1 \end{cases}$     |
| SUPERBEE                   | <i>superbee</i>       | $[\alpha, \beta] = \begin{cases} [1, 0] & \tilde{\phi}_C \leq 0 \vee \tilde{\phi}_C \geq 1 \\ [1/2, 1/2] & 0 < \tilde{\phi}_C < 1/2 \\ [3/2, 0] & 1/2 \leq \tilde{\phi}_C \leq 2/3 \\ [0, 1] & 2/3 < \tilde{\phi}_C < 1 \end{cases}$     |
| <sup>3</sup> no convection | <i>none</i>           | —  |

<sup>1</sup> Corresponds to the name entry identifying the scheme in the source code.<sup>2</sup> See Eq. (3.20).<sup>3</sup> When this option is used, the convective term is deleted.

values, for which there is a change of branch in the function defined in Eq. (3.20). Thus, function *lims()* defines Eq. (3.20) for the selected scheme.

- *fvmDiv()*: this function also exists for *Gauss* schemes and returns the matrix of coefficients and the source term resulting from the discretization of the implicit convective operator *fvm::div()*. Function *phifDefC()* is called from here, whenever the selected scheme is different from *upwind* or *none*. Note that both *Gauss* and *GaussDefCmpw* classes implement the *upwind* scheme in the same way – it is the only scheme for which this happens.
- *fvcDiv()*: evaluates explicitly the operator *fvc::div()*.
- *interpolate()*: returns face-interpolated values, by simplifying calling

*phifDefC()*, with the adequate boolean value.

- *flux()*: returns the field interpolated on face centers multiplied by the flux on each face (*phi*).

The class *GaussDefCmpw* easily allows modifying or adding a new piecewise-linear HRS, by simply adding a new instance or modifying an existing one in function *lims()*, in file `limiters.H`. It is also possible to include HRSs not defined as piecewise-linear functions, although this also requires modifying function *phifDefC()*.

#### 4.7.2 Generic post-processing: *ppUtil*

In version 1.0 of *rheoTool* for OpenFOAM® versions, the computation and writing of quantities of interest after and/or during the simulations of the tutorial cases was mainly exemplified by the use of *coded FunctionObjects*. The reader will easily notice this throughout Chapter 5, where we even included a short Section devoted to those utilities (Section 5.1.2). On the other hand, the same tasks accomplished by such *coded FunctionObjects* were assembled in a library for the *rheoTool* version running in foam-extend, since *coded FunctionObjects* are not available there. While we recognize that *coded FunctionObjects* are a very useful tool, it is also true that they do not allow the efficient execution of some advanced tasks. Therefore, since *rheoTool* version 2.0 we generalized the post-processing dedicated library already present for foam-extend versions to all *rheoTool* versions, while still keeping the examples making use of *coded FunctionObjects*.

The post-processing library is named *libpostProcessingRheoTool* and it can be found in directory `src/libs/postProcessing/postProcUtils/`. The base class is named *ppUtil* and it is accessible from all the solvers included in *rheoTool* through the *ppUtilInterface* class. Creating a new *ppUtil* is straightforward for a user with some knowledge on OpenFOAM® programming:

- copy and paste the folder of an already existing *ppUtil* and give it a new name of your choice. Delete the *.dep* file in that folder.
- *find & replace* the old name of the *ppUtil* by the name that you gave to the folder. This should be done for both the *.C* and *.H* files (there are several ways to do it automatically, for example, *Ctrl + H* in *gedit*).
- modify the source code in order to do what you want.
- add the source file that was just created to the list of files for compilation in the `Makefile` of the library.
- run the `Allwmake` script in `src/` to compile, and it should be ready to use.

Several *ppUtil* can be used simultaneously in a given simulation. They should be defined in subDict *PostProcessing*, located in dictionary `fvSolution`. Each *ppUtil* should be provided as a different entry of group *functions*, as shown in Listing 4.18. In this example, two *ppUtil* are selected and a name is given to each one (*ciMonitor* and *jMonitor*; any name can be attributed).

```

PostProcessing
2 {

4 functions
(
6   ciMonitor
8   {
10     funcType      calcBalance;
11     enabled       true;
12     evaluateInterval 100;
13   }

14   jMonitor
15   {
16     funcType      calcJpatch;
17     ListOfPatches
18     (
19       "cylinder"
20     );
21     enabled       true;
22     evaluateInterval 100;
23   }
24 }

25 );
26
}

```

**Listing 4.18:** Example of a *PostProcessing* subDict.

For each *ppUtil* selected, at least three keywords must be defined:

- *funcType*: should specify the *TypeName* of the given *ppUtil*. To obtain a full list of all the available utilities, simply insert any random letter.
- *enabled*: should be *true* or *false* and it determines whether the *ppUtil* is active or not;
- *evaluateInterval*: should be any integer value  $> 0$  and corresponds to the number of time-steps between consecutive calls to the given *ppUtil*. Currently, the execution interval can be only controlled by the number of time-steps.

When a given *ppUtil* is active and programmed to write some quantity (or several) of interest, a folder named `rheoToolPP/startTimeName/ppUtilName/` is created in the case directory and the output is forwarded to there.

The class *ppUtil* not only allows to create case-specific post-processing tools, as it also offers the possibility to build generic post-processing applications. In Table 4.10 we present some generic *ppUtil* which are included in *rheoTool* and that can be useful in a number of cases.

**Table 4.10:** General-purpose *ppUtil* available in *rheoTool*.

| Type               | Name | Description  |
|--------------------|------|--|
| <i>calcWSS</i>     |      | Computes the wall shear-stress magnitude for any constitutive equation: $WSSmag =  \mathbf{n} \cdot \boldsymbol{\tau}' - \mathbf{n}(\mathbf{n} \cdot \boldsymbol{\tau}' \cdot \mathbf{n}) $ (Pa), where we remember that $\boldsymbol{\tau}'$ represents the total extra-stress tensor (see Section 3.1). This <i>ppUtil</i> is used in the tutorial of Section 5.1.8.   |
| <i>calcJpatch</i>  |      | Computes the surface-averaged current density, for each ionic specie, in the patches specified by the user: $J_i = \frac{z_i F}{ \mathbf{S}_{\text{patch}} } \sum_{f=1}^{N_f} [(c_{i,f} \mathbf{u}_f - D_i \nabla c_{i,f} - D_i \frac{e z_i}{kT} c_{i,f} \nabla \Psi_f) \cdot \mathbf{S}_f]$ (A/m <sup>2</sup> ). This <i>ppUtil</i> is only meaningful for the PNP model (an example can be found in the tutorial of Section 5.4.4).  |
| <i>calcBalance</i> |      | Computes the average concentration for each ionic specie: $\bar{c}_i = \frac{1}{V_{\text{domain}}} \sum_{j=1}^{N_C} c_{i,j} V_j$ (mol/m <sup>3</sup> ). It also retrieves the net, surface-averaged flux of each ionic specie through all the domain boundaries (equivalent to run <i>calcJpatch</i> for all the boundaries, sum the fluxes and divide by $z_i F$ ). This <i>ppUtil</i> is only meaningful for the PNP model (an example can be found in the tutorial of Section 5.4.3). |

### 4.7.3 *writeEfield*

By default, the solver *rheoEFoam* does not write the electric field to the time directories. The purpose of utility *writeEfield* is to read the electric potential variable(s) and write the electric field, for each time directory. This means that this utility can only be called after the simulation has been run. The utility sums up all the electric potential variables available in the directories:  $\Psi$  (*psi*),  $\phi_{\text{Ext}}$  (*phiE*) and/or  $\psi$  (*psi*).

The utility can be used by typing *writeEfield* in the terminal, without any other requirements, except that at least one electric potential variable must exist in the time directories. In addition, the time directories can not be decomposed among processors (reconstruct the case if it is decomposed).

Note that the electric field can be also computed from the electric potential in most of the visualization software, as for example Paraview, since a simple differentiation operation is required.

#### 4.7.4 *initMolecules*

The purpose of utility *initMolecules* is to generate a set of files representing the molecules that can be read by solver *rheoBDFoam*. The users can interpret this utility as a sort of *blockMesh* application that generates molecules instead of a computational mesh.

This utility reads its controls from dictionary *initMoleculesDict*, which should be located inside folder *constant/*. An example of such dictionary is presented in Listing 4.19. We will now analyze its entries. However, we should first remember that solver *rheoBDFoam* can handle simultaneously multiple groups of molecules with different physical properties. As such, both the physical properties and the beads positions should be defined for each group. In the example of Listing 4.19, there are two groups of molecules defined inside dictionary *groups*, which were arbitrarily named *G1* (line 3) and *G2* (line 27). The user can introduce and define as many groups as needed (at least one should exist). For each group, the following data must be present (we will only analyze group *G1* in Listing 4.19):

- number of molecules (line 5): this is specified in entry *nMolecules* and should be an integer  $\geq 1$ . All the molecules generated inside a group will share the same physical properties.
- physical properties (lines 7-12): these are the input parameters needed by the physical model. We can find the diffusion coefficient (*D*), the beads radius (*a*; only used if HI are active), the number of Kuhn steps per spring (*Nks*), the exclusion volume parameter (*nuEV*; only used if EV forces are active) and the maximum length of a fully-stretched spring (*Ls*). See Section 3.8 for details about these parameters.
- spatial distribution and topology of the molecules (lines 15-24): these settings should all be defined inside dictionary *spatialDistributionCoeffs* (lines 15-24). Currently, the molecules can be only distributed uniformly over a straight line defined by its extreme points, *p0* and *p1*. For a group with *M* molecules, this means that the first bead of the first molecule will be at position *p1* and the first bead of the remaining molecules will be spaced apart consecutively by vector  $\Delta\mathbf{s} = (\mathbf{p1} - \mathbf{p0})/(M - 1)$  (the first bead of the last molecule will be at position *p2*). Note that *p0* and *p1* can be assigned the same vector positions, in which case all the molecules have their first bead at the same position. We remember that solver *rheoBDFoam* does not account for inter-molecular interactions (for all the effects considered, each molecule behaves as if it was alone in the surrounding fluid). The last entry of dictionary *spatialDistributionCoeffs*, named *branches()* (lines 20-23), controls the position of the remaining beads in each molecule. The molecules are built branch-by-branch, thus each line of *branches()* should fully define a branch according to a fixed syntax:

(A B C) (*d0 d1 d2*) (E F) (G H)

A - index of the master branch (integer).

- B - local index of the connecting bead in master branch (integer).
- C - number of beads in the branch (integer).
- (*d0 d1 d2*) - growth vector of the branch. Each component is expressed as a fraction of *Ls* (vector of doubles).
- E - is the branch growth random? Random (*true*) or not random (*false*) (boolean).
- F - does the last bead of the branch connects to any other branch? Yes (*true*) or no (*false*) (boolean).
- G - (*optional*) if F = *true*, then specify the local index of the connecting bead in master branch (integer).
- H - (*optional*) if F = *true*, then specify the index of the master branch (integer).

In order to simplify the understanding of this syntax, three examples are provided in Fig. 4.4. Each line specified inside *branches* corresponds to a branch of the molecule. The index automatically attributed to each branch simply follows the order in which they are entered in the list. Importantly, a given branch can only connect to a branch which has been already entered in the list. All the examples provided have E = *false*, which means that the current bead position is obtained from the previous bead position by adding vector (*d0 d1 d2*)*Ls*. In these cases, this vector is simply the spring vector. However, when E = *true*, each component of the vector provided is multiplied by a random number between -1 and 1. In either case, it is user's responsibility to ensure that the vector provided does not violate the maximum spring length:  $d0^2 + d1^2 + d2^2 < 1$

```

1 groups
(
3   G1
{
5     nMolecules    1000;

7     // Physical properties
9       D           0.065e-12;
11      a           .077e-6;
13      Nks          20;
15      nuEV         1.2e-21;
17      Ls           2.1e-6;

19     // Spatial distribution
21     spatialDistibutionCoeffs
{
23       p0           (0 0 0);
25       p1           (0 0.001 0);

27     branches
29     (
31       (0 0 11)  ( 0.2 0 0)  (true true)

```

```

23           );
25       }
27   G2
28   {
29     nMolecules    700;
30
31     // Physical properties
32     D            0.15e-12;
33     a            .053e-6;
34     Nks          15;
35     nuEV         4e-22;
36     Ls           2.1e-6;
37
38     // Spatial distribution
39     spatialDistributionCoeffs
40     {
41       p0           (0 0 0);
42       p1           (0.005 0 0);
43
44       branches
45       (
46         (0 0 3) ( 0.1 -0.1 0 ) (false true)
47         (0 2 2) ( -0.1 -0.1 0 ) (false true)
48         (1 1 2) ( -0.1 0.1 0 ) (false true)
49         (1 1 1) ( 0.1 0.1 0 ) (false false) ( 0 0 )
50         (2 1 3) ( -0.1 0 0 ) (false true)
51       );
52     }
53   }
54 ;

```

**Listing 4.19:** Example of a `initMoleculesDict` dictionary used to generate molecules with utility `initMolecules`.

The execution of `initMolecules` generates a directory named `lagrangian/molecules/` inside the `startTime` folder. The directory contains 5 files:

`indices-` field of triplets where the first value is the global bead index, the second is the local bead index inside the molecule to which it belongs, and the third is the index of the group to which the molecule belongs.

`molcID-` field of labels corresponding to the index of the molecule which contains the given bead.

`origID-` field of labels corresponding to the global bead index. In most of the cases, this field is equal to the first element of field `indices`. This field is kept to ensure compatibility with the generic particle-tracking engine of OpenFOAM®.

`origProcID-` field of labels corresponding to the index of the processor containing the bead. Since `rheoBDFoam` is still not able to run in parallel, this will be always a field of zeros. Again, this field is kept to ensure compatibility with the generic particle-tracking engine of OpenFOAM®.

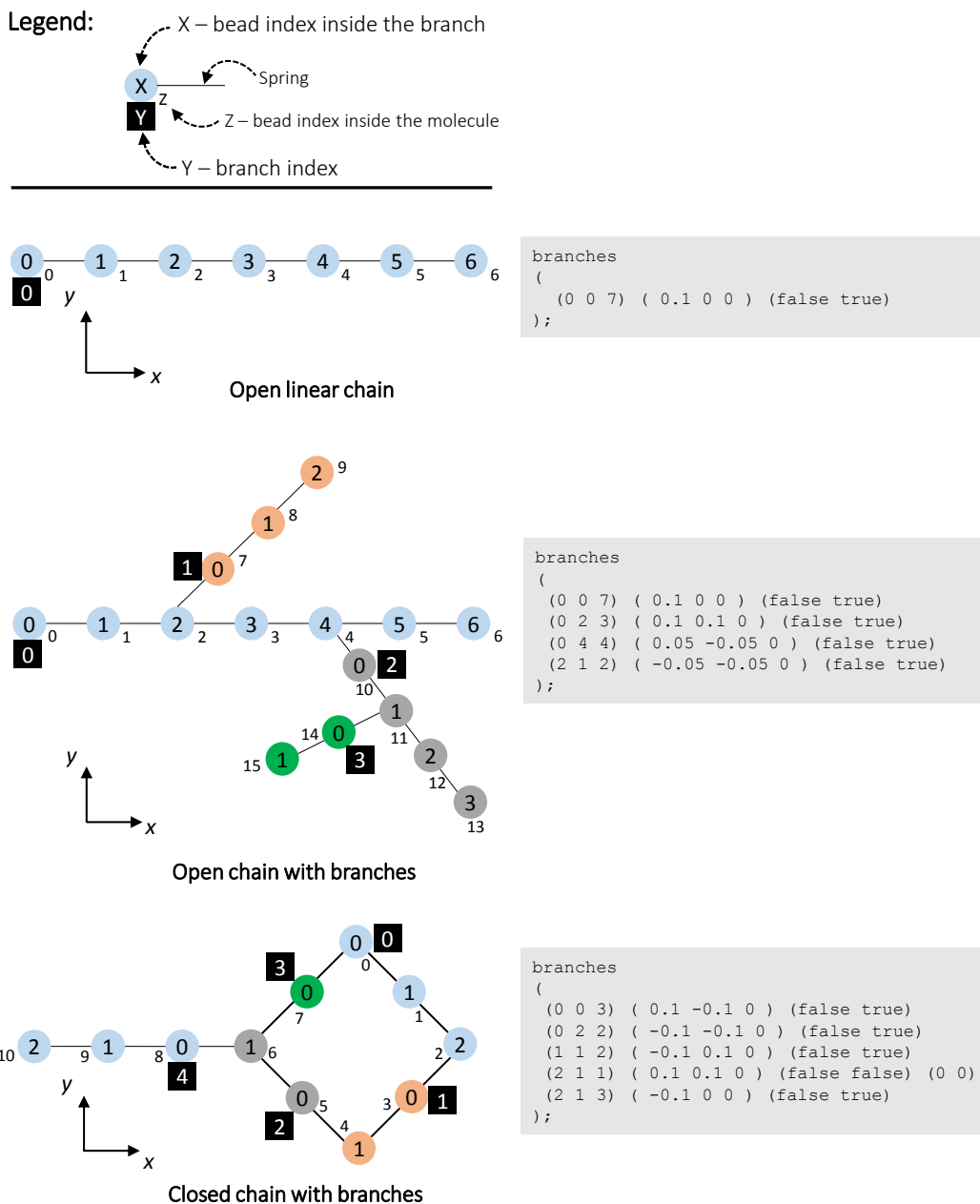


**Figure 4.4:** Example of 3 molecules and corresponding *branches* settings to generate them with utility *initMolecules*.

positions- list of bead's positions. This list has a special format defined by OpenFOAM®. Each entry is composed by the barycentric coordinates of the bead (inside parentheses), the mesh cell index containing the bead, the index of the face owning the tetrahedron containing the bead and the point index defining that face. For more information, the user is advised to check the source code of `src/lagrangian/basic/particle/partic1e.H` and `src/lagrangian/basic/particle/particleIO.C` provided with OpenFOAM® (version 5.0 or newer).

In addition to these files, *initMolecules* creates directory `constant/runTimeInfo/StartTime` containing two files:

`MoleculesInfo-` holds information on the active molecules, as the physical properties of each group of molecules. It also lists the index, number of beads and the group that each active molecule belongs to.

`springs-` a list of triplets defining the springs of the active molecules (similarly to faces in a mesh). The first element is the first-bead global index, the second element is the second-bead global index and the third element is the molecule index. A spring can be unequivocally defined with these elements.

The seven files described above are generated upon execution of *initMolecules*, and they are automatically written by *rheoBDFoam* during a simulation, since they are needed for an eventual restart. Note that all the information in dictionary `initMoleculesDict` is only read by utility *initMolecules*; changing this dictionary after having run the utility or just before running solver *rheoBDFoam* will change nothing. This is not a valid way to change the molecules' physical properties after having created the molecules. Such changes can be done manually in file `MoleculesInfo`, although it is generally not recommended (it is preferable to re-run *initMolecules*).

#### 4.7.5 *averageMolcN*

The results obtained with solver *rheoBDFoam* usually require averaging over several molecules due to the random nature of the Brownian term. Utility *averageMolcN* averages the molecular length over all the valid molecules registered at a given time. This utility is mostly useful for homogeneous flows, where the molecular extension does not depend on the spatial position.

The argument to this utility should be provided in the command line, following this syntax:

```
~$ averageMolcN time
```

where *time* is the *startTime*.

The results for each group of molecules are written to file `rheoToolPP/startTime/moleculesStats/groupName/Stretch_Naverage.txt`, where the first column corresponds to time and the second column is the ensemble averaged molecular length. Note that untracked/overstretched molecules are not accounted in the average.

This utility requires (uses) the registry of the molecules' position and stretch over time, optionally written and saved by solver *rheoBDFoam* (see Section 4.3.8). Therefore, this post-processing utility can only be called after a call to the solver.

#### 4.7.6 *averageMolcX*

In some cases, it is useful to compute the average evolution of the molecules' length over space. Utility *averageMolcX* is intended for this purpose, since it retrieves the average molecular length over a line defined by the user. This line can have any

orientation and is divided in a finite number of bins. For example, consider line connecting point (0,0,0) to point (10,0,0), that is divided in 10 bins. Then, all the molecules whose center of mass, at a given instant, had its  $x$ -coordinate between  $x = 0$  and  $x = 1$  will contribute to the average in the first bin. The second bin is between  $x = 1$  and  $x = 2$ , and so on for the remaining bins.

The arguments to this utility should be all provided in the command line, following this syntax:

```
~$ averageMolcX time -biased bool -startPoint "sP" -endPoint "eP" -nBins nB
```

where *time* is the *startTime*, *sP* is the position of the first point of the line, *eP* is the position of the second point of the line and *nB* is the number of bins. The option *-biased* should receive a boolean and stands for the averaging method used. The biased average (*bool = true*) takes all the hits in a given bin and averages among all with equal weights per hit. This results, in general, in a biased average, because the molecules with more hits in a given bin (for example the ones with slower velocity) will have a higher representation in the results. The unbiased average (*bool = false*; default option if none is specified) first computes the average length of each molecule inside the bin, collecting all the hits of that molecule in the bin, and then averages between all the molecules, attributing equal weights to each one.

The results for each group of molecules are written to file *rheoToolPP/startTime/moleculesStats/groupName/Stretch\_Xaverage.txt*, where the first three columns correspond to the  $x$ -,  $y$ - and  $z$ -coordinates of each bin's center, the fourth column contains the average molecular length in that bin and the fifth column contains the number of values used in the average (number of molecules for unbiased average, or total number of hits for biased average).

This utility requires (uses) the registry of the molecules' position and stretch over time, optionally written and saved by solver *rheoBDFoam* (see Section 4.3.8). Therefore, this post-processing utility can only be called after a call to the solver.

# Chapter 5

## Tutorials

In this Chapter, we provide a step-by-step guide on how to use the solvers of *rheoTool*. For each solver, general guidelines are first discussed, regarding the new fields and dictionaries required by that application. Then, specific tutorials are presented, which will illustrate the application of *rheoTool* to relevant problems. These tutorials cover the full process to obtain results, from the mesh generation to the post-processing stage.

The approach used in this Chapter assumes that the reader is familiar with the typical folder organization of OpenFOAM® cases and has basic knowledge on how to run simulations in OpenFOAM®.

**ⓘ** The tutorials in this Chapter are mainly intended for learning purposes. It is not our primary goal to obtain highly accurate results with such examples, but solely to show how to run the solvers, preferably using fast-running cases. Higher accuracy can be obtained in all the cases by increasing the resolution in space and time.

### 5.1 *rheoFoam*

#### 5.1.1 General guidelines

Before proceeding, we note that the sequence of operations required to prepare a case in OpenFOAM® does not need to be ordered as presented next (`constant/ → 0/ → system/`). This sequence was organized in such a way to be (hopefully) logic and easy to follow and execute.

##### **constant/**

Inside folder `constant/` there are two main components of the simulation: the mesh, in folder `polyMesh/`, and the dictionary `constitutiveProperties`, which is a dictionary specific of *rheoTool*. Since the mesh is an element required by almost all OpenFOAM® solvers, it will not be discussed here and we assume that a valid mesh already exists in folder `polyMesh/`.

The dictionary `constitutiveProperties` used by *rheoFoam* includes information about the constitutive model and the passive scalar transport which can optionally be activated in the simulation (Listing 5.1).

```

parameters
2 {
    type          Oldroyd-BLog;
4
    rho           rho [1 -3 0 0 0 0] 1.;
6    etaS          etaS [1 -1 -1 0 0 0] 0.01;
8    etaP          etaP [1 -1 -1 0 0 0] 0.99;
10   lambda        lambda [0 0 1 0 0 0] 1.;

10  stabilization  coupling;
}
12
passiveScalarProperties
14 {
    solvePassiveScalar off;
16    D              D [ 0 2 -1 0 0 0 ] 1e-9;
}

```

**Listing 5.1:** Example of a `constitutiveProperties` dictionary used with *rheoFoam*.

The dictionary `constitutiveProperties` has two different sub-dictionaries (`subDict`), which must necessarily exist: *parameters*, with information on the constitutive model, and *passiveScalarProperties*, related with the scalar-transport equation.

Regarding `subDict parameters`, in line 3 we define the `TypeName` of the constitutive model to be used, which can be found in Table 4.1. In the example displayed in Listing 5.1, we are using the Oldroyd-B model, solved with the log-conformation approach (*Oldroyd-B + Log*). If we would like to use the same model without solving it with the log-conformation approach (solving the constitutive equation for the extra-stress tensor), then the type would be simply *Oldroyd-B* – this naming rule is valid for all viscoelastic models. Lines 5 to 8 specify the fluid properties required by the constitutive model being solved. The density is a property common to all models (it is not related with the constitutive equation) and should always be present, while the model-dependent properties can be checked in Table 4.1. Anyway, if some required parameter is not specified, the solver will retrieve an error complaining for its absence.

The reader might be surprised with the unphysical parameters displayed in Listing 5.1 (even just being an example), particularly the density of the fluid, which is not realistic for any known viscoelastic liquid. The use of a unitary density ( $\rho = 1 \text{ kg/m}^3$ ) and many other unitary variables is simply to facilitate the calculations. In the tutorials presented next, we frequently make use of this kind of approach, since the computation of dimensionless parameters does not require physically realistic quantities.

At line 10, the stabilization method is selected (recall that C++ is case-sensitive): *none* for no stabilization; *BSD* to use the both-sides-diffusion technique; *coupling* to use the stress-velocity coupling discussed in Section (3.3.2). Note that

this option is only meaningful for viscoelastic models.

For multi-mode viscoelastic models, the TypeName is *multimode* and lines 3-10 need to be included for each mode, enclosed in a dictionary identified with the mode's name. An example is provided in the tutorials (`tutorials/rheoFoam/OtherTests/`).

For the FENE-type models not using the log-conformation approach, several formulations are available, as discussed in Section 4.1.2. The selection between them is also performed in subDict *parameters*. If nothing is specified, FENE models are evaluated using the (complete) formulation in **A**. In order to solve the complete formulation in **Tau**, the keyword *solveInTau* should be defined and set to *true*. If the modified formulation in **Tau** is intended, both *solveInTau* and *modifiedForm* keywords should be defined and set to *true*. Some examples are provided in the tutorials (`tutorials/rheoFoam/OtherTests/`). Note that the selection between the available formulations of FENE-type models is **not** achieved by specifying different TypeNames for each one: the TypeName is the same for all the formulations within the same model (FENE-CR or FENE-P) and the selection is based on the keywords just described.

Focusing now on subDict *passiveScalarProperties*, only two entries are present. In line 15, the user can select to solve (*on*, *true* or *yes*), or not (*off*, *false* or *no*), the transport equation of a passive scalar. If the equation is solved, then line 16 should specify the diffusion coefficient and field *C* (the name of the scalar being transported) should be defined in the folder corresponding to the start-time. Otherwise, none of these two actions is required. Importantly, if the option to solve the transport equation is enabled, but field *C* is not provided, then *rheoFoam* will solve a transport equation (you can confirm it on the solver output) for a scalar not present in the domain (its concentration will remain null over all the simulation time), since this is how the field is internally initialized when there is no entry for it in the start-time folder.

For a moving mesh, dictionary *dynamicMeshDict* is also required in directory `constant/`. This dictionary contains information on the mesh motion and its entries depend on the type of motion specified. Since this is a generic topic of OpenFOAM®, we will not present further details. Starting from *rheoTool* v3.0, dictionary *dynamicMeshDict* should always exist, even for static meshes. If not defined by the user, the solver will create a *dynamicMeshDict* with the *type* set to *staticFvMesh*, i.e., a static mesh. In that case, the solver for foam-extend and OpenFOAM® versions prior to v5.1 automatically add that dictionary to directory `constant/`. Therefore, for simulations in static meshes, the user does not need to take any action related with dictionary *dynamicMeshDict*.

## 0/

At this point, both the mesh and the fluid are defined and some decisions have been made about the numerical method. It is now time to create and define the initial and boundary conditions for the variables used in the simulation, which will depend on the constitutive equation selected. At least three scenarios are possible:

- **GNF fluid:** those cases only require defining pressure (divided by the density), *p* (in this guide represented by  $\frac{p}{\rho}$ ), and velocity, *U* (in this guide rep-

resented by  $\mathbf{u}$ ) fields. For all the GNF models, except for the Newtonian case, the solver will automatically write the shear-rate dependent viscosity at subsequent times.

- **viscoelastic model using the standard extra-stress approach:** those cases require defining pressure (divided by the density),  $p$ , velocity,  $\mathbf{U}$ , and the polymeric extra-stress field,  $\tau$  (in this guide represented by  $\boldsymbol{\tau}$ ). The novelty relative to the GNF cases is in variable  $\tau$ , which is of type *symmTensor*. All the three variables will be automatically written at future times. When a multi-mode viscoelastic model is used, each mode owns a variable  $\tau$ , which should be present in folder `0/`. The name given to each variable should be consistent with the names attributed to each mode in `constitutiveProperties`, i.e., this name should be appended at the end of name  $\tau$ . For example, having defined mode names `M1` and `M2`, then the names for the respective  $\tau$  should be `tauM1` and `tauM2`.
- **viscoelastic model using the log-conformation approach:** comparing with the previous case, it requires defining the additional variable `theta`, which represents the natural logarithm of the conformation tensor (in this guide represented by  $\boldsymbol{\Theta}$ ), which is also a *symmTensor*. In order to define boundary conditions for `theta`, we suggest the reader to take a look at Eqs. (3.6) and (3.7). For example, if the polymeric extra-stress ( $\tau$ ) is a null tensor, then variable `theta` is also a null tensor. At subsequent times, the solver will automatically write fields  $p$ ,  $\mathbf{U}$ ,  $\tau$ , `theta` and both the eigenvectors, `eigVecs` (in this guide represented by  $\mathbf{R}$ ), and eigenvalues, `eigVals` (in this guide represented by  $\Lambda$ ), which are obtained from the diagonalization of the conformation tensor. Note that the fields `eigVecs` and `eigVals` do not need to be present to start a simulation, although they are read if they are present (for example, to restart a simulation from the exact point where it finished). For a multi-mode model, the same considerations previously described apply, including for variable `theta`.

When using FENE-type models solved in the conformation tensor, without the logarithmic transformation (see Section 4.1.2), the conformation tensor field ( $\mathbf{A}$ ) can be optionally defined in folder `0/`, being read by the solver in that case. However, if not defined, the solver automatically initializes the conformation tensor field from  $\boldsymbol{\tau}$ , that should always be present. Independently of being or not present in the starting time folder, field  $\mathbf{A}$  will be written to the case directory for the remaining of the simulation.

For any of the previous cases, if the option to solve the transport equation of a passive scalar has been enabled, then a field  $C$  should also be present in folder `0/`. The utility `setFields` of OpenFOAM® can be particularly helpful to initialize this field, since it allows to assign different values of  $C$  in different regions of the domain.

If the simulation includes a moving mesh, depending on the type of mesh motion, some fields may need to be defined inside folder `0/`. For example, if the mesh is being deformed by solving some equations, e.g. a Laplace equation, then

boundary conditions need to be defined to solve such equations (see the tutorial in Section 5.1.9). On the other hand, rigid-body like motions, for example, do not need such procedure, since the whole mesh is simply transformed by some geometric operation.

### system/

The last steps before starting the simulation are related with the dictionaries located in folder `system/`, which mainly control the numerical method. In particular, we will focus our attention on the following dictionaries: `controlDict`, `fvSchemes` and `fvSolution`. All the three dictionaries must be present for the simulation to run, as required by most of the OpenFOAM® solvers. Since most of the entries in those dictionaries are transversal to both *rheoFoam* and any OpenFOAM® solver, we will limit our description to the new features introduced by *rheoFoam*.

In `controlDict` dictionary, the options allowing to automatically control the time-step by imposing a Courant number limit are available in *rheoFoam* and can be used (following the same principles of other OpenFOAM® solvers). Those options are `adjustTimeStep (on/off)`, `maxCo` (the value of the limiting Courant number) and `maxDeltaT` (the maximum admissible time-step). Furthermore, and although not being a feature exclusive of *rheoFoam*, *coded functionObjects* can be defined in `controlDict` and used with *rheoFoam* to extract and monitor quantities of interest (this is not possible in *foam-extend*). This kind of functions are frequently used in the tutorials of this Chapter.

Regarding dictionary `fvSchemes`, we remember that *GaussDefCmpw* schemes (Section 4.7.1) are available for selection and can be used to discretize any convective term with the generic form `div(phi,variable)`, where *variable* is either *U*, *tau*, *theta* or *C*. Still in the `divSchemes` subDict, the term `div(grad(U))` is part of the stress-velocity coupling algorithm (see line 44 of Listing 4.2) and should (always) be discretized using a central differencing scheme (*Gauss linear*), if used. In the `gradSchemes` subDict, the entry `linExtrapGrad` is for the gradient of the tensor components when using linear extrapolation of polymeric extra-stress at a given boundary, as discussed in Section 4.6.1. Apart from this, the remaining entries in `fvSchemes` should be familiar to the user and the selection of appropriate discretization schemes for each one is essential to keep the numerical method accurate and stable.

The dictionary `fvSolution` is the only remaining to be adjusted before running the simulation. In subDict *solvers*, the matrix solver for each equation being solved should be specified (remember that there will be *N* equations to solve for *theta/tau* in a model using *N* modes; wildcard characters are useful in those cases). If the user forgets to specify any, the solver will retrieve an error message asking for it. Only the pressure equation results in a symmetric matrix of coefficients, while all the others generate non-symmetric matrices. The only exception is the momentum equation without the convective term included, which also results in a symmetric matrix. This should be taken into account when selecting the type of matrix solver, since some are specific for some type of matrices. If a coupled solver or a sparse matrix solver from an external library is used, then check the instructions provided in Section 4.4. In the *SIMPLE* subDict, there

is a new entry specific of *rheoFoam*, which is *nInIter*. This variable was defined in Section 4.5.1 and controls the number of inner-iterations (see Fig. 4.2). If not defined, the solver will execute 1 inner-iteration as the default behavior. Still in the *SIMPLE* subDict, the entry *residualControl* allows the solver to automatically stop the simulation once the residuals for all the specified variables drop below the prescribed value. This is mainly a characteristic of steady-state solvers of OpenFOAM® and it can be also used in *rheoFoam*. However, if the goal is to run *rheoFoam* until the *endTime* specified in *controlDict*, simply leave this entry empty. The last subDict in *fvSolution* is the *relaxationFactors*, that determines the amount of explicit (*fields*) and implicit (*equations*) under-relaxation for each field or equation. When using the SIMPLEC algorithm for pressure-velocity coupling, as a rule of thumb, the pressure does not need to be explicitly under-relaxed to correct the velocity (see Ref. [2]). The only exception occurs for non-orthogonal grids, where a small amount of under-relaxation may eventually be needed for pressure. The under-relaxation factor, ranging between 1 (no under-relaxation) and 0 (total under-relaxation, pressure does not evolve in time), is case-specific and should be as high as possible (it can be conditioned by stability issues). Regarding implicit under-relaxation (*equations*), it only makes sense to be used with steady-state solvers, where the absence of a time-derivative term requires under-relaxation for stability reasons. Since *rheoFoam* is by default a transient solver, where time-derivatives are present in all the transport equations, implicit under-relaxation is not needed. In practice, it is possible to run *rheoFoam* without those time-derivatives by selecting a default steady-state discretization scheme in the *ddtSchemes* subDict of *fvSchemes* and, by this way, *rheoFoam* will run as a typical steady-state solver of OpenFOAM®, requiring implicit under-relaxation. However, in some situations (viscoelastic models solved with the log-conformation approach) the user will probably face stability issues, due to the poor diagonal dominance of the base matrix of coefficients. For this reason, unless the user is experienced and knows what is doing, we strongly recommend to use *rheoFoam* in transient mode. Note that, if it exists, the steady-state will be reached after some time of a transient simulation (typically after several relaxation times, of the order of 10 or above for higher *Wi*, for viscoelastic models). If the transient analysis is not important, a high Courant number ( $\gg 1$ ) can be defined to reach this state faster, as long as the computations remain stable.

In all the tutorials presented next, a steady-state is reached for the range of parameters used in the examples. However, in none of them we use the residuals as the termination criteria. Indeed, we prefer to set a very long *endTime* and monitor a relevant variable at sensitive points over time. It can be the extra-stress near a singular point, the drag coefficient over a surface, a vortex length, or any other relevant quantity for the problem at hand. This is usually achieved either through a *probe* (when the variable exists within the solver) or a *ppUtil* or *codedFunctionObject* (when the variable does not exist within the solver and needs to be computed), in dictionary *controlDict*. The termination criteria is then based on this variable. Of course, we have set the *endTime* in the tutorials based on that analysis. The residuals displayed on the screen should not be used alone as the termination criteria.

As mentioned in Section 4.7.2, the *PostProcessing* subDict enabling the use of the *ppUtil* class is also defined in dictionary *fvSolution*. A detailed discussion on this subject can be found in Section 4.7.2.

### 5.1.2 A note on *coded FunctionObjects*

Most of the tutorials presented next use a *coded FunctionObject*. This is a run time compilable code, executing run time functions coded by the user, which can be defined in dictionary *controlDict*.

These functions allow to access almost all the data of the case, from field variables to information about the mesh. The frequency at which they are evaluated can be controlled using the keywords *outputControl* and *outputInterval*. It is also possible to disable these functions by setting the keyword *enabled* to *off*.

The *coded FunctionObjects* included in the tutorials are usually divided in three sections: a section which reads data, a section which computes quantities of interest from this data and a writing section. Usually, we create a dynamic list to accommodate the data to be written, so that any extra quantity can be easily added to the list. This also eases the writing step. The meaning of each column of the data being written is usually displayed as a comment in the source code of the *coded FunctionObject*, being of course dependent on the tutorial case.

Among the several possibilities to write the variables computed by *coded FunctionObjects*, we chose to use a *.sh* executable, named *writeData*. This executable simply receives as arguments the name of the file to write to (the user can change it in the *codedStream functionObjects*), along with the data to be written, both provided by a system call from the *coded FunctionObject*. If the executable is not present in the case directory, but it is being called by the *FunctionObject*, a warning is displayed in the terminal informing about this situation (it is also possible to copy this script to a location loaded by default in each OpenFOAM® session, in order to avoid the need of having it in the case directory). Keep in mind that this *.sh* executable only writes to a file the data it receives as argument, so that it is unlikely that the user would need to change it.

One main advantage of *coded FunctionObjects* is that they are case-specific, instead of solver-specific, which means that the code of the solver does not need to be changed. They are probably also a good entry point to start programming in OpenFOAM®, since the compilation steps are automatically handled.

**Note for foam-extend users:** as mentioned in Section 2.2, *coded* objects are not available in foam-extend. For these versions, functions executing the same tasks as the *coded* objects are available in a dedicated post-processing library, as discussed in Section 4.7.2.

The boundary conditions implemented in OpenFOAM® versions as *coded* functions were added to library *libBCRheoTool.so* in the foam-extend version.

**i** For most of the tutorials presented next, the commands required to run them are specified. It is instructive for the less experienced users to type each one in the command line, in order to exactly know what is being done. However, in the directory for each tutorial we also provide a script named `Allrun` that automatically runs all these commands. On the other hand, the script `Allclean` also included cleans the directory, deleting everything that has been created.

### 5.1.3 Case 1: flow between parallel plates

 `tutorials/rheoFoam/Channel/Oldroyd-BLog/`

#### ❖ Overview

In this tutorial, the flow between two infinite parallel plates is simulated for an Oldroyd-B fluid. Although apparently simple, this case can pose formidable difficulties using the UCM and Oldroyd-B models at high Weissenberg number flows [41]. This example also shows that the log-conformation approach is effective in solving this stability issue, while retrieving the predicted analytical profiles.

Following Ref. [42], the Reynolds number for this problem is defined as  $Re = \frac{\rho U w}{\eta_0}$  and the Weissenberg number as  $Wi = \frac{\lambda U}{w}(1 - \beta)$ , where  $\beta = \frac{\eta_s}{\eta_s + \eta_p} = \frac{\eta_s}{\eta_0}$ . The case reproduced in the tutorial is for  $Re = 0$  (the convective term in the momentum equation is suppressed),  $Wi = 0.99$  and  $\beta = 0.01$ .

#### ❖ Geometry & Mesh

The geometry is a planar channel (two parallel plates) with half-width  $w$ , Fig. 5.1. The mesh is composed of 50 cells in the  $x$ -direction and 60 cells in the  $y$ -direction, uniformly distributed in both directions.

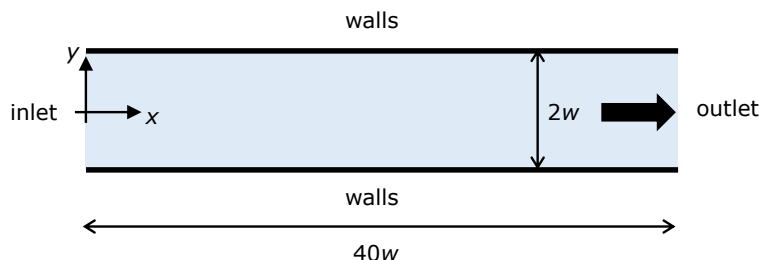


Figure 5.1: Planar channel geometry.

#### ❖ Boundary conditions

This flow is 2D, being solved in the  $xy$ -plane. A uniform velocity profile ( $U$ ) is set at the inlet, along with zero-gradient for pressure and polymeric extra-stress components. At the outlet, fully-developed flow conditions are assumed

(zero-gradient for all variables, except pressure, which is fixed to a constant value,  $p = 0$ ). A no-slip boundary condition is assigned at the walls (velocity is null, polymeric extra-stress components are linearly extrapolated and a zero-gradient is assumed for pressure in the normal direction to the wall).

### ❖ Command-line

1–Build the mesh:

```
~$ blockMesh
```

2–Run the solver:

```
~$ rheoFoam
```

3–Extract profiles for  $\mathbf{u}$  and  $\boldsymbol{\tau}$  along line  $x = 35$ :

```
~$ sample
```

### ❖ Results

Figure 5.2 presents the fully-developed profiles at line  $x = 35$ . The variables were normalized as follows: length is normalized with  $w$ , time with  $w/U$ , velocity with  $U$  and polymeric components of the extra-stress with  $\frac{\eta_0 U}{w}$ , as in Ref. [42]. A good agreement is observed between the numerical results and the analytical solution written in dimensionless form [42]:

$$\begin{aligned} u_x &= \frac{3}{2}(1 - y^2) \\ \tau_{xy} &= -3(1 - \beta)y \\ \tau_{xx} &= 18Wi(1 - \beta)y^2 \end{aligned}$$

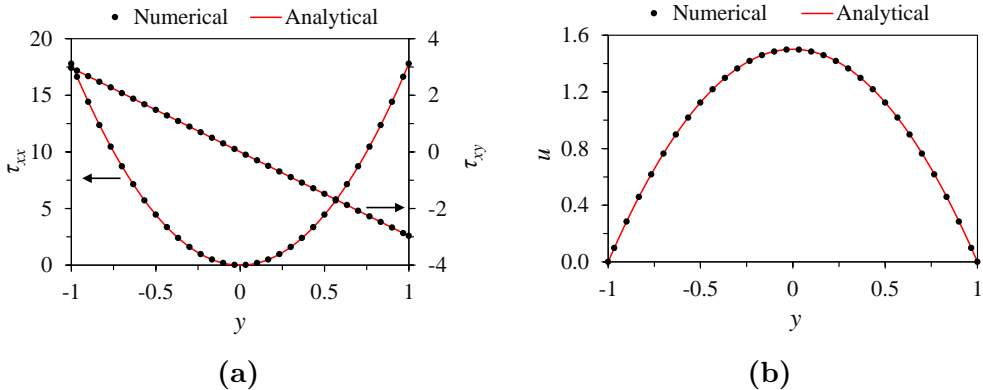


**Figure 5.2:** (a) Polymeric extra-stress components and (b) velocity, at  $x = 35$ , for  $Re = 0$ ,  $Wi = 0.99$  and  $\beta = 0.01$ .

The user can test the solver with a UCM fluid ( $\beta = 0$ ) and confirm that an accurate solution is still achieved, without facing any numerical issue. However, running the same cases without the log-conformation approach leads to numerical divergence (try it!).

This tutorial probes a point in the flow over time (to check for convergence), which has been specified in `controlDict` dictionary. The data is written to a directory named `probes/`, whose location in the case directory depends on the OpenFOAM® version.

### 5.1.4 Case 2: lid-driven cavity flow

 `tutorials/rheoFoam/Cavity/Oldroyd-BLog/`

#### ❖ Overview

The flow in a lid-driven cavity is a common benchmark for numerical solvers, for both Newtonian and viscoelastic fluids, being one of the mostly used geometries for such purposes. One reason explaining the popularity is its simple geometry: a square in 2D or a cube in 3D.

For viscoelastic fluids, stress boundary layers develop at the walls and, at high Deborah numbers, the flow becomes time-dependent. A similar behavior is observed with Newtonian fluids at high Reynold numbers.

The case reproduced in this tutorial is for an Oldroyd-B fluid with  $\beta = \frac{\eta_s}{\eta_s + \eta_p} = 0.5$ . The Deborah number is defined here as  $De = \frac{\lambda U}{L}$ , while the Reynolds number is  $Re = \frac{\rho U L}{\eta_0}$ . In this tutorial, we set  $De = 1$  and  $Re = 0.01$ , so that the creeping flow assumption is still adequate, notwithstanding the finite  $Re$ .

#### ❖ Geometry & Mesh

The planar lid-driven cavity is simply a square, with side length  $L$ , Fig. 5.3. The coordinate axis is located at the bottom-left corner. The mesh consists of one single block with 127 cells uniformly distributed in both directions.

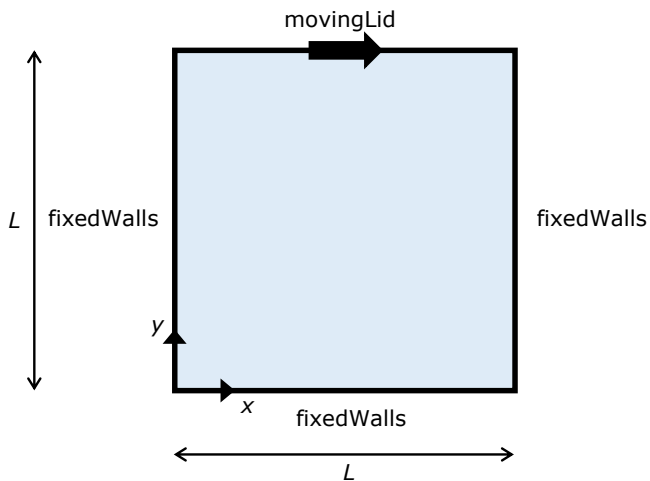


**Figure 5.3:** Geometry for the lid-driven cavity flow.

#### ❖ Boundary conditions

The flow is assumed to be 2D, being solved in the  $xy$ -plane. For the three stationary walls, a no-slip boundary condition is assigned, with null velocity, linearly extrapolated polymeric extra-stresses and zero normal gradient for pressure. At the moving lid wall, the same boundary conditions are used for pressure and polymeric extra-stresses. Regarding the velocity, a time-space dependent condition is employed in order to impose a smooth start of the flow, and to avoid a local singularity with infinite acceleration at the top-right and top-left corners [13]:

$$U_{\text{lid}}(x, t) = 8U [1 + \tanh \{8(t - 0.5)\}] x^2(1 - x)^2 \quad (5.1)$$

Eq. (5.1) is directly implemented as a *codedFixedValue* boundary condition in file *0/U*. The variables were normalized as follows: length is normalized with  $L$ , time with  $L/U$ , velocity with  $U$ , and polymeric extra-stresses with  $\frac{\eta_0 U}{L}$ .

### ⌚ Command-line

1–Build the mesh:

```
~$ blockMesh
```

2–Run the solver:

```
~$ rheoFoam
```

3–Extract profiles for  $\mathbf{u}$  and  $\boldsymbol{\tau}$  along lines  $x = 0.5$  and  $y = 0.75$ :

```
~$ sample
```

### ⌚ Results

Figure 5.4 presents spatial profiles for the  $x$ -component of the velocity and for  $\Theta_{xy}$ , along with the evolution over time of the volume-averaged "kinetic energy", defined as

$$E_k = \frac{1}{2V_t} \int |\mathbf{u}|^2 dV = \frac{1}{2V_t} \sum_{k=1}^N |\mathbf{u}_k|^2 V_k = \frac{1}{2N} \sum_{k=1}^N |\mathbf{u}_k|^2 \quad (5.2)$$

where  $N$  is the number of cells of the mesh and  $V_t = NV_k$  for a uniform mesh. A good agreement is observed between the results obtained by *rheoFoam* and the reference data [13], which shows the good accuracy of the solver, both in space and time. The contour maps for the components of  $\boldsymbol{\Theta}$  are also provided in Fig. 5.5, together with the flow streamlines.

The "kinetic energy" is written on run time to the case directory, using a *codedFunctionObject*, defined in dictionary *controlDict*. The reader can check in this function how Eq. (5.2) has been implemented.

#### 5.1.5 Case 3: flow in a 4:1 planar contraction

 `tutorials/rheoFoam/Contraction41/Oldroyd-BLog/`

### ⌚ Overview

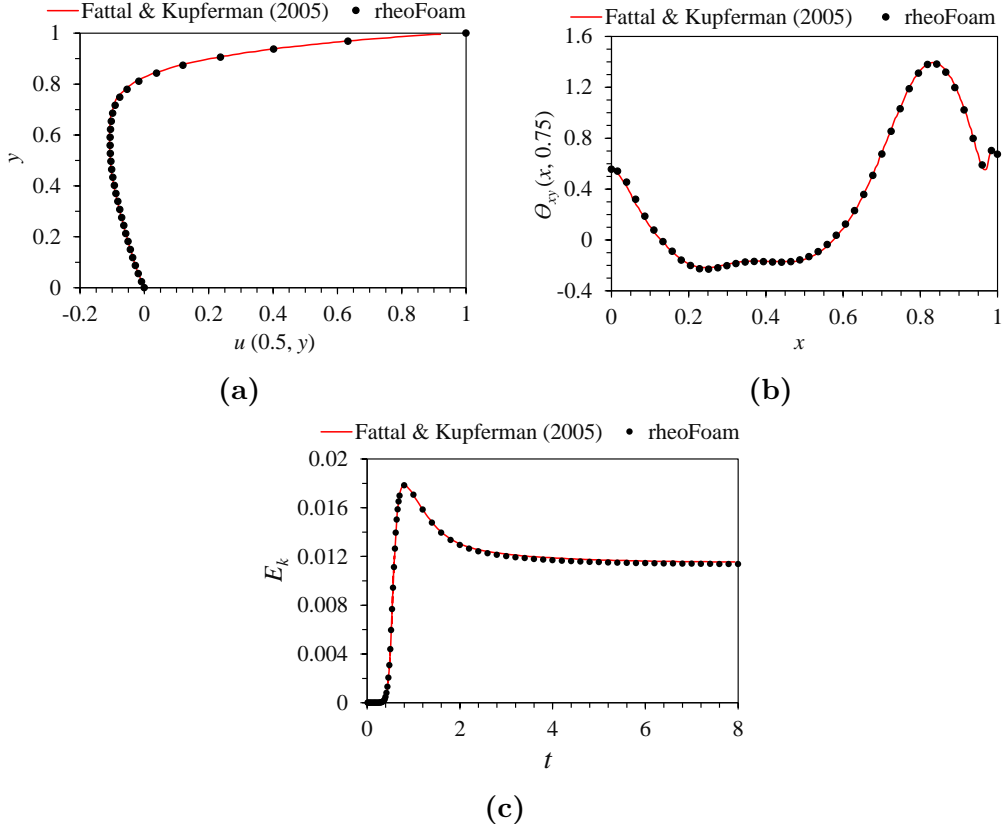


**Figure 5.4:** (a) Velocity profile along line  $x = 0.5$  (at  $t = 8$ ), (b)  $\Theta_{xy}$  profile along line  $y = 0.5$  (at  $t = 8$ ) and (c) evolution of the average "kinetic energy" over time. All the results are for  $Re = 0.01$ ,  $De = 1$  and  $\beta = 0.5$ .

The 4:1 planar contraction is another traditional benchmark flow problem for viscoelastic fluid flow solvers. The existence of singular points at the re-entrant corners, where stresses grow exponentially as the corner is approached, make this problem challenging from a numerical perspective.

This tutorial reproduces the work that we developed in Ref. [2] using an early version of *rheoFoam*, where an Oldroyd-B fluid ( $\beta = \frac{1}{9}$ ) was studied for  $De = 0\text{--}12$ . The `constitutiveProperties` dictionary is adjusted to reproduce the case for  $De = 1$  and  $Re = 0.01$ .

### ❖ Geometry & Mesh

The geometry for this case is reproduced in Fig. 5.6. The mesh corresponds to mesh M1 of Ref. [2].

### ❖ Boundary conditions

The boundary conditions used are described in Ref. [2]. It is worth mentioning that the time-varying inlet velocity is implemented as a `codedFixedValue` boundary condition in file `0/U`. The function is implemented as

$$\mathbf{u}(t) = \begin{cases} \frac{1-\cos(\pi \frac{t}{tlim})}{fac} \mathbf{dirN} & t \leq tlim \\ \mathbf{Uav} & t > tlim \end{cases} \quad (5.3)$$

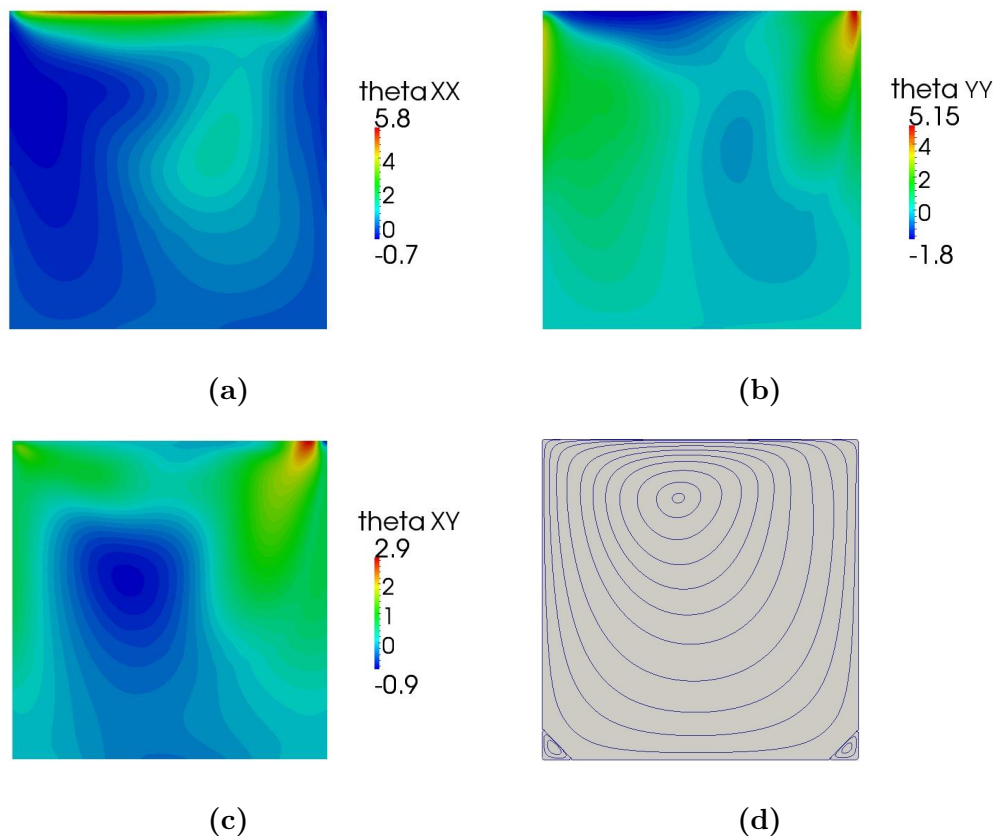


**Figure 5.5:** Contours of (a)  $\Theta_{xx}$ , (b)  $\Theta_{yy}$  and (c)  $\Theta_{xy}$ . In (d), the streamlines are plotted. All the results are for  $Re = 0.01$ ,  $De = 1$ ,  $\beta = 0.5$  and  $t = 8$ .

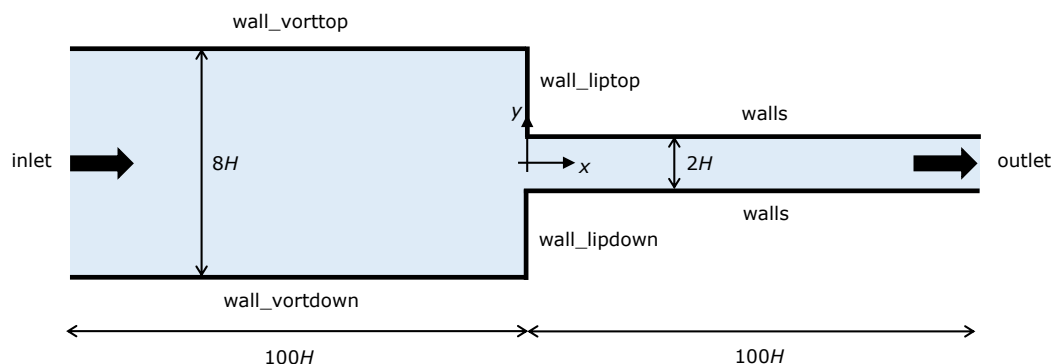


**Figure 5.6:** Geometry for the 4:1 planar contraction.

where  $\mathbf{U}_{av}$  and  $\mathbf{dirN}$  are vectors, and  $fac$  and  $tlim$  are scalar parameters. For  $\mathbf{U}_{av} = (0.25, 0, 0)$ ,  $\mathbf{dirN} = (1, 0, 0)$ ,  $fac = 8$  and  $tlim = 1$ , this generates an inlet velocity profile aligned with the  $x$ -axis and whose magnitude increases from 0, at  $t = 0$ , to 0.25, at  $t = 1$ .

## ✓ Command-line

### 1–Build the mesh:

```
~$ blockMesh
```

2–Run the solver:

```
~$ rheoFoam
```

3–Extract  $\mathbf{u}$  and  $\boldsymbol{\tau}$  at the cell centers immediately upstream and downstream of vertical line  $x = 0$ :

```
~$ sample
```

## ❖ Results

The results obtained with mesh M1 can be found in Ref. [2].

A *coded FunctionObject* returns the points where the wall-parallel velocity component changes of sign (for both the walls near to the upper lip and corner vortices). Those points are delimiting the lip and corner vortices (if present). The user can easily add two extra *coded FunctionObjects* for the vortices in the lower-half of the contraction.

### 5.1.6 Case 4: flow around a confined cylinder

 tutorials/rheoFoam/Cylinder/Oldroyd-BLog/

## ❖ Overview

The planar flow past a confined cylinder is another traditional benchmark problem in computational rheology. Since this flow has no singular points and because extra-stresses can grow significantly in the wake of the cylinder, this problem is particularly well-suited to test the accuracy and stability of numerical methods. Furthermore, it is also a good problem to test the non-orthogonality handling by the algorithms, both in terms of accuracy and stability, since the grids used for this problem usually require some degree of non-orthogonality.

The Oldroyd-B model is used in this tutorial, since a reasonable amount of data is available in the literature for comparison purposes. The Reynolds number for this flow is defined as  $Re = \frac{\rho U R}{\eta_0}$  and the Weissenberg number as  $Wi = \frac{\lambda U}{R}$ . In order to establish comparable conditions with Refs. [43, 44], the solvent viscosity ratio ( $\beta$ ) is fixed at 0.59, the blockage ratio (diameter of cylinder/width of the channel) is 50 % and  $Re = 0$  (the convective term in the momentum equation is removed). The case at  $Wi = 0.7$  is simulated in this tutorial.

## ❖ Geometry & Mesh

The geometry used in this case is composed of a channel with a cylinder of radius  $R$  vertically centered between its walls – spaced apart  $4R$  –, and placed at a distance of  $20R$  from the inlet, Fig. 5.7. The length of the channel downstream of the cylinder is  $60R$ . The mesh for this geometry is composed of 8 blocks (upper-half), with a high cell-density near the wall of the cylinder. The minimum cell length in the radial direction of the cylinder is  $0.0049R$ , while in the tangential direction it is  $0.0053R$ .

## ❖ Boundary conditions

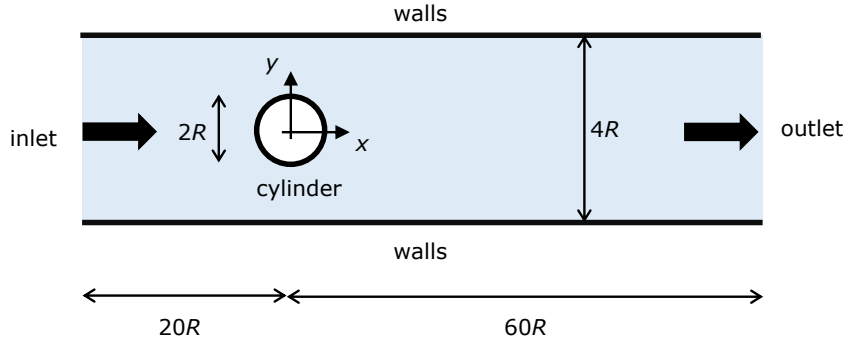


**Figure 5.7:** Cylinder vertically centered in a planar channel with 50 % blockage ratio.

The flow is assumed to be 2D, being solved in the  $xy$ -plane. At the inlet, a uniform velocity profile with magnitude  $U$  is imposed, the polymeric extra-stresses are null and zero-gradient is assigned to pressure. Channel and cylinder walls are static (velocity is null, polymeric extra-stresses are linearly extrapolated to the walls and a zero-gradient is imposed for pressure). At the outlet, fully-developed conditions are assumed: zero-gradient for all variables, except pressure, which is fixed to a constant value,  $p = 0$ .

### ❖ Command-line

1–Create half of the mesh:

```
~$ blockMesh
```

2–Reflect the half-mesh using plane  $xz$  as mirror, to obtain the full mesh:

```
~$ mirrorMesh -noFunctionObjects
```

3–Run the solver:

```
~$ rheoFoam
```

### ❖ Results

Figure 5.8 presents the contour plots for the first normal stress difference and for the velocity magnitude (with superimposed streamlines), at  $Re = 0$ ,  $Wi = 0.7$  and  $\beta = 0.59$ , using the Oldroyd-B model with the log-conformation approach. Note that the velocity is normalized with  $U$ , time with  $R/U$  and polymeric extra-stresses with  $\frac{\eta_0 U}{R}$ . The drag coefficient obtained in such conditions is  $C_d = 117.357$ , which is in reasonable agreement with  $C_d = 117.323$  [44] and  $C_d = 117.315$  [43]. Refining the mesh would further increase the accuracy of the numerical solution. The drag coefficient was computed as

$$C_d = \frac{1}{\eta_0 U h} \int_S (p \mathbf{I} + \boldsymbol{\tau}') \cdot \hat{\mathbf{i}} \cdot dS = \frac{1}{\eta_0 U h} \sum_{k=1}^{N_f} \mathbf{S}_f \cdot (p_f \mathbf{I} + \boldsymbol{\tau}'_f) \cdot \hat{\mathbf{i}}$$

where  $\mathbf{S}_f$  is a vector normal to each face of the cylinder boundary, whose magnitude is equal to the face's area,  $h$  is the depth of the cylinder in the neutral (empty) direction and  $\hat{\mathbf{i}}$  is a unitary vector aligned with the streamwise direction. The drag coefficient is retrieved on run time by a *coded FunctionObject*, which can be found in `controlDict` dictionary.

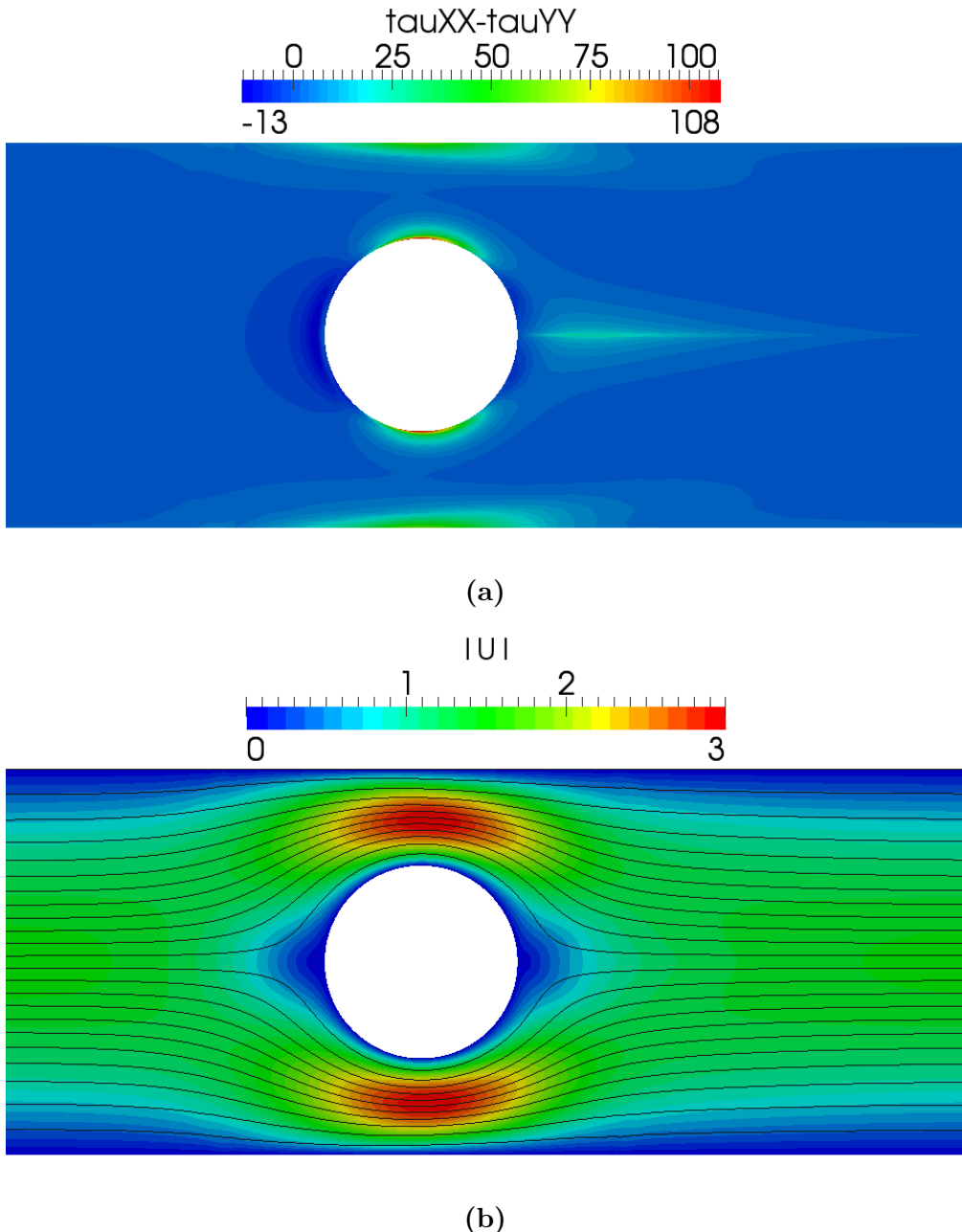


**Figure 5.8:** (a) First-normal stress difference and (b) velocity magnitude contours with superimposed streamlines, at  $t = 15$ , for  $Wi = 0.7$ ,  $Re = 0$  and  $\beta = 0.59$ .

Since version 4.0 of *rheoTool*, this tutorial is solved with a semi-coupled solver ( $p\text{-}\mathbf{u}$  coupled and  $\boldsymbol{\tau}$  segregated) in OpenFOAM® versions. Under this setup, a higher time-step can be used, no pressure under-relaxation is needed and the

non-orthogonality corrector loop is not used, notwithstanding the mesh non-orthogonality. Overall, this allows a fast convergence to the final solution. Note, however, that these conditions are not appropriate for a transient study.

### 5.1.7 Case 5: bifurcation in a 2D cross-slot flow

 `tutorials/rheoFoam/CrossSlot/Oldroyd-BLog/`

#### ❖ Overview

While the previous tutorials were based on traditional benchmark flow problems, the case selected for this tutorial is a recent benchmark: the 2D cross-slot flow [45]. For sufficiently high Deborah numbers, the flow in such geometry becomes asymmetric (steady or unsteady) [45]. At the stagnation point generated by the two opposite-flowing streams, fluid elements can remain for a virtually infinite amount of time. Because the local strain-rate is non-zero, the accumulated strain is high (theoretically infinite at the stagnation point), and this is especially problematic for models based on springs with an infinite extension – the tensile normal stress grows exponentially over time near that point. Thus, a singular point exists in this case, although not being located at a wall, as commonly seen in other geometries with singularities.

In directory `tutorials/rheoFoam/CrossSlot/`, there are four tutorials for this case, each one using a different model or solution method. The tutorial described here is the one solving the Oldroyd-B model with the log-conformation approach (`Oldroyd-BLog/`). The remaining cases are: `Oldroyd-BRootk/`, which solves the Oldroyd-B model using the root<sup>k</sup> kernel, with  $k = 8$ ; `Oldroyd-B-Sqrt/`, which solves the Oldroyd-B model using the square-root transformation approach; and `PTTlinearLog/`, which solves the linear PTT model with the log-conformation approach. All the tutorials with the Oldroyd-B model are for the same conditions:  $De = 0.33$ ,  $Re = 0$  and  $\beta = 0$  (UCM fluid). The tutorial solving the linear PTT model is for  $De = 0.6$ ,  $Re = 0$ ,  $\beta = 1/9$ ,  $\varepsilon = 0.02$  and  $\zeta = 0$  (simplified PTT). This group of tutorials also solves the transport equation of a passive scalar, exemplifying how this extra-feature can be used.

The dimensionless numbers for this problem are defined as:  $Re = \frac{\rho UW}{\eta_0}$ ,  $Wi = \frac{\lambda U}{W}$ ,  $\beta = \frac{\eta_s}{\eta_0}$  and  $Pe = \frac{WU}{D}$ . The Péclet number ( $Pe$ ) is only relevant for the scalar transport equation and  $D$  is the diffusion coefficient of the passive tracer. We set  $Pe = 500$  in all the cases (representative, for example, of rhodamine-B in water flowing in a 200  $\mu\text{m}$  wide channel, at 1 mm/s).

#### ❖ Geometry & Mesh

The cross-slot geometry for this tutorial is depicted in Fig. 5.9. It consists of four identical arms (width  $W$ ; length  $10W$ ), where the two vertically opposite arms are inlets and the remaining are outlets. Each arm is meshed as a single block with 60 cells in the streamwise direction (cells are compressed near the origin) and 51 cells uniformly distributed in the transverse direction. As a consequence, the central square block,  $(x, y) \in [-0.5W, 0.5W]$ , has 51x51 uniformly spaced cells. The use of an odd number of cells in both directions of the central square

generates a cell exactly centered at the stagnation point, which is advantageous for the post-processing of quantities of interest at this location.

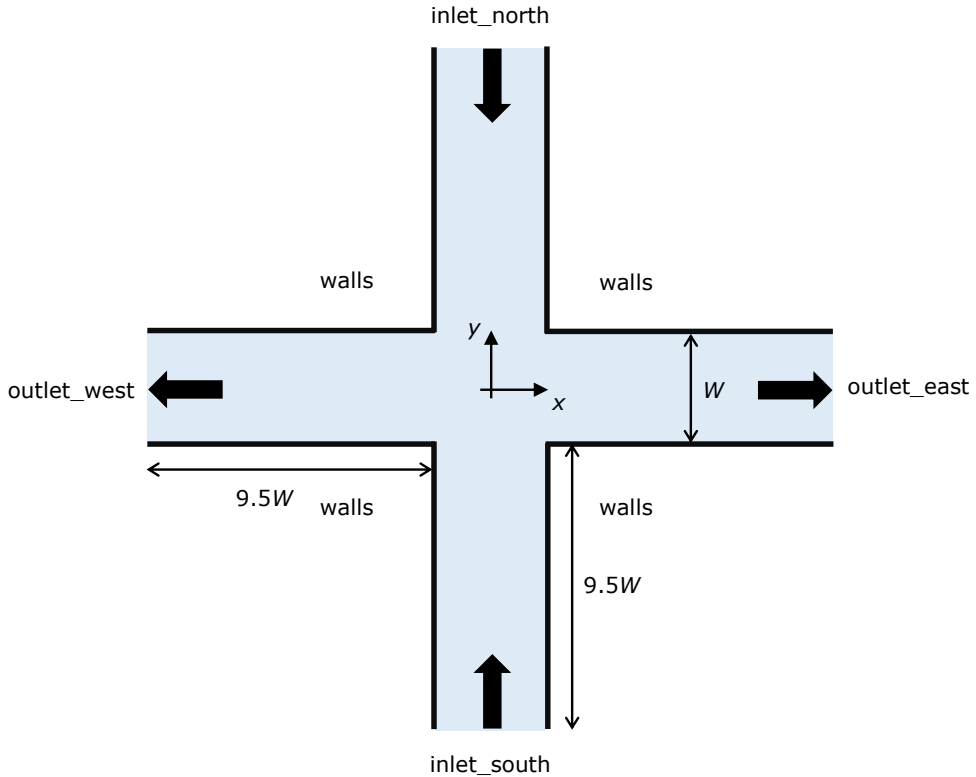


**Figure 5.9:** Cross-slot geometry composed of 4 arms with two balanced inlets and two outlets.

### ❖ Boundary conditions

The flow is assumed to be 2D, being solved in the  $xy$ -plane. At both inlets, a uniform velocity profile is specified, with magnitude  $U$  and pointing to the origin, so that those two streams are flowing in opposite directions. The polymeric extra-stresses are null and for pressure a zero-gradient is used. The walls are stationary, thus velocity is null, polymeric extra-stresses are linearly extrapolated and the pressure is assumed to not change in the normal direction. Fully-developed flow conditions are assigned at the outlets: null normal gradient for all variables, except pressure, which is fixed at  $p = 0$ .

A passive scalar (tracer field  $C$ ) is added to the problem, which requires the assignment of initial and boundary conditions. We impose a continuous injection of  $C$  at *inlet\_north* ( $C = 1$ ), while no tracer is injected at *inlet\_south* ( $C = 0$ ). In the remaining boundaries, we impose null normal gradient (meaning no flux of  $C$  across the walls and fully-developed flow conditions at both outlets). At time  $t = 0$ , when the simulation is started, the  $y$ -positive portion of the cross-slot is filled with the tracer ( $C = 1, y > 0 \wedge t = 0$ ).

### ❖ Command-line

1–Build the mesh:

```
~$ blockMesh
```

2–Create field C by copying one already present, which is not initialized in the interior domain:

```
~$ cp 0/C.org 0/C
```

3–Initialize field C in the interior domain ( $C = 1, y > 0 \wedge t = 0$ ):

```
~$ setFields
```

4–Run the solver:

```
~$ rheoFoam
```

### ❖ Results

The contours for some important variables are displayed in Fig. 5.10, for  $Re = 0$ ,  $Wi = 0.33$ ,  $\beta = 0$  (UCM model) and  $Pe = 500$ . The variables are normalized with  $U$  (velocity),  $W/U$  (time) and  $\frac{\eta_0 U}{W}$  (stresses).

The local Weissenberg number at the origin, defined in Ref. [45] as the product of the relaxation time by the velocity gradient magnitude at the stagnation point streamlines, is  $Wi_0 = 0.523$ , which is close to the benchmark value obtained in a similar mesh,  $Wi_0 = 0.509$  (Ref. [45], for mesh M1). The local Weissenberg number at the origin is retrieved by the solver to the case directory, through a *coded FunctionObject* that can be found in dictionary `controlDict`.

The importance of stress-velocity coupling in this case can be evaluated by re-running the tutorial with either BSD only or no stabilization method (*stabilization = none* or *BSD*, in dictionary `constitutiveProperties`).

Checkerboard fields easily develop in such conditions (this is a critical case due to the use of a UCM fluid).

Note that this tutorial makes use of a variable time-step, controlled by a maximum Courant number fixed at 0.4. This strategy is used because only steady-state results are of interest. This is also the reason to use a high tolerance in the sparse matrix solvers, in `fvSolution` dictionary – the steady asymmetry in the flow develops faster with these conditions, since the transient numerical error is higher.

## 5.1.8 Case 6: blood flow simulation in a real-model aneurysm

 `tutorials/rheoFoam/Aneurysm/HerschelBulkley/`

### ❖ Overview

The tutorial presented in this Section addresses the simulation of blood flow in a real-model aneurysm. Contrarily to the previous tutorials, this case is based on a 3D polyhedral (non-orthogonal) mesh and uses a GNF model. Furthermore, the flow is simulated for a moderate Reynolds number, which will test the robustness of the solver for such conditions, where inertia already plays an important role.

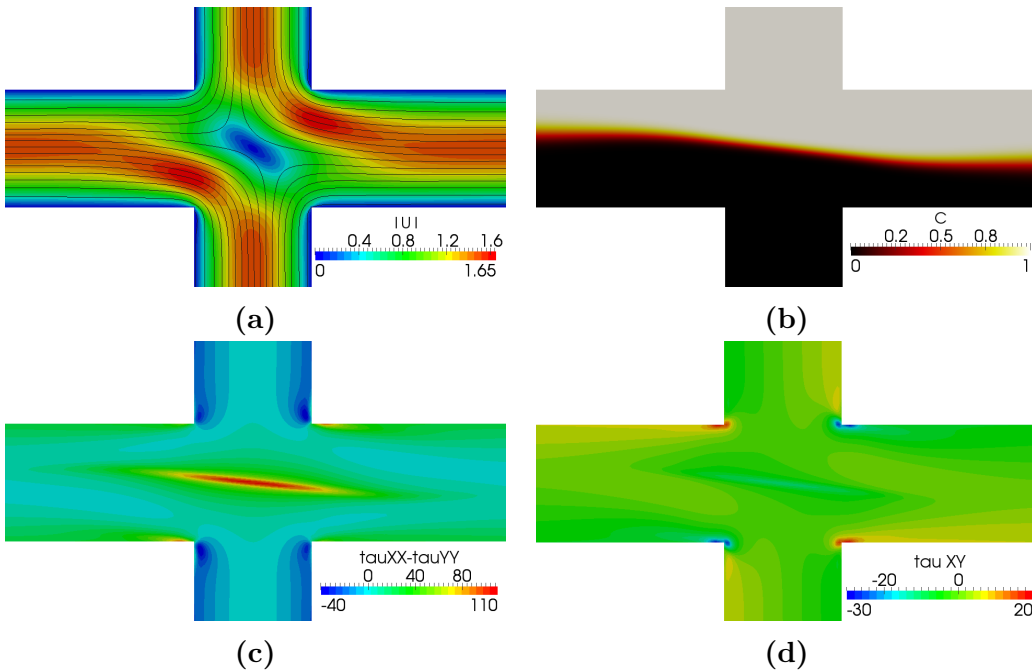


**Figure 5.10:** (a) Velocity magnitude contours with superimposed streamlines, (b) contours of  $C$ , (c) first-normal stress difference and (d)  $\tau_{xy}$  contours, for  $Re = 0$ ,  $Wi = 0.33$ ,  $\beta = 0$  and  $Pe = 500$ .

The Herschel-Bulkley model was selected to simulate the blood rheology, following Ref. [46]. The generalized Reynolds number for this model, assuming  $\tau_0 = 0$  – the power-law limit –, is [46]:

$$Re_{GN} = \frac{\rho(2R_{in1})^n \bar{U}^{2-n}}{k \left(\frac{3n+1}{4n}\right)^n 8^{n-1}}$$

This tutorial simulates the flow at  $Re_{GN} = 420$ .

### ⌚ Geometry & Mesh

The STL file of the aneurysm surface was downloaded from a repository with real-model aneurysms [47], extracted from 3D rotational angiographies of diseased patients. From the list of available models, case ID *C0005* was selected, which refers to an aneurysm in the internal carotid artery (ICA).

The surface is composed of one main entry vessel (*in1*, the ICA), which bifurcates into two smaller vessels (*out1* and *out2*), Fig. 5.11a. The aneurysm is located near the bifurcation point. Due to the long extension of vessels upstream and downstream of the aneurysm in the original STL file, all the vessels were shortened and a cylindrical extension was connected to each one, in order to minimize entry/exit effects in the region near the aneurysm. The locations where those connections were established are highlighted in Fig. 5.11a using red arrows. The transition length between the tube connectors and the vessels is typically 10 % of the vessel radius and the radius of those tubes is equal to the equivalent radius of the vessels at the connection point. The radius of each inlet/outlet is:  $R_{in1} = 1.66$  mm,  $R_{out1} = 1.17$  mm and  $R_{out2} = 0.95$  mm.

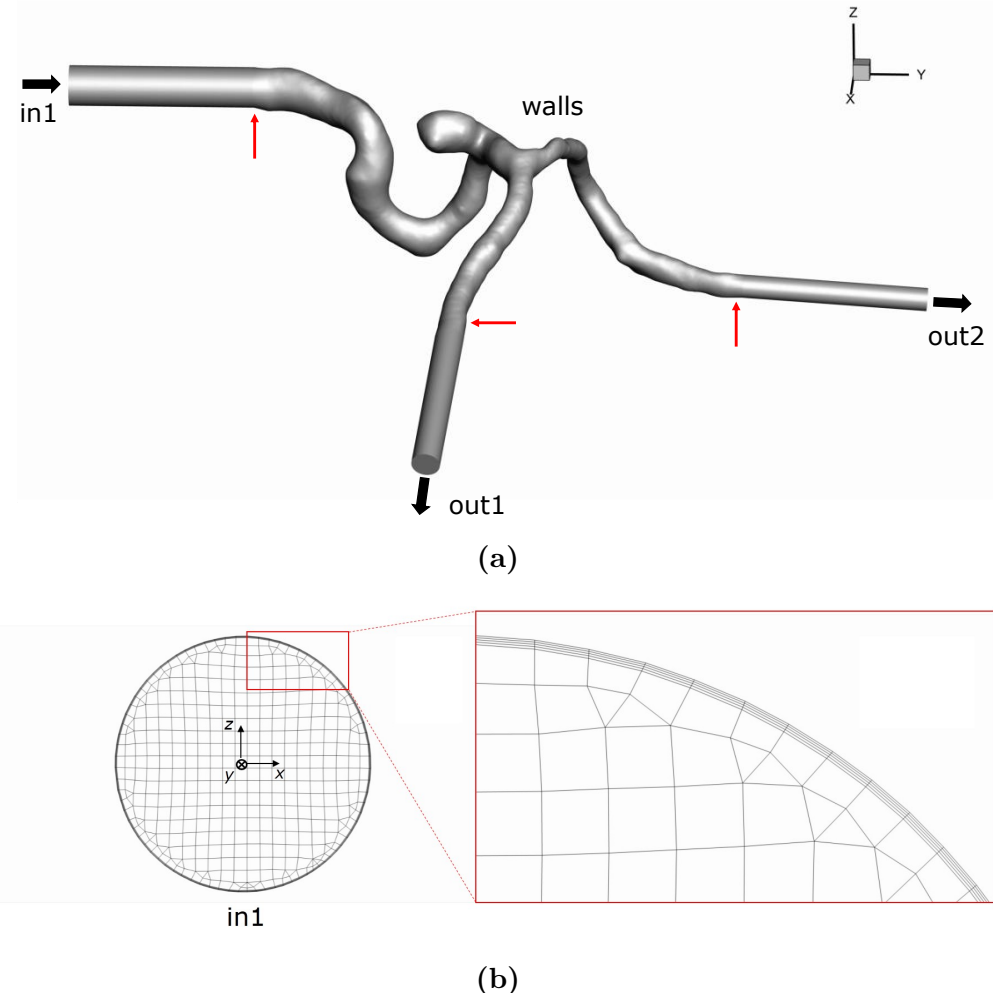


**Figure 5.11:** (a) Geometry of the aneurysm considered in the tutorial. Red arrows point to the transition regions between the aneurysm and the cylindrical extensions. The radius of each inlet/outlet is:  $R_{\text{in}1} = 1.66 \text{ mm}$ ,  $R_{\text{out}1} = 1.17 \text{ mm}$  and  $R_{\text{out}2} = 0.95 \text{ mm}$ . (b) Detailed view of the mesh on patch  $\text{in}1$ , zooming the cell layers near the wall. The reference axis for the geometry is centered on patch  $\text{in}1$ , with the normal vector of the patch pointing in the negative direction of the  $y$ -axis.

The mesh was built using <sup>1</sup>*cfMesh*, a meshing tool available in foam-extend since version 3.2. The maximum cell size was limited to 5 mm and boundary cell layers were generated near to the vessel walls in order to accurately solve the gradients developed there, Fig. 5.11b. The mesh provided with this tutorial has around 280 kcells.

### ❖ Boundary conditions

The boundary conditions and fluid properties used in this tutorial are based in Ref. [46], where also ICA aneurysms were studied. Accordingly, blood is modeled with a Herschel-Bulkley model, with  $\tau_0 = 0.0175 \text{ Pa}$ ,  $k = 8.9721 \times 10^{-3} \text{ Pa.s}^n$ ,

<sup>1</sup><http://cfmesh.com/>

$n = 0.8601$  and  $\eta_0 = 0.15$  Pa.s. Note that  $\eta_0$  (see Table 4.1) is a parameter characteristic of the model implementation in *rheoTool*, which limits the viscosity for low strain-rate values – otherwise it would generate infinite values at points with zero shear-rate. A relatively high value was attributed to  $\eta_0$  in order to not affect the results. Furthermore, a density of 1050 kg/m<sup>3</sup> is considered.

For this fluid model, a fully-developed velocity profile is imposed at the inlet (*in1*), along with a null pressure gradient. For small  $\tau_0$ , we can use (approximately) the fully-developed velocity profile for a power-law fluid:

$$U = \bar{U} \frac{3n+1}{n+1} \left[ 1 - \left( \frac{r}{R} \right)^{\frac{n+1}{n}} \right] \quad (5.4)$$

where  $\bar{U}$  is the mean velocity. In our case,  $\bar{U}$  is constant over time, thus steady conditions are simulated, instead of the cardiac cycle (this is to shorten the simulation time, since transient solutions would require a lower time-step, leading to a higher computational time). Regarding the walls, a no-slip boundary condition is imposed. At the outlets, the pressure is fixed to zero and the velocity is assumed to be fully-developed (zero gradient for velocity). Since the Reynolds number used in the tutorial is well below the critical value for transition to the turbulent regime, no special conditions need to be defined regarding turbulence modeling.

## ❖ Command-line

The mesh is already built and can be found in folder `polyMesh/`.

1–Decompose the case among 2 processors to speed-up the computations (with 2 processors, it takes around 1h to reach convergence in a laptop with an Intel i5-3210M processor, 2.5 GHz):

```
~$ decomposePar
```

2–Run the solver in parallel, using 2 processors:

```
~$ mpirun -np 2 rheoFoam -parallel
```

3–Reconstruct the last time-step of the case for post-processing:

```
~$ reconstructPar -latestTime
```

## ❖ Results

The results obtained at  $Re_{GN} = 420$  are displayed in Fig. 5.12, where both the streamlines and the wall shear-stress magnitude (*WSSmag*) contours are shown. The wall shear-stress magnitude is computed through a *ppUtil* (described in Section 4.7.2), whose settings can be found in dictionary *fvSolution*, under subDict *PostProcessing*.

This tutorial is defined to run with an adjustable time-step, controlled by a maximum Courant number fixed at 50. The high Courant number is to quickly achieve the steady-state, without the need to cancel the time-derivatives. The non-orthogonality corrector loop was turned on, with 1 iteration *per* time-step (the pressure is also under-relaxed with a factor of 0.9), in order to avoid possible numerical issues due to non-orthogonality. The convergence can be monitored by a probe located at one of the exit vessels, downstream of the aneurysm.

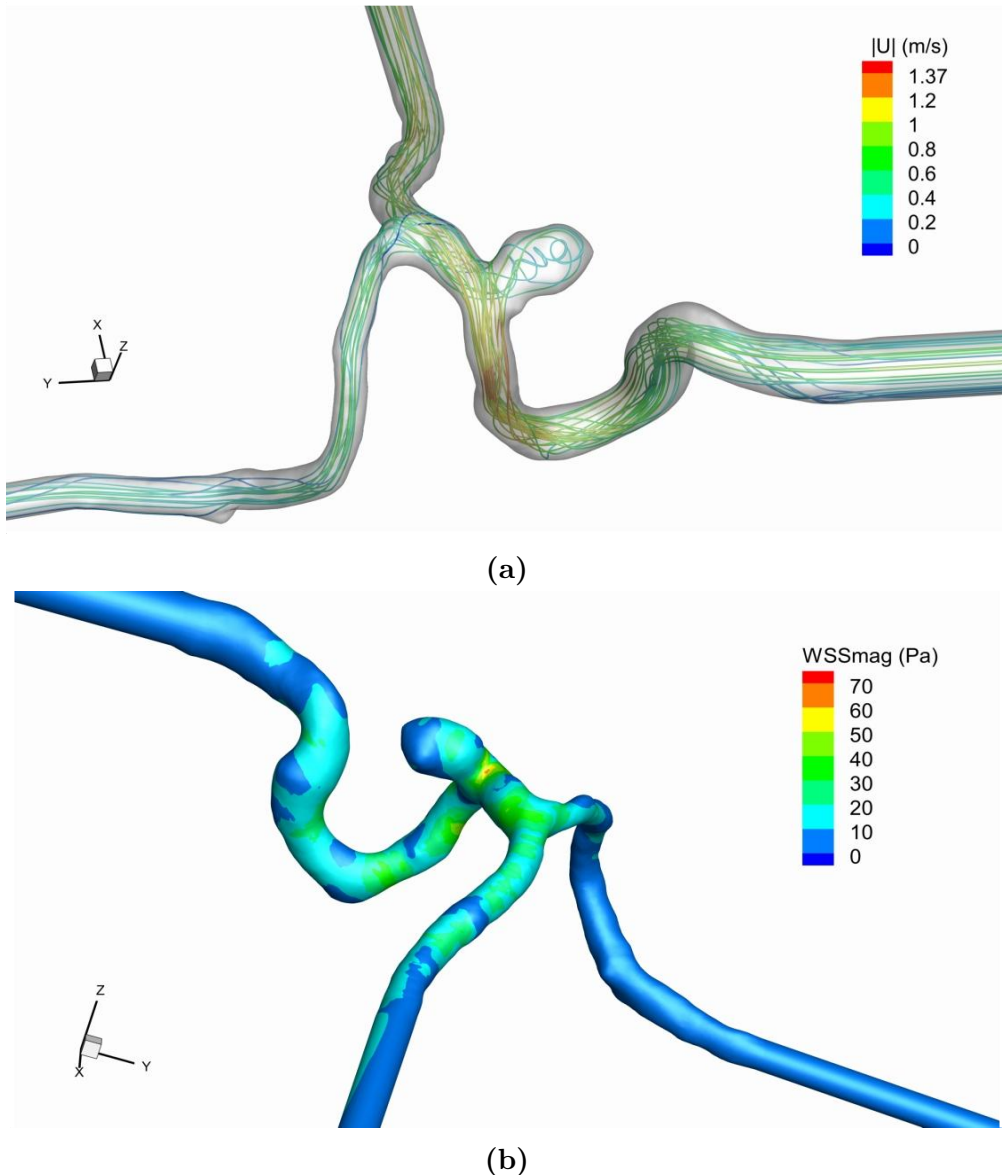


**Figure 5.12:** (a) Streamlines (colored with the velocity magnitude) and (b) wall shear-stress magnitude contours, at steady-state and for  $Re_{GN} = 420$ .

### 5.1.9 Case 7: viscous fluid damper (moving mesh)

[tutorials/rheoFoam/fluidDamper/CarreauYasuda/](#)

#### ❖ Overview

Viscous fluid dampers react to applied loads with the generation of a back pressure due to the high resistance experienced by a viscous fluid flowing through narrow orifices. These mechanical elements are typically composed of a moving piston enclosed inside a cage filled with a viscous fluid, with a narrow gap left between the piston and the cage wall. The motion of the piston and the shaft to which it is connected drive the fluid flow inside the cage. This tutorial aims to simulate the fluid dynamics inside a damper subjected to an oscillatory load,

whereby the piston and shaft motion are represented by a moving mesh.

The setup adopted in this tutorial aims to closely reproduce the conditions presented by Syrakos et al. [48]. The case represented in this tutorial is for the Careau-Yasuda fluid, named *CY-100* in [48], at 32 Hz. Other conditions can be easily tested by simple adjustment of the input parameters.

### ❖ Geometry & Mesh

The fluid damper geometry is depicted in Fig. 5.13. The geometry is equal to that presented in [48], and the piston edges are rounded by the same radius of curvature ( $R_{\text{curv}} = 0.75$  mm) as therein. The damper is axisymmetric, thus only a slice of the total domain is simulated (Fig. 5.13). A Cartesian system of coordinates is shown in Fig. 5.13 because that is the one used by OpenFOAM® to solve the problem, although keep in mind that symmetry around axis  $Ox$  holds.

The mesh is built using *blockMesh* and has a spatial resolution in the gap region between patches *top* and *piston*, which is approximately half of mesh M1 in [48].

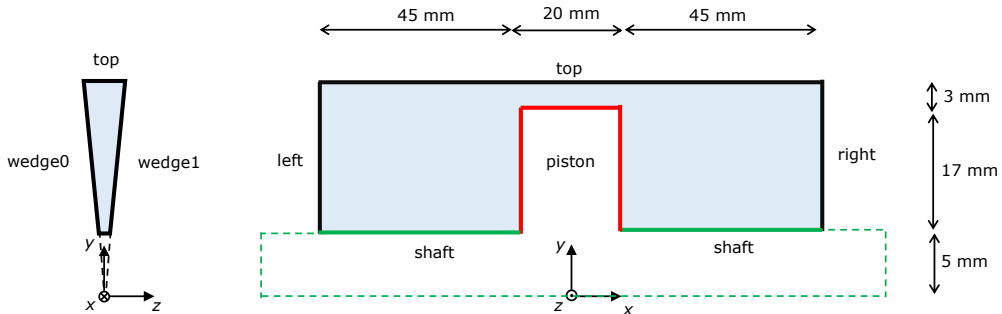


**Figure 5.13:** Fluid damper geometry. The geometry is symmetric around axis  $Ox$ , thus the computational domain corresponds to only a slice of the whole geometry.

### ❖ Boundary conditions

The Navier slip boundary condition is applied to the velocity field in all the boundaries (except on wedges), in agreement with [48]. In addition, the velocity of patches *shaft* and *piston* receive an extra contribution due to their own oscillatory motion,

$$\mathbf{u}_{\text{shaft, piston}} = \mathbf{u}_{\text{NS}} + \boldsymbol{\alpha} \omega \cos(\omega t) \quad (5.5)$$

where  $\boldsymbol{\alpha} = (\alpha, 0, 0)$  is the amplitude vector,  $\alpha = 0.012$  m and  $\omega = 64\pi$  rad/s. Note that Syrakos et al. [48] used a sine function for the motion, whereas a cosine is used here for convenience (the two functions are offset by  $\pi/2$  rad). A zero-gradient condition is imposed for pressure.

Although physically both the shaft and piston move, in practice we only let the *piston* patch to follow exactly the motion described by Eq. 5.5, while the faces of patch *shaft* stretch or shrink according to the motion imposed by patch

*piston* (*slip* boundary condition). The same happens for patch *top*, while the remaining patches remain static. The mesh motion is obtained from the solution of a Laplace equation with the previously described boundary conditions and a variable diffusivity coefficient (see `dynamicMeshDict` dictionary). Note that the boundary conditions presented in this paragraph are not related with the fluid velocity field, whose boundary conditions were reported in the previous paragraph. Still, such coupling can be obtained with boundary condition *movingWallVelocity*, whereby the given patch velocity is used as boundary condition to the fluid velocity (this can be used, for example, for patch *piston*, but not for patch *shaft*).

### ❖ Command-line

1–Build the mesh:

```
~$ blockMesh
```

2–Run the solver:

```
~$ rheoFoam
```

3–Check file *Ffl* generated by the solver.

### ❖ Results

The oscillatory piston motion can be directly observed in Paraview. In addition, the solver writes in runtime the reaction force exerted by the fluid on the piston and shaft (file *Ff1*),

$$F_{\text{fl}} = \int_S (-p\mathbf{I} + \boldsymbol{\tau}') \cdot \hat{\mathbf{i}} \cdot d\mathbf{S} = \sum_{k=1}^{N_f} \mathbf{S}_f \cdot (-p_f \mathbf{I} + \boldsymbol{\tau}'_f) \cdot \hat{\mathbf{i}}$$

where  $\mathbf{S}_f$  is a vector normal to each face of the shaft/piston boundary, whose magnitude is equal to the face's area, and  $\hat{\mathbf{i}}$  is a unitary vector aligned with the  $Ox$  axis. Since  $x_{\text{piston}} = \alpha \sin(\omega t)$  is the known  $x$ -position of the piston midpoint over time, then the force can be plotted against the displacement (Fig. 5.14). Note that two periods of oscillation are simulated in the tutorial, and we can consider that the first period is already in the steady regime. Moreover, in a plot such as the one of Fig. 5.14 (considering the steady periodic regime), it is not relevant if a sine or cosine function is used in Eq. (5.5).

## 5.2 *rheoTestFoam*

### 5.2.1 General guidelines

In Section 4.5.2, *rheoTestFoam* was presented as a testing application for the constitutive models implemented in *rheoTool*, being not a general-purpose solver. For this reason, some of the steps usually required to setup a generic simulation in OpenFOAM® are not necessary with *rheoTestFoam*, while, on the other hand, extra-inputs need to be specified.

 **constant/**

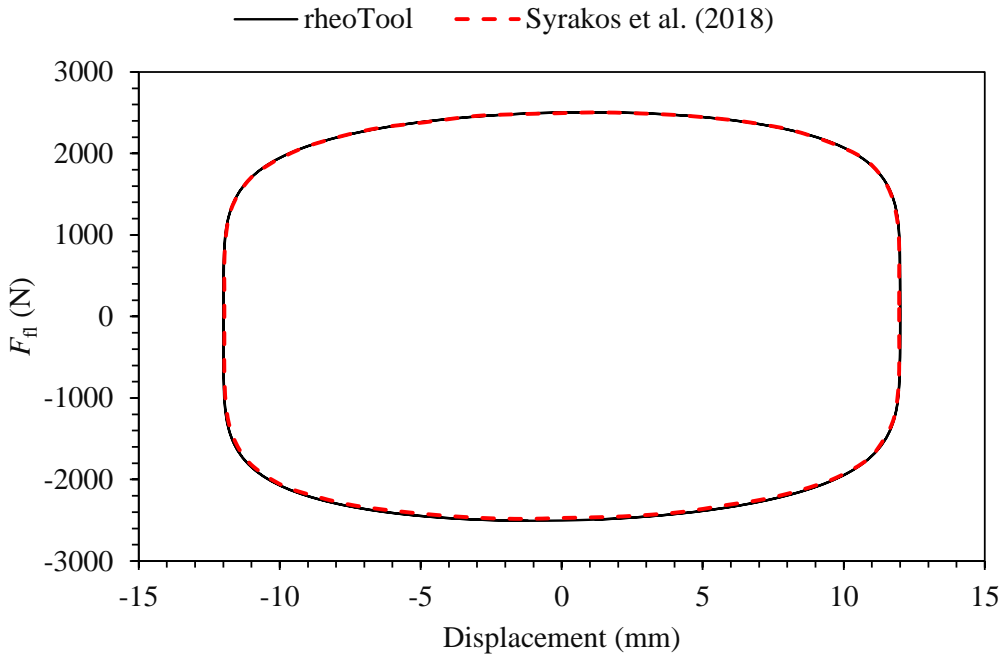


**Figure 5.14:** Reaction force exerted by the Carreau-Yasuda fluid on the piston and shaft over time, for  $f = 32$  Hz. The results of Syrakos et al. [48] are also plotted for reference.

One main difference of *rheoTestFoam* cases regarding, for example, *rheoFoam* cases is in the mesh: the user should always use the same single-cell unitary mesh when working with *rheoTestFoam*. Thus, changing the mesh from case to case is unnecessary and not recommended.

The dictionary `constitutiveProperties` is composed of two subDict: `parameters` and `rheoTestFoamParameters`, as displayed in Listing 5.2. The entries in `parameters` have exactly the same meaning as previously discussed for *rheoFoam*. However, there are two entries which remain inactive in *rheoTestFoam*: `rho` and `stabilization`. Remember from Section 4.5.2 that *rheoTestFoam* is only solving the constitutive equations for a given  $\nabla\mathbf{u}$  tensor, thus those two parameters related with the momentum equation are useless. Nevertheless, they should be present (with any assigned value) to avoid a run time error. `rheoTestFoamParameters` is a subDict specific of *rheoTestFoam*, in the same way as `passiveScalarProperties` is a particular subDict of *rheoFoam*. The keyword `ramp` stands for the operation mode (see Section 4.5.2): `ramp (true)` or `transient (false)`. The other two entries define tensor  $\nabla\mathbf{u}$ , since we consider  $\nabla\mathbf{u} = \text{gammaEpsilonDotL}[i] \cdot \text{gradU}$ , where  $i$  is the index representing each entry of list `gammaEpsilonDotL`. If `ramp = false`, the mode is transient and only one entry is expected in `gammaEpsilonDotL` – the solver is testing the transient behavior of the constitutive model, for a (single) given  $\nabla\mathbf{u}$ . On the other hand, in ramp mode (`ramp = true`), `gammaEpsilonDotL` may have as many entries as defined by the user and steady-state variables will be returned by the solver for each entry. Any combination of components is admissible for `gradU`, although only some correspond to canonical rheometric flows. The

one displayed in Listing 5.2 is for a pure-shear flow:  $\mathbf{u} = (\dot{\gamma}y, 0, 0)$ , where  $\dot{\gamma}$  is the *gammaEpsilonDotL* value.

```

1 parameters
{
3     type          Oldroyd-B;
5     etaS          etaS [1 -1 -1 0 0 0 0] 1.;
6     etaP          etaP [1 -1 -1 0 0 0 0] 1.;
7     lambda        lambda [0 0 1 0 0 0 0] 0.1;

9 // Place-holder variables in rheoTestFoam
10    stabilization   none;
11    rho            rho [1 -3 0 0 0 0 0] 0.;
}
13
rheoTestFoamParameters
15 {
16     ramp           false;
17
18     gradU          (0. 0. 0.
19                      1. 0 0.
20                      0. 0. 0.);
21
22     gammaEpsilonDotL
23     (
24         1.
25     );
}

```

**Listing 5.2:** Example of a `constitutiveProperties` dictionary used with *rheoTestFoam*.

### 0/

When using *rheoTestFoam*, the same fields as for *rheoFoam* should be present in folder 0/. However, any value can be assigned to their internal/boundary fields, since the solver will internally manipulate those values (only for velocity) in order to fulfill the specified  $\nabla \mathbf{u}$  (Fig. 4.3). **Shortly, both the mesh and folder 0/ provided in the tutorials can be readily applied to any fluid, without any change.**

### system/

When running *rheoTestFoam* in ramp mode, the user does not have control on *deltaT* (time-step), nor on the *endTime*. The time step is automatically set based on the relaxation time and strain-rate values for viscoelastic fluids or is simply set to 1 s for GNF models (in this case, the value is not important since no equation is solved implicitly). The *endTime* in ramp mode is not important, since the stopping criteria is based on an hard-coded threshold for the residuals and for the number of iterations. On the other hand, in transient mode, both variables should be specified by the user in `controlDict`. Regarding the discretization schemes (`fvSchemes` dictionary), only time-derivatives and *grad(U)* are used by the solver. The discretization of *grad(U)* should be kept as *Gauss linear*, while

any valid time-scheme can be selected (except steady-state), although in ramp mode this should not make any difference, since we are looking for steady-state solutions. In dictionary `fvSolution`, the matrix solvers required by the constitutive equations must be defined and the number of inner-iterations may also be controlled if running in transient mode. Note that since the mesh has only one cell, a good time accuracy can be achieved by selecting a small time-step, without compromising the CPU time (in general, simulations will be always fast). The use of under-relaxation is not needed, as long as time-derivatives are not disabled in `fvSchemes` (this is our recommendation).

### 5.2.2 Case I: Herschel-Bulkley model

 `tutorials/rheoTestFoam/HerschelBulkley/`

#### ❖ Overview

This tutorial illustrates the behavior of the Herschel-Bulkley model used in tutorial *Case 6* to model the blood rheology (Section 5.1.8). A steady shear flow is considered for this purpose.

#### ❖ Geometry & Mesh

The geometry used with *rheoTestFoam* is always the same (see Sections 5.2.1 and 4.5.2). The mesh is already built (do not change it).

#### ❖ Boundary conditions

The boundary conditions to be used with *rheoTestFoam* are always the same (see Sections 5.2.1 and 4.5.2). Folder `0/` should not be changed.

#### ❖ Command-line

1–Run the solver:

```
~$ rheoTestFoam
```

The file `Report` is created in the case directory, which contains the results.

#### ❖ Results

For a GNF model, only the ramp mode of *rheoTestFoam* makes sense to be used, since thixotropy is not considered in any of the GNF models implemented. A steady shear flow is used, thus  $\frac{\partial u}{\partial y}$  is the only non-zero component of tensor  $\nabla \mathbf{u}$ . For the range of shear-rates between  $0.01 \text{ s}^{-1}$  and  $10000 \text{ s}^{-1}$ , the Herschel-Bulkley model behavior is displayed in Fig. 5.15. The model predicts a shear-thinning behavior for  $\dot{\gamma} > \dot{\gamma}_0$ , where  $\dot{\gamma}_0$  is the critical strain-rate at which  $\eta = \eta_0$ . For the parameters defined in this example,  $\dot{\gamma}_0 = 0.13 \text{ s}^{-1}$ .

### 5.2.3 Case II: FENE-CR model

 `tutorials/rheoTestFoam/FENE-CR/`

#### ❖ Overview

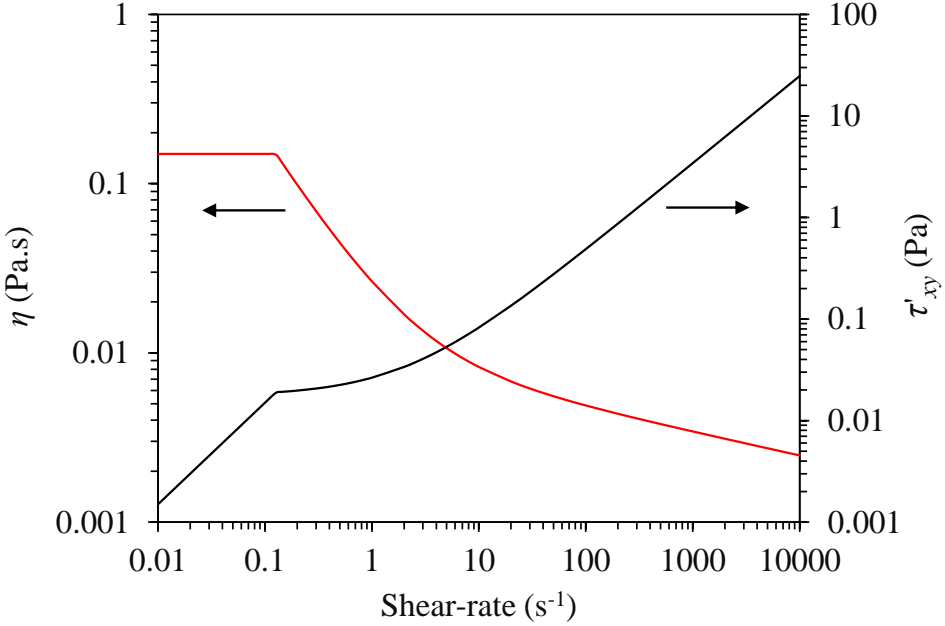


**Figure 5.15:** Shear viscosity and  $\tau'_{xy}$  (the only non-zero component of the symmetric extra-stress tensor) as a function of the shear-rate, in a steady shear flow, for the Herschel-Bulkley model with parameters:  $\tau_0 = 0.0175$  Pa,  $k = 8.9721 \times 10^{-3}$  Pa.s $^n$ ,  $n = 0.8601$  and  $\eta_0 = 0.15$  Pa.s.

This tutorial exemplifies the use of *rheoTestFoam*, both in transient and ramp modes, with a constitutive equation for a viscoelastic fluid. The FENE-CR model is selected and its behavior will be assessed for uniaxial extensional flow.

The uniaxial extensional flow may be described by the following velocity gradient

$$\nabla \mathbf{u} = \dot{\varepsilon} \begin{bmatrix} 1 & 0 & 0 \\ 0 & -\frac{1}{2} & 0 \\ 0 & 0 & -\frac{1}{2} \end{bmatrix}$$

where  $\dot{\varepsilon}$  is the extensional rate. The Weissenberg number,  $Wi = \lambda\dot{\varepsilon}$ , is the dimensionless group controlling the rate of stretch induced in the fluid and it was varied between 0.01 and 100, by increasing the extensional rate from 0.01 to 100  $s^{-1}$ . The fluid properties used in the FENE-CR model are:  $\eta_s = 0.1$  Pa.s,  $\eta_p = 0.9$  Pa.s,  $\lambda = 1$  s and different values of  $L^2$  were tested (10, 100 and 1000). In such conditions, the extensional viscosity, defined as  $\eta_E = \frac{\tau'_{xx} - \tau'_{yy}}{\dot{\varepsilon}}$ , is given by [34]

$$\eta_E = 3\eta_s + \eta_p \left( \frac{2}{1 - 2\lambda\dot{\varepsilon}/f} + \frac{1}{1 + \lambda\dot{\varepsilon}/f} \right) \quad (5.6)$$

where  $f$  is the solution of the cubic equation

$$(L^2 - 3)f^3 - [(\lambda\dot{\varepsilon})(L^2 - 3) + L^2]f^2 - [2(\lambda\dot{\varepsilon})^2(L^2 - 3) - (\lambda\dot{\varepsilon})L^2 + 6(\lambda\dot{\varepsilon})^2]f + 2(\lambda\dot{\varepsilon})^2L^2 = 0 \quad (5.7)$$

The geometry used with *rheoTestFoam* is always the same (see Sections 5.2.1 and 4.5.2). The mesh is already built (do not change it).

### ❖ Boundary conditions

The boundary conditions to be used with *rheoTestFoam* are always the same (see Sections 5.2.1 and 4.5.2). Folder 0/ should not be changed.

### ❖ Command-line

As it is, the tutorial will run in ramp mode.

1–Run the solver:

```
~$ rheoTestFoam
```

Take a look to file *Report* created in the case directory, which contains the results.

### ❖ Results

The results computed by *rheoTestFoam*, and displayed in Fig. 5.16a, show that the FENE-CR model is correctly implemented, since the difference to the analytical solution is negligible.

In addition to the "steady" results in Fig. 5.16a, also the transient evolution of the extensional viscosity (commonly denoted as  $\eta_E^+$  in the literature) can be obtained with *rheoTestFoam*. For that purpose, simply switch the keyword *ramp* (in *constitutiveProperties*) from *true* to *false* and define the desired extensional rate as the first entry of list *gammaEpsilonDotL* (the remaining entries can be left, since they will not be read). The results obtained for  $Wi = 2, 5$  and  $10$  are displayed in Fig. 5.16b.

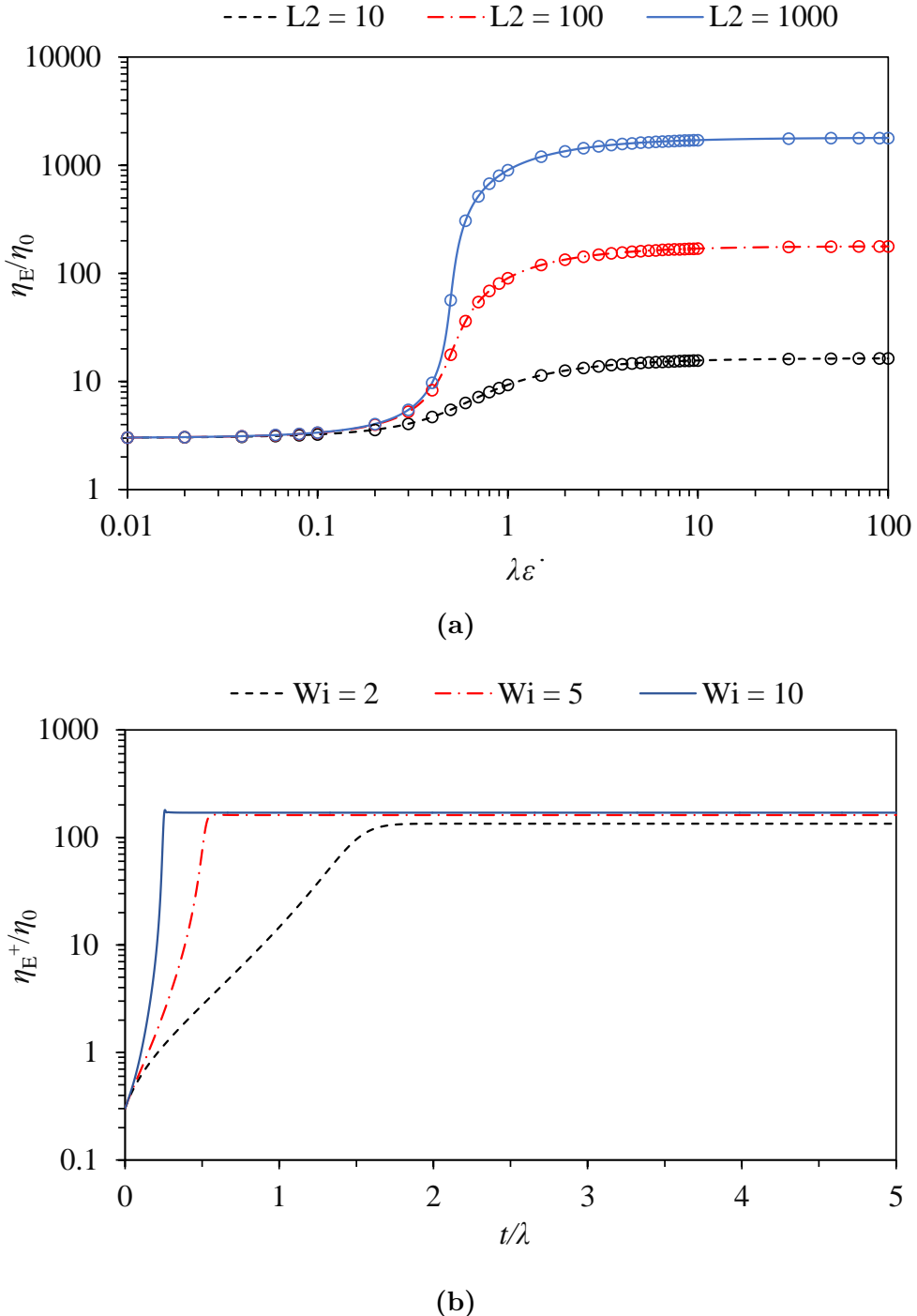


**Figure 5.16:** (a) Steady extensional viscosity ( $\eta_E$ ) as a function of  $Wi = \lambda\dot{\varepsilon}$ , for different values of  $L^2$  (points represent the numerical results of *rheoTestFoam* and the lines correspond to the analytical solution of Eq. 5.6); (b) transient extensional viscosity  $\eta_E^+$  for different  $Wi$ , at fixed  $L^2 = 100$ . The remaining parameters of the FENE-CR model are  $\eta_s = 0.1$  Pa.s and  $\eta_p = 0.9$  Pa.s.

## 5.3 *rheoInterFoam*



*Section 5.3* is under development.

### 5.3.1 General guidelines

Since most of the steps required to set up a case for *rheoInterFoam* are the same as for *rheoFoam*, only the major differences will be pointed out.

#### constant/

The dictionary `constitutiveProperties` should contain the same information as detailed for *rheoFoam* (Section 5.1.1), for each phase. The principle is the same as for the default two-phase solvers of OpenFOAM® (e.g. *interFoam*), where each phase owns a dictionary defining its physical properties. Importantly, `subDict passiveScalarProperties`, related with the transport of a passive scalar, is general for the two phases and should only be defined once, outside each phase. Finally, the surface tension between the two phases – parameter *sigma* – should also be present.

Note that when using default names *phase1* and *phase2* for each phase, without specifying the name of the phases in a *wordList*, then it is automatically assumed that the phases are labeled 1 and 2, respectively. Recent versions of OpenFOAM® have a slightly different behavior regarding phases labeling.

#### 0/

In folder 0/, the internal and boundary field for the indicator (color) function used by the VOF method should be defined. The indicator has a value of 1 for one of the phases and 0 for the other phase. Ideally, and assuming that boundary conditions were correctly assigned, the indicator should remain bounded in this range. The name given to the file representing the indicator field should be consistent with the naming in dictionary `constitutiveProperties`. If the default names *phase1* and *phase2* were used, then the indicator function should be named *alpha1*. If other name was used instead, then the indicator would be named *alpha* suffixed with that name, without spaces in-between (recent versions of OpenFOAM® require a separation point). Although there are always two phases, only one indicator field should be defined, since the indicator for the other phase is computed from this one. In opposition to what is done in *rheoFoam*, the pressure field used by *rheoInterFoam* is not divided by the density, thus retaining its natural units (Pa.s).

Given that a constitutive equation is being defined and solved individually for each phase, variables *tau* and *theta* should be labeled (suffixed) with the respective phase name. Considering a viscoelastic model for each phase and default naming of phases, we would have *tau1*, *theta1* and *tau2*, *theta2*. If a multimode mode model is assigned to a given phase, then the name of each mode should also be appended.

## system/

The main novelty comparing to *rheoFoam* is that when using *rheoInterFoam* the user has the possibility to choose between PIMPLE and SIMPLEC for pressure-velocity coupling. This is controlled in dictionary *fvSolution*, in subDict *PIMPLE*, where the keyword *SIMPLEC* can be assigned to *true* or *false*. Independently of the choice, the momentum equation is always solved. The variable *nCorrectors* works in its usual way (looping the pressure equation) and the variable *nInIter* assumes the same function as *nOuterCorrectors*. In a future release of *rheoInterFoam*, this workflow will most likely change. There are currently these two options because it is still not clear which one is more advantageous. Still in dictionary *fvSolution*, other keywords must be assigned in subDict *PIMPLE*, which are related with the VOF method and that the reader can found in the tutorials. If a sparse matrix solver from an external library is used, then check the instructions provided in Section 4.4.

In dictionary *fvSchemes*, the discretization schemes for the two phases should be defined, as well as the discretization schemes related with the VOF method, which can also be found in the tutorials.

Besides the Courant number, the solvers using VOF, as *rheoInterFoam*, can also restrict the time-step based on an interface Courant number, which should be defined in dictionary *controlDict*.

The dictionary *setFields*, used to initialize parts of the domain with specified values, should also be present in folder *system/* whenever used.

### 5.3.2 Case 1: impacting drop

#### tutorials/rheoInterFoam/ImpactDrop/Oldroyd-BLog/

##### Overview

In this tutorial, a liquid drop composed of a viscoelastic fluid falls under gravity and its shape (the drop width, more precisely) is monitored before and after the drop impacts a rigid plate. Under such conditions, the drop width oscillates after the impact. This problem has been used in the literature as a benchmark case for viscoelastic two-phase flow solvers (e.g. [49, 50]).

The configuration adopted in the tutorial reproduces the conditions in Ref. [49], where an axisymmetric geometry has been used. The dimensionless numbers governing the flow are:  $Fr = \frac{U_0}{\sqrt{gD}}$ ,  $Re = \frac{\rho U_0 D}{\eta_0}$ ,  $Wi = \frac{\lambda U_0}{D}$  and  $\beta = \frac{\eta_s}{\eta_s + \eta_p}$ , where  $U_0$  is the initial velocity of the drop,  $g$  is the gravitational acceleration,  $D$  is the drop diameter,  $\rho$  is the fluid density,  $\eta_0$  is the total viscosity (polymer plus solvent) and  $\lambda$  is the relaxation time (all these fluid properties are for the drop phase). The problem was simulated for  $Fr = 2.26$ ,  $Re = 5$ ,  $Wi = 1$  and  $\beta = 0.1$ . Note that the surface tension is set to zero and we assign low (but finite) density and viscosity values to the fluid surrounding the drop.

##### Geometry & Mesh

The geometry is composed by a plate on its bottom, while the other patches simply act as open boundaries, representing the atmosphere. Axisymmetry is

considered around the  $y$ -axis. All the dimensions are expressed as a function of the drop diameter, Fig. 5.17. The domain is big enough so that we can neglect the influence of the open boundaries location in the results.

The domain is meshed uniformly with 120 cells in both the radial and axial directions.

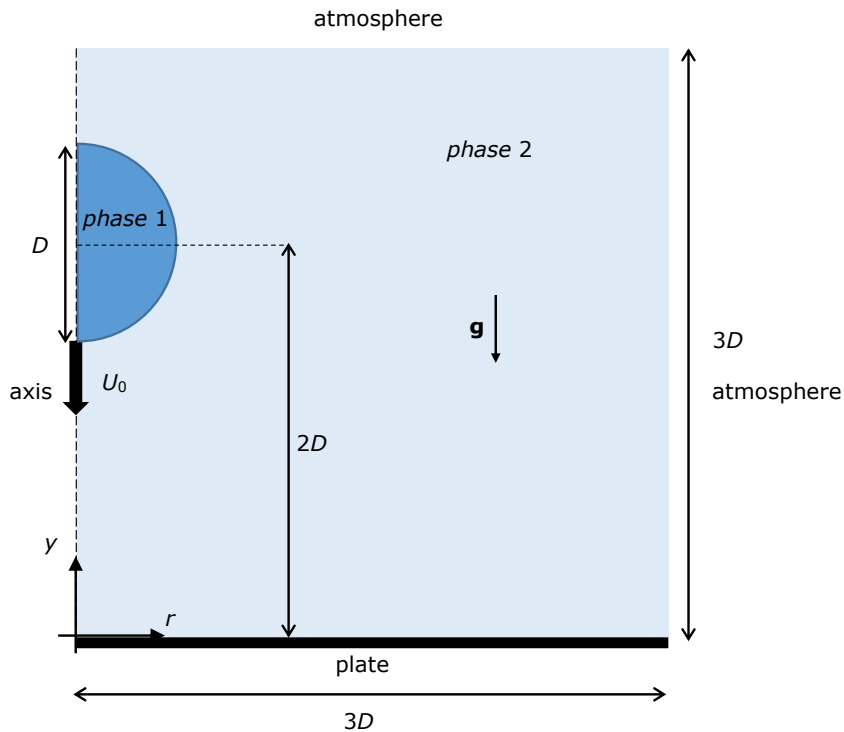


**Figure 5.17:** Geometry for the impacting drop problem.

### ❖ Boundary conditions

At the plate, no-slip boundary conditions are imposed with a null velocity, linearly extrapolated polymeric extra-stress components and zero normal gradient for the indicator field. We assign a *fixedFluxPressure* BC to the pressure, as discussed in Section 4.6.8, for multiphase flows. The patches representing the open boundaries (atmosphere) are assumed to not interfere with the dynamics of the drop, so that zero-gradient is assumed for all variables, except the pressure, which is fixed at  $p = 0$ .

Following Ref. [49], the drop has an initial velocity  $U_0$ , in the vertical direction (pointing downwards), and its center of mass is at a distance  $2D$  from the plate.

### ❖ Command-line

1–Build the mesh:

```
~$ blockMesh
```

2–Initialize the indicator and velocity fields in the drop region:

```
~$ cp 0/alpha1.org 0/alpha1
~$ cp 0/U.org 0/U
~$ setFields
```

3–Run the solver:

```
~$ rheoInterFoam
```

### ➊ Results

The evolution of the drop width over time is plotted in Fig. 5.18. The width is normalized with  $D$  (its initial diameter) and time with  $D/U_0$ . The evolution of the drop width over time is written to a file by a *coded FunctionObject*.

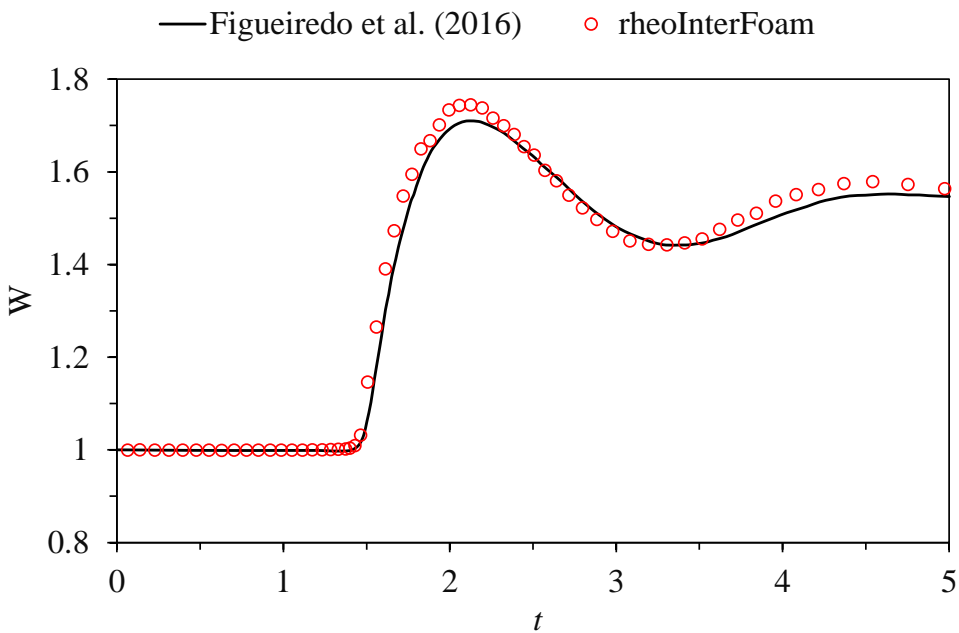


**Figure 5.18:** Evolution of the drop width over time for  $Fr = 2.26$ ,  $Re = 5$ ,  $Wi = 1$  and  $\beta = 0.1$ . The profile obtained with *rheoInterFoam* is compared with the data of Figueiredo et al. [49].

### 5.3.3 Case 2: planar die swell

⬇️ [tutorials/rheoInterFoam/DieSwell/](#)

#### ➊ Overview

A significant number of plastic objects that we use in our everyday life are produced by extrusion of molten polymers. In this process, the polymeric phase can swell significantly at the exit of the die due to the development of normal stresses. Predicting the amount of swell is important for the processing. Moreover, undesirable sharkskin defects in the extrudate surface can occur under certain conditions, and the ability to predict such conditions can potentially reduce industrial wastes.

This tutorial presents the swell of non-Newtonian fluids flowing through a planar rectangular die. The three cases provided reproduce the results obtained in Ref. [51] using *rheoTool*, for mesh M1 and three different fluids: Carreau-Yasuda fluid with  $n = 0.3$  (directory `CarreauYasuda/`); Oldroyd-B fluid with  $\beta = \frac{1}{9}$  and  $Wi = 2$  (directory `Oldroyd-BLog/`); Giesekus fluid with  $\beta = \frac{1}{9}$ ,  $\alpha = 0.5$  and  $Wi = 4$  (directory `GiesekusLog/`). The viscoelastic fluid models are solved with the log-conformation approach. Note that both gravity and surface-tension effects are neglected in this tutorial. In addition, only the steady-state solution is of interest.

### ❖ Geometry & Mesh

The geometry for this case is displayed in Fig. 5.19. The mesh corresponds to mesh M1 of Ref. [51]. Note that this is a kind of stick-slip configuration, which represents a die with negligible wall thickness. Accordingly, patch *wallOut* overlaps part of the *wallIn* patch.

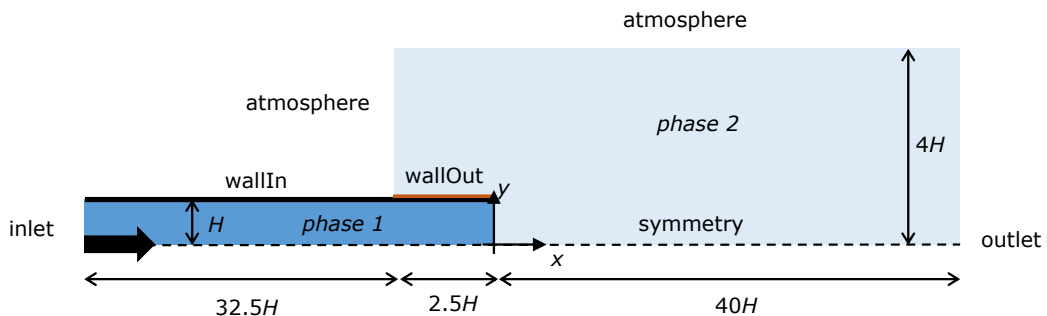


**Figure 5.19:** Geometry for the planar die swell tutorial.

### ❖ Boundary conditions

The boundary conditions used are described in Ref. [51]. In order to avoid the definition of an analytical solution at the *inlet*, a long entrance channel is used.

### ❖ Command-line

1–Build the mesh:

```
~$ blockMesh
```

2–Initialize the color function field:

```
~$ cp 0/alpha1.org 0/alpha1
```

```
~$ setFields
```

3–Run the solver:

```
~$ rheoInterFoam
```

## ❖ Results

The results obtained with mesh M1 can be found in Ref. [51]. The users of the foam-extend version (*fe40*) will notice an instability in the extrudate surface close to the die exit, which eventually vanishes with time. Such instability is not present in the OpenFOAM® versions.

Several methods can be used to compute the amount of swell far from the die exit. Assuming that the free-surface of the extrudate corresponds to  $\alpha = 0.5$ , for  $\alpha \in [0, 1]$ , this isoline can be directly extracted with Paraview. Another option is to extract the profile of the color function ( $\alpha$ ) over a vertical line far from the die exit, using the *sample* utility of OpenFOAM®. Then, the value  $\alpha = 0.5$  can be simply interpolated from the nearest values. A more complex, still more versatile option is to code a *ppUtil* function (Section 4.7.2) retrieving in run time the maximum free-surface position in a predefined region. This would also allow to check for convergence of the free-surface position. Slight differences can be found among the results from the different methods.

## 5.4 *rheoEFoam*

### 5.4.1 General guidelines

The first steps to set up a case for *rheoEFoam* are the same as for *rheoFoam* (Section 5.1.1). After that, the hydrodynamic component of the problem will be ready, and only the electric component will remain to be defined – this is the subject of this section.

#### ❖ constant/

The *electricProperties* dictionary should be added to folder `constant/`. It contains most of the information about the EDF model to be used, as shown in Listing 5.3, illustrating an example for the PNP model.

```

parameters
2 {
    type           NernstPlanck;
4
    T              T [ 0 0 0 1 0 0 0 ] 298;
6    relPerm        relPerm [ 0 0 0 0 0 0 0 ] 80.1;
8
    psiContrib     true;
    extraEField    extraEField [ 1 1 -3 0 0 -1 0 ] (5000 0
10
    species
12 (
    cCation
14 {
        z             z [ 0 0 0 0 0 0 0 ] 1;
16     D             D [ 0 2 -1 0 0 0 0 ] 1e-9;
18
    cAnion

```

```

20          {
21              z           z [ 0 0 0 0 0 0 0 ] -1;
22              D           D [ 0 2 -1 0 0 0 0 ] 1e-9;
23          }
24      );
}

```

**Listing 5.3:** Example of a `electricProperties` dictionary used with `rheoEFoam` – the settings displayed are for the PNP model.

The electric properties in dictionary `electricProperties` are defined inside a subDict named `parameters` (line 1, Listing 5.3). The EDF model is selected through keyword `type`, where the `TypeName` of any model in Table 4.2 can be used (the user may type any random word to get the list of all available EDF models). Apart from the `type` keyword, all the remaining entries are model-specific. In the case of the PNP model in Listing 5.3, `T` is the absolute temperature and `relPerm` corresponds to the relative permittivity (dielectric constant) of the electrolyte,  $\epsilon_R$ , such that  $\epsilon = \epsilon_R \epsilon_0$ , where  $\epsilon_0$  is the vacuum permittivity. In line 8, the entry `psiContrib` set to `true` indicates that variable `psi` (either  $\Psi$  or  $\psi$ ) should contribute to the electric field used in the definition of the electric body-force. The default behavior, i.e., if the entry is not defined, is `psiContrib = true`. The next line (line 9) is also optional and allows the user to define an additional uniform electric field, `extraEField` (units are in SI, as always). This electric field will **only** enter in the computation of the electric body-force in the momentum equation ( $\mathbf{f}_E = \rho_E(\mathbf{E} + \text{extraEField})$ ); `extraEField` corresponds to vector  $\mathbf{E}_a$  in Table 4.2). Then, from line 11 to 24 each specie of the electrolyte is defined. In the example, only two species are modeled: `cCation` and `cAnion`, each having its own charge valence (`z`) and diffusivity (`D`). Note that the charge valence is a signed integer: positive for cations and negative for anions. The user can add as many species as desired to the list, for the model under analysis. The name given to each specie is user-defined, but consistence must be kept when further defining the respective fields, as explained next.

The example in Listing 5.3 should not be generalized to all the EDF models, as stated before. The best way for the user to know how the `electricProperties` dictionary should look like for a given EDF model is to analyze a tutorial provided for that model (at least one tutorial is provided for each model).

## 0 /

In addition to the fields related with the hydrodynamics (pressure, velocity and eventually extra-stress), when using `rheoEFoam` for EDFs, the fields specific to the given EDF model should be specified in folder 0 / (or the equivalent starting time folder when different from 0).

For the PNP model illustrated in Listing 5.3, we need to define 3 or 4 fields, depending if we use one single electric potential or two, respectively. In the first case, the fields would be `psi` (in this guide represented by  $\Psi$ ), `cCation` and `cAnion` (in this guide represented by  $c_i$ ). In the second case, field `psi` would be replaced by `psi` (in this guide represented by  $\psi$ ) and `phiE` (in this guide represented by  $\phi_{\text{Ext}}$ ). Note that although having the same name in both cases, field `psi` has different meanings for each one: it is either the total, unique electric potential ( $\Psi$ ),

or the intrinsic electric potential ( $\psi$ ) – in practice, the Poisson equation to be solved is different in each case. The selection between both cases is made through variable `phiE`: when present, `psi` is considered the intrinsic electric potential,  $\psi$ . It is important to highlight that the fields representing the concentration of each specie (in mol/m<sup>3</sup>) should keep the name defined in dictionary `electricProperties`, in a one-to-one correspondence for each specie. These names are user-defined, in opposition to the names for the electric potential variables, which are fixed: `psi` and `phiE`.

The PNP model is the only to require the definition of fields for the concentration of each ionic specie. The other EDF models only require the electric potential (one or two variables, depending on the model and on the user's choice) to be defined. The exception is the Ohmic model, which also requires a field for the conductivity (`sigma`, in this guide represented by  $\sigma$ ). Still for this model, only one electric potential variable may exist and its name should be `phiE`. In case of doubt, checking the tutorials is always a good starting point.

### system/

Since additional equations are solved for EDFs (comparing to pressure-driven flows), the discretization schemes for the terms entering these equations need to be defined, as well as the sparse matrix solvers and respective settings.

The discretization schemes are defined in dictionary `fvSchemes`. The new entries to add to the dictionary are model-dependent and can be found in the tutorials. If the discretization scheme for any term is missing, an error will be retrieved complaining for it.

Regarding dictionary `fvSolution`, keep in mind when defining the matrix solvers for the new fields that Poisson-type equations require, in general, a symmetric matrix solver, while generic transport equations (including advection) are usually handled with an asymmetric matrix solver. If a coupled solver or a sparse matrix solver from an external library is used, then check the instructions provided in Section 4.4. Regarding under-relaxation, our recommendations are the same as the ones expressed for `rheoFoam`: by default, do not use under-relaxation, except, eventually for pressure in non-orthogonal grids, if needed. Note that the Nernst-Planck equations for each specie in the PNP model are collectively solved under the name `ci`, instead of the name given to the specie (this should be taken into account when defining the matrix solver and the under-relaxation factors).

Still in dictionary `fvSolution`, a new subDict needs to be defined for EDFs, named `electricControls`, Listing 5.4. In the code sample analyzed in Section 4.2.5, we have seen that each equation of a given EDF model is solved inside a *while* loop, controlled by a maximum allowable number of iterations and the initial residual of the equation being solved (the loop is exited when the first of the two criteria is met). These loops are intended to converge explicit terms inside each equation, since this can be critical for some EDFs. Thus, the controlling parameters of these cycles – the maximum number of iterations and the threshold residual – are defined in subDict `electricControls`. This needs to be done for each equation, or default values are assumed otherwise (`maxIter: 50; residuals: 10-7`). For non-stiff problems and when the mesh non-orthogonality is kept low, 1 iteration can be enough. When the PNP model is used, the number of electrokinetic coupling

iterations (see Section 4.2.3) can also be defined in this subDict, as shown in line 3 of Listing 5.4 (if not defined,  $nIterPNP = 2$  is assumed by default). As mentioned in Section 4.2.3, we recommend a minimum of 2 electrokinetic coupling iterations for any generic case using this model.

```

1 electricControls
{
3   nIterPNP          2;
5   phiEEqn
{
7     residuals 1e-7;
8     maxIter      1;
9   }

11  psiEqn
{
13    residuals 1e-7;
14    maxIter      1;
15  }

17  ciEqn
{
19    residuals 1e-7;
20    maxIter      1;
21  }
}
```

**Listing 5.4:** Example of an *electricControls* subDict in dictionary fvSolution – the settings displayed are for the PNP model.

### 5.4.2 Case I: EDF of power-law and PTT fluids in a microchannel

Our first tutorial for *rheoEFoam* is aimed to predict the velocity profile for a purely EDF of a power-law fluid (**Part A**) and for the mixed pressure-/electrically-driven flow of a linear PTT fluid (**Part B**) in a slit microchannel. The numerical profiles are compared with analytical solutions.

#### ➊ Part A - Power-law fluid

 `tutorials/rheoEFoam/channelEDF/PowerLaw/PoissonBoltzmann`

##### ❖ Overview

The analytical solution for the EDF of a power-law fluid in a slit microchannel can be found in Ref. [52] for a generic flow behavior index ( $n$ ) of the power-law model, under the Debye-Hückel approximation. For fully-developed flow conditions, the velocity profiles depend on  $n$  and on  $\tilde{\kappa} = \kappa H = \frac{H}{\lambda_D} = \sqrt{\frac{2(zH)^2 e c_0 F}{\varepsilon k T}}$ , where  $\lambda_D$  is the Debye length for a binary, symmetric electrolyte, as defined in Eq. (3.34), and  $H$  is the channel half-width. Although we will only present results for the PB model, we also provide the corresponding cases for the PNP and DH

models – as you will see, the results are indistinguishable between the models, for the conditions simulated.

### ❖ Geometry & Mesh

The geometry is a 2D (slit) microchannel with half-width  $H$ , Fig. 5.20. Due to the periodic boundary conditions assumed on the inlet/outlet, the mesh has one single cell in the  $x$ -direction and 300 non-uniformly distributed cells in the  $y$ -direction, normal to the applied electric field.

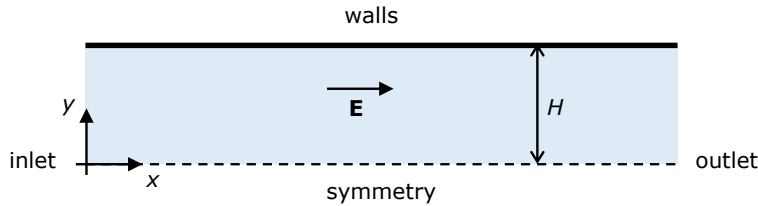


**Figure 5.20:** Planar channel geometry.

### ❖ Boundary conditions

The flow is 2D in the  $xy$ -plane. At both the inlet and outlet, periodicity is imposed. Thus, we assume from the beginning that this condition will retrieve the fully developed profiles for an infinitely long microchannel. A symmetry condition is imposed at  $y = 0$ . The walls are impermeable ( $\mathbf{u} = \mathbf{0}$  and zero-gradient for pressure) and have a fixed intrinsic electric potential. Due to the simple geometry of the channel, the flow is generated by imposing a uniform electric field throughout the channel, parallel to the walls ( $\mathbf{E}$ ). Therefore, there is no need to solve for the external electric potential variable ( $\phi_{IE}$ ): the electric field is directly imposed through the `extraField` entry of dictionary `electricProperties`. These boundary conditions hold for both the PB and DH models. In order to use the PNP model, a boundary condition must be defined at the wall for the ionic species. Since Boltzmann equilibrium holds and only the steady-solution is sought, the easiest way is to simply compute the ionic concentration from the potential distribution (check the `boltzmannEquilibrium` boundary condition described in Section 4.6.4). The flow is initially at rest and the intrinsic electric potential is zero.

### ❖ Command-line

1–Build the mesh:

```
~$ blockMesh
```

2–Run the solver:

```
~$ rheoEFoam
```

3–Extract the profile of  $\mathbf{u}$  along the vertical direction:

```
~$ sample -latestTime
```

### ❖ Results

The velocity profiles over the  $y$ -direction are depicted in Fig. 5.21 for varying  $n = 0.25, 0.5, 0.75, 1$  and  $1.5$ , at fixed  $\tilde{\kappa} = 15$ . The velocity profiles are normalized by the velocity at the centerline of the channel, while the spatial coordinate is normalized by the channel half-width. The numerical results reproduce accurately the analytical solution [52] and show that shear-thinning fluids ( $n < 1$ ) display an apparently compressed EDL, while the opposite is observed for shear-thickening fluids ( $n > 1$ ).

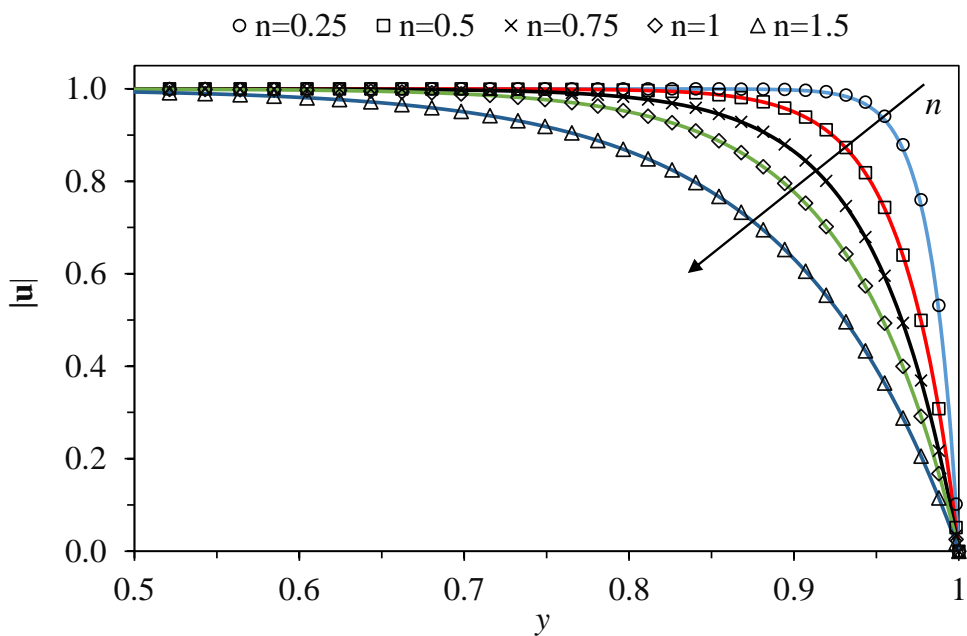


**Figure 5.21:** Velocity magnitude over the direction transverse to the applied electric field for a power-law fluid with different flow behavior index, at fixed  $\tilde{\kappa} = 15$ . The points represent numerical values, while the lines are the analytical solution [52]. Note that the  $x$ -scale has been truncated and only represents one-quarter of the channel width (this is to have a zoomed view near the wall).

As aforementioned, the same results would be obtained with the PNP and DH models and the user may confirm that from the cases provided. All the cases are prepared for  $n = 0.75$  (this can be easily changed in dictionary `constitutiveProperties`) and will converge in the total time of simulation defined in `controlDict`. However, we should note that for low  $n$ , where  $n = 0.25$  can be included, the simulation will take a much longer time to reach the steady-state, because of the low viscosity that develops near the wall, where the shear-rate attains very high values (it becomes even worse for higher  $\tilde{\kappa}$ ). Furthermore, care should be taken in defining the upper and lower bounds for the viscosity (check the power-law model implementation in Table 4.1), since stringent bounds may influence the numerical solution.

### ⌚ Part B - linear PTT fluid

 `tutorials/rheoEFoam/channelEDF/PTTlinear/DebyeHuckel`

### ❖ Overview

Afonso et al. [53] derived an analytical expression for the mixed pressure-electrically-driven flow of simplified ( $\zeta = 0$ ) linear PTT fluids in slit channels with an homogeneous zeta-potential at the walls, under the Debye-Hückel approximation. For creeping flow conditions ( $Re = 0$ ), the velocity profiles depend on  $\Gamma = -\frac{H^2}{\epsilon\psi_0} \frac{|\nabla p|}{|\mathbf{E}|}$  (ratio between pressure and electric forcing),  $\tilde{\kappa} = \kappa H = \frac{H}{\lambda_D} = \sqrt{\frac{2(zH)^2 ec_0 F}{\varepsilon k T}}$  and  $\sqrt{\varepsilon} De = \sqrt{\varepsilon} \lambda \kappa U$ , where  $\varepsilon$  is the extensibility parameter of the PTT model,  $U = -\frac{\epsilon\psi_0 |\mathbf{E}|}{\eta_0}$  is the Helmholtz-Smoluchowski velocity and  $\psi_0$  is the zeta-potential at the wall. Both  $\nabla p$  and  $\mathbf{E}$  only have a single non-zero component, in our case, the  $x$ -component. Note that in this tutorial we use exceptionally  $\epsilon$  to represent the electric permittivity (instead of  $\varepsilon$ ), in order to distinguish it from  $\varepsilon$  that we use to represent the extensibility parameter of the PTT model.

In this tutorial, we analyze the effect of varying  $\Gamma$ , while keeping the remaining dimensionless parameters fixed.

### ❖ Geometry & Mesh

The geometry is similar to the one used in **Part A** for the power-law fluid example. However, the physical dimensions are different and, importantly, we do not consider periodicity between the *inlet* and *outlet*. Instead, the flow is also solved in the  $x$ -direction. We note that this is not mandatory and that cyclic conditions would also provide the right solution. However, considering the full channel in the  $x$ -direction eases the definition of the pressure gradient, at the expense of having a higher number of cells in the mesh. Several options would allow to keep the cyclic patches and to impose directly the pressure gradient in the momentum equation, as the *fvOptions* tool, but we consider them less straightforward than our choice (at least for less experienced users).

### ❖ Boundary conditions

The boundary conditions are similar to the ones used in **Part A**, with some modifications required by the use of a viscoelastic model and due to the different conditions assigned to patches *inlet* and *outlet*. Since pressure gradients are allowed, we fix the pressure at the *outlet* and adjust the *inlet* pressure as required to get the desired  $\Gamma$ . Remember that in *rheoEFoam* field  $p$  represents the pressure divided by the density. A zero-gradient condition is imposed for the remaining variables at those two patches. Regarding the wall, the polymeric extra-stresses are linearly extrapolated.

### ❖ Command-line

1–Build the mesh:

```
~$ blockMesh
```

2–Run the solver:

```
~$ rheoEFoam
```

3—Extract the profile of  $\mathbf{u}$  along the vertical direction for the latest time (the  $x$ -position of the sampling line should not be important):

```
~$ sample -latestTime
```

### ❖ Results

Fig. 5.22 shows the velocity profiles under different forcing ratios. The velocity is normalized by the Helmholtz–Smoluchowski velocity ( $U$ , defined above), while the spatial coordinate is normalized by the channel half-width. Note that for a Newtonian case and  $\Gamma = 0$  (pure EDF), the (normalized) velocity profile at the centerline would have a value very close to 1 (the higher  $\tilde{\kappa}$ , the closer it is) and we can see that this value is significantly higher for a linear PTT fluid due to shear-thinning.

The parameters provided in the tutorial are for  $\Gamma = 4$ .

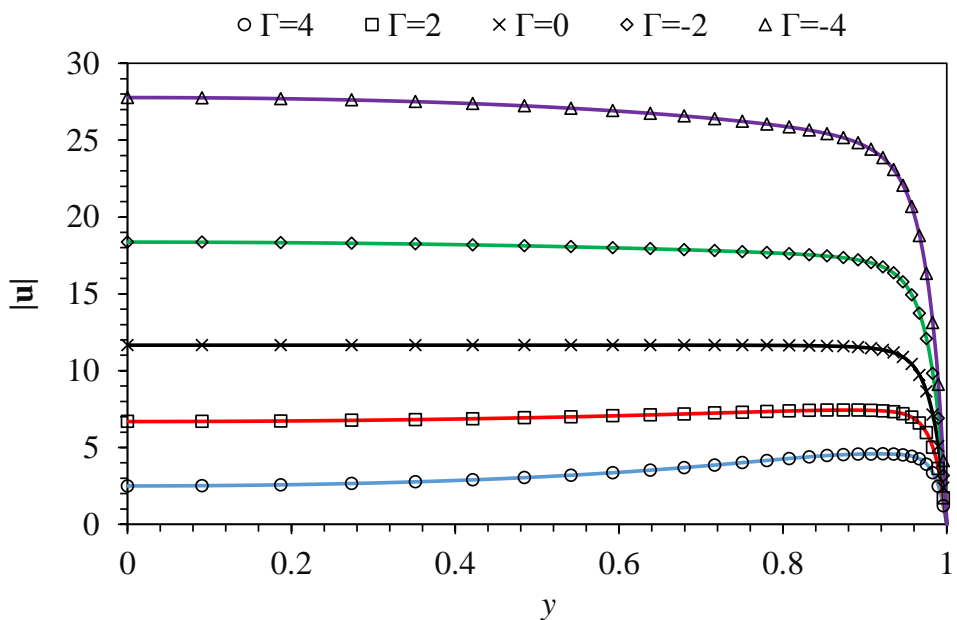


**Figure 5.22:** Velocity magnitude along the direction transverse to the applied electric field and pressure gradient for a simplified linear PTT fluid, at different forcing ratios  $\Gamma$ , for  $\tilde{\kappa} = 20$  and  $\sqrt{\epsilon}De = 4$ . The points represent numerical values, while the lines are the analytical solution [53].

### 5.4.3 Case II: induced-charge electroosmosis around a cylinder

☛ [tutorials/rheoEFoam/ICEO/NernstPlanckCoupled](#)

### ❖ Overview

This tutorial analyzes the DC induced-charge electroosmosis (ICEO) around a conducting cylinder. We have investigated this problem in Ref. [3] and we present in this tutorial the setup used for  $\tilde{V} = 0.01$  and  $\tilde{\kappa} = 10$ , in mesh M1.

In directory `tutorials/rheoEFoam/ICEx/`, the same case is available under different EDF models (PNP, PB and DH). For the conditions aforementioned, all give similar results in steady-state. The case for the PNP model uses one potential ( $\Psi$ ), while the remaining cases are solved under the splitting approach for the electric potential (both  $\phi_{\text{Ext}}$  and  $\psi$  are defined). For the last ones, you can also see the use of the *inducedPotential* boundary condition described in Section 4.6.5.

The case for the PNP model (OpenFOAM® versions only) uses a semi-coupled solver, where the PNP system of equations is solved coupled, but separated from continuity and momentum equations, which are themselves solved coupled.

### ❖ Geometry & Mesh

The geometry used in this tutorial is displayed in Fig. 5.23, being the same as in Ref. [3]. The mesh corresponds to mesh M1 of that work, and more details on the problem definition can be found therein.

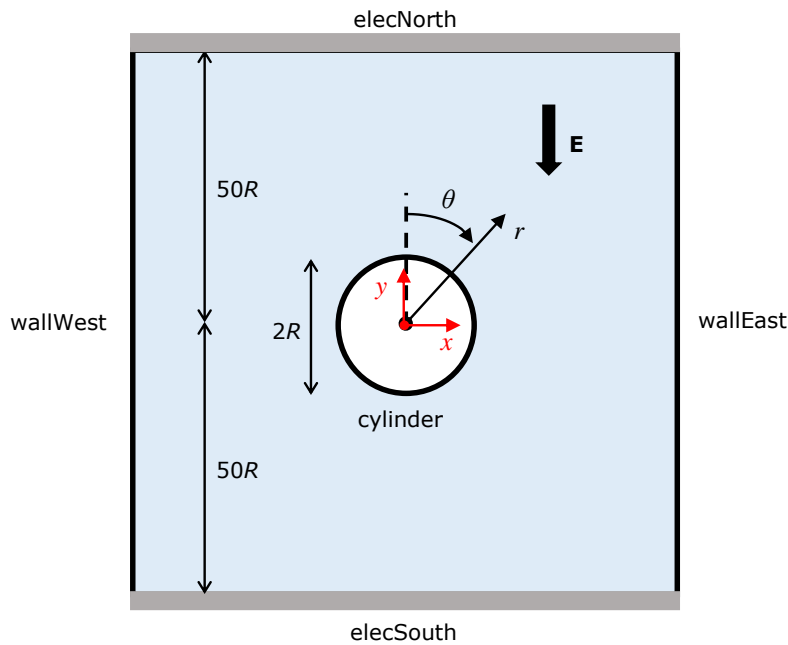


**Figure 5.23:** Metallic cylinder placed over an electric field. The surrounding domain is square (edge size:  $100R$ ) and the cylinder lays on its center. The cylindrical coordinate system ( $r, \theta$ ) is plotted in black, while the Cartesian coordinate system ( $x, y$ ) is represented in red (remember that OpenFOAM® uses the Cartesian system for computations).

### ❖ Boundary conditions

The boundary conditions are described in detail in Ref. [3]. The only difference is on the boundary condition for pressure on the cylinder surface, which has been changed to zero-gradient. This change is due to the use of a coupled solver.

### ❖ Command-line

1–Build the mesh:

```
~$ blockMesh
```

2–Run the solver:

```
~$ rheoEFoam
```

3–Extract profiles of  $\mathbf{u}$  along the line  $\theta = 45^\circ$ :

```
~$ sample -latestTime
```

## ❖ Results

You may find the following relation useful in converting the velocity from the Cartesian base where it is computed, to the cylindrical base used in Ref. [3] to display the results:

$$\begin{bmatrix} U_r \\ U_\theta \end{bmatrix} = \begin{bmatrix} \sin(\theta) & \cos(\theta) \\ \cos(\theta) & -\sin(\theta) \end{bmatrix} \begin{bmatrix} U_x \\ U_y \end{bmatrix} \quad (5.8)$$

Note that two *ppUtil* (cf. Section 4.7.2) are used in this tutorial, returning both the global balance of ions (*calcBalance*) and the current density through the cylinder surface (*calcJpatch*). The latter allows to verify, in this specific case, that the no-flux boundary conditions for the two ionic species is working as expected, since a *quasi*-null current density is retrieved at the boundary where it is assigned.

### 5.4.4 Case III: charge transport across an ion-selective membrane

 `tutorials/rheoEFoam/selecMembrane/NernstPlanck`

## ❖ Overview

This tutorial presents the charge transport across an ion-selective membrane and will show the development of the so-called electroconvective instabilities (e.g. [54]). We addressed this EDF in Ref. [3] and we present in this tutorial the setup used for  $\tilde{V} = 120$ , in mesh M1. The case is adjusted to run until  $\tilde{t} = 0.01$ , but this time can be easily increased in `controlDict`.

## ❖ Geometry & Mesh

The geometry for this tutorial is displayed in Fig. 5.24, being the same as in Ref. [3]. The mesh corresponds to mesh M1 of that work, and more details on the problem definition can be found therein.

## ❖ Boundary conditions

The boundary conditions were described in detail in Ref. [3]. For the users of OpenFOAM® v4.x, if the *fixedFluxExtrapolatedPressure* is intended to be used at the membrane boundary – this is the most correct option –, then function *adjustPhi()* must be disabled in solver *rheoEFoam*, as discussed in Section 4.6.8. Since this would require a permanent change in the solver, we have chosen to use a *zeroGradient* BC in replacement.

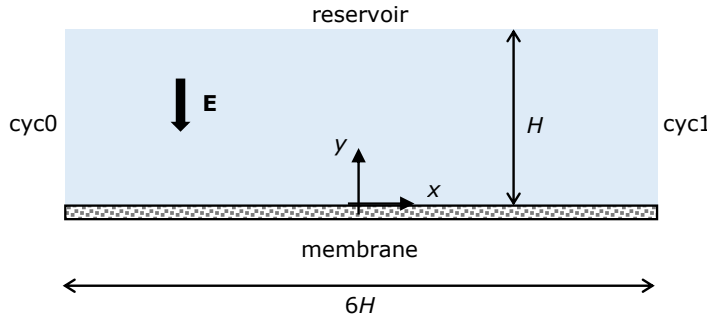


**Figure 5.24:** Planar reservoir with an ion-selective membrane (only permeable to cations) on its bottom.

### ❖ Command-line

This tutorial is slightly different from the previous ones regarding the command-line sequence to run. This is because the problem is first solved in a 1D configuration and the resulting solution is then disturbed and used as the starting solution of the 2D configuration. Thus, we recommend to use directly the `Allrun` script to run this tutorial, although we also explain next the main steps accomplished by that script.

Firstly, in the directory of the main case you will find a folder named `solution1D/`. This is where the 1D problem is solved – script `Allrun` inside this folder is the first call of the `Allrun` in the main directory. Computing the 1D solution is relatively straightforward in what respects the commands to be executed, since it only requires building the mesh (`blockMesh`) and running the solver (`rheoEFoam`). You may note that the hydrodynamic component of the solver is switched off through the `solveFluid` keyword in dictionary `fvSolution`, which is set to `false`. Thus, only the Poisson and Nernst-Planck equations are being solved. The 1D solution is obtained by solving the PNP system of equations coupled (see Sections 4.2.4 and 4.4.8). Under the current settings, the lower the voltage on patch `reservoir`, the higher the time for the 1D solution to converge (the `endTime` should be increased accordingly in these situations). Our criteria for convergence relies in the monitor for the current density.

After the 1D solution is computed, the resulting fields are mapped to the 2D domain (also created with `blockMesh` beforehand), using the `mapFields` utility available by default in OpenFOAM®. Then, the fields for the cationic and anionic concentration are locally disturbed by a 1 % random perturbation. This is accomplished by a pre-processing utility named `rndPerturbation`, which has been specifically created for this task and that can be found in directory `src/libs/preProcessing/rndPerturbation/`. The case is ready to be run with `rheoEFoam`, noticing that now `solveFluid = true`.

While the case is running, a `ppUtil` (cf. Section 4.7.2) is simultaneously being executed (`calcJpatch`), which retrieves the surface-averaged current density over time on both the `reservoir` and `membrane` patches (Fig. 5.24).

## ➊ Results

The current density can be plotted over time and the contours of charge density can be computed and visualized in Paraview (these are just some suggestions).

The electric field intensity can be controlled by changing the voltage in file `solution1D/0/psi`, under the entry for patch `reservoir`. Note that any change in the initial/boundary conditions of any field must be done in the files inside folder `solution1D` due to the mapping procedure. By running the `Allrun` script in the main folder, the 1D solution will be always computed first.

### 5.4.5 Case IV: electrokinetic instabilities in a flow-focusing device

 `tutorials/rheoEFoam/EKI/Ohmic`

## ➋ Overview

This tutorial aims to reproduce qualitatively the electrokinetic instabilities arising in a flow-focusing device, when electrolytes of different conductivity join at the converging region. The problem has been extensively studied in Ref. [55], both experimentally and theoretically.

The use of the Ohmic model is illustrated in this tutorial, which also includes the transport of a passive, neutral scalar.

As shown by Posner et al. [55], the dynamics of the problem is essentially governed by three dimensionless numbers: the electric Rayleigh number,  $Ra_E = \frac{\varepsilon E_a^2 h^2}{\eta D}$ , the conductivity ratio  $\gamma = \frac{\sigma_W}{\sigma_S}$  and the voltage ratio  $\beta = \frac{V_W}{V_S}$ . The indices refer to the north (N), south (S), west (W) and outlet (O) arms of the flow-focusing device and  $h = 0.8H$  is the channel depth. Furthermore, an apparent electric field is computed as  $E_a = \frac{V_N - V_O}{L_N + L_O}$ , where the denominator of  $E_a$  represents the summed distance of the north and east arms (distance between the ends of each arm, passing by the center of the geometry:  $L_N + L_O = 24H$  in this tutorial). The parameters of the tutorial are chosen in order to simulate  $Ra_E = 839$ ,  $\gamma = 10$  and  $\beta = 1.05$ .

## ➌ Geometry & Mesh

The geometry is a 3D flow-focusing device (Fig. 5.25) composed of three converging inlets and one outlet. The width and the depth of the channel are uniform over all the geometry:  $2H$  and  $0.8H$ , respectively. The inlet arms (west, south and north) are all  $8H$  long, while the outlet arm (east) is  $16H$  long.

The geometry is divided into 12 blocks for meshing purposes. The dimensions of the cells at the junction corners are approximately:  $(\Delta x, \Delta y, \Delta z) \approx (0.1, 0.1, 0.07)H$ .

## ➍ Boundary conditions

Since the Ohmic model is used in this simulation, we have to define boundary conditions for pressure, velocity, electric potential and conductivity. We consider that all the arms are open to the atmosphere, thus  $p = 0$  and a zero-gradient is assumed for the velocity. At `inletNorth` and `inletSouth`, the conductivity of the fluid entering those arms is the same, but ten times lower than the conductivity of

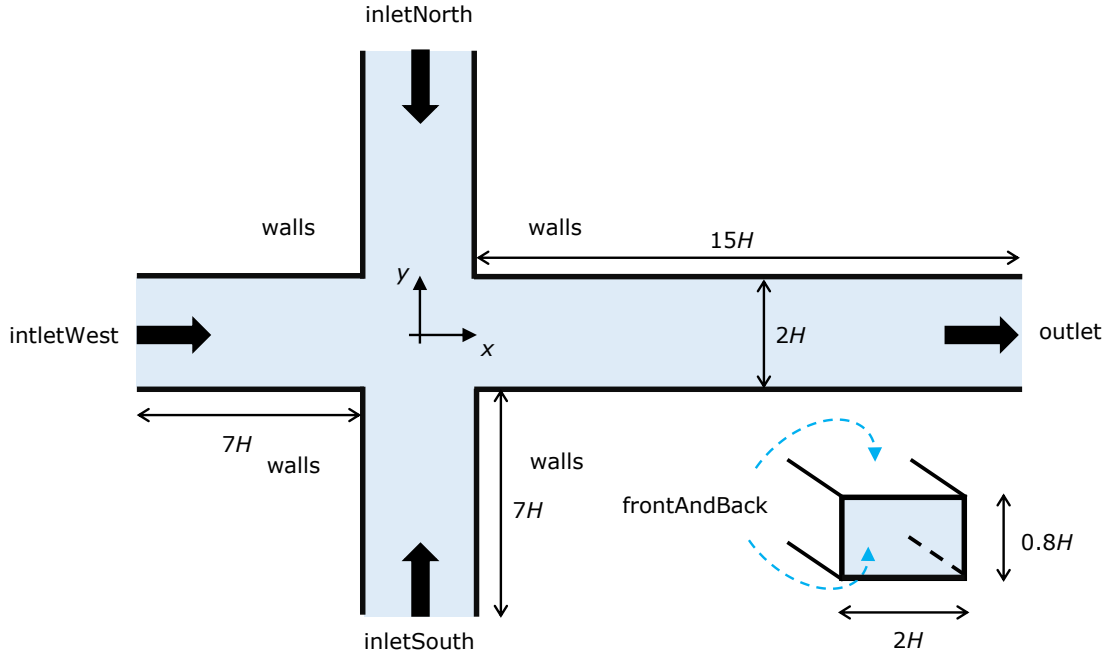


**Figure 5.25:** Three-dimensional flow-focusing device.

the fluid entering *inletWest* ( $\gamma = 10$ ). A passive scalar (neutral dye) is also entering the geometry through *inletWest*, only. A zero-gradient condition is imposed for both the conductivity and the passive-scalar concentration at the *outlet*. At the *walls* we assume zero-gradient for all variables, except the velocity. As discussed in Section 3.7.6, the Ohmic model is usually complemented with a conductivity-dependent slip velocity (Eq. 3.42). In this tutorial, we use  $m = -0.3$  for the power-law index (see Section 4.6.7). Regarding the electric potential, the *outlet* is grounded, while the potential at *inletNorth* and *inletSouth* are the same, being adjusted in order to impose the desired  $Ra_E$ . The potential at *inletWest* is set according to  $\beta$ .

Note that the passive-scalar (dye) has a diffusivity which is one order of magnitude lower than the diffusivity of the ions (conductivity), in agreement with typical real conditions.

### ❖ Command-line

1–Build the mesh:

```
~$ blockMesh
```

2–Create fields *C* and *sigma* by copying the ones already present, but which are not initialized in the interior domain:

```
~$ cp 0/C.org 0/C
```

```
~$ cp 0/sigma.org 0/sigma
```

3–Initialize fields *C* and *sigma* in the interior domain ( $C = 1 \wedge \sigma = \sigma_W$  for  $x < -H$  and  $t = 0$ ):

```
~$ setFields
```

4–Run the solver:

```
~$ rheoFoam
```

5–Post-process in Paraview (hint: slice the channel at the midplane in the  $z$ -direction and plot the contours of C):

```
~$ paraFoam
```

## ❖ Results

The contours for the passive-scalar are displayed in Fig. 5.26 at the mid-plane in  $z$ , for different  $Ra_E$ . The reader will probably note similarities between these instabilities and von-Kármán vortex streets.

The patterns are qualitatively similar to those obtained in Ref. [55] (see Fig. 4 therein, although our  $Ra_E$  is defined differently from the one used in that work). The periodicity or the chaotic behavior of the instabilities can be further evaluated by looking to the probes of C and U.

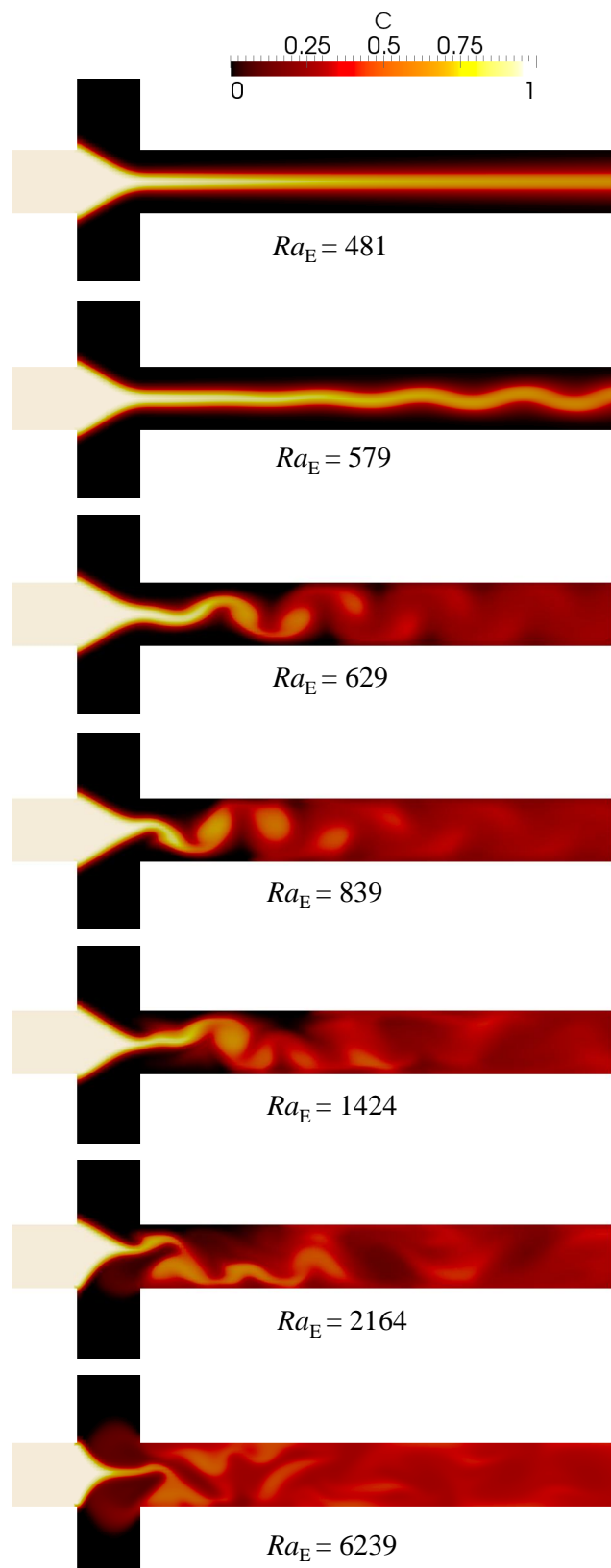


**Figure 5.26:** Instantaneous contours of  $C$  at the mid-plane in  $z$  for different  $Ra_E$  ( $\gamma = 10$  and  $\beta = 1.05$ ). The case provided in the tutorial is for  $Ra_E = 839$  and the remaining ones can be easily obtained by simply scaling the applied voltage (phiE) at the inlets (see the definition of  $Ra_E$ ).

Note that we do not use exactly the same parameters as in Posner et al. [55], since our purpose was solely to illustrate the qualitative behavior of electrokinetic instabilities, through a fast-running case. The large time-step used (Courant-controlled, with  $Co = 1.5$ ) is also inadequate to capture accurately the transient behavior of this case.

### 5.4.6 Case V: electrokinetic mixer

 `tutorials/rheoEFoam/EKmixer/slipSmoluchowski`

#### ❖ Overview

The main purpose of this tutorial is to illustrate the use of the *slipSmoluchowski* EDF model (see Section 3.7.5 and Table 4.2). Although simple, this model is very useful to simulate Newtonian fluid flows in complex geometries, being accurate for thin EDL and low intrinsic potentials. In addition, in this tutorial we also use AC fields, combined with the transport of a passive-scalar.

The case that we propose is an electrokinetic-based micromixer, inspired on the work of Coleman et al. [56]. In that work, the authors showed that a flow-focusing geometry followed by an expansion can achieve a good degree of mixing between two fluids, under AC-driven injection.

Note that this tutorial does not reproduce exactly the same geometrical dimensions, nor the same operating conditions of Ref. [56].

#### ❖ Geometry & Mesh

The 2D electrokinetic mixer is shown in Fig. 5.27 (the user can check the dimensions by opening the mesh in Paraview or by inspecting the corresponding `blockMeshDict` file). The device consists of a flow-focusing region where one fluid is injected through `inletWest` and the other fluid is injected in `inletNorth`. The geometry is made symmetric relative to the  $x$ -axis and an expansion region exists downstream to the flow-focusing, which is where the mixing mainly occurs.

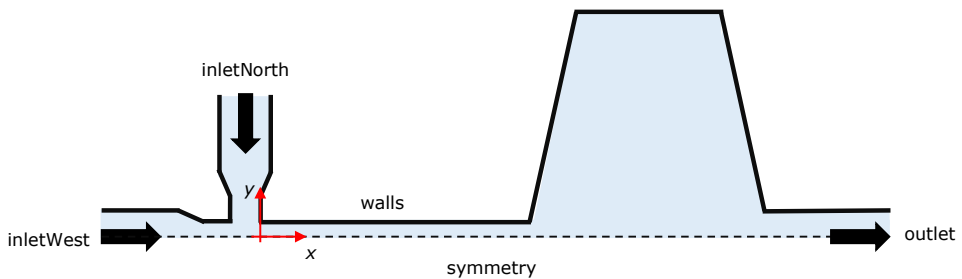


**Figure 5.27:** Electrokinetic mixer similar to the device used by Coleman et al. [56].

#### ❖ Boundary conditions

We consider a purely EDF, thus  $p = 0$  at both inlets and outlet boundaries, and a zero-gradient condition is simultaneously assigned to the velocity. Regarding the

externally applied potential, it is fixed at 0 V in the *outlet* and a custom sinusoidal boundary condition is imposed at each inlet,

$$\phi_{\text{Ext}}(t) = \phi_{\text{Ext, DC}} + \phi_{\text{Ext, AC}} \sin(2\pi ft + \theta) \quad (5.9)$$

As long as  $\phi_{\text{Ext}}(t) > 0$  at each inlet, there is a unidirectional net flow of fluid in the region  $x > 0$ , although the fluid can move both forward and backward in the region  $x \leq 0$ , which constitutes the injecting mechanism of the mixer [56]. By changing  $\phi_{\text{Ext, DC}}$ ,  $\phi_{\text{Ext, AC}}$ ,  $f$  and/or  $\theta$  at each inlet, different degrees of mixing can be achieved. At the wall, zero-gradient is considered for pressure and electric potential and the Helmholtz-Smoluchowski equation (Eq. 3.35) is used for the slip velocity.

A passive-scalar is injected at *inletWest* and the purpose of the mixer is precisely to achieve the perfect mixing of the passive-scalar stream (*inletWest*), with the stream devoid of that scalar (*inletNorth*) – perfect mixing means  $C = 0.5$  for a passive-scalar in the range  $[0, 1]$ . Note that, as stated in Ref. [56], the operating conditions can be also tuned in order to obtain a pre-defined degree of mixture different than a 0.5/0.5 stream at the outlet.

### ⌚ Command-line

Since the list of commands to run is rather extensive, we recommend the user to simply run the script `Allrun`. The commands executed by `Allrun` that might seem new, regarding what has been done in the previous tutorials, are `topoSet` and `refineMesh`. Those commands select the cells in the expansion region and perform a refinement in the  $y$ -direction, respectively.

### ⌚ Results

Fig. 5.28 shows the contours of the passive-scalar when either the stream devoid of  $C$ , or rich in  $C$ , are injected. Both snapshots were taken after the system has reached a periodic state. As can be seen, the conditions defined ensure a good mixing between the streams, since  $C \approx 0.5$  at the outlet.

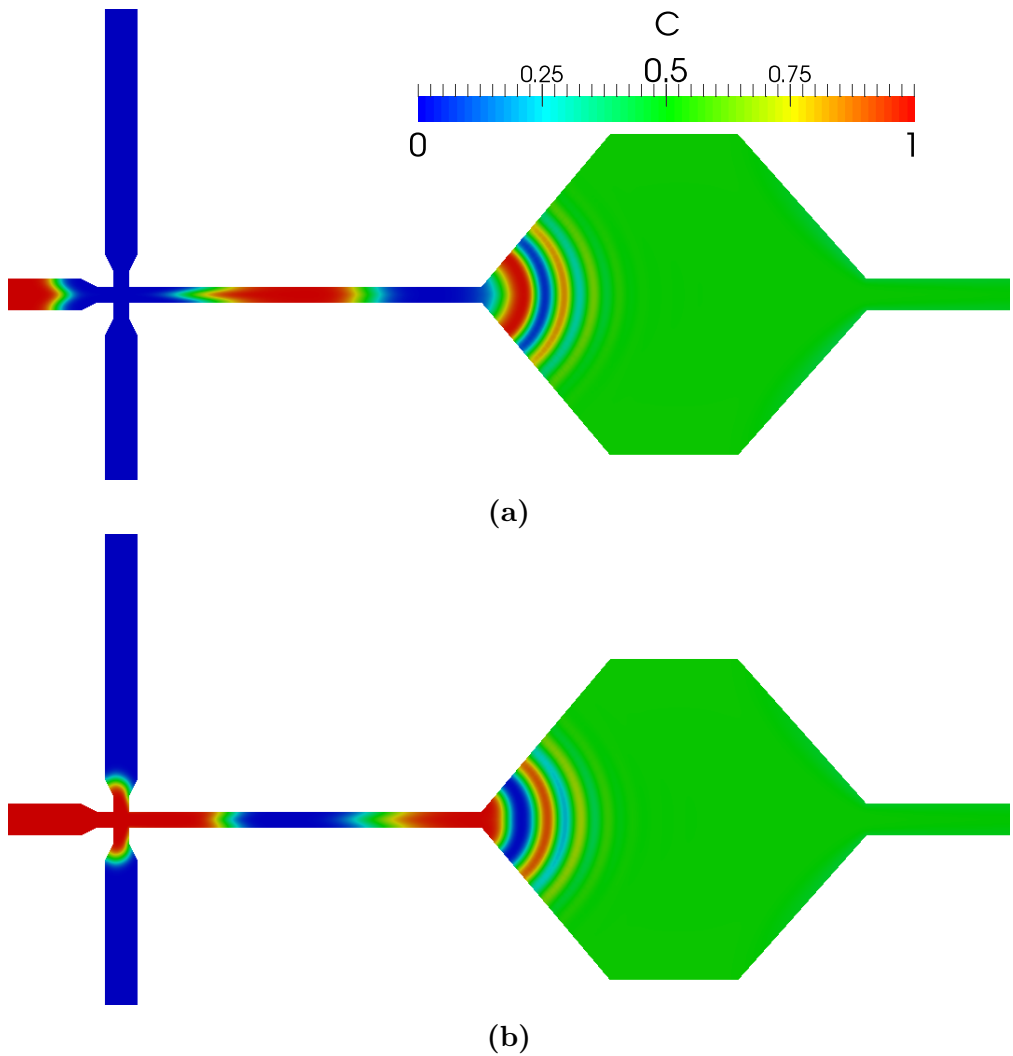


**Figure 5.28:** Snapshots of the passive scalar concentration field at different instants: (a) injecting the phase devoid of  $C$  (*inletNorth*) and (b) injecting the phase rich in  $C$  (*inletWest*). Note that the geometry has been reflected relative to the  $x$ -axis (in Paraview) for presentation purposes – only the upper-half of the geometry is simulated.

The user can play with the several degrees of freedom of the electric potential boundary conditions in order to achieve different degrees of mixing. Note that the time-step used in the tutorial has been adjusted to obtain results in a reasonable amount time, but it should be lowered to achieve higher accuracy in time. Such a high time-step, as well as the "coarse" mesh used, would not be possible to use if, for instance, the full PNP model was used instead – the simulation would most likely diverge due to stability issues.

#### 5.4.7 Case VI: electro-elastic instabilities in cross-shaped geometries

[tutorials/rheoEFoam/EEI/PoissonBoltzmann/](#)

### ❖ Overview

The electrically-driven flow of high-molecular weight polyacrylamide solutions in cross-slot and flow-focusing devices was seen to become unstable after a threshold electric potential is exceeded [57]. This tutorial addresses the numerical simulation of such phenomena, as presented in Ref. [57]. This tutorial merges electrically-driven flows with viscoelastic fluid models, where the electric charge distribution is computed by the Poisson-Boltzmann model and the extra-stress tensor of the viscoelastic fluid is evolved using the Oldroyd-B model ( $\beta = 0.4$ ). The settings of the tutorial reproduce the case with  $\Delta V = 160$  V,  $Wi_B = 2.06$ ,  $Wi_\kappa = 103$  (CrossSlot/) and  $\Delta V = 160$  V,  $Wi_B = 1.03$ ,  $Wi_\kappa = 154$  (FlowFocusing/) of Ref. [57]. The physical time of the simulations is  $t_f = 0.5$  s =  $10\lambda$ .

### ❖ Geometry & Mesh

The geometry for this case is displayed in Fig. 5.29. Both the geometry and the mesh correspond to the ones used in Ref. [57]. The flow is assumed to be 2D, being solved in the  $xy$ -plane. Note that the patch names for the cross-slot and flow-focusing geometries differ in the west arm, which is either an outlet or an inlet (Fig. 5.29).

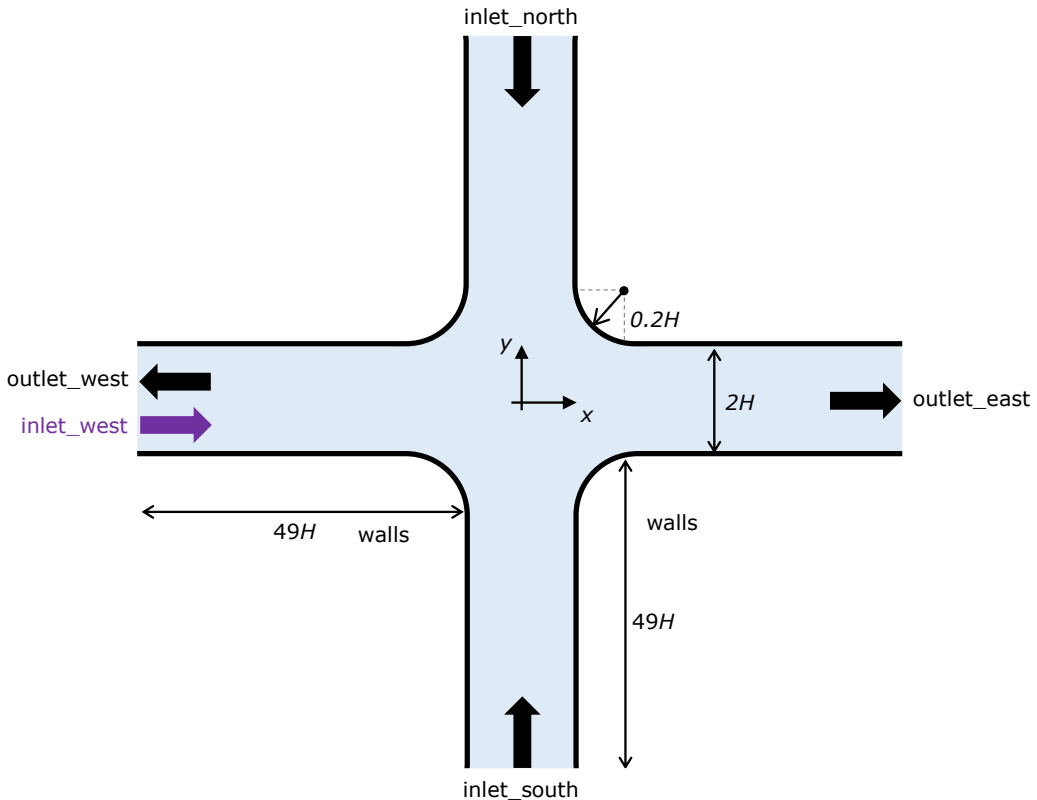


**Figure 5.29:** Cross-slot and flow-focusing geometries. In the west arm, the black arrow is for the cross-slot configuration (*outlet\_west*) and the purple arrow is for the flow-focusing configuration (*inlet\_west*). In the tutorial,  $H = 5 \times 10^{-5}$  m.

### ❖ Boundary conditions

The boundary conditions used are described in Ref. [57]. The tutorials also include the transport of a passive tracer. Note that the pressure extrapolation boundary condition at the wall is replaced by a zero-gradient condition in version *fe40*, since it is not available therein.

### ❖ Command-line

Before presenting the command line sequence, it is worth to note that the mesh for this case is built in a slightly different way. Indeed, the `blockMesh` application only builds one-quarter of the geometry/mesh, the one in the first quadrant (+,+). The remaining of the geometry/mesh is built by 2 sequential mirroring operations (`mirrorMesh`): first using the  $Oyz$  plane and then using the  $Oxz$  plane. Afterwards, patches should be renamed accordingly, which requires selecting, splitting and removing faces of already existing patches (`topoSet`) and creation of new ones (`createPatch`).

1–Build the mesh:

```
~$ blockMesh
~$ cp system/mirrorMeshDict0 system/mirrorMeshDict
~$ mirrorMesh
~$ cp system/mirrorMeshDict1 system/mirrorMeshDict
~$ mirrorMesh
~$ topoSet
~$ createPatch -overwrite
```

2–Initialize field  $C$  in the interior domain:

```
~$ cp 0/C.org 0/C
~$ setFields
```

3–Run the solver:

```
~$ rheoEFoam
```

### ❖ Results

The dye patterns (field  $C$ ) of the unstable flows can be visualized in Paraview.

## 5.5 *rheoBDFoam*

### 5.5.1 General guidelines

 **constant/**

All the elements needed in directory `constant/` for a simulation with *rheoEFoam* (Section 5.4.1) should also be present in a simulation with *rheoBDFoam*. This includes a valid mesh and dictionaries `electricProperties` and `constitutiveProperties`. If the simulation will not require the electric module of *rheoBDFoam*, then simply set the electric model *type* to *noModel* inside dictionary `electricProperties` (see the tutorial examples).

In addition to the above elements, the molecules' structure and physical properties should also be present in subdirectory `runTimeInfo`. The easiest and recommended way to generate this subdirectory and the files needed is running utility *initMolecules*, as described in Section 4.7.4. The last element that must be present in directory `constant/` is dictionary `moleculesControls`. This dictionary controls all the options specifically related with the Brownian dynamics algorithm, discussed in Section 4.3. Listing 5.5 presents an example of a `moleculesControls` dictionary, that we now analyze entry-by-entry:

- subDict *externalFlow*

*writeFields* – the continuum fields needed for the simulation must be present in the `startTime` directory, but during the simulation it is possible to suppress their write. This entry controls the writing of continuum fields during the simulation. For example, when using a frozen field, there is no need to write this constant field to the subsequent time directories (usually to save disk space), unless we expect to restart the simulation from one of those times. Even in the situation where a restart is expected, it is always possible to keep the *writeFields* option disabled and later copy manually the continuum fields to the new `startTime` directory. (boolean)

*frozenFlow* – as pointed out by the entry name, it should indicate if the flow (more generically all continuum fields) is frozen or not. A frozen flow does not change over time. (boolean)

*tethered* – indicates whether the molecules are tethered or not. Remember that if this option is enabled, all the molecules (of all groups) will be tethered by their first bead (see Section 4.3.6). (boolean)

*pushBackCmp* – each component of this vector should be either 1, if the molecules' center of mass is fixed in that direction, or 0 otherwise (see Section 4.3.6). (vector of 0/1's)

*pushBackFreq* – when the molecules' center of mass is to be fixed in any direction, then this entry corresponds to the frequency at which this is done (number of time-steps between calls) (see Section 4.3.6). This entry is ignored if all components of *pushBackCmp* are zero. (integer)

*interpolation* – the user should specify any valid interpolation method for the external forcing (see Section 4.3.4). (string)

*gradU* – if *interpolation* = *Analytical*, then  $\nabla \mathbf{u}$  should be defined in this entry. If any other interpolation method is selected, this entry is not used (see Section 4.3.3). (tensor)

- subDict *outputOptions*

*writeStats* – this option enables writing the index, position and stretch of all the molecules over time (see Section 4.3.8). (boolean)

*outputStats Interval* – number of time-steps between consecutive calls to the statistics writer. It is independent from the writing of time directories. Only effective if the previous option is enabled. (integer)

*writeVTK* – this option enables writing the molecules' structure and properties in VTK format, which should be readable by any version of Paraview. (boolean)

- subDict *exclusionVolumeProperties*

*activeExclusion Volume* – this option allows to include or suppress exclusion volume forces between beads (see Section 3.8.2). (boolean)

*activeWall Repulsion* – this option enables to impose a minimum approximation distance of the beads to the walls, upon collision. If not enabled, the beads are repositioned at the collision point, inside the computational domain (see Section 4.3.7). (boolean)

*repulsiveDistance* – if *activeWallRepulsion = true*, this entry defines the repositioning distance of the beads in the wall-normal direction, starting from the collision point on the wall (see Section 4.3.7). (double)

- subDict *HIProperties*

*activeHI* – this option allows to include or suppress hydrodynamic interactions, where the latter corresponds to the free-draining approach (see Section 3.8.2). (boolean)

- subDict *electrophoresis*

*active* – enabling this option adds an electrophoretic force (computed numerically) acting on the beads center of mass. (boolean)

*mobility* – if *active = true*, this entry should correspond to the electrophoretic mobility of **each individual** bead. (double)

- subDict *springModelProperties*

*springModel* – this entry should correspond to one of the available spring models (see Section 4.3.5). (string)

*timeScheme* – this entry should correspond to one of the available time integration schemes (see Section 4.3.5). (string)

*maxIter* – maximum number of iterations of the Newton-Raphson method if a semi-implicit time integration scheme is used. (integer)

*relTol* – minimum normalized spring length variation below which the Newton-Raphson method stops. (double)

*thresholdF* – fraction of the maximum spring length which triggers the algorithm to add implicitly the diagonal spring force terms contribution. This is the  $\alpha$  variable defined in Section 3.8.4, which should take values in the range  $]0, 1]$ . (double)

*cutOffStretch* – variable used to stabilize the Newton-Raphson method. In one given iteration of the Newton-Raphson method, it may happen that a spring exceeds its maximum admissible length ( $l$ ). As such, when the springs length needs to be used to compute  $\mathbf{f}^k$  and  $\mathbf{J}^k$  (see Section 3.8.4), we replace its value by  $\min(R_i, \text{cutOffStretch} \times l)$ . However, the resulting beads positions **are never** corrected. In order to ensure that this stabilization method will not affect the simulation results, this variable should always be higher than the maximum expected fractional extension and  $\leq 1$ . In most of the cases, a value between 0.990 and 0.999 will be a good choice (FENE and Cohen Padé models will typically require higher values, as 0.999 or even 1). (double)

*solver* – this entry should correspond to the name of one of the available matrix solvers to be used in the Newton-Raphson method (see Section 4.3.5). (string)

```

1  externalFlow
2 {
3     writeFields false;
4     frozenFlow true;
5
6     tethered false;
7     pushBackCmp (0 0 0);
8     pushBackFreq 1;
9
10    interpolation BarycentricWeights;
11    gradU
12    (
13        0 0 0
14        0 0 0
15        0 0 0
16    );
17}
18
19 outputOptions
20 {
21     writeStats true;
22     outputStatsInterval 10;
23
24     writeVTK true;
25 }
26
27 exclusionVolumeProperties
28 {
29     // bead-bead
30     activeExclusionVolume true;
31
32     // wall-bead
33 }
```

```

    activeWallRepulsion true;
34   repulsiveDistance 1e-7;
}
36
HIPProperties
38 {
    activeHI  true;
40 }

42 electrophoresis
{
44   active  false;
    mobility 5.95767e-10;
46 }

48 springModelProperties
{
50   springModel  MarkoSiggia;

52   timeScheme  semiImplicit;
    maxIter 20;
54   relTol 1e-6;
    thresholdF 0.85;
56   cutOffStretch .99;
    solver QR;
58 }

```

**Listing 5.5:** Example of a `moleculesControls` dictionary used with `rheoBDFoam`.

## 0 /

As we have seen for directory `constant/`, a simulation with `rheoBDFoam` requires all the elements that would be needed for a simulation with `rheoEFoam` (Section 5.4.1). Therefore, continuum fields `p` and `U` must always be present, and `phiE` and/or `psi` should also be defined for an electrically-driven flow, or if molecular electrophoresis is accounted for. Note that in case molecular electrophoresis is considered, only the electric field represented by `phiE` (the externally applied electric field) is used. Consider now three typical situations where `rheoBDFoam` is likely to be used:

- I-** steady numerical external forcing. In this case, the continuum fields defined in the `startTime` directory will be used and kept constant during the simulation. The continuum is frozen in time. The usual procedure in this scenario is to simulate the continuum flow elsewhere, in a separate simulation/case, and then copy the steady-state continuum fields to the `startTime` directory of the Brownian dynamics case.
- II-** transient numerical external forcing. In this situation, the continuum evolves in time simultaneously with the molecules. Therefore the continuum fields in the `startTime` directory should include initial and boundary conditions.
- III-** steady analytical external forcing. Although in this case the external forcing is defined by an analytical expression, the continuum fields that would be

needed for a numerical forcing should also be present. However, they are just placeholders and are **not used**, such that their content is not important, but needs to respect the expected syntax (have defined internal and boundary fields compliant with the boundary types).

In addition to files for the continuum fields, the `startTime` directory still needs to have a subdirectory `lagrangian/molecules/` containing the fields for the molecules. The easiest and recommended way to generate this subdirectory and the files needed is running utility `initMolecules`, as described in Section 4.7.4.

Note that if any viscoelastic fluid model is used in the continuum flow, which should probably be unusual, then also the corresponding variables should be defined in the `startTime` directory (see Section 5.1.1). No additional files are needed for a (non-elastic) generalized Newtonian fluid model.

### system/

Again, directory `system/` for a *rheoBDFoam* case should have the same elements as any *rheoEFoam* case. Moreover, most of the dictionaries do not require any change. The only modifications (additions) needed are in dictionary `fvSolution`, in subDict *SIMPLE*:

- solveFluid* – this entry allows to switch on/off the resolution of the constitutive, momentum and pressure equations. This option is typically set as *false* when the external forcing is analytical, or when the external forcing is numerical but frozen in time. (Switch)
- solveElecM* – this entry allows to switch on/off the resolution of the electric-related equations, independently of the option selected for *solveFluid*. (Switch)
- nSubCycles* – the Eulerian time-step – the one defined in `controlDict` – divided by *nSubCycles* corresponds to the time-step used to solve the governing equations of beads motion (see Section 4.5.5). (integer)

## 5.5.2 Molecules visualization with Paraview

The purpose of this short Section is to briefly explain the procedure to visualize the molecules in Paraview. There are at least two methods that can be used.

In the first method, open the case in Paraview in the usual way, for example, running *paraFoam* in the terminal. In the *Properties* panel, on the left, under *Mesh Parts* there is an entry named *molecules-lagrangian*. If not yet, check this box. Then, scroll-down in the same panel and check the box for all *Lagrangian Fields*. After clicking the *Apply* button, the molecules will be rendered in the screen. However, this does not mean that you will immediately see them, because the mesh is also represented and the molecules should lie inside the mesh. The easiest way to solve this issue is to uncheck *internalMesh* in the *Properties* panel (do not forget clicking the *Apply* button to update the changes). You should now be able to see (very) small dots in the screen, where each dot is a bead. The size of the dot is not related with the bead diameter (it is simply a setting of Paraview). However, although you can now see the beads, you do not have a spatial reference.

The ideal scenario would be to have both the mesh and the beads represented together. Therefore, open (*File → Open*) again the same *filename.OpenFOAM* file and select only the *internalMesh* under *Mesh Parts*. Depending on the geometry of the case, you may be able to slice the mesh behind the position of the molecules, ending with the representation of both. An alternative to the slice is to extract the feature edges of the geometry, whereby you will obtain the external edges of the geometry and be able to see the interior. The options are numerous. Nevertheless, this method is not very fruitful in information, since the only "interesting" field associated to each bead is the molecule index (*molcID*) to which they belong. The most one can do is to filter the beads by the molecule index, and isolate all the beads of a given molecule. However, there is no information on the beads connectivity, neither on the molecules' group, which may be relevant variables. There is still an additional issue: the position file associated to the Lagrangian particles will not be read by old Paraview versions, thus the beads cannot be visualized therein.

In order to solve these issues, *rheoBDFoam* can optionally output in runtime the molecules data in VTK format. This option can be enabled in dictionary *moleculesControls*, as seen in the previous Section, and it will create a directory named *VTKMolecules*, to which the molecules' data is written for each *outputTime*. When the molecules are visualized in VTK format, we recommend also to convert the mesh and continuum fields to VTK format by running the default OpenFOAM® utility *foamToVTK*. Then, simply open the two stacks of VTK files in Paraview. If using the *paraFoam* application, delete the object automatically created in the *Pipeline Browser* and *File → Open* the two VTK stacks (a stack *contains* the files generated for all the time-steps, under the same prefix name). Note that the stack directly sent to directory VTK by OpenFOAM® is the one for the internal field data. If you open that one, then the slicing procedure described above is also needed. The fields associated to each bead are *globalID*, *groupID*, *localID* and *molcID*. Following a top-down approach, filters can be used (*Threshold* in particular) to select a group of molecules (e.g. *groupID* = 0), a particular molecule of the group (e.g. *molcID* = 0) and finally the  $k^{\text{th}}$  bead in that molecule (*localID* =  $k$ ). You can also color the beads of a given molecule by their *localID* to see the connections. The *Glyph* filter may help to obtain nice images (Fig. 5.30). In general, the VTK files will be read by any Paraview version.

Summarizing, we recommend using the fist method to routinely check a case being prepared for simulation and to monitor the simulation. The second method should be used to debug, to obtain good-quality images, or if an old Paraview version is to be used.

### 5.5.3 Case 1: $\lambda$ -DNA extension in a planar extensional flow

 [tutorials/rheoBDSFoam/planarExtensionalFlow](#)

#### Overview

This tutorial aims to illustrate the use of an analytical external forcing. The

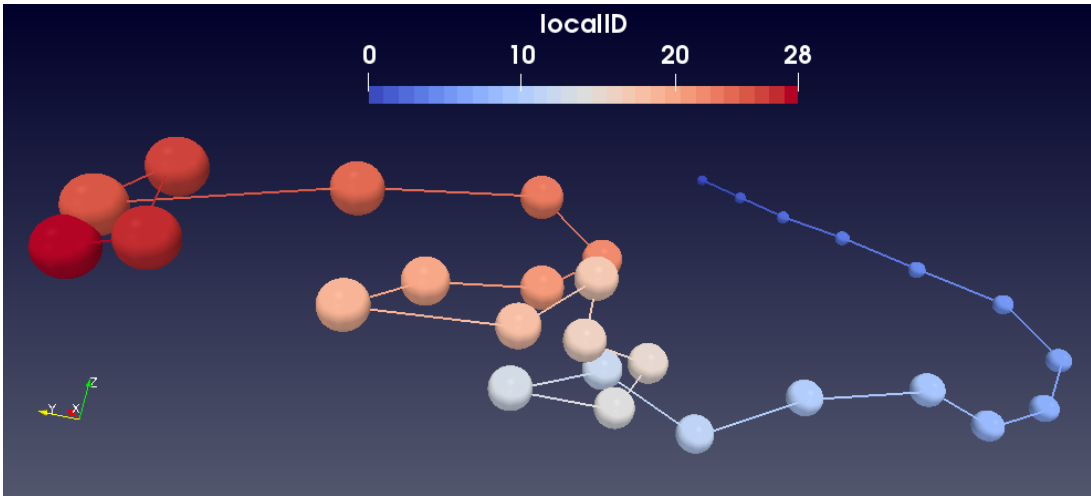


**Figure 5.30:** Screenshot of a molecule represented in Paraview, where the beads are colored by the local index. Springs are represented by straight lines between beads.

stretching of  $\lambda$ -DNA molecules in a planar extensional flow was selected for such purpose, since this is a well-studied case. Before imposing the planar extensional flow, the molecules are initialized in a stretched state and left to relax in no-flow conditions. This allows one to estimate the relaxation time of the molecules and also provides the starting molecular configurations for the planar extensional flow.

The  $\lambda$ -DNA molecules are modeled with the set of parameters provided in [25]:  $N = 11$  beads,  $D = 0.065 \text{ } \mu\text{m}^2/\text{s}$ ,  $a = 0.077 \text{ } \mu\text{m}$ ,  $N_{k,s} = 19.81$ ,  $\nu^{EV} = 0.0012 \text{ } \mu\text{m}^3$  and  $L_{\max} = 21 \text{ } \mu\text{m}$ . The planar extensional flow is simulated for  $Wi = \lambda\dot{\epsilon} = 2$ , where  $\dot{\epsilon}$  is the extensional-rate and  $\lambda$  is the relaxation time of  $\lambda$ -DNA molecules ( $\lambda \approx 4.1 \text{ s}$ , as determined in the first part of the tutorial). The simulations are run for an ensemble of 1000 molecules using the Marko-Siggia spring model.

### ❖ Geometry & Mesh

Since the forcing is analytical, a simple single-cell mesh can be used. The dimensions are set large enough so that the molecules can be fully contained inside the computational domain, even if fully-stretched. Furthermore, the molecules' center of mass is held at a fixed position. The flow is unconfined.

### ❖ Boundary conditions

Due to the analytical nature of the forcing, any arbitrary, but consistent, boundary condition can be attributed to the continuum fields (pressure and velocity); however, they will not be used. Consistent means here that if we assigned a *patch* type to a given boundary while building the mesh, then we cannot assign, for example, a *symmetryPlane* boundary condition to that boundary.

### ❖ Command-line

As aforementioned, in the first part of the tutorial the molecules are initialized in a stretched configuration ( $L = 0.7L_{\max}$ ) in order to study their relaxation to equilibrium in no-flow conditions. This is carried out inside directory `relaxation/`:

1–Build the mesh:

```
~$ blockMesh
```

2–Initialize the molecules:

```
~$ initMolecules
```

3–Run the solver:

```
~$ rheoBDFoam
```

4–Extract the ensemble average molecular length over time:

```
~$ averageMolcN 0
```

In the last time outputted by the solver ( $t = 50$  s), the molecules display an equilibrium configuration in no-flow conditions. These configurations are used in the start of the planar extensional flow, thus they should be copied to the case directory. The data needed is contained inside 50/lagrangian and constant/runTimeInfo/50.

1–Build the mesh:

```
~$ blockMesh
```

2–Copy the equilibrium molecular configurations from directory relaxation/:

```
~$ cp -rf relaxation/50/lagrangian 0/
~$ mkdir -p constant/runTimeInfo/50
~$ cp -rf relaxation/constant/runTimeInfo/50/constant/run
TimeInfo
~$ mv constant/runTimeInfo/50 constant/runTimeInfo/0
```

3–Run the solver:

```
~$ rheoBDFoam
```

4–Extract the ensemble average molecular length over time:

```
~$ averageMolcN 0
```

## ⌚ Results

Firstly, we will estimate the relaxation time of the molecules. It can be obtained from the ensemble average relaxation curve output to file relaxation/rheoToolPP/0/moleculesStats/G1/Stretch\_Naverage.txt by utility *averageMolcN*. The molecular length should decay over time as [24],

$$L^2(t) = L_I^2 \exp(-t/\lambda) + L_0^2$$

where  $L_I$  is the initial length of the molecules and  $L_0$  is the equilibrium length for  $t \rightarrow \infty$ . Therefore, when plotting  $\ln(L^2(t) - L_0^2)$  as a function of  $t$ , the inverse of the slope corresponds to  $-\lambda$ . The estimation is more accurate in the range of time where  $L$  is below  $0.3L_{\max}$  [24]. The results obtained are presented in Fig. 5.31a, where we can estimate  $\lambda = -1/-0.2429 \approx 4.1$  s.

The evolution of the fractional molecular length over time, obtained in the planar extensional flow at  $Wi = 2$  (second part of the tutorial), is plotted in Fig. 5.31b, along with the numerical results of [25].

Experimenting new  $Wi$  is as easy as changing the `gradU` entry in `constant/moleculesControls` (the time-step may need adjustments). There is no need to run again the initial molecules' relaxation step. Also, the components of `gradU` can easily be set to represent a shear flow.

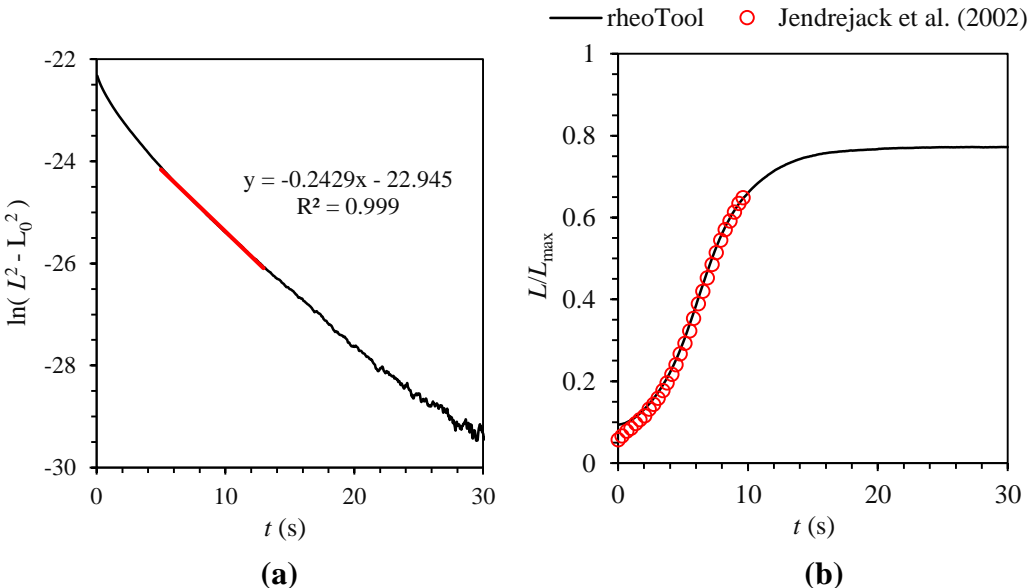


**Figure 5.31:** (a) Decay of the molecular length over time during relaxation in no-flow conditions. The red line represents a linear fit to the data for  $5 \leq t \leq 13$  s. (b) Fractional molecular length evolution over time in a planar extensional flow at  $Wi = 2$ . The symbols represent the numerical results from [25].

#### 5.5.4 Case 2: $7\lambda$ -DNA extension in a flow-focusing device

☞ [tutorials/rheoBDSFoam/flowFocusing](#)

##### ❖ Overview

This tutorial illustrates the application of *rheoBDSFoam* in a case with a steady numerical external forcing, where the forcing is either a pressure-driven flow (`directory pressureDrivenFlow/`) or electrophoresis (`directory electrophoresis/`). The geometry used is a flow-focusing device, which imposes a non-homogeneous extensional flow along its centerline.

The molecule selected for this tutorial is  $7\lambda$ -DNA, which is modeled with the following set of parameters [58]:  $N = 29$  beads,  $D = 0.257 \mu\text{m}^2/\text{s}$ ,  $a = 0.101 \mu\text{m}$ ,  $N_{k,s} = 40$ ,  $\nu^{EV} = 0.0034 \mu\text{m}^3$  and  $L_{\max} = 150 \mu\text{m}$ . According to [58], these parameters give  $\lambda = 21 \text{ s}$  in a 8.4 cP Newtonian buffer.

Considering a low Reynolds number flow ( $Re < 0.01$ ), the relevant dimensionless numbers are the velocity ratio ( $VR = U_N/U_W$ ) and the centerline Weissenberg number ( $Wi = \lambda\dot{\epsilon}$ ), where  $\dot{\epsilon} = \frac{2.1U_N}{H}$ , with factor 2.1 corresponding approximately

to the ratio between the centerline velocity and the average velocity in the fully-developed region of the north arm (valid for a pressure-driven laminar flow in a straight channel with a square cross-section). Subscripts N and W point to the North and West arms of the device. For the electrophoresis case,  $\dot{\epsilon} = \frac{U_N}{H}$  and  $U = \mu E$  is the relation between the electric field magnitude and the electrophoretic velocity magnitude. Both  $\mu$  (the electrophoretic mobility) and  $E$  can be adjusted interchangeably to impose a given  $U$ . Note that a given electrophoretic  $VR$  can not be obtained by an equal ratio of electric potentials (exception is for  $VR = 1$ ).

The simulations are run for an ensemble of 1000 molecules, divided over two groups of 500 molecules. The Marko-Siggia spring model is used.

## ❖ Geometry & Mesh

The 3D flow-focusing geometry used is similar to the one in the tutorial of Section 5.4.5 (see Fig. 5.25). However, the height considered in this example is equal to the width,  $h = 2H$ , and  $H = 100 \mu\text{m}$ .

## ❖ Boundary conditions

### Pressure-driven flow

The velocity magnitude in the north and south inlets is equal, and  $20\times$  higher than the velocity magnitude in the west arm ( $VR = 20$ ). The velocities are selected in order to have  $Wi = 20$ . The pressure is fixed at zero at the outlet and no-slip boundary conditions hold at the walls.

### Electrophoresis

For the electrophoresis case, the sole purpose of the continuum simulation is to obtain the electric potential distribution. Thus, we need to define field `phiE` and select any model for electrically-driven flows that allows one to compute Laplace's equation. Note that we are not interested in solving for the electroosmotic flow; we only need the electric potential distribution, but this requires selecting a complete model. The `slipSmoluchowski` model (see Section 4.2.1) is the one displaying the simplest `electricProperties` dictionary to define, thus this one has been selected. The electric field is assumed to be tangential to the walls, and the potential at the inlets is fixed in order to have an electric field (velocity) ratio  $\approx 20$  between the north (south) and west arms. Then, we select  $\mu$  in order to match the  $U$  velocity corresponding to  $Wi = 20$  (we are not concerned with the physical admissibility of  $\mu$  in the tutorial).

## ❖ Command-line

The sequence of commands to run these cases is somewhat long. Thus, we recommend to use directly the `Allrun` scripts inside directories `pressureDrivenFlow/` and `electrophoresis/`. Each of these scripts will first run the solver to obtain the steady-state continuum fields (either `rheoFoam` or `rheoEFoam`), and then they run the Brownian dynamics solver (`rheoBDFoam`, inside directory `BDS/`). Regarding the Brownian dynamics simulations, the molecules are first left to equilibrate in the local fully-developed flow of the west arm ( $x = -4H$ ) for around  $20\lambda \approx 400\text{s}$ . This requires fixing the molecules center of mass (see Section 4.3.6). Then, this constraint is removed and the molecules flow freely until they exit the geometry through the `outlet` patch. Both steps are carried out in the

same directory (`BDS/`); the second simulation starts from the last time-step of the first simulation. The second simulation stops when no molecule remains inside the geometry. At the end of the simulation, we use utility `averageMolcX` (see Section 4.7.6) to extract the average molecular length over a line starting at  $x = -3H$  and ending at  $x = 15H$ , partitioned in 100 bins. You can see that the application is called for `time = 400` because this is the `startTime` of the second simulation.

The comments in the `Allrun` scripts should help to understand all the steps. Nevertheless, we would like to highlight two points that may seem less clear. Firstly, the commands

```
~$ foamDictionary -entry ...
```

simply use utility `foamDictionary` of OpenFOAM® to automatically change a given entry in a given dictionary from the command-line (or via scripting). More information can be found in the OpenFOAM® website. The second point is related with the copy operations performed. For example, script `pressureDrivenFlow/BDS/Allrun` includes these lines,

```
~$ cp -rf ../flowSimulation/0.01/p* 0/
~$ cp -rf ../flowSimulation/0.01/U* 0/
```

which are simply intended to copy the steady-state ( $t = 0.01$  s in this case) fields  $U$  and  $p$  from the continuum simulation directory, to directory `BDS/`. Some lines below, you will find,

```
~$ cp -rf 0/p* 400/
~$ cp -rf 0/U* 400/
```

which have a related function. These lines of code are executed after the first Brownian dynamics simulation (equilibrating the molecules in the local flow) has been run, and we call them to copy again the continuum fields  $U$  and  $p$  to the `startTime` directory (in this case `startTime = 400`) of the next Brownian dynamics simulation, where they still do not exist, but are needed. The user may be wondering why `rheoBDFoam` do not automatically wrote these fields during the first run. This was because it was our option, by setting `writeFields = false` inside dictionary `moleculesControls` (see Section 5.5.1). This option was considered simply to save disk space (the advantage would be clearer if we would have to save 1000 time-steps or if the mesh was much denser).

## ⌚ Results

The fractional molecular length obtained for the pressure-driven flow and for electrophoresis ( $VR = Wi = 20$ ) are plotted in Fig. 5.32. This data is the result outputted by the call to `averageMolcX`. You can find it in `rheoToolPP/400/moleculesStats/G1/Stretch.txt` and `rheoToolPP/400/moleculesStats/G2/Stretch.txt` for each of the two groups, and compute the average between both groups. The pressure-driven flow seems to be slightly more effective in stretching the molecules, eventually due to its higher flow heterogeneity over the channel width. You can also visualize the molecules in Paraview using one of the methods described in Section 5.5.1.

It would be easy to run a case with the superposition of the two external forcings, pressure-driven flow and electrophoresis. Moreover, we could even add an electroosmotic flow. This exercise is left as a challenge.

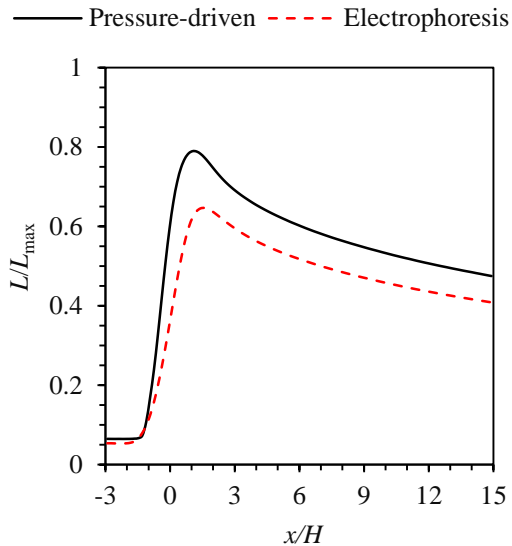


**Figure 5.32:** Fractional molecular length of  $7\lambda$ -DNA in the flow-focusing geometry, under two types of external forcing. Results are for  $VR = Wi = 20$ .

### 5.5.5 Case 3: $\lambda$ -DNA dynamics in LAOE

 [tutorials/rheoBDSFoam/LAOE](#)

#### ❖ Overview

The previous tutorials used a steady external forcing, either analytical or numerical. This tutorial exemplifies the use of *rheoBDFoam* in a case with a time-varying numerical forcing. In such situations, both the continuum and Brownian dynamics equations need to be evolved in time.

The case selected is the large-amplitude oscillatory extension (LAOE) of  $\lambda$ -DNA molecules, as proposed in [59]. The working principle of LAOE is very similar to LAOS (large-amplitude oscillatory shear), but the flow is extensionally-dominated instead of shear-dominated [59]. This type of flow can be generated in the vicinity of the stagnation point of a microfluidic cross-slot device with oscillatory inlet streams.

This tutorial aims to reproduce one of the experiments presented in [59], for  $Wi = \lambda\dot{\epsilon} = 6.5$  and  $De = \lambda f = 0.45$ , where  $\lambda$  is the molecules' relaxation time,  $\dot{\epsilon}$  is the peak extensional-rate at the stagnation point of the cross-slot and  $f$  is the oscillatory frequency of the inlet streams. The geometry used in [59] has a channel width of 400  $\mu\text{m}$  and the height is 90  $\mu\text{m}$ . However, we use a 2D geometry (width = 400  $\mu\text{m}$ ) in this tutorial to reduce the computation time. Since  $1/f$  is much higher than the diffusion time-scale of the channel, the different diffusion time-scale of the 2D geometry will not effect appreciably the results (momentum diffusion can

still be considered "instantaneous"). In addition, the  $z$ -component of the velocity field is likely to have a negligible influence, as the molecules analyzed are all at the channel mid-height. Hence, the 2D approximation seems to be reasonable *a priori*. Remember that although the mesh and continuum fields are assumed 2D, the three Cartesian components of the beads motion equation are solved for (see Section 4.3.3).

The simulations are run for an ensemble of 500 molecules. The spring model and physical parameters used to represent  $\lambda$ -DNA molecules are the same as those presented in Section 5.5.3. We remember that those parameters give  $\lambda = 4.1$  s in a 43.3 cP buffer, which has a viscosity close to that of the buffer used in [59]. In [59], the molecules are immobilized at the stagnation point of the cross-slot using a Stokes trap. Hence, in the tutorial we also fix the molecules center of mass in the vicinity of the stagnation point. We remember that fixing the molecules center of mass in *rheoTool* is not the same as tethering the molecules (see Section 4.3.6).

### ❖ Geometry & Mesh

The geometry of the 2D cross-slot device is similar (same boundary names) to the one used in the tutorial of Section 5.1.7. For the scheme of Fig. 5.9,  $W = 400 \mu\text{m}$  and the four arms are 2 mm long.

### ❖ Boundary conditions

The  $y$ -component of the velocity in the *inlet\_north* boundary follows a sinusoidal profile,

$$v_N(t) = -v_0 \sin(2\pi ft)$$

where  $v_0$  is selected such that the maximum extensional-rate at the stagnation point (computed numerically) is  $Wi/\lambda$ . In the *inlet\_south* boundary,  $v_S(t) = -v_N(t)$ . These sinusoidal velocity profiles are imposed using a *functionObject* (check file 0/U). No-slip boundary conditions are assigned at the walls.

### ❖ Command-line

The list of commands to be run is somewhat lengthy. Thus, we recommend the user to directly run the Allrun script provided in the tutorial.

The tutorial performs two calls to *rheoBDFoam*. In the first call, the molecules are equilibrated in no-flow conditions for approximately  $10\lambda$  (40 s). In the second call, starting from the equilibrium configurations ( $t = 40$  s), the flow is switched-on and the simulation runs up to  $t = 80$  s.

### ❖ Results

The evolution of the fractional molecular length over time is plotted in Fig. 5.33. The data of this figure can be found in file rheoToolPP/40/moleculeStats/G1/Stretch\_Naverage.txt. The first cycles should be discarded, since they are in the non-periodic regime (we need then to translate the curve in time).

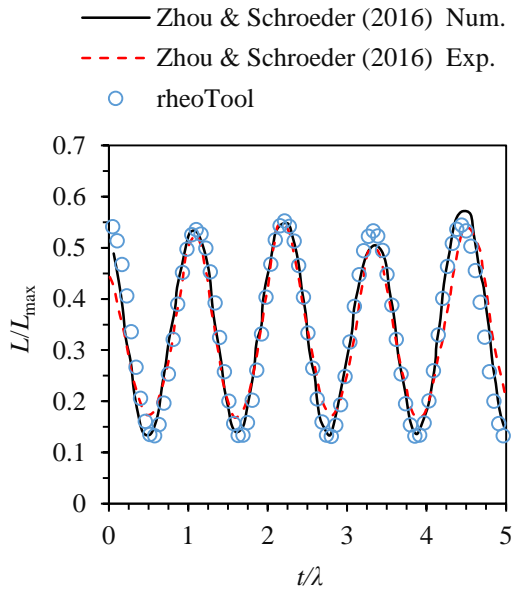


**Figure 5.33:** Fractional molecular length of  $\lambda$ -DNA in LAOE, for  $Wi = 6.5$  and  $De = 0.45$ . The lines are for the experimental (dashed) and numerical (solid) results in [59], while the symbols represent the numerical results obtained with *rheoTool*.

The reader may wonder if it would be possible to prescribe an analytical sinusoidal planar extensional flow, instead of simulating the full cross-slot flow, as it was done in [59] (even if simulating the full flow is possibly more realistic). Shortly, it is not possible to use a time-varying analytical flow in the form *rheoTool* is provided, but anyone with some programming experience can easily change the code to do so. It would just require changing one line of code in *AnalyticalI.H*. Indeed, line

```
return (gradU_.T() & sP.position());
```

should be replaced, for example, by

```
1 scalar e0 = 1.5854 * Foam::sin(2*M_PI*mesh_.time().timeOutputValue
() * 0.10976);
3 return vector(-e0*sP.position().x(), e0*sP.position().y(), 0.);
```

The reader can easily try this, and check if the results are comparable, as expected.

# Chapter 6

## FAQS

It is important for any new user of *rheoTool* to read this user-guide, if not entirely, at least the Sections referring to the components that will be used. This will prepare the user for any apparently unexpected behavior from the software. Since the first version of *rheoTool*, we received some common questions about the code, that we list below in the hope they can help future users.

### **While installing *rheoTool* the compilation fails with the error message: fatal error: Eigen/Dense: No such file or directory. How to solve it?**

This means that variable `$EIGEN_RHEO` is not pointing to Eigen's directory. Either your `~/.bashrc` file was not sourced before compiling *rheoTool* and after downloading Eigen (this is why it is important to compile *rheoTool* in a terminal **different** from the one used to download Eigen), or the path is not valid anymore (perhaps you moved Eigen to a different directory or you renamed it). In the terminal where the error was retrieved, check the path with command `echo $EIGEN_RHEO` and be sure that Eigen is there, i.e. inside that directory you should find folders `bench`, `blas`, `cmake`, etc. If an empty path is retrieved, then this variable was not exported to your `~/.bashrc`. If nothing is inside the directory, then the variable was wrongly assigned and should be exported again. See the installation instructions in Chapter [2](#).

### **My simulation is running for $Re \gg 1$ but behaves as if it was laminar ( $Re = 0$ ). Is this a bug?**

Check the convective scheme assigned to `div(phi, U)` in `system/fvSchemes`. If it corresponds to `GaussDefCmpw none` then this means that momentum convection is being ignored and that explains your results. Simply select a convective scheme different from that one to fix the 'problem' (see Section [4.7.1](#)). This happens often when deriving a case from a tutorial running in inertialess conditions.

### **The results of my transient simulations with a viscoelastic fluid model are very sensitive to the time-step. Is it normal?**

When simulating a transient case, all the existing time-scales (momentum diffusion, polymer relaxation, ion diffusion, etc.) should be taken into account and the user should ensure that the time-step is low enough to resolve all of them. In addition to this, care should be taken when using the *coupling* stabilization method in cases where  $\eta_P \gg \eta_S$ , since explicit stabilizing terms are introduced in

the momentum equation. To test if the stabilization method is the main reason for exaggerated time-step sensitivity, simply disable it (set it equal to *none*). Note, however, that the simulation will likely become more unstable and lower time-steps might be needed. The *BSD* stabilizing option is less explicit than *coupling* and could be also tried. The explicitness can be reduced by increasing the number of inner iterations. Note that the explicitness of the *coupling* stabilization method requires refinement in both time and space to disappear. See Sections 3.2 and 4.1.4 .

If your question is not in the list above and you can not find an answer for it in this user-guide, then feel free to contact us (see contacts in Section 1.5).

# Appendix A

## Parameters and variables in *rheoTool*

**Table A.1:** List of some relevant parameters and variables used by *rheoTool* and correspondence with the nomenclature used in this guide. The list is not exhaustive.

| Name in the guide | Name in the code | Dimensions [kg m s K mol A cd] | Definition  |
|-------------------|------------------|--------------------------------|---|
| $\alpha$          | alpha            | [0 0 0 0 0 0]                  | Anisotropy parameter of Giesekus and eXtended Pom-Pom models (scalar)       |
| $\alpha$          | alpha            | [0 0 0 0 0 0]                  | Parameter of the piecewise-linear HRS functions (scalar)                    |
| $\alpha$          | alpha            | [0 0 0 0 0 0]                  | Indicator/Color function of the VOF method (scalar)                         |
| <b>A</b>          | A                | [0 0 0 0 0 0]                  | Conformation tensor (symmTensor)  |
| $a$               | a                | [0 0 0 0 0 0]                  | Dimensionless parameter of Carreau-Yasuda and White-Metzner models (scalar) |
| $a$               | a                | [0 0 0 0 0 0]                  | Variable of FENE-P model (scalar)   |
| $a$               | a                | [0 1 0 0 0 0]                  | Bead radius (scalar)  |
| -                 | AK_-             | [0 0 0 0 -1 0 0]               | Avogrado's constant (scalar)  |
| $\beta$           | beta             | [0 0 0 0 0 0]                  | Parameter of the piecewise-linear HRS functions (scalar)                    |

|                      |               |                   |   |
|----------------------|---------------|-------------------|---|
| $\beta$              | beta          | [0 0 0 0 0 0]     | CCR coefficient of Rolie-Poly model (scalar)  |
| $b$                  | b             | [0 0 0 0 0 0]     | Dimensionless parameter of White-Metzner model (scalar)                                       |
| -                    | b             | [0 0 0 0 0 0]     | Square-root conformation tensor of Ref. [15], for the <i>Oldroyd-BSqrt</i> model (symmTensor) |
| $\chi_{\max}$        | chiMax        | [0 0 0 0 0 0]     | Maximum stretch ratio in Rolie-Poly model (scalar)  |
| -                    | C             | [0 0 0 0 0 0]     | Passive scalar (scalar)   |
| $c_i$                | -             | [0 -3 0 0 1 0 0]  | Concentration of specie $i$ in mol/m <sup>3</sup> (scalar)                                    |
| $c_0$                | c0            | [0 -3 0 0 1 0 0]  | Reference ionic concentration (scalar)  |
| $\delta$             | delta         | [0 0 0 0 0 0]     | Exponent of Rolie-Poly model (scalar)   |
| $D$                  | D             | [0 2 -1 0 0 0 0]  | Diffusion coefficient in the passive scalar transport equation (scalar)                       |
| $D$                  | D             | [0 2 -1 0 0 0 0]  | Isotropic diffusion coefficient of a bead (scalar)  |
| $D_i$                | Di            | [0 2 -1 0 0 0 0]  | Diffusion coefficient of ionic specie $i$ (scalar)  |
| $\mu$                | elecMobility  | [-1 0 2 0 0 1 0]  | Electroosmotic mobility (scalar)  |
| $\mu_0$              | elecMobility0 | [-1 0 2 0 0 1 0]  | Electroosmotic mobility at a reference conductivity (scalar)                                  |
| $\varepsilon$        | epsilon       | [0 0 0 0 0 0]     | Extensibility parameter of PTT-type models (scalar)   |
| $\varepsilon$        | -             | [-1 -3 4 0 0 2 0] | Electric permittivity (scalar)  |
| $\varepsilon_0$      | epsilonK_     | [-1 -3 4 0 0 2 0] | Electric permittivity of vacuum (scalar)  |
| $\eta$               | eta           | [1 -1 -1 0 0 0 0] | Newtonian viscosity (scalar)  |
| $\eta(\dot{\gamma})$ | eta           | [1 -1 -1 0 0 0 0] | Shear-rate dependent viscosity from a GNF model (scalar)                                      |

|                    |             |                   |  |
|--------------------|-------------|-------------------|--|
| $\eta_0$           | eta0        | [1 -1 -1 0 0 0 0] | Zero shear-rate viscosity (scalar)   |
| $\eta_0$           | eta0        | [1 -1 -1 0 0 0 0] | Limiting viscosity in the Herschel-Bulkley model (scalar)                          |
| $\eta_\infty$      | etaInf      | [1 -1 -1 0 0 0 0] | Infinite shear-rate viscosity (scalar)   |
| $\eta_{\max}$      | etaMax      | [1 -1 -1 0 0 0 0] | Upper bound for the viscosity in the power-law model (scalar)                      |
| $\eta_{\min}$      | etaMin      | [1 -1 -1 0 0 0 0] | Lower bound for the viscosity in the power-law model (scalar)                      |
| $\eta_p$           | etaP        | [1 -1 -1 0 0 0 0] | Polymeric viscosity coefficient (scalar)   |
| $\eta_s$           | etaS        | [1 -1 -1 0 0 0 0] | Solvent viscosity (scalar)   |
| $\mathbf{\Lambda}$ | eigVals     | [0 0 0 0 0 0 0]   | Eigenvalues obtained in the diagonalization of $\mathbf{A}$ (tensor)               |
| $\mathbf{R}$       | eigVecs     | [0 0 0 0 0 0 0]   | Eigenvectors obtained in the diagonalization of $\Theta$ and $\mathbf{A}$ (tensor) |
| $e$                | eK_-        | [0 0 1 0 0 1 0]   | Elementary charge (scalar)   |
| $\mathbf{E}_a$     | extraEField | [1 1 -3 0 0 -1 0] | Constant and uniform extra electric field (vector)                                 |
| $f$                | f           | [0 0 0 0 0 0 0]   | Variable of FENE-type models (scalar)  |
| $F$                | FK_-        | [0 0 1 0 -1 1 0]  | Faraday's constant (scalar)  |
| $k$                | k           | [1 -1 -1 0 0 0 0] | Consistency index of power-law model (scalar)                                      |
| $k$                | k           | [0 0 1 0 0 0 0]   | Time-scale in the Carreau-Yasuda model (scalar)                                    |
| $K$                | K           | [0 0 1 0 0 0 0]   | Time-scale for $\eta_p$ in the White-Metzner model (scalar)                        |
| $k$                | kbK_-       | [1 2 -2 -1 0 0 0] | Boltzmann's constant (scalar)  |
| $\lambda$          | lambda      | [0 0 1 0 0 0 0]   | Relaxation time (scalar)   |
| $\lambda_B$        | lambdaB     | [0 0 1 0 0 0 0]   | Relaxation time of the backbone tube orientation (scalar)                          |
| $\lambda_D$        | lambdaD     | [0 0 1 0 0 0 0]   | Reptation time (scalar)  |

|                               |          |                   |  |
|-------------------------------|----------|-------------------|--|
| $\lambda_R$                   | lambdaR  | [0 0 1 0 0 0 0]   | Rouse or stretch time (scalar)   |
| $\lambda_S$                   | lambdaS  | [0 0 1 0 0 0 0]   | Relaxation time for the tube stretch (scalar)  |
| $L$                           | L        | [0 0 1 0 0 0 0]   | Time-scale for $\lambda$ in the White-Metzner model (scalar)                               |
| $L^2$                         | L2       | [0 0 0 0 0 0 0]   | Extensibility parameter of FENE-type models (scalar)                                       |
| $l$                           | Ls       | [0 1 0 0 0 0 0]   | Maximum length of a spring (scalar)  |
| $m$                           | m        | [0 0 0 0 0 0 0]   | Dimensionless parameter of White-Metzner model (scalar)                                    |
| $m$                           | m        | [0 0 0 0 0 0 0]   | Power-law exponent for the conductivity-dependent Helmholtz-Smoluchowski velocity (scalar) |
| $\mu$                         | mobility | [-1 0 2 0 0 1 0]  | Electrophoretic mobility of a bead (scalar)  |
| $\nu_{EV}$                    | nuEV     | [0 3 0 0 0 0 0]   | Exclusion-volume parameter (scalar)  |
| $n$                           | n        | [0 0 0 0 0 0 0]   | Flow behavior index for shear-rate dependent viscosity models (scalar)                     |
| $N_{k,s}$                     | Nks      | [0 0 0 0 0 0 0]   | Number of Kuhn steps lengths per spring (scalar)   |
| $\phi_{Ext}$                  | phiE     | [1 2 -3 0 0 -1 0] | Externally-applied electric potential (scalar)   |
| $\Psi$                        | psi      | [1 2 -3 0 0 -1 0] | Total electric potential (scalar)  |
| $\psi$                        | psi      | [1 2 -3 0 0 -1 0] | Intrinsic electric potential (scalar)  |
| $p$                           | p        | [1 -1 -2 0 0 0 0] | Pressure, in <i>rheoInterFoam</i> (scalar)   |
| $\frac{p}{\rho}$              | p        | [0 2 -2 0 0 0 0]  | Pressure divided by the density, in <i>rheoFoam</i> and <i>rheoEFoam</i> (scalar)          |
| $\mathbf{u} \cdot \mathbf{S}$ | phi      | [0 3 -1 0 0 0 0]  | Face fluxes (scalar)   |

|                 |              |                   |   |
|-----------------|--------------|-------------------|---|
| $q$             | q            | [0 0 0 0 0 0]     | Amount of arms at the end of the polymer backbone (scalar)  |
| $\rho$          | rho          | [1 -3 0 0 0 0]    | Density (scalar)  |
| $\rho_E$        | -            | [0 -3 1 0 0 1 0]  | Charge density (per unit volume) (scalar)   |
| $\varepsilon_R$ | relPerm      | [0 0 0 0 0 0]     | Relative electric permittivity or dielectric constant (scalar)  |
| $\sigma$        | sigma        | [-1 -3 3 0 0 2 0] | Electric conductivity (scalar)  |
| $\sigma_0$      | sigma0       | [-1 -3 3 0 0 2 0] | Reference electric conductivity (scalar)  |
| $\dot{\gamma}$  | strainRate() | [0 0 -1 0 0 0 0]  | Shear-rate (scalar)   |
| $\tau$          | tau          | [1 -1 -2 0 0 0 0] | Polymeric extra-stress tensor (symmTensor)  |
| $\tau_0$        | tau0         | [1 -1 -2 0 0 0 0] | Yield stress (scalar)   |
| -               | tauMF        | [1 -1 -2 0 0 0 0] | Polymeric extra-stress tensor weighted by the indicator function in <i>rheoInterFoam</i> (symmTensor) |
| $\Theta$        | theta        | [0 0 0 0 0 0]     | Natural logarithm of the conformation tensor (symmTensor)   |
| $T$             | T            | [0 0 0 1 0 0 0]   | Absolute temperature (scalar)   |
| $\mathbf{u}$    | U            | [0 1 -1 0 0 0 0]  | Velocity (vector)   |
| $\zeta$         | zeta         | [0 0 0 0 0 0]     | Slip parameter of PTT-type models (scalar)  |
| $z_i$           | zi           | [0 0 0 0 0 0]     | Charge valence of specie $i$ (scalar)   |

# Bibliography

- [1] J. Favero, A. Secchi, N. Cardozo, and H. Jasak, “Viscoelastic fluid analysis in internal and in free surface flows using the software OpenFOAM,” *Computers & Chemical Engineering*, vol. 34, no. 12, pp. 1984 – 1993, 2010. 10th International Symposium on Process Systems Engineering, Salvador, Bahia, Brasil, 16-20 August 2009.
- [2] F. Pimenta and M. Alves, “Stabilization of an open-source finite-volume solver for viscoelastic fluid flows,” *Journal of Non-Newtonian Fluid Mechanics*, vol. 239, pp. 85 – 104, 2017.
- [3] F. Pimenta and M. Alves, “Simulation of electrically-driven flows using Open-FOAM,” *arXiv:1802.02843*, 2018.
- [4] F. Pimenta, R. G. Sousa, and M. A. Alves, “Optimization of flow-focusing devices for homogeneous extensional flow,” *Biomicrofluidics*, vol. 12, no. 5, p. 054103, 2018.
- [5] F. Pimenta and M. Alves, “A coupled finite-volume solver for numerical simulation of electrically-driven flows,” *arXiv:1904.02138*, 2019.
- [6] R. Fattal and R. Kupferman, “Constitutive laws for the matrix-logarithm of the conformation tensor,” *Journal of Non-Newtonian Fluid Mechanics*, vol. 123, no. 2–3, pp. 281 – 285, 2004.
- [7] R. Bird and O. Hassager, *Dynamics of Polymeric Liquids: Fluid mechanics*, vol. 1-2 of *Dynamics of Polymeric Liquids*. Wiley, 1987.
- [8] M. G. Baltussen, W. M. Verbeeten, A. C. Bogaerds, M. A. Hulsen, and G. W. Peters, “Anisotropy parameter restrictions for the extended pom-pom model,” *Journal of Non-Newtonian Fluid Mechanics*, vol. 165, no. 19, pp. 1047 – 1054, 2010.
- [9] S. Balay, S. Abhyankar, M. F. Adams, J. Brown, P. Brune, K. Buschelman, L. Dalcin, A. Dener, V. Eijkhout, W. D. Gropp, D. Kaushik, M. G. Knepley, D. A. May, L. C. McInnes, R. T. Mills, T. Munson, K. Rupp, P. Sanan, B. F. Smith, S. Zampini, H. Zhang, and H. Zhang, “PETSc Web page.” <http://www.mcs.anl.gov/petsc>, 2018.
- [10] S. Balay, S. Abhyankar, M. F. Adams, J. Brown, P. Brune, K. Buschelman, L. Dalcin, A. Dener, V. Eijkhout, W. D. Gropp, D. Kaushik, M. G. Knepley,

- D. A. May, L. C. McInnes, R. T. Mills, T. Munson, K. Rupp, P. Sanan, B. F. Smith, S. Zampini, H. Zhang, and H. Zhang, “PETSc users manual,” Tech. Rep. ANL-95/11 - Revision 3.10, Argonne National Laboratory, 2018.
- [11] S. Balay, W. D. Gropp, L. C. McInnes, and B. F. Smith, “Efficient management of parallelism in object oriented numerical software libraries,” in *Modern Software Tools in Scientific Computing* (E. Arge, A. M. Bruaset, and H. P. Langtangen, eds.), pp. 163–202, Birkhäuser Press, 1997.
- [12] X. Chen, H. Marschall, M. Schäfer, and D. Bothe, “A comparison of stabilisation approaches for finite-volume simulation of viscoelastic fluid flow,” *International Journal of Computational Fluid Dynamics*, vol. 27, no. 6-7, pp. 229–250, 2013.
- [13] R. Fattal and R. Kupferman, “Time-dependent simulation of viscoelastic flows at high weissenberg number using the log-conformation representation,” *Journal of Non-Newtonian Fluid Mechanics*, vol. 126, no. 1, pp. 23 – 37, 2005.
- [14] A. Afonso, F. Pinho, and M. Alves, “The kernel-conformation constitutive laws,” *Journal of Non-Newtonian Fluid Mechanics*, vol. 167–168, pp. 30 – 37, 2012.
- [15] N. Balci, B. Thomases, M. Renardy, and C. R. Doering, “Symmetric factorization of the conformation tensor in viscoelastic fluid models,” *Journal of Non-Newtonian Fluid Mechanics*, vol. 166, no. 11, pp. 546 – 553, 2011. XVIth International Workshop on Numerical Methods for Non-Newtonian Flows.
- [16] Ž. Tuković and H. Jasak, “A moving mesh finite volume interface tracking method for surface tension dominated interfacial fluid flow,” *Computers & Fluids*, vol. 55, pp. 70 – 84, 2012.
- [17] H. Jasak, “Pressure-velocity coupling in FOAM, Consistent derivation for steady and transient flow solvers.” OFW11, Guimarães, Portugal, 2016.
- [18] F. Moukalled, A. A. Aziz, and M. Darwish, “Performance comparison of the NWF and DC methods for implementing high-resolution schemes in a fully coupled incompressible flow solver,” *Applied Mathematics and Computation*, vol. 217, no. 11, pp. 5041 – 5054, 2011.
- [19] H. Jasak, H. Weller, and A. Gosman, “High resolution NVD differencing scheme for arbitrarily unstructured meshes,” *International Journal for Numerical Methods in Fluids*, vol. 31, no. 2, pp. 431 – 449, 1999.
- [20] J. Ferziger and M. Peric, *Computational Methods for Fluid Dynamics*. Springer Berlin Heidelberg, 2001.
- [21] A. Afonso, F. Pinho, and M. Alves, “Electro-osmosis of viscoelastic fluids and prediction of electro-elastic flow instabilities in a cross slot using a finite-volume method,” *Journal of Non-Newtonian Fluid Mechanics*, vol. 179–180, pp. 55 – 68, 2012.

- [22] C.-H. Chen, H. Lin, S. K. Lele, and J. G. Santiago, “Convective and absolute electrokinetic instability with conductivity gradients,” *Journal of Fluid Mechanics*, vol. 524, pp. 263–303, 2005.
- [23] A. Persat and J. G. Santiago, “An ohmic model for electrokinetic flows of binary asymmetric electrolytes,” *Current Opinion in Colloid & Interface Science*, vol. 24, pp. 52 – 63, 2016.
- [24] R. G. Larson, “The rheology of dilute solutions of flexible polymers: Progress and problems,” *Journal of Rheology*, vol. 49, no. 1, pp. 1–70, 2005.
- [25] R. M. Jendrejack, J. J. de Pablo, and M. D. Graham, “Stochastic simulations of DNA in flow: Dynamics and the effects of hydrodynamic interactions,” *The Journal of Chemical Physics*, vol. 116, no. 17, pp. 7752–7759, 2002.
- [26] “Brownian dynamics simulations of bead-rod and bead-spring chains: numerical algorithms and coarse-graining issues,” *Journal of Non-Newtonian Fluid Mechanics*, vol. 108, no. 1, pp. 227 – 255, 2002.
- [27] K. K. Kabanemi and J.-F. Hétu, “Nonequilibrium stretching dynamics of dilute and entangled linear polymers in extensional flow,” *Journal of Non-Newtonian Fluid Mechanics*, vol. 160, no. 2–3, pp. 113 – 121, 2009.
- [28] P. A. Vasquez, G. H. McKinley, and L. P. Cook, “A network scission model for wormlike micellar solutions: I. model formulation and viscometric flow predictions,” *Journal of Non-Newtonian Fluid Mechanics*, vol. 144, no. 2, pp. 122 – 139, 2007.
- [29] S. Dutta and M. D. Graham, “Mechanistic constitutive model for wormlike micelle solutions with flow-induced structure formation,” *Journal of Non-Newtonian Fluid Mechanics*, vol. 251, pp. 97 – 106, 2018.
- [30] F. Bautista, J. de Santos, J. Puig, and O. Manero, “Understanding thixotropic and antithixotropic behavior of viscoelastic micellar solutions and liquid crystalline dispersions. i. the model,” *Journal of Non-Newtonian Fluid Mechanics*, vol. 80, no. 2, pp. 93 – 113, 1999.
- [31] P. Saramito, “A new elastoviscoplastic model based on the herschel–bulkley viscoplastic model,” *Journal of Non-Newtonian Fluid Mechanics*, vol. 158, no. 1, pp. 154 – 161, 2009. Visco-plastic fluids: From theory to application.
- [32] P. Saramito, “A new constitutive equation for elastoviscoplastic fluid flows,” *Journal of Non-Newtonian Fluid Mechanics*, vol. 145, no. 1, pp. 1 – 14, 2007.
- [33] Y. Wei, M. J. Solomon, and R. G. Larson, “A multimode structural kinetics constitutive equation for the transient rheology of thixotropic elastoviscoplastic fluids,” *Journal of Rheology*, vol. 62, no. 1, pp. 321–342, 2018.
- [34] P. J. Oliveira, “Asymmetric flows of viscoelastic fluids in symmetric planar expansion geometries,” *Journal of Non-Newtonian Fluid Mechanics*, vol. 114, no. 1, pp. 33 – 63, 2003.

- [35] G. Guennebaud, B. Jacob, *et al.*, “Eigen v3.” <http://eigen.tuxfamily.org>, 2010.
- [36] W. H. Press, B. P. Flannery, S. A. Teukolsky, and W. T. Vetterling, “Numerical recipes (FORTRAN version),” *Press Syndicate of the University of Cambridge, Cambridge, UK*, 1989.
- [37] LLNL, “Hypre: High performance preconditioners.” <http://www.llnl.gov/CASC/hypre>, 2010.
- [38] F. Habla, A. Woitalka, S. Neuner, and O. Hinrichsen, “Development of a methodology for numerical simulation of non-isothermal viscoelastic fluid flows with application to axisymmetric 4:1 contraction flows,” *Chemical Engineering Journal*, vol. 207, no. Supplement C, pp. 772 – 784, 2012. 22nd International Symposium on Chemical Reaction Engineering (ISCRE 22).
- [39] L. L. Ferrás, A. M. Afonso, J. M. Nóbrega, and F. T. Pinho, “A numerical and theoretical study on viscoelastic fluid slip flows,” *Physics of Fluids*, vol. 29, no. 5, p. 053102, 2017.
- [40] Z. Wu and D. Li, “Mixing and flow regulating by induced-charge electrokinetic flow in a microchannel with a pair of conducting triangle hurdles,” *Microfluidics and Nanofluidics*, vol. 5, no. 1, pp. 65–76, 2008.
- [41] S. Xue and G. W. Barton, “An unstructured finite volume method for viscoelastic flow simulations with highly truncated domains,” *Journal of Non-Newtonian Fluid Mechanics*, vol. 233, pp. 48 – 60, 2016. Papers presented at the Rheology Symposium in honor of Prof. R. I. Tanner on the occasion of his 82nd birthday, in Vathi, Samos, Greece.
- [42] Y. Na and J. Y. Yoo, “A finite volume technique to simulate the flow of a viscoelastic fluid,” *Computational Mechanics*, vol. 8, no. 1, pp. 43–55, 1991.
- [43] M. A. Hulsen, R. Fattal, and R. Kupferman, “Flow of viscoelastic fluids past a cylinder at high weissenberg number: Stabilized simulations using matrix logarithms,” *Journal of Non-Newtonian Fluid Mechanics*, vol. 127, no. 1, pp. 27 – 39, 2005.
- [44] M. Alves, F. Pinho, and P. Oliveira, “The flow of viscoelastic fluids past a cylinder: finite-volume high-resolution methods,” *Journal of Non-Newtonian Fluid Mechanics*, vol. 97, no. 2–3, pp. 207 – 232, 2001.
- [45] F. Cruz, R. Poole, A. Afonso, F. Pinho, P. Oliveira, and M. Alves, “A new viscoelastic benchmark flow: Stationary bifurcation in a cross-slot,” *Journal of Non-Newtonian Fluid Mechanics*, vol. 214, pp. 57 – 68, 2014.
- [46] A. Valencia, A. Zarate, M. Galvez, and L. Badilla, “Non-newtonian blood flow dynamics in a right internal carotid artery with a saccular aneurysm,” *International Journal for Numerical Methods in Fluids*, vol. 50, no. 6, pp. 751–764, 2006.

- [47] Aneurisk-Team, “AneuriskWeb project website, <http://ecm2.mathcs.emory.edu/aneuriskweb>.” Web Site, 2012.
- [48] A. Syrakos, Y. Dimakopoulos, and J. Tsamopoulos, “Theoretical study of the flow in a fluid damper containing high viscosity silicone oil: Effects of shear-thinning and viscoelasticity,” *Physics of Fluids*, vol. 30, no. 3, p. 030708, 2018.
- [49] R. Figueiredo, C. Oishi, A. Afonso, I. Tasso, and J. Cuminato, “A two-phase solver for complex fluids: Studies of the weissenberg effect,” *International Journal of Multiphase Flow*, vol. 84, pp. 98 – 115, 2016.
- [50] C. Oishi, F. Martins, M. Tomé, and M. Alves, “Numerical simulation of drop impact and jet buckling problems using the extended pom-pom model,” *Journal of Non-Newtonian Fluid Mechanics*, vol. 169–170, pp. 91 – 103, 2012.
- [51] R. Comminal, F. Pimenta, J. H. Hattel, M. A. Alves, and J. Spangenberg, “Numerical simulation of the planar extrudate swell of pseudoplastic and viscoelastic fluids with the streamfunction and the VOF methods,” *Journal of Non-Newtonian Fluid Mechanics*, vol. 252, pp. 1 – 18, 2018.
- [52] C. Zhao and C. Yang, “An exact solution for electroosmosis of non-newtonian fluids in microchannels,” *Journal of Non-Newtonian Fluid Mechanics*, vol. 166, no. 17–18, pp. 1076 – 1079, 2011.
- [53] A. Afonso, M. Alves, and F. Pinho, “Analytical solution of mixed electroosmotic/pressure driven flows of viscoelastic fluids in microchannels,” *Journal of Non-Newtonian Fluid Mechanics*, vol. 159, no. 1–3, pp. 50 – 63, 2009.
- [54] C. L. Druzgalski, M. B. Andersen, and A. Mani, “Direct numerical simulation of electroconvective instability and hydrodynamic chaos near an ion-selective surface,” *Physics of Fluids*, vol. 25, no. 11, p. 110804, 2013.
- [55] J. D. Posner and J. G. Santiago, “Convective instability of electrokinetic flows in a cross-shaped microchannel,” *Journal of Fluid Mechanics*, vol. 555, pp. 1–42, 05 2006.
- [56] J. T. Coleman, J. McKechnie, and D. Sinton, “High-efficiency electrokinetic micromixing through symmetric sequential injection and expansion,” *Lab Chip*, vol. 6, pp. 1033–1039, 2006.
- [57] F. Pimenta and M. Alves, “Electro-elastic instabilities in cross-shaped microchannels,” *Journal of Non-Newtonian Fluid Mechanics*, vol. 259, pp. 61 – 77, 2018.
- [58] C. M. Schroeder, E. S. G. Shaqfeh, and S. Chu, “Effect of hydrodynamic interactions on DNA dynamics in extensional flow: Simulation and single molecule experiment,” *Macromolecules*, vol. 37, no. 24, pp. 9242–9256, 2004.
- [59] Y. Zhou and C. M. Schroeder, “Single polymer dynamics under large amplitude oscillatory extension,” *Physical Review Fluids*, vol. 1, p. 053301, 2016.